POPULATION GENETIC AND PHENOTYPIC ANALYSES OF *ASPERGILLUS FUMIGATUS* STRAINS FROM GLOBAL SOIL SAMPLES

POPULATION GENETIC AND PHENOTYPIC ANALYSES OF *ASPERGILLUS FUMIGATUS* STRAINS FROM GLOBAL SOIL SAMPLES

by

GREG KORFANTY, B.Sc., M.Sc.

A Thesis
Submitted to the School of Graduate Studies
in the Partial Fulfillment of the Requirements for the Degree
Doctor of Philosophy

McMaster University

DOCTOR OF PHILOSOPHY (2023) McMaster University

Department of Biology Hamilton, Ontario, Canada

TITLE: POPULATION GENETIC AND PHENOTYPIC ANALYSES OF *ASPERGILLUS FUMIGATUS* STRAINS FROM GLOBAL SOIL SAMPLES

AUTHOR: Gregory Korfanty

B.Sc. (Molecular Biology and Genetics)

M.Sc. (Biology)

McMaster University, Hamilton, Canada

SUPERVISOR: Dr. Jianping Xu

NUMBER OF PAGES: xvii, 203

Lay Abstract

Aspergillus fumigatus is a cosmopolitan mold that causes opportunistic infections in humans termed aspergillosis. To better understand the environmental reservoirs of aspergillosis infection, I investigated soil populations of this fungus, as soil is likely the largest reservoir of *A. fumigatus*. I isolated *A. fumigatus* strains from 11 countries across 6 continents and genetically compared these soil populations to each other and to clinical *A. fumigatus* populations. I found extensive genetic diversity within most local soil populations, along with different relationships among geographic populations. When a sample of these global strains were sexually crossed, I uncovered high variation in their sexual fecundity, which lowered at higher geographic distances. Lastly, strains exhibited high variations in growth at different temperatures regardless of climatic, genetic, and geographic factors from where they were isolated. My thesis highlights the extraordinary phenotypic variations and complex population structure of *A. fumigatus* populations isolated from soil across the globe.

Abstract

Fungal populations occupy a vast number of ecological niches across many geographic areas around the planet. Fungi act as essential nutrient recyclers, playing key roles as saprophytes, mutualists, and pathogens. As humans, we use these broad properties of fungi in biochemical and pharmaceutical industries, creating a plethora of products ranging from antimicrobials to food products. However, certain fungal species have become a devastating burden on human public health. Of these fungal species, my PhD thesis has focused on the critically important mold *Aspergillus fumigatus*. This mold is an opportunistic human pathogen, being the leading etiological cause of the spectrum of diseases termed aspergillosis that yearly affects over 8,000,000 people worldwide. In addition, the rising number of antifungal resistant strains around the world, especially within environmental populations, is of critical concern. Given that almost all aspergillosis infections result from environmental strains, and that soil is a major ecological niche for *A. fumigatus*, my thesis focused on characterizing genetic and phenotypic aspects of soil isolates of *A. fumigatus* obtained from many geographic and climatic regions around the world. My analyses revealed extensive allelic and genotypic diversity within and among populations. These *A. fumigatus* populations were defined by both historical differentiations, high gene flow, non-random recombination, and high susceptibility to triazole antifungals. Additionally, I tested the sexual fecundity of a subset of these global strains and found that geographic and genetic distance between the pairs of parental strains had little effect on sexual fecundity. Lastly, my research found broad variations in growth of a global sample of *A. fumigatus* strains at different temperatures. Again, no relationship of either geographic or genetic distance on strain growth was observed. Overall, my research highlights the extraordinary nature of *A. fumigatus* populations to quickly spread and adapt across diverse and complex environments.

Acknowledgments

To start, I would like to thank my amazing supervisor Dr. Jianping Xu. I joined his lab in 2016 for my fourth-year undergraduate thesis course, where I initially began my work on *Aspergillus fumigatus*. Since then, I have continued my research on *A. fumigatus* in his lab, starting my master's thesis in 2017 and completing it in 2019, followed by the start of my PhD. Since the beginning, JP has been a fantastic supervisor, always being supportive, patient, flexible, and highly knowledgeable. I thank him greatly for all the professional development he has provided me over these seven years to become a better leader and a thorough researcher. I would also like to thank my supervisory committee, Dr. Turlough Finan and Dr. Brian Golding, for all their critical and helpful feedback, and the great support they provided throughout my graduate career.

I have met many wonderful lab members throughout my graduate career. I would like to thank my mentor Eta Ashu, as, along with JP, sowed the passion I have for fungal genetics that helped me get to where I am now. I thank all my past and current lab members for all their support and friendship, as they all helped me grow as a researcher and highlighted the value of collaboration in science; Heather Yoell, Adrian Forsythe, Himeshi Samarasinghe, Lijun Liu, Renad Aljohani, Sarah Sandor, Yuying Fan, Man You, Yue Wang, Megan Archer, Chadabhorn Insuk, Megan Hitchcock, Veronica Thorn, Viraj Whabi, Nicolas Popescu, Jezreel Dalmieda and Carlos Colangelo. I also thank all my wonderful undergraduate thesis students who offered tremendous contributions to my PhD thesis presented here; Mykaelah Dixon, Arshia Kazerouni, Kaitlin Stanley, Kaitlyn Lammers, Joy Heifetz, Paola Gomez, Michala Trajkovski. I wish all the best for their future endeavours.

Lastly, I would like to thank my parents, Anna and Jack, my brother Viktor, and all my friends for all their love and support throughout my PhD. I deeply value all the encouragements they provided and the great times we spent together.

Table of Contents

List of Figures

List of Tables

Abbreviations

ABPA – Allergic bronchopulmonary aspergillosis

BSH – Broad sense heritability

CPA – Chronic pulmonary aspergillosis

CSP – Cell surface protein

DAPC – Discriminant analysis of principal components

IA – Invasive aspergillosis

MAT – Mating type

ME – Malt extract

MIC – Minimum inhibitory concentration

MLG – Multilocus locus genotype

MSN – Minimum spanning network

NJ – Neighbor joining

SD – Sabouraud dextrose

STR – Short tandem repeat

Chapter 1

Introduction

1.1 Fungi: Ecology and Biotechnology

Fungi are an incredibly diverse and heterogeneous eukaryotic kingdom estimated to be composed of 2.2 to 2.8 million species where ~120,000 have been described (Hawksworth & Lücking, 2017). With so many species, fungi thrive in almost all ecological niches, functioning as mutualists (such as endophytes and mycorrhizae), saprobes or pathogens that use a diverse suite of metabolic processes to produce a plethora of secondary metabolites. Given all these properties of fungi, they have been extensively researched and used in biotechnology to benefit humanity (Mapook et al., 2022). Even before the advent of modern biotechnology following the initial production of citric acid by *Aspergillus niger* in 1917 (Cairns et al., 2018), fungi were used for food and therapeutic applications for centuries. For instance, in China, *Saccharomyces cerevisiae*, known today as brewer's or baker's yeast, was used to ferment beverages in the neolithic period (McGovern et al., 2004). Today, fungi are used in the production of alcohols, food, chemicals, medicines, composite materials, and as recyclers (e.g. plastics) (Meyer et al., 2020). Indeed, current research aims to better understand how fungi interact with their environment as well as other species. For example, within agriculture and forestry settings, a better understanding of mycorrhizal networks and their association with their host plant will help contribute to higher plant yields and lower fungicide/pesticides use (Khaliq et al., 2022).

1.2 Fungal Plant and Human Pathogens

The fungal kingdom includes many pathogens, with the majority affecting plants. Global crop yield losses due to fungal pathogens is between 30% to 40% and is estimated to cost the global economy hundreds of billions of dollars each year (Fones et al., 2020; Xu, 2022). Fungi also pose direct threats to human health, either by contaminating our food with

mycotoxins, pose as allergens in the atmosphere, or directly cause fungal infections. In immunocompetent individuals, fungal infections are primarily superficial infections of the skin, hair, or nails. In immunocompromised populations, mucosal infections, that include those of the mouth, throat, or genitalia, or chronic/invasive infections can occur. Approximately one billion people suffer from superficial fungal infections and 150 million suffer from serious to life-threatening infections, where on average 1.5 million people die from fungal infections per year (Bongomin et al., 2017; Brown et al., 2012). Concerningly, the prevalence of severe fungal infection is increasing due to the rising immunocompromised population around the world (Bongomin et al., 2017; Rayens & Norris, 2022). These severe and typically nosocomial infections are primarily caused by species in three genera: *Candida*, *Cryptococcus*, and *Aspergillus* (Bongomin et al., 2017). The yeast *Candida auris* has only recently been discovered and has already been designated a critically important fungal pathogen by the WHO due to its high mortality rate (between 30% and 60%) and resistance to almost all clinical antifungals (Chowdhary et al., 2023; World Health Organization, 2022). Indeed, systemic fungal infections pose a great risk to human health and research is continually ongoing to identify potential therapeutic targets and novel antifungals to help alleviate the burden caused by the fungal species (Lionakis et al., 2023).

1.3 *Aspergillus fumigatus*: Environmental and Pathogenic Roles

The saprophyte, *Aspergillus fumigatus*, is a cosmopolitan ascomycete mold found globally. The *Aspergillus* genus is closely related to both *Neosartorya* and *Penicillium* genera and consists of 344 species, some of which have roles in biotechnology, food production, and human health (Samson et al., 2014). *A. fumigatus* is part of the subgenera *Fumigati*, which consists of up to 63 morphologically similar mold species (Frisvad & Larsen, 2016; Samson et al., 2014). *A. fumigatus* has many physiological adaptations to the environment that contribute to the ubiquitous presence around the world. As a saprobe, *A. fumigatus* favour habitats with decaying organic matter, such as soil, compost heaps, and flower bulb wastes, contributing to the recycling carbon and nitrogen worldwide. As hydrolysis of organic matter produces excess heat that elevates temperatures in these environments, *A. fumigatus* has evolved high thermotolerance, capable of maintaining growth at 60 °C (Bhabhra & Askew,

2005; Kwon-Chung & Sugui, 2013; Verweij, Chowdhary, et al., 2016). From these niches, *A. fumigatus* ejects billions of highly volatile conidia (asexual spores) into the atmosphere, where, on average, the concentration of conidia is ~100 per m^3 of air (Kwon-Chung & Sugui, 2013). The high atmospheric abundance of *A. fumigatus* conidia and both historical and contemporary dispersal events led to the global presence of this species. Indeed, *A. fumigatus* conidia have been found and successfully cultured from the stratosphere and within the International Space Station (Dassarma et al., 2020; Knox et al., 2016).

The high atmospheric abundance, small conidia, and high thermotolerance allow *A. fumigatus* spores to enter and survive within human respiratory tracts. Macrophages from the host immune system normally clear the foreign conidia within the mucosal membranes in the lungs (Latgé & Chamilos, 2020). However, in individuals with past lung pathologies (e.g. asthma, cystic fibrosis, or tuberculosis) or those who are immunocompromised (either through HIV or immunosuppressive therapies), inhalation of these conidia can result in a range of pulmonary infections termed aspergillosis that affects over 8,000,000 globally (Bongomin et al., 2017; Latgé & Chamilos, 2020). Compared to other pathogenic *Aspergillus* species, *A. fumigatus* is the leading cause of aspergillosis, accounting for approximately 70% of all aspergillosis infections (Rokas et al., 2020). These chronic infections include allergic bronchopulmonary aspergillosis (ABPA), aspergilloma growth, and chronic pulmonary aspergillosis (CPA) (Figure 1.1). The most severe form of aspergillosis infection, invasive aspergillosis (IA), develops from prior CPA infections and affects at least 300,000 patients annually (Bongomin et al., 2017). The mortality rate of IA ranges between 40-90% without treatment (Latgé & Chamilos, 2020; Verweij, Chowdhary, et al., 2016). Severe aspergillosis infections occur typically in immunocompromised patients, however, the COVID-19 pandemic created a relatively large immunocompetent population with or recovering from severe COVID-19 infections (Verweij et al., 2021). These patients are susceptible to aspergillosis (co)infection, termed covid associated pulmonary aspergillosis (CAPA) that can develop into IA (Peláez-García de la Rasilla et al., 2022; Verweij et al., 2021). Patient mortality rate with CAPA is between 43-52% (Janssen et al., 2021).

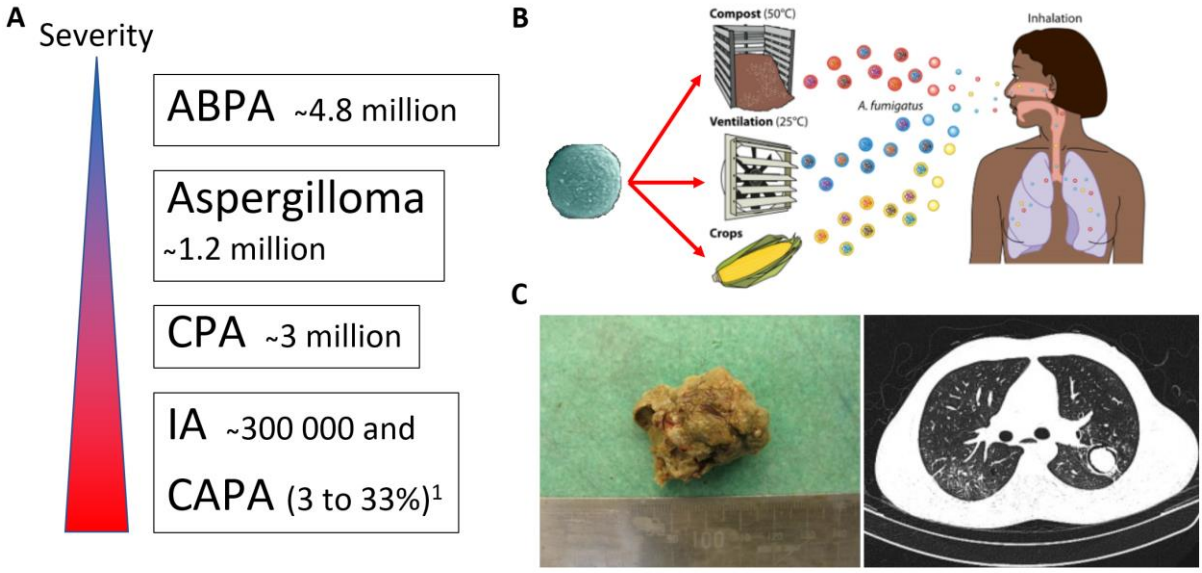

Figure 1.1: Aspergillosis infections and severity. (A) Severity and yearly prevalence of aspergillosis types. [1]CAPA infection prevalence varies between medical centers (Alanio et al., 2020; Machado et al., 2021; Prattes et al., 2022; Segrelles-Calvo et al., 2021; Verweij et al., 2020). (B) Route of *A. fumigatus* conidial colonization into the lungs. (C) Fungal ball and CT scan of aspergilloma extracted from a patient. Panel C was adapted from Figures 2 and 3 in Moodley et al., (2014). ABPA – allergic bronchopulmonary aspergillosis, CPA – chronic pulmonary aspergillosis, IA – invasive aspergillosis, CAPA – covid associated pulmonary aspergillosis.

Triazole antifungals are the first line pharmaceuticals in the treatment and prophylaxis of aspergillosis (Latgé & Chamilos, 2020). Triazoles target the biosynthesis pathway of ergosterol, the cholesterol analog within fungal cell membranes. Unfortunately, multiple triazole resistance mechanisms have been reported. The most common are point mutations and tandem repeat duplications within the triazole target lanosterol 14α-demethylase and its regulatory regions and mutations that increase triazole efflux pumps or limit drug uptake (Rybak et al., 2019). These mutations can occur in tandem with each other, resulting in *A. fumigatus* strains that are multi- and pan-azole resistant (Chowdhary et al., 2014; MacEdo et al., 2020; Siopi et al., 2020). Concerningly, triazole resistance rates are rising and resistance mutations are spreading around the world (Abdolrasouli et al., 2018; Buil et al., 2019; Chowdhary et al., 2013; Heo et al., 2017; Latgé & Chamilos, 2020). As a result, increasing numbers of triazole naïve patients have been reported with triazole resistant aspergillosis. Other antifungal classes used to treat aspergillosis include the echinocandins and polyenes.

Echinocandins target the FKS1, the catalytic subunit of (1,3)-β-D-glucan synthase, a protein complex vital in the development of the fungal cell wall. However, due to their limited and fungistatic activity against *Aspergillus* spp., they are used as an alternative treatment strategy against IA (Aruanno et al., 2019). The polyene amphotericin B is highly effective against fungal cells, as it binds directly to ergosterol, forming pores that lead to the leakage of cellular ions and eventually cell death (Stone et al., 2016). However, this exact process is unknown. During IA treatment, the high nephrotoxicity of amphotericin B relegates it for salvage therapy against triazole resistant infections. Unfortunately, *A. fumigatus* strains resistant to echinocandins and amphotericin B have been detected around the world (Ashu et al., 2018; Chen et al., 2023; Fan et al., 2020; Jiménez-Ortigosa et al., 2017).

1.4 Global *A. fumigatus* Populations and Drug Resistance

The rising number of triazole resistant *A. fumigatus* strains is a growing burden on aspergillosis management. Investigations into the rising triazole resistance rates have been conducted within medical centres over the last two decades (Abdolrasouli et al., 2018; Erjavec et al., 2009; Heo et al., 2017; Lestrade et al., 2020; Shelton et al., 2022; Verweij, Zhang, et al., 2016; Wu et al., 2020). Many of these studies have focused on clinically isolated *A. fumigatus* strains, with fewer including environmental sampling within their dataset (Chowdhary et al., 2012; Snelders et al., 2009). Within the last decade, environmental samples have been obtained from areas within and around hospitals (areas include hospital atmosphere, flower beds, and nearby soils) where, on average, the triazole susceptibility was lower than clinical isolates (Chowdhary et al., 2012). Triazoles used in agricultural practices have a similar mode of action to medical triazoles, and cross-resistance between medical and environmental azoles is common (Rodriguez-Tudela et al., 2008). The use of triazoles in agriculture was thought to be responsible for the rising number of drug resistant strains around the world in addition to promoting clonal expansions of multi- and pan-azole resistant genotypes found in many countries around the planet (Ahangarkani et al., 2020; Chowdhary et al., 2012; Verweij et al., 2009). Recent literature has found triazole resistant strains in flower bulb waste, green waste material, and wood chippings (Fraaije et al., 2020; Jeanvoine et al., 2017; Schoustra et al., 2019). Triazole fungicides are commonly used during the

manufacturing of a variety of goods and can accumulate within the organic waste, leading to resistance development of resident *A. fumigatus* strains. Interestingly, the study by Barber et al. (2020) found no significant effect on *A. fumigatus* population structure and genetic diversity after the application of fungicides on an agricultural field.

Several molecular methods have been used to genotype *A. fumigatus* strains and populations throughout the years. These methods provide key insight on *A. fumigatus* population structure in many clinics and environments and allow for the monitoring and surveillance of antifungal resistant *A. fumigatus* genotypes. However, some *A. fumigatus* typing methods suffered from one of two main issues for broad population genetic analyses. The first being poor lab to lab reproducibility. These methods included random amplified polymorphic DNA (RAPD) (Loudon et al., 1993), amplified fragment length polymorphism analysis (AFLP) (Warris et al., 2003), restriction fragment length polymorphism analysis (RFLP) (Neuveglise et al., 1996), and minisatellite length polymorphism (MLP) (Bart-Delabesse et al., 1998). The second issue was low discriminatory power at the subspecies levels. These methods included retrotransposon insertion-site context (RISC) typing (de Ruiter et al., 2007) and multilocus sequence typing (MLST) (Bain et al., 2007). The current standard reference method for *A. fumigatus* typing is a panel of nine microsatellite (STR*Af*) loci used in multiplex PCR approaches (de Valk et al., 2005). These loci are highly polymorphic and offer high discriminatory power when differentiating strains and results are far more reproducible between laboratories than the previously listed methods. However, this method is expensive, as it requires trained personal to operate the expensive capillary-based or acrylamide-based electrophoresis platforms (Balajee et al., 2007). The expense and expertise requirements make STR*Af* typing of *A. fumigatus* strains difficult in many clinical laboratories. To combat these issues, cell surface protein A (CSP) sequence typing, based on hypervariable tandem repeats within its exons, which only requires amplification and sequencing of the CSP gene, was developed (Balajee et al., 2007). However, while easily reproducible and available in most lab settings, the discriminatory power of CSP typing is much lower than STR*Af t*yping. Nevertheless, both STR*Af* and CSP have been widely used and are accepted typing techniques in many *A. fumigatus* studies in recent years. Recently, the discriminatory power

of CSP typing was enhanced with the addition of three additional targets for typing, termed TRESPERG, that boasts equal discriminatory power to STR*Af* typing (Garcia-Rubio et al., 2016, 2018). Unfortunately, due to the novelty of TRESPERG, few studies have used this method in their analysis. Given the long history of STR*Af* genotyping, it is still a great option for *A. fumigatus* typing as STR*Af* populations from past studies can be incorporated into modern population genetic analyses. For example, using STR*Af* genotypes and combining genotype data from studies spanning ~ two decades, the global population structure *of A. fumigatus* was found to be highly shaped by gene flow between distant geographic populations (Ashu et al., 2017; Korfanty et al., 2019; Sewell et al., 2019).

With regards to triazole resistance, the global population of *A. fumigatus* is defined into two genetic clusters, with one cluster having a higher abundance of triazole resistant strains and the other containing a higher proportion of triazole susceptible strains (Sewell et al., 2019). Two main factors could have facilitated the spread of *A. fumigatus* genotypes and drug-resistant genes among geographic populations: the high dispersal ability of its asexual spores by wind and contemporary anthropogenic influences such as travel and trade (Kwon-Chung & Sugui, 2013). Additionally, as aspergillosis is one of the leading causes of fungal deaths in avian species, bird migration may also be a factor in *A. fumigatus* dispersal (Cacciuttolo et al., 2009; Melo et al., 2020). Further research into *A. fumigatus* populations from underrepresented niches and geographic locations will aid in the understanding of the global population structure of this species. Results from these efforts will develop better stewardship strategies and aid in the control and management of Aspergillosis outbreaks.

1.5 Thesis Objectives

My PhD thesis focused on understanding and broadening our knowledge on *A. fumigatus* populations. I analyzed *A. fumigatus* strains obtained from many international and domestic soil samples in their genetic and phenotypic variations. My thesis is formatted as a sandwich thesis, consisting of one protocol chapter and four data chapters that provide a comprehensive exploration into these *A. fumigatus* soil populations, with a conclusion chapter that summarizes my findings and provides broader context for my thesis work. Further

information and descriptions regarding the data chapters is found below within chapters two to six. Chapter 2 describes a high throughput protocol to harvest yeasts and *A. fumigatus* from soil. In Chapter 3, I focused on investigating two *A. fumigatus* populations obtained from two arctic regions. In Chapter 4, I investigated *A. fumigatus* populations obtained from soils within 69 sites representing 11 countries on 6 continents and conducted population genetic analysis on these populations on country, continental, and global levels and to their clinical co-populations. In Chapter 5 of my thesis, using a global subset of 60 strains, I investigated the patterns of fertility among geographic and genetically distinct strains. In Chapter 6, I investigated the variation in growth among 89 *A. fumigatus* strains that were obtained from different climate and ecological regions around the world.

1.6 References

Abdolrasouli, A., Petrou, M. A., Park, H., Rhodes, J. L., Rawson, T. M., Moore, L. S. P., Donaldson, H., Holmes, A. H., Fisher, M. C., & Armstrong-James, D. (2018). Surveillance for azole-resistant *Aspergillus fumigatus* in a centralized diagnostic mycology service, London, United Kingdom, 1998–2017. *Frontiers in Microbiology*, *9*(SEP), 2234. https://doi.org/10.3389/fmicb.2018.02234

Ahangarkani, F., Badali, H., Abbasi, K., Nabili, M., Khodavaisy, S., de Groot, T., & Meis, J. F. (2020). Clonal expansion of environmental triazole resistant *Aspergillus fumigatus* in Iran. *Journal of Fungi*, *6*(4), 199. https://doi.org/10.3390/jof6040199

Alanio, A., Dellière, S., Fodil, S., Bretagne, S., & Mégarbane, B. (2020). Prevalence of putative invasive pulmonary aspergillosis in critically ill patients with COVID-19. *The Lancet Respiratory Medicine*, *8*(6), e48–e49. https://doi.org/10.1016/S2213-2600(20)30237-X

Aruanno, M., Glampedakis, E., & Lamoth, F. (2019). Echinocandins for the treatment of invasive aspergillosis: from laboratory to bedside. *Antimicrobial Agents and Chemotherapy*, *63*(8). https://doi.org/10.1128/AAC.00399-19

Ashu, E. E., Hagen, F., Chowdhary, A., Meis, J. F., & Xu, J. (2017). Global population genetic analysis of *Aspergillus fumigatus*. *MSphere*, *2*(1), e00019-17. https://doi.org/10.1128/mSphere.00019-17

Ashu, E. E., Korfanty, G. A., Samarasinghe, H., Pum, N., You, M., Yamamura, D., & Xu, J. (2018). Widespread amphotericin B-resistant strains of *Aspergillus fumigatus* in Hamilton, Canada. *Infection and Drug Resistance*, *11*, 1549–1555. https://doi.org/10.2147/IDR.S170952

Bain, J. M., Tavanti, A., Davidson, A. D., Jacobsen, M. D., Shaw, D., Gow, N. A. R., & Odds, F. C. (2007). Multilocus sequence typing of the pathogenic fungus *Aspergillus fumigatus*. *Journal of Clinical Microbiology*, *45*(5), 1469–1477. https://doi.org/10.1128/JCM.00064-07/

Balajee, S. A., Tay, S. T., Lasker, B. A., Hurst, S. F., & Rooney, A. P. (2007). Characterization of a novel gene for strain typing reveals substructuring of *Aspergillus fumigatus* across North America. *Eukaryotic Cell*, *6*(8), 1392–1399. https://doi.org/10.1128/EC.00164-07

Barber, A. E., Riedel, J., Sae-Ong, T., Kang, K., Brabetz, W., Panagiotou, G., Deising, H. B., & Kurzai, O. (2020). Effects of agricultural fungicide use on *Aspergillus fumigatus* abundance, antifungal susceptibility, and population structure. *MBio*, *11*(6). https://doi.org/10.1128/mbio.02213-20

Bart-Delabesse, E., Humbert, J. F., Delabesse, É., & Bretagne, S. (1998). Microsatellite markers for typing *Aspergillus fumigatus* isolates. *Journal of Clinical Microbiology*, *36*(9), 2413–2418. https://doi.org/10.1128/JCM.36.9.2413-2418.1998

Bhabhra, R., & Askew, D. S. (2005). Thermotolerance and virulence of *Aspergillus fumigatus*: Role of the fungal nucleolus. In *Medical Mycology* (Vol. 43, Issue SUPPL.1, pp. 87–93). Oxford Academic. https://doi.org/10.1080/13693780400029486

Bongomin, F., Gago, S., Oladele, R., & Denning, D. (2017). Global and multi-national prevalence of fungal diseases—Estimate precision. *Journal of Fungi*, *3*(4), 57. https://doi.org/10.3390/jof3040057

Brown, G. D., Denning, D. W., Gow, N. A. R., Levitz, S. M., Netea, M. G., & White, T. C. (2012). Hidden killers: Human fungal infections. *Science Translational Medicine*, *4*(165). https://doi.org/10.1126/scitranslmed.3004404

Buil, J. B., Snelders, E., Denardi, L. B., Melchers, W. J. G., & Verweij, P. E. (2019). Trends in azole resistance in *Aspergillus fumigatus*, the Netherlands, 1994–2016 Jochem.

Emerging Infectious Diseases, *25*(1), 176–178. https://doi.org/10.3201/eid2501.171925

Cacciuttolo, E., Rossi, G., Nardoni, S., Legrottaglie, R., & Mani, P. (2009). Anatomopathological aspects of avian aspergillosis. *Veterinary Research Communications*, *33*(6), 521–527. https://doi.org/10.1007/S11259-008-9199-7

Cairns, T. C., Nai, C., & Meyer, V. (2018). How a fungus shapes biotechnology: 100 years of *Aspergillus niger* research. *Fungal Biology and Biotechnology*, *5*(1), 1–14. https://doi.org/10.1186/S40694-018-0054-5

Chen, M. M., Shi, G. H., Dai, Y., Fang, W. X., & Wu, Q. (2023). Identifying genetic variants associated with amphotericin B (AMB) resistance in *Aspergillus fumigatus* via k-mer-based GWAS. *Frontiers in Genetics*, *14*, 1133593. https://doi.org/10.3389/fgene.2023.1133593

Chowdhary, A., Jain, K., & Chauhan, N. (2023). *Candida auris* genetics and emergence. *Https://Doi.Org/10.1146/Annurev-Micro-032521-015858*, *77*(1), 583–602. https://doi.org/10.1146/annurev-micro-032521-015858

Chowdhary, A., Kathuria, S., Xu, J., & Meis, J. F. (2013). Emergence of azole-resistant *Aspergillus fumigatus* Strains due to agricultural azole use creates an increasing threat to human health. *PLoS Pathogens*, *9*(10). https://doi.org/10.1371/journal.ppat.1003633

Chowdhary, A., Kathuria, S., Xu, J., Sharma, C., Sundar, G., Singh, P. K., Gaur, S. N., Hagen, F., Klaassen, C. H., & Meis, J. F. (2012). Clonal expansion and emergence of environmental multiple-triazole-resistant *Aspergillus fumigatus* strains carrying the TR34/L98H mutations in the *cyp51A* gene in India. *PLoS ONE*, *7*(12), e52871. https://doi.org/10.1371/journal.pone.0052871

Chowdhary, A., Sharma, C., van den Boom, M., Yntema, J. B., Hagen, F., Verweij, P. E., & Meis, J. F. (2014). Multi-azole-resistant *Aspergillus fumigatus* in the environment in Tanzania. *Journal of Antimicrobial Chemotherapy*, *69*(11), 2979–2983. https://doi.org/10.1093/jac/dku259

Dassarma, P., Antunes, A., Simões, M. F., & Dassarma, S. (2020). Earth's stratosphere and microbial life. *Current Issues in Molecular Biology*, *38*, 197–244. https://doi.org/10.21775/cimb.038.197

de Ruiter, M. T., de Valk, H. A., Meis, J. F. G. M., & Klaassen, C. H. W. (2007).

Retrotransposon insertion-site context (RISC) typing: A novel typing method for *Aspergillus fumigatus* and a convenient PCR alternative to restriction fragment length polymorphism analysis. *Journal of Microbiological Methods*, *70*(3), 528–534. https://doi.org/10.1016/J.MIMET.2007.06.009

de Valk, H. A., Meis, J. F. G. M., Curfs, I. M., Muehlethaler, K., Mouton, J. W., & Klaassen, C. H. W. (2005). Use of a novel panel of nine short tandem repeats for exact and high-resolution fingerprinting of *Aspergillus fumigatus* isolates. *Journal of Clinical Microbiology*, *43*(8), 4112–4120. https://doi.org/10.1128/JCM.43.8.4112-4120.2005

Erjavec, Z., Kluin-Nelemans, H., & Verweij, P. E. (2009). Trends in invasive fungal infections, with emphasis on invasive aspergillosis. *Clinical Microbiology and Infection*, *15*(7), 625–633. https://doi.org/10.1111/J.1469-0691.2009.02929.X

Fan, Y., Wang, Y., & Xu, J. (2020). Comparative genome sequence analyses of geographic samples of *Aspergillus fumigatus*—Relevance for amphotericin B resistance. *Microorganisms*, *8*(11), 1673. https://doi.org/10.3390/microorganisms8111673

Fones, H. N., Bebber, D. P., Chaloner, T. M., Kay, W. T., Steinberg, G., & Gurr, S. J. (2020). Threats to global food security from emerging fungal and oomycete crop pathogens. *Nature Food 2020 1:6*, *1*(6), 332–342. https://doi.org/10.1038/s43016-020-0075-0

Fraaije, B., Atkins, S., Hanley, S., Macdonald, A., & Lucas, J. (2020). The Multi-Fungicide Resistance Status of *Aspergillus fumigatus* populations in arable soils and the wider European environment. *Frontiers in Microbiology*, *11*, 3199. https://doi.org/10.3389/fmicb.2020.599233

Frisvad, J. C., & Larsen, T. O. (2016). Extrolites of *Aspergillus fumigatus* and other pathogenic species in *aspergillus* section *fumigati*. *Frontiers in Microbiology*, *6*(JAN), 1485. https://doi.org/10.3389/fmicb.2015.01485

Garcia-Rubio, R., Escribano, P., Gomez, A., Guinea, J., & Mellado, E. (2018). Comparison of two highly discriminatory typing methods to analyze *Aspergillus fumigatus* azole resistance. *Frontiers in Microbiology*, *9*(JUL), 399560. https://doi.org/10.3389/fmicb.2018.01626

Garcia-Rubio, R., Gil, H., Monteiro, M. C., Pelaez, T., & Mellado, E. (2016). A new *Aspergillus fumigatus* typing method based on hypervariable tandem repeats located

within exons of surface protein coding genes (TRESP). *PLOS ONE*, *11*(10), e0163869. https://doi.org/10.1371/journal.pone.0163869

Hawksworth, D. L., & Lücking, R. (2017). Fungal diversity revisited: 2.2 to 3.8 million species. *Microbiology Spectrum*, *5*(4). https://doi.org/10.1128

Heo, S. T., Tatara, A. M., Jiménez-Ortigosa, C., Jiang, Y., Lewis, R. E., Tarrand, J., Tverdek, F., Albert, N. D., Verweij, P. E., Meis, J. F., Mikos, A. G., Perlin, D. S., & Kontoyiannis, D. P. (2017). Changes in in vitro ausceptibility patterns of *Aspergillus* to triazoles and correlation with aspergillosis outcome in a tertiary care cancer center, 1999–2015. *Clinical Infectious Diseases*, *65*(2), 216–225. https://doi.org/10.1093/cid/cix297

Janssen, N. A. F., Nyga, R., Vanderbeke, L., Jacobs, C., Ergün, M., Buil, J. B., Van Dijk, K., Altenburg, J., Bouman, C. S. C., Van der Spoel, H. I., Rijnders, B. J. A., Dunbar, A., Schouten, J. A., Lagrou, K., Bourgeois, M., Reynders, M., Van Regenmortel, N., Rutsaert, L., Lormans, P., … Verweij, P. E. (2021). Multinational observational cohort study of COVID-19–associated pulmonary aspergillosis. *Emerging Infectious Diseases*, *27*(11), 2892. https://doi.org/10.3201/EID2711.211174

Jeanvoine, A., Rocchi, S., Reboux, G., Crini, N., Crini, G., & Millon, L. (2017). Azole-resistant *Aspergillus fumigatus* in sawmills of eastern France. *Journal of Applied Microbiology*, *123*(1), 172–184. https://doi.org/10.1111/jam.13488

Jiménez-Ortigosa, C., Moore, C., Denning, D. W., & Perlin, D. S. (2017). Emergence of echinocandin resistance due to a point mutation in the *fks1* Gene of *Aspergillus fumigatus* in a patient with chronic pulmonary aspergillosis. *Antimicrobial Agents and Chemotherapy*, *61*(12), e01277-17. https://doi.org/10.1128/AAC.01277-17

Khaliq, A., Perveen, S., Alamer, K. H., Ul Haq, M. Z., Rafique, Z., Alsudays, I. M., Althobaiti, A. T., Saleh, M. A., Hussain, S., & Attia, H. (2022). Arbuscular mycorrhizal fungi symbiosis to enhance plant–soil interaction. *Sustainability 2022, Vol. 14, Page 7840*, *14*(13), 7840. https://doi.org/10.3390/SU14137840

Knox, B. P., Blachowicz, A., Palmer, J. M., Romsdahl, J., Huttenlocher, A., Wang, C. C. C., Keller, N. P., & Venkateswaran, K. (2016). Characterization of *Aspergillus fumigatus* isolates from air and surfaces of the International Space Station. *MSphere*, *1*(5), e00227-16. https://doi.org/10.1128/msphere.00227-16

Korfanty, G. A., Teng, L., Pum, N., & Xu, J. (2019). Contemporary gene flow is a major force shaping the *Aspergillus fumigatus* population in Auckland, New Zealand. *Mycopathologia*, *184*(4), 479–492. https://doi.org/10.1007/s11046-019-00361-8

Kwon-Chung, K. J., & Sugui, J. A. (2013). *Aspergillus fumigatus*--what makes the species a ubiquitous human fungal pathogen? *PLoS Pathogens*, *9*(12), e1003743. https://doi.org/10.1371/journal.ppat.1003743

Latgé, J. P., & Chamilos, G. (2020). *Aspergillus fumigatus* and aspergillosis in 2019. *Clinical Microbiology Reviews*, *33*(1). https://doi.org/10.1128/CMR.00140-18

Lestrade, P. P. A., Buil, J. B., Van Der Beek, M. T., Kuijper, E. J., Dijk, K. Van, Kampinga, G. A., Rijnders, B. J. A., Vonk, A. G., De Greeff, S. C., Schoffelen, A. F., Dissel, J. Van, Meis, J. F., Melchers, W. J. G., & Verweij, P. E. (2020). Paradoxal trends in azole-resistant *Aspergillus fumigatus* in a national multicenter surveillance program, the Netherlands, 2013-2018. In *Emerging Infectious Diseases* (Vol. 26, Issue 7, pp. 1447–1455). Centers for Disease Control and Prevention (CDC). https://doi.org/10.3201/eid2607.200088

Lionakis, M. S., Drummond, R. A., & Hohl, T. M. (2023). Immune responses to human fungal pathogens and therapeutic prospects. *Nature Reviews Immunology 2023 23:7*, *23*(7), 433–452. https://doi.org/10.1038/s41577-022-00826-w

Loudon, K. W., Burnie, J. P., Coke, A. P., & Matthews, R. C. (1993). Application of polymerase chain reaction to fingerprinting *Aspergillus fumigatus* by random amplification of polymorphic DNA. *Journal of Clinical Microbiology*, *31*(5), 1117–1121. https://doi.org/10.1128/jcm.31.5.1117-1121.1993

MacEdo, D., Devoto, T. B., Pola, S., Finquelievich, J. L., Cuesta, M. L., & Garcia-Effron, G. (2020). A novel combination of CYP51A mutations confers pan-azole resistance in *Aspergillus fumigatus*. *Antimicrobial Agents and Chemotherapy*, *64*(8). https://doi.org/10.1128/aac.02501-19

Machado, M., Valerio, M., Álvarez-Uría, A., Olmedo, M., Veintimilla, C., Padilla, B., De la Villa, S., Guinea, J., Escribano, P., Ruiz-Serrano, M. J., Reigadas, E., Alonso, R., Guerrero, J. E., Hortal, J., Bouza, E., Muñoz, P., Alcalá, L., Aldámiz, T., Álvarez, B., … Vicente, T. (2021). Invasive pulmonary aspergillosis in the COVID-19 era: An

expected new entity. *Mycoses*, *64*(2), 132–143. https://doi.org/10.1111/MYC.13213

Mapook, A., Hyde, K. D., Hassan, K., Kemkuignou, B. M., Čmoková, A., Surup, F., Kuhnert, E., Paomephan, P., Cheng, T., de Hoog, S., Song, Y., Jayawardena, R. S., Al-Hatmi, A. M. S., Mahmoudi, T., Ponts, N., Studt-Reinhold, L., Richard-Forget, F., Chethana, K. W. T., Harishchandra, D. L., … Stadler, M. (2022). Ten decadal advances in fungal biology leading towards human well-being. *Fungal Diversity 2022 116:1*, *116*(1), 547–614. https://doi.org/10.1007/S13225-022-00510-3

McGovern, P. E., Zhang, J., Tang, J., Zhang, Z., Hall, G. R., Moreau, R. A., Nuñez, A., Butrym, E. D., Richards, M. P., Wang, C. S., Cheng, G., Zhao, Z., & Wang, C. (2004). Fermented beverages of pre- and proto-historic China. *Proceedings of the National Academy of Sciences of the United States of America*, *101*(51), 17593–17598. https://doi.org/10.1073/PNAS.0407921102

Melo, A. M., Stevens, D. A., Tell, L. A., Veríssimo, C., Sabino, R., & Xavier, M. O. (2020). Aspergillosis, Avian Species and the One Health Perspective: The Possible Importance of Birds in Azole Resistance. *Microorganisms*, *8*(12), 1–22. https://doi.org/10.3390/microorganisms8122037

Meyer, V., Basenko, E. Y., Benz, J. P., Braus, G. H., Caddick, M. X., Csukai, M., De Vries, R. P., Endy, D., Frisvad, J. C., Gunde-Cimerman, N., Haarmann, T., Hadar, Y., Hansen, K., Johnson, R. I., Keller, N. P., Kraševec, N., Mortensen, U. H., Perez, R., Ram, A. F. J., … Wösten, H. A. B. (2020). Growing a circular economy with fungal biotechnology: a white paper. *Fungal Biology and Biotechnology 2020 7:1*, *7*(1), 1–23. https://doi.org/10.1186/S40694-020-00095-Z

Moodley, L., Pillay, J., & Dheda, K. (2014). Aspergilloma and the surgeon. *Journal of Thoracic Disease*, *6*(3), 202. https://doi.org/10.3978/J.ISSN.2072-1439.2013.12.40

Neuveglise, C., Sarfati, J., Latge, J. P., & Paris, S. (1996). Afut 1, a retrotransposon-like element from *Aspergillus fumigatus*. *Nucleic Acids Research*, *24*(8), 1428–1434. https://doi.org/10.1093/nar/24.8.1428

Peláez-García de la Rasilla, T., González-Jiménez, I., Fernández-Arroyo, A., Roldán, A., Carretero-Ares, J. L., García-Clemente, M., Telenti-Asensio, M., García-Prieto, E., Martínez-Suarez, M., Vázquez-Valdés, F., Melón-García, S., Caminal-Montero, L.,

Fernández-Simón, I., Mellado, E., & Sánchez-Núñez, M. L. (2022). COVID-19 Associated Pulmonary Aspergillosis (CAPA): hospital or home environment as a source of life-threatening *Aspergillus fumigatus* infection? *Journal of Fungi 2022, Vol. 8, Page 316*, *8*(3), 316. https://doi.org/10.3390/jof8030316

Prattes, J., Wauters, J., Giacobbe, D. R., Salmanton-García, J., Maertens, J., Bourgeois, M., Reynders, M., Rutsaert, L., Van Regenmortel, N., Lormans, P., Feys, S., Reisinger, A. C., Cornely, O. A., Lahmer, T., Valerio, M., Delhaes, L., Jabeen, K., Steinmann, J., Chamula, M., … Muñoz, P. (2022). Risk factors and outcome of pulmonary aspergillosis in critically ill coronavirus disease 2019 patients—a multinational observational study by the European Confederation of Medical Mycology. *Clinical Microbiology and Infection*, *28*(4), 580–587. https://doi.org/10.1016/j.cmi.2021.08.014

Rayens, E., & Norris, K. A. (2022). Prevalence and healthcare burden of fungal infections in the United States, 2018. *Open Forum Infectious Diseases*, *9*(1). https://doi.org/10.1093/ofid/ofab593

Rodriguez-Tudela, J. L., Alcazar-Fuoli, L., Mellado, E., Alastruey-Izquierdo, A., Monzon, A., & Cuenca-Estrella, M. (2008). Epidemiological cutoffs and cross-resistance to azole drugs in *Aspergillus fumigatus*. *Antimicrobial Agents and Chemotherapy*, *52*(7), 2468–2472. https://doi.org/10.1128/AAC.00156-08

Rokas, A., Mead, M. E., Steenwyk, J. L., Oberlies, N. H., & Goldman, G. H. (2020). Evolving moldy murderers: *Aspergillus* section *Fumigati* as a model for studying the repeated evolution of fungal pathogenicity. *PLOS Pathogens*, *16*(2), e1008315. https://doi.org/10.1371/journal.ppat.1008315

Rybak, J. M., Fortwendel, J. R., & Rogers, P. D. (2019). Emerging threat of triazole-resistant *Aspergillus fumigatus*. *Journal of Antimicrobial Chemotherapy*, *74*(4), 835–842. https://doi.org/10.1093/jac/dky517

Samson, R. A., Visagie, C. M., Houbraken, J., Hong, S. B., Hubka, V., Klaassen, C. H. W., Perrone, G., Seifert, K. A., Susca, A., Tanney, J. B., Varga, J., Kocsubé, S., Szigeti, G., Yaguchi, T., & Frisvad, J. C. (2014). Phylogeny, identification and nomenclature of the genus *Aspergillus*. *Studies in Mycology*, *78*(1), 141–173. https://doi.org/10.1016/j.simyco.2014.07.004

Schoustra, S. E., Debets, A. J. M., Rijs, A. J. M. M., Zhang, J., Snelders, E., Leendertse, P. C., Melchers, W. J. G., Rietveld, A. G., Zwaan, B. J., & Verweij, P. E. (2019). Environmental hotspots for azole resistance selection of *Aspergillus fumigatus*, the netherlands. *Emerging Infectious Diseases*, *25*(7), 1347–1353. https://doi.org/10.3201/eid2507.181625

Segrelles-Calvo, G., Araújo, G. R. S., Llopis-Pastor, E., Carrillo, J., Hernández-Hernández, M., Rey, L., Rodríguez Melean, N., Escribano, I., Antón, E., Zamarro, C., García-Salmones, M., & Frases, S. (2021). Prevalence of opportunistic invasive aspergillosis in COVID-19 patients with severe pneumonia. *Mycoses*, *64*(2), 144–151. https://doi.org/10.1111/MYC.13219

Sewell, T. R., Zhu, J., Rhodes, J., Hagen, F., Meis, J. F., Fisher, M. C., & Jombart, T. (2019). Nonrandom distribution of azole resistance across the global population of *Aspergillus fumigatus*. *MBio*, *10*(3), e00392-19. https://doi.org/10.1128/mBio.00392-19

Shelton, J. M. G., Collins, R., Uzzell, C. B., Alghamdi, A., Dyer, P. S., Singer, A. C., & Fisher, M. C. (2022). Citizen science surveillance of triazole-resistant *Aspergillus fumigatus* in united kingdom residential garden soils. *Applied and Environmental Microbiology*, *88*(4). https://doi.org/10.1128/aem.02061-21

Siopi, M., Rivero-Menendez, O., Gkotsis, G., Panara, A., Thomaidis, N. S., Alastruey-Izquierdo, A., Pournaras, S., & Meletiadis, J. (2020). Nationwide surveillance of azole-resistant *Aspergillus fumigatus* environmental isolates in Greece: detection of pan-azole resistance associated with the TR46/Y121F/T289A cyp51A mutation. *Journal of Antimicrobial Chemotherapy*, *75*(11), 3181–3188. https://doi.org/10.1093/jac/dkaa316

Snelders, E., Huis In 't Veld, R. A. G., Rijs, A. J. M. M., Kema, G. H. J., Melchers, W. J. G., & Verweij, P. E. (2009). Possible environmental origin of resistance of *Aspergillus fumigatus* to medical triazoles. *KorApplied and Environmental Microbiology*, *75*(12), 4053–4057. https://doi.org/10.1128/aem.00231-09

Stone, N. R. H., Bicanic, T., Salim, R., & Hope, W. (2016). Liposomal Amphotericin B (AmBisome®): A review of the pharmacokinetics, pharmacodynamics, clinical experience and future directions. *Drugs*, *76*(4), 485–500. https://doi.org/10.1007/s40265-016-0538-7

Verweij, P. E., Brüggemann, R. J. M., Azoulay, E., Bassetti, M., Blot, S., Buil, J. B., Calandra, T., Chiller, T., Clancy, C. J., Cornely, O. A., Depuydt, P., Koehler, P., Lagrou, K., de Lange, D., Lass-Flörl, C., Lewis, R. E., Lortholary, O., Liu, P. W. L., Maertens, J., … Martin-Loeches, I. (2021). Taskforce report on the diagnosis and clinical management of COVID-19 associated pulmonary aspergillosis. *Intensive Care Medicine*, *47*(8), 819. https://doi.org/10.1007/S00134-021-06449-4

Verweij, P. E., Chowdhary, A., Melchers, W. J. G., & Meis, J. F. (2016). Azole resistance in *Aspergillus fumigatus*: Can we retain the clinical use of mold-active antifungal azoles? *Clinical Infectious Diseases*, *62*(3), 362–368. https://doi.org/10.1093/cid/civ885

Verweij, P. E., Rijnders, B. J. A., Brüggemann, R. J. M., Azoulay, E., Bassetti, M., Blot, S., Calandra, T., Clancy, C. J., Cornely, O. A., Chiller, T., Depuydt, P., Giacobbe, D. R., Janssen, N. A. F., Kullberg, B. J., Lagrou, K., Lass-Flörl, C., Lewis, R. E., Liu, P. W. L., Lortholary, O., … van de Veerdonk, F. L. (2020). Review of influenza-associated pulmonary aspergillosis in ICU patients and proposal for a case definition: an expert opinion. *Intensive Care Medicine*, *46*(8), 1524–1535. https://doi.org/10.1007/S00134-020-06091-6

Verweij, P. E., Snelders, E., Kema, G. H., Mellado, E., & Melchers, W. J. (2009). Azole resistance in *Aspergillus fumigatus*: a side-effect of environmental fungicide use? *The Lancet Infectious Diseases*, *9*(12), 789–795. https://doi.org/10.1016/S1473-3099(09)70265-8

Verweij, P. E., Zhang, J., Debets, A. J. M., Meis, J. F., van de Veerdonk, F. L., Schoustra, S. E., Zwaan, B. J., & Melchers, W. J. G. (2016). In-host adaptation and acquired triazole resistance in *Aspergillus fumigatus*: a dilemma for clinical management. In *The Lancet Infectious Diseases* (Vol. 16, Issue 11, pp. e251–e260). Lancet Publishing Group. https://doi.org/10.1016/S1473-3099(16)30138-4

Warris, A., Klaassen, C. H. W., Meis, J. F. G. M., De Ruiter, M. T., De Valk, H. A., Abrahamsen, T. G., Gaustad, P., & Verweij, P. E. (2003). Molecular epidemiology of *Aspergillus fumigatus* isolates recovered from water, air, and patients shows two clusters of genetically distinct strains. *Journal of Clinical Microbiology*, *41*(9), 4101–4106. https://doi.org/10.1128/JCM.41.9.4101-4106.2003

WorldHealthOrganization. (2022). *WHO fungal priority pathogens list to guide research, development and public health action*. World Health Organization. https://www.who.int/publications/i/item/9789240060241

Wu, C. J., Liu, W. L., Lai, C. C., Chao, C. M., Ko, W. C., Wang, H. C., Dai, C. T., Hsieh, M. I., Choi, P. C., Yang, J. L., & Chen, Y. C. (2020). Multicenter study of azole-resistant *Aspergillus fumigatus* clinical isolates, Taiwan. *Emerging Infectious Diseases*, *26*(4), 806–809. https://doi.org/10.3201/eid2604.190840

Xu, J. (2022). Assessing global fungal threats to humans. *MLife*, *1*(3), 223–240. https://doi.org/10.1002/MLF2.12036

Chapter 2

Isolation of Culturable Yeasts and Molds from Soils to Investigate Fungal Population Structure

Summary This protocol is an effective, speedy method of culturing yeasts and the mold *Aspergillus fumigatus* from large sets of soil samples in as little as 7 days. The methods can be easily modified to accommodate a range of incubation media and temperatures as needed for experiments.

Abstract Soil is host to an incredible amount of microbial life, with each gram containing up to billions of bacterial, archaeal, and fungal cells. Multicellular fungi such as molds and unicellular fungi, broadly defined as yeasts, fulfill essential roles in soil ecosystems as decomposers of organic material and as food sources for other soil dwellers. Fungal species diversity in soil is dependent on a multitude of climatic factors such as rainfall and temperature, as well as soil properties including organic matter, pH, and moisture. Lack of adequate environmental sampling, especially in regions of Asia, Africa, South America, and Central America, hinders the characterization of soil fungal communities and the discovery of novel species.

We characterized soil fungal communities in nine countries across six continents using ~4,000 soil samples and a protocol developed in the laboratory for the isolation of yeasts and molds. This protocol begins with separate selective enrichment for yeasts and the medically relevant mold *Aspergillus fumigatus*, in liquid media while inhibiting bacterial growth. Resulting colonies are then transferred to solid media and further processed to obtain pure cultures, followed by downstream genetic characterization. Yeast species identity is established via sequencing of their internal transcribed spacer (ITS) region of the nuclear ribosomal RNA gene cluster, while global population structure of *A. fumigatus* is explored via microsatellite marker analysis.

The protocol was successfully applied to isolate and characterize soil yeast and *A. fumigatus* populations in Cameroon, Canada, China, Costa Rica, Iceland, Peru, New Zealand, and Saudi Arabia. These findings revealed much-needed insights on global patterns in soil yeast diversity, as well as global population structure and antifungal resistance profiles of *A. fumigatus*. This paper presents the method of isolating both yeasts and *A. fumigatus* from international soil samples.

For the study in this chapter, I created the *A. fumigatus* isolation protocol. I am a co-first author of the following publication reprinted for this chapter:

Samarasinghe, H., Korfanty, G., & Xu, J. (2022). Isolation of Culturable Yeasts and Molds from Soils to Investigate Fungal Population Structure. *JoVE (Journal of Visualized Experiments)*, *2022*(183), e63396. https://doi.org/10.3791/63396

2.1 Introduction

Fungi in soil ecosystems play essential roles in organic matter decomposition, nutrient cycling, and soil fertilization (Frac et al., 2018). Both culture-independent (i.e., high-throughput sequencing) and culture-dependent approaches are widely used in the study of soil fungi (Egidi et al., 2019; Tedersoo et al., 2014). While the large amount of data generated by high-throughput meta-barcode sequencing is useful for elucidating broad-scale patterns in community structure and diversity, the culture-dependent approach can provide highly complementary information on the taxonomic and functional structures of fungal communities, as well as more specific profiles of individual organisms through downstream diversity and functional analyses due to the availability of pure fungal cultures.

Despite rarely exceeding thousands of cells per gram of soil, yeasts, broadly defined as unicellular fungi, are essential decomposers and food sources for other soil dwellers (Botha, 2011; Andrey M. Yurkov, 2018). In fact, yeasts may be the predominant soil fungi in cold biospheres such as continental Antarctica (Connell et al., 2008; Vishniac, 2006). Soil is also a primary reservoir of medically relevant yeasts that cause serious opportunistic infections in

humans and other mammals (Kurtzman et al., 2011). Despite morphological similarities, yeast species are phylogenetically diverse and occur among filamentous fungi in two major phyla, Ascomycota and Basidiomycota, within the fungal kingdom (Samarasinghe et al., 2021). Yeasts lack a defining DNA signature at the fungal barcoding gene, the internal transcribed spacer (ITS) region of the nuclear ribosomal RNA gene cluster (Xu, 2016), making them indistinguishable from other fungi in metagenomics investigations and thus necessitating the use of culture-dependent methods to isolate yeast species.

The protocol below was implemented to characterize soil yeast communities of nine countries and identify global trends and patterns in soil yeast diversity (Aljohani et al., 2018; Samarasinghe et al., 2019, 2021). Metagenomics approaches are of limited use when studying targeted groups of organisms such as yeasts (Egidi et al., 2019; Tedersoo et al., 2014). Due to their phylogenetic diversity, yeasts cannot be distinguished from other fungi based on DNA sequence alone. Thus, studying yeast populations requires the continued use of culture-dependent isolation. However, culturing is often significantly more time consuming and requires more personnel to perform the experiments. Therefore, the protocol has been optimized and streamlined for faster processing with limited personnel. The main advantage of culturing is that the yeast species identified are living yeasts and not dead ones, and thus are more likely to be true soil dwellers rather than transient cells present in the soils. It has been estimated that approximately 40% of fungal DNA in soil are either contaminants from other environments, extracellular, or come from cells that are no longer intact, causing high-throughput sequencing approaches to overestimate fungal richness by as much as 55% (Carini et al., 2016). Culture-dependent isolation can readily confirm yeast species identity with the added benefit of securing pure culture to be used in downstream analyses. Indeed, pure cultures of 44 putative new yeast species were identified using this soil isolation protocol that allowed the use of a range of methods to study their taxonomic and functional properties in detail (Xu, 2020).

The protocol below can also be used to isolate molds present within soil, such as *A. fumigatus*. *Aspergillus fumigatus* is a thermophilic and saprophytic mold with a wide, global distribution

in soil (Brakhage & Langfelder, 2002). It has been isolated from numerous clinical and non-clinical environments. Non-clinical sampling commonly includes air, organic debris (compost, saw dust, tulip bulb waste), and soil (agricultural, garden, and natural soils) (Alcazar-Fuoli et al., 2008; Bongomin et al., 2017; Chowdhary et al., 2012; Rocchi et al., 2021). *Aspergillus fumigatus* is a human opportunistic pathogen causing a range of infections collectively termed aspergillosis, affecting over 8 million people worldwide (Bongomin et al., 2017; Kwon-Chung & Sugui, 2013). Approximately 300,000 people around the globe suffer from invasive aspergillosis, which is the most severe form of aspergillosis (Bongomin et al., 2017). Depending on factors such as the patient population, site of infection, and efficacy of antifungal therapy, mortality rate can be as high as 90%. Over the past several decades, resistance to antifungal therapies has increased, requiring global surveillance efforts in both clinical and environmental populations to track these resistance genotypes (Eta Ebasi Ashu et al., 2017; Heo et al., 2017; Sewell et al., 2019). Given its ability to grow at temperatures upward of 50 °C, this temperature can be exploited to select for *A. fumigatus* isolates from soil using culture-dependent methods. *Aspergillus fumigatus* isolates are commonly genotyped at nine highly polymorphic short tandem repeat (STR) loci, shown to have high discriminatory power between strains (de Valk et al., 2005). These STR genotypes can be compared to other previously surveyed populations to track the spread of *A. fumigatus* genotypes, including drug resistance genes, around the world.

Below we describe a protocol for the speedy isolation of yeasts and *A. fumigatus* from soil samples in a culture dependent manner. Depending on the amount of soil obtained per sample, the soil samples can be shared between the two protocols. In comparison to similar methods that isolate yeast and *A. fumigatus* from soil, this protocol uses 10x less soil per isolate obtained. Studies attempting to isolate *A. fumigatus* from soil require between 1 and 2 g of soil per isolate, whereas this protocol requires only 0.1-0.2 g of soil (Chowdhary et al., 2012; Rocchi et al., 2021; A. M. Yurkov et al., 2012). This protocol utilizes smaller plastics and containers that facilitate its high-throughput design. Therefore, a larger number of samples can be processed using less space for equipment such as incubators and roller drums.

Soil samples can be fully processed to obtain isolates in as little as 7 days. This protocol has been optimized to allow processing of up to 150-200 samples per day per person.

2.2 Protocol

NOTE: Any steps utilizing international soil samples and/or *A. fumigatus* spores and mycelia require working within a biosafety cabinet for level 2 organisms (BSCII).

2.2.1 Isolation of yeast from soil

2.2.1.1 Preparation of antibacterial and antifungal solutions

1. Suspend chloramphenicol powder in 70% ethanol to prepare a 50 g/L stock solution. Sterilize by syringe filtration and store at 4 °C.

   NOTE: This antibiotic will prevent the growth of most bacteria during soil yeast isolation. As chloramphenicol-resistant bacteria may still grow, colony morphology must be carefully taken into consideration when distinguishing yeasts from bacteria. Additional antibiotics may be added to media when working with soil suspected of containing antibiotic-resistant bacterial strains. Bacterial contamination in chloramphenicol supplemented media was not an issue encountered when isolating yeasts from environmental soils.
2. Suspend benomyl powder in DMSO to prepare a 5 g/L stock solution. Sterilize by syringe filtration and store at 4 °C.

   NOTE: This selective antifungal drug prevents the growth of most filamentous fungi without affecting yeast growth during soil yeast isolation (Calhelha et al., 2006; Thomas et al., 1985).

2.2.1.2 Preparation of culture media and sterile equipment

1. To prepare YEPD (Yeast Extract-Peptone-Dextrose) broth, add 10 g of Yeast Extract, 20 g of peptone, and 20 g of dextrose to 1 L of double distilled water. Stir until well-mixed and autoclave for 40 min at 121 °C. Store at room temperature until use.
2. YEPD solid agar medium

1. Mix 10 g of yeast extract, 20 g of peptone, 20 g of dextrose, and 20 g of agar in 1 L of water. Stir well to mix and autoclave for 40 min at 121 °C.
2. Once sufficiently cooled, add 1 mL of chloramphenicol and benomyl from stock solutions to bring the final concentrations of the two antimicrobials to 50 mg/L and 5 mg/L, respectively.
3. Mix well by stirring and pour into 10 cm diameter Petri dishes. Leave at room temperature overnight to set and store at 4 °C until use.
   NOTE: From 1 L of YEPD, approximately 80 plates can be poured.

3. Sterilize wooden plain-tipped applicator sticks and reusable cell spreaders by autoclaving and store at room temperature.

2.2.1.3 Incubation of soil in liquid broth

1. Prepare a set of sterile 13 mL culture tubes by labeling them with soil sample ID.
2. Using a serological pipette, add 5 mL of YEPD broth supplemented with chloramphenicol and benomyl into each tube.
3. Working in a BSCII, transfer ~0.1 g of soil into the appropriate culture tube using a sterile, wooden plain-tipped applicator.
   NOTE: Use a fresh applicator for each soil sample and discard immediately upon use to avoid cross-contamination between samples.
4. Cap the tube securely to the first stop to prevent spillage but still allow air exchange during incubation. Incubate the culture tubes in a roller drum for 24 h at a temperature deemed optimum for maximizing yeast growth.
   NOTE: The incubation temperature should be decided based on the mean annual temperature of the soil samples' country of origin. For example, when isolating soil yeasts from Iceland, the culture tubes were incubated at 14 °C, whereas soils from Saudi Arabia were incubated at 30 °C. Due to slower yeast growth at lower temperatures, incubation time might have to be extended for up to 72 h.

2.2.1.4 Transfer the supernatant to the solid medium

1. Using the set of YEPD + chloramphenicol + benomyl agar plates prepared in Step 2.2.1.2, label them with the soil sample ID.
2. Remove the culture tubes prepared in Step 2.2.1.3 from the roller drum. Working in a BSCII, briefly vortex the tube to draw soil particles and cells that may have settled at the bottom back into suspension.
3. Using a micropipette, transfer 100 µL of the supernatant onto a plate. Use a sterile, reusable cell spreader to spread the liquid thoroughly and evenly over the agar surface.

   NOTE: Working in sets of 10 samples can significantly speed up this process. Pipette the supernatant onto 10 plates first and then perform spreading. Use a fresh spreader for each sample to avoid cross-contamination between samples.
4. Stack the plates in plastic bags, seal, and incubate upside down for 2-3 days at the same temperature used previously for liquid broth incubation until microbial growth is visible.

2.2.1.5 Detection of yeasts and streaking for single colonies

1. After allowing for sufficient incubation time (typically 2-3 days, but may take longer at lower temperatures), inspect the plates in a BSCII for any yeast growth. Look for creamy, round, matte-like yeasts that are easily distinguished from bacterial and mold colonies.

   NOTE: Some yeasts produce colored pigments and may appear black/brown, yellow, or red, but their overall colony texture and shape would be similar to non-pigmented yeasts
2. Select one yeast-like colony from each plate for further processing.

   NOTE: If more than one type of morphology is observed on a single plate, select one representative colony for each morphological type.
3. Using sterile, wooden plain-tipped applicator sticks, transfer each selected colony onto a fresh YEPD + chloramphenicol + benomyl plate and streak for single colonies. Perform three separate streaks.

Streak back and forth over a third of the plate using an applicator stick. Begin the second and third streak by streaking the applicator across the preceding streak once. Use a new applicator stick for every streak.

NOTE: Use one plate per isolate. Discard applicators immediately upon use to avoid cross-contamination between samples.

4. Stack the plates in plastic bags, seal, and incubate upside down for 2-3 days at the same temperature used previously until single colonies become visible.

2.2.1.6 Identification of yeast species via ITS sequencing

1. Select a well-separated, single colony per soil isolate and subculture onto a fresh YEPD + chloramphenicol + benomyl plate to obtain more cells. Incubate for 2-3 days at the same temperature used previously.
2. Harvest the freshly grown cells and suspend them in -80 °C freezer tubes containing 1 mL of sterilized 30% glycerol in double-distilled water to create cell suspensions. Maintain these suspensions at -80 °C as stock solutions.
3. Use fresh cells to perform colony PCR (polymerase chain reaction) with primers ITS1 (5' TCCGTAGGTGAACCTGCGG 3') and ITS4 (5' TCCTCCGCTTATTGATATGC 3') to amplify the fungal barcoding gene, ITS9. Use the following thermocycling conditions: an initial denaturation step at 95 °C for 10 min followed by 35 cycles of (i) 95 °C for 30 s, (ii) 55 °C for 30 s, and (iii) 72 °C for 1 min.

   NOTE: Colony PCR has a high success rate and a faster turnaround time than DNA extraction followed by PCR
4. If colony PCR repeatedly fails for a strain, extract DNA using the protocol of choice and perform ITS PCR using extracted genomic DNA as template (use same thermocycling conditions as above).

   NOTE: A relatively inexpensive chloroform-based DNA extraction is recommended (Xu et al., 2000).
5. Perform Sanger sequencing to determine the DNA sequence of the amplified ITS region for each strain.

6. Compare the obtained ITS sequence of the yeast strains to sequences deposited in public databases such as NCBI GenBank and UNITE to establish species identity.

2.2.2 Isolation of *Aspergillus fumigatus* from soil

2.2.2.1 Prepare 1 mL of sterile Sabouraud dextrose broth (SDB) supplemented with the antibiotic chloramphenicol per soil sample.

1. Add 10 g of peptone and 20 g of dextrose to 1 L of distilled water. Autoclave at 121 °C for 40 min.
2. Allow the SDB to cool to ~50 °C, add 1 mL of 50 g/ L chloramphenicol to bring the concentration to 50 mg/L.

   NOTE: Chloramphenicol is prepared the same as described above for yeast isolation. Aside from inhibiting bacterial growth, chloramphenicol also prevents the production of gas from bacteria that will cause the tubes to open during the incubation step detailed in Step 2.2.2.2.
3. Aseptically aliquot 1 mL of SDB into a 1.5 mL microcentrifuge tube per soil sample using a mechanical pipette.

2.2.2.2 Add soil to 1.5 mL microcentrifuge tubes.

1. Lay bench coat or absorbent padding inside a BSCII to aid in the disposal of spilt soil.
2. Using autoclaved applicator sticks, transfer approximately 0.1 g of soil into a 1.5 mL microcentrifuge tube containing 1 mL of SBD. Close the tube and vortex. Incubate the suspended soil at 50 °C for 3 days.

   NOTE: Shaking during incubation is not required.

2.2.2.3 Mycelial harvest of soil-inoculated broth

1. Prepare malt extract agar (MEA) plates.
    1. Per liter of MEA: add 20 g of malt extract, 20 g of dextrose, 6 g of peptone, and 15 g of agar to 1 L of distilled water. Autoclave at 121 °C for 40 min.

2. Allow the MEA to cool to ~50 °C, then add 1 mL of 50 g/L chloramphenicol to bring to a final concentration of 50 mg/L.

2. Transfer the mycelia from the soil-inoculated broth onto MEA plates.
    1. Identify soil inoculums that have visible mycelial growth at the SDB to air boundary.
    2. Use sterilized wooden plain-tipped applicator sticks to transfer the mycelia to the center of a MEA plate. Incubate the MEA plates at 37 °C for 3 days.

2.2.2.4 Selection of mycelia with *A. fumigatus* morphological properties.

1. Identify mold colonies that have characteristic *A. fumigatus* morphological properties (green suede like growth).
2. Working in a BSCII, use sterilized wooden plain tipped applicator sticks or an inoculation loop to harvest conidia/mycelia by scraping the surface once. Transfer the spores/mycelia to the center of a MEA plate by streaking onto the agar for single colonies. Incubate at 37 °C for 2 days.

   NOTE: As multiple *A. fumigatus* strains and/or other fungi may be present on the plate, it is important to streak for single colonies. The single-colony streaking protocol in Step 2.2.1.5 in the yeast isolation protocol can be used.
3. After incubation, using a sterile applicator stick or inoculation loop, subculture a single colony generated onto MEA by streaking the colony once. Spread the harvested spores into the center of the plate. Incubate at 37 °C for 2 days.

2.2.2.5 Harvesting of *A. fumigatus* spores/mycelia for culture storage

1. Prepare a sterile 30% glycerol solution (for a 100 mL solution, add 30 mL of 100% glycerol mixed with 70 mL of double-distilled water, sterilized at 121 °C for 40 min).
2. Working in a BSCII, use a p1000 pipette to aspirate 1 mL of the 30% glycerol solution. Dispense the 1 mL of glycerol solution onto the *A. fumigatus* colony to harvest spores/mycelia.
    1. Due to the hydrophobicity *of A. fumigatus* spores/mycelia, use the pipette tip to scratch a densely sporulated region of the plate.

NOTE: When glycerol is dispensed in the scratch, the glycerol would adhere to the scratch area rather than rolling over the agar.

2. Slowly dispense the glycerol onto the scratch area to dislodge the spores and suspend them in the glycerol solution.
3. Once fully dispensed, lightly tip the plate and aspirate the glycerol spore/mycelia suspension.

   NOTE: Approximately 750 to 800 µL will be aspirated.
4. Transfer the aspirate to a sterile freezer tube and store at -80 °C. If required, create working stock by repeating step 2.2.2.5.

2.2.2.6 Phenotypic identification of *A. fumigatus* strains

1. Using the spore stock created from step 2.2.2.5, create a 100x dilution in water. To do this, Aspirate 10 µL of the mycelial and spore stocks and dispense in 990 µL of water. Vortex the suspension.
2. Dispense 10 µL of the diluted spore suspension onto a standard microscope slide.
3. OPTIONAL: Stain the mycelial and spore suspension with methylene blue.
   1. To stain with methylene blue, fix the conidia and conidiophores to the slide by passing the slide over a Bunsen burner until dry.
   2. Apply methylene blue for 1-2 min and wash off with water.
   3. Dry the slide with blotting paper.
2. Using a compound microscope at 400x magnification, view the suspension and locate conidiophores. Compare the observed conidiophore morphology with *A. fumigatus* conidiophore morphology.

2.2.2.7 Molecular identification of *A. fumigatus* strains

1. Extract DNA from each isolate following common fungal DNA extraction protocols.
2. Using primers specific to the *Aspergillus* β-tubulin genes (β-tub1 and β-tub4), run PCR and obtain the sequence for the amplified products, following protocols described by Alcazar-Fuoli et al., (2008).

1. Compare the obtained sequences to sequences deposited in public databases such as NCBI GenBank using BLAST.
2. Confirm the strain sequences are a top match to *A. fumigatus* sequences in the database.

3. Alternative to the previous step, run a multiplex PCR reaction targeting the *A. fumigatus* mating types *MAT1-1* and *MAT1-2* (Paoletti et al., 2005).
    1. Use the following three primer sequences in the multiplex PCR reaction:
       AFM1: 5' - CCTTGACGCGATGGGGTGG-3';
       AFM2: 5′ - CGCTCCTCATCAGAACAACTCG-3′;
       AFM3: 5′ - CGGAAATCTGATGTCGCCACG-3′.
    2. Use the following thermocycler parameters: 5 min at 95 °C, 35 cycles of 30 s at 95 °C, 30 s at 60 °C, and 1 min at 72 °C before a final 5 min at 72 °C.
    3. Run gel electrophoresis to identify the products; look for 834 bp MAT-1 or 438 bp *MAT1-2*. Use *A. fumigatus* strains that have confirmed mating type amplification as positive and negative controls.

2.2.2.8 Microsatellite genotyping of *A. fumigatus* strains through fragment analysis

NOTE: Although the steps listed below broadly cover genotyping *A. fumigatus* at nine microsatellite (STR) loci, only a few important considerations have been highlighted. For details on *A. fumigatus* STR genotyping, refer to De Valk et al. (de Valk et al., 2005; De Valk et al., 2007).

1. Prepare three PCR multiplex master mixes using the STRAf primers previously described by De Valk et al. (2005).
    1. Fluorescently label forward primers to determine fragment size through capillary electrophoresis. Ensure that the concentration of the forward primers is half (0.5 μM) that of the reverse primers (1 μM) within the master mix.
       NOTE: For the best results, use fluorescent labels that have absorbance wavelengths that match those of the chosen dye standard used during capillary electrophoresis
    2. Use a hot start DNA polymerase for best results.

3. Use a DNA concentration of 0.1 ng per reaction.

2. Run the multiplex PCR for each strain using the following PCR program: 95 °C for 10 min, 40 cycles of 95 °C for 30 s, 60 °C for 30 s, and 72 °C for 60 s, followed by 72 °C for 10 min and a hold at 4 °C.
3. Check for amplified products through gel electrophoresis.
4. Dilute the products to the desired level (typically ~50x) as recommended by fragment analyses specialists and run capillary electrophoresis. Perform three runs for each strain, with each run covering three multiplexed reactions with three different fluorescent probes.
5. To determine the correct fragment size for each of the nine STR loci, use software capable of fragment analysis.
    1. Retrieve the raw data obtained from capillary electrophoresis. Score the fragment sizes based on the largest peak using the fragment analysis software (e.g., Osiris).
    2. Convert the fragment sizes to repeat numbers for each of the nine loci. Use the fragment sizes of the repeat numbers of the reference strain Af293 as previously described by De Valk et al. (2005).

       NOTE: Slight variations in fragment sizes may occur between different capillary electrophoresis platforms. Thus, it is important to include a common reference strain (and an internal ladder) with known fragment size for each of the nine loci for genotyping strains.

2.3 Representative Results

2.3.1 Yeast isolation from soil

The above yeast isolation protocol was implemented to culture yeasts from soil samples originating from 53 locations in nine countries (Aljohani et al., 2018; Samarasinghe et al., 2021). In total, 1,473 yeast strains were isolated from 3,826 soil samples. Given the different climatic conditions of the nine originating countries, the best incubation temperature for each country was determined based on its mean annual temperature (Table 2.1). Given the slower yeast growth at 14 °C, soil samples from Iceland were incubated on a roller drum for an

additional 48 h (96-120 h total). Following 2-3 days of incubation on solid medium, microbial growth was visible on plates for all samples (Figure 2.1A). A randomly selected colony for each yeast morphology present on a plate was streaked for single colonies on fresh plates (Figure 2.1B).

Table 2.1: Soil yeast isolation from nine countries in six continents. Incubation temperature for soil samples from each country was determined based on its mean annual temperature. Results presented here are adapted from (Aljohani et al., 2018; Samarasinghe et al., 2021).

Country	Incubation temperature (°C)	Soil samples	Yeast isolates	Known species/ Novel species
Cameroon	30	493	110	10/9
Canada	23	300	261	34/12
China	23	340	230	23/5
Costa Rica	30	388	95	20/2
France	23	327	175	12/2
Iceland	14	316	211	11/0
New Zealand	23	610	155	14/4
Peru	23	490	139	30/9
Saudi Arabia	30	562	97	8/1
Total		3826	1473	90/44

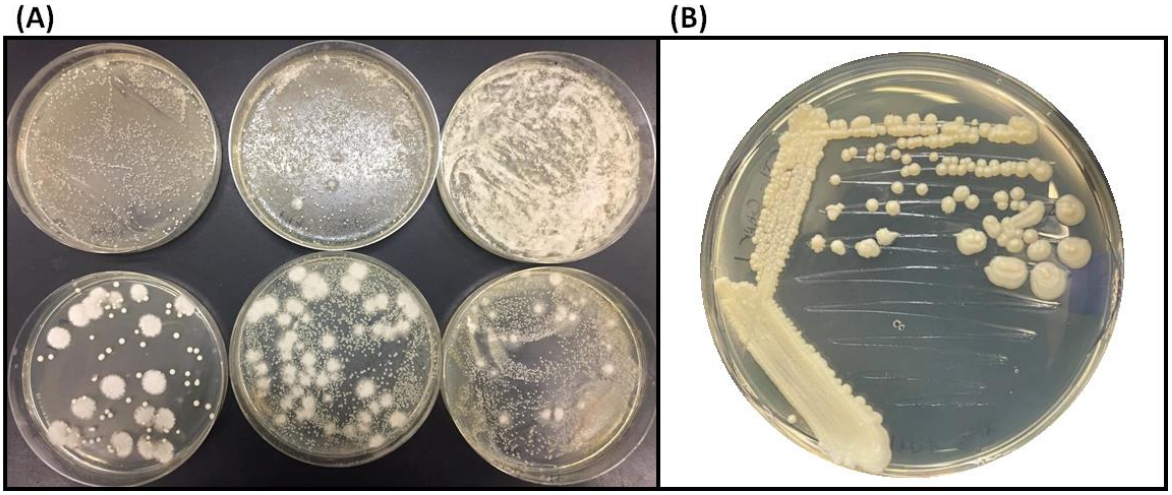

Figure 2.1: Yeasts isolation from soil samples. (A) Microbial growth is visible on solid agar following 2-3 days of incubation. Yeast colonies can be seen interspersed among other fungal/bacterial colonies. One representative yeast colony for each morphological type on a plate is selected to streak for single colonies. (B) Three streaks are performed to obtain single colonies of yeast isolates. One plate was used to obtain each soil isolate.

The rate of successful yeast isolation differed between countries (Table 2.1). For example, 97 yeast strains were cultured from 562 Saudi Arabian soil samples (17.3%), whereas 261 yeasts were cultured from 300 Canadian soil samples (87%). A rarefaction analysis should be performed to determine if sufficient soil sampling has been conducted to obtain accurate estimates of the true yeast diversity in sampled locations. An example rarefaction analysis for each country was preformed where the Shannon diversity index was used as a measure of soil yeast diversity (Figure 2.2). The resulting rarefaction curves approached the saturation asymptote indicating that additional sampling was not likely to have yielded more yeast diversity.

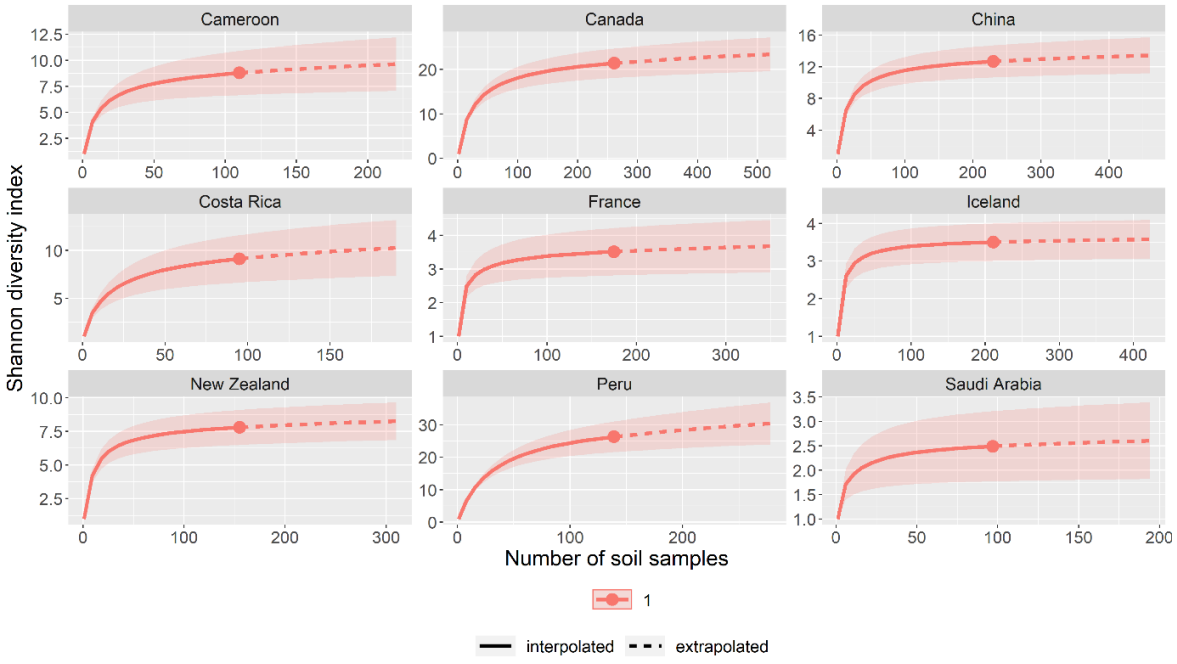

Figure 2.2: Rarefaction analysis of soil sampling. In each of the nine sampled countries, soil yeast diversity, as quantified by Shannon diversity index, approaches saturation as the number of soil samples increases. This figure was adapted from (Samarasinghe et al., 2021).

Sequencing of the ITS region revealed that the 1,473 yeast isolates can be categorized into 134 distinct species. This included 90 known species and 44 potentially novel species. We applied a mixed-effects model to identify predictors of global culturable soil yeast diversity, as quantified by the Shannon diversity index (Bates et al., 2015). In this model, mean annual precipitation, mean annual temperature, elevation, and distance to equator of the sampling

locations were fitted as fixed effects, while sampling country was set as a random effect (Samarasinghe et al., 2021). This model identified mean annual precipitation to be significantly correlated with the Shannon diversity index ($p = 0.012$), while no significant correlations were found between other predictor variables and the Shannon diversity index (Samarasinghe et al., 2021).

To compare this culture-based protocol to culture independent methods, we compared these findings to a previous study by Tedersoo and colleagues that investigated global diversity of soil fungi using metagenomics (Tedersoo et al., 2014). Tedersoo and colleagues performed high-throughput sequencing of the ITS region on DNA directly extracted from soil samples of 39 countries, four of which, namely Cameroon, Canada, China, and New Zealand, were also sampled in this study. We performed BLAST searches to identify ITS sequences present in both datasets (Camacho Christiam et al., 2022), and found 26% of the ITS sequences had a significant match (>98.41% nucleotide identity) in the metagenomics dataset. However, <3% matched a fungal sequence from the same country, while the remaining 23% matched a fungal sequence found in a different country (Samarasinghe et al., 2021). We were more successful than the metagenomics study in annotating the ITS sequences with yeast species identity. Tedersoo and colleagues reported a total of 50,589 fungal operational taxonomic units (OTUs), with the number of yeast OTUs not known. Of these fungal OTUs, 33% were merely annotated as environmental_sequence (724, 1.4%), uncultured_soil_fungus (2,405, 4.8%), uncultured_ectomycorrhizal_fungus (1,407, 2.8%), or uncultured_fungus (11,898, 23.5%).

2.3.2 *Aspergillus fumigatus* isolation from soil

After 3 days of soil incubation at 50 °C in 1 mL of SDB in a microcentrifuge tube, mycelia may be found growing within the SDB, on the SDB to air boundary, and/or on the inside walls. *Aspergillus fumigatus* mycelia are typically found growing on the SDB to air boundary but can also be harvested from just below the SDB surface. After this step, the mycelia are transferred to MEA and grown for 3 days at 37 °C. Mycelial growth on plates may only form the green suede morphology typical of *A. fumigatus* (Figure 2.3A). More commonly, other

thermotolerant molds may be present within the same soil and grow with *A. fumigatus* on the same plate or by themselves (Figure 2.3B-D). *Aspergillus fumigatus* isolation rates may vary between geographic locations, similar to what has been found for soil yeasts. For example, within Vancouver, Canada, 251 isolates were obtained through this method from 540 soil samples (46.5%) (unpublished results). By contrast, within Cameroon, 51 *A. fumigatus* isolates were harvested from 495 soil samples (10.3%) (Eta E. Ashu et al., 2017).

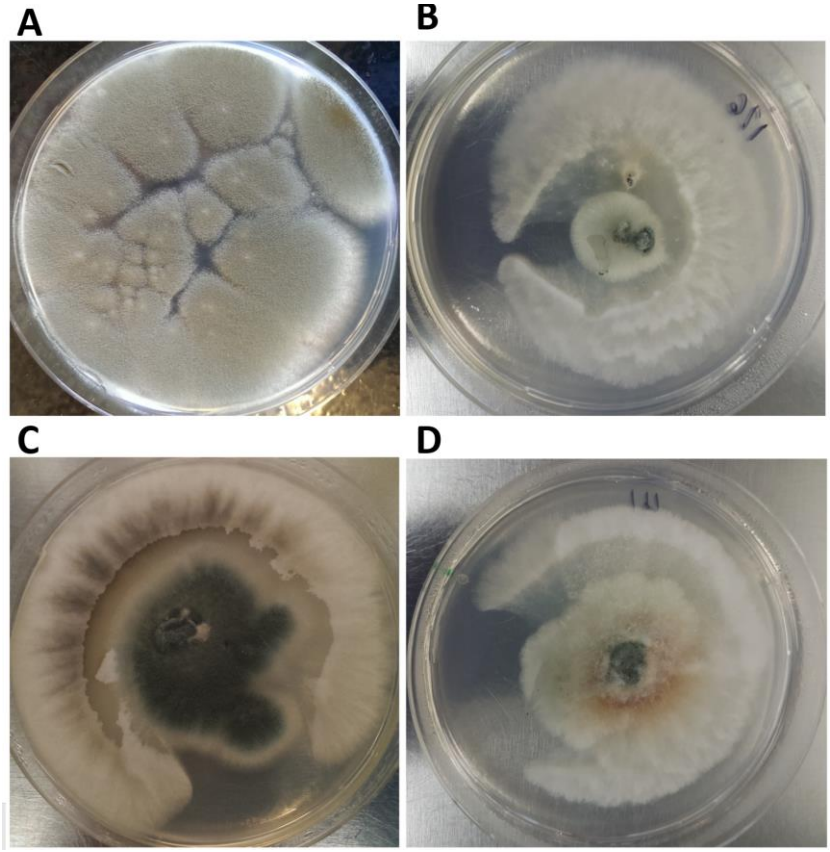

Figure 2.3: *Aspergillus fumigatus* morphology on Sabouraud dextrose agar. (A) Green suede-like *A. fumigatus* growth morphology. (B-D) *A. fumigatus* growth with other thermophilic molds present within the soil sample. *A. fumigatus* conidiation is visibly reduced in B and D.

A. fumigatus conidiophore structure can be viewed and identified using light microscopy. Conidiophores have a ball on stick morphology (Figure 2.4). Additionally, *A. fumigatus* conidiophores are uniseriate, where the phialides, attached to the conidia chains, are attached directly to the spherical vesicle. In other *Aspergillus* species, conidiophores are biseriate, where the phialides are connected to metulae attached to the vesicle.

Figure 2.4: Photo of an *A. fumigatus* conidiophore under a light microscope. Scale bar = 10 µm.

Several software programs are available to perform fragment analysis of the raw data from capillary electrophoresis, converting the capillary electrophoresis spectrum to fragment sizes. Figure 2.5 is a chromatogram generated by the program Osiris. The three channels visualizing the fragment lengths of *A. fumigatus* dinucleotide (2A, 2B, and 2C), trinucleotide (3A, 3B, and 3C), and tetranucleotide (4A, 4B, and 4C) STR loci are shown. In addition, PCR artifacts that occur if the sample DNA concentration during PCR is too high are also shown. The highest peaks of each color represent the fragment sizes of the three STR loci in this plot.

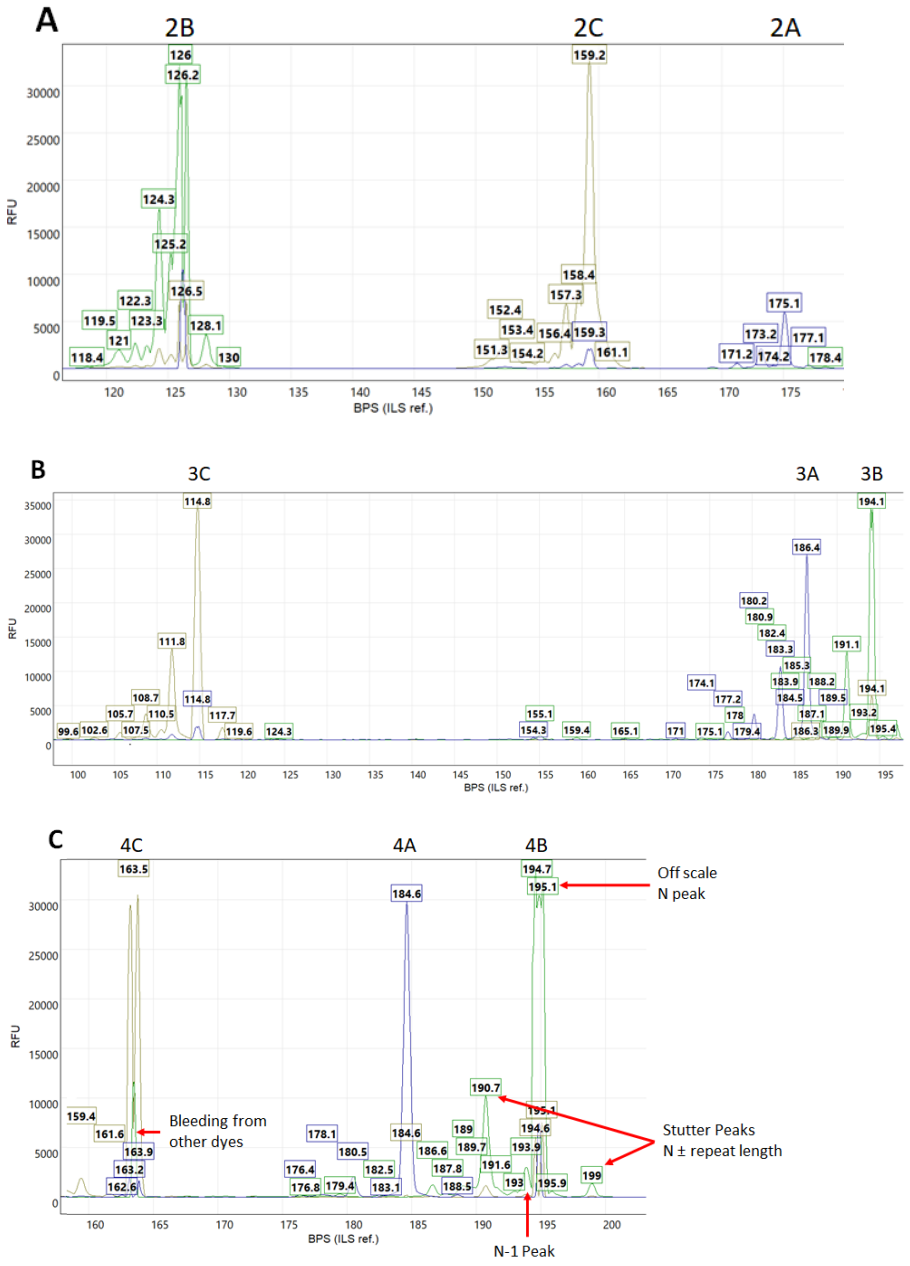

Figure 2.5: Osiris output of nine microsatellite loci from an *A. fumigatus* strain. The outputs correspond to the (A)Dinucleotide (2A, 2B and 2C), (B) trinucleotide (3A, 3B and 3C) and (C) tetranucleotide (4A, 4B and 4C) short tandem repeat (STR) loci. Forward primer 5` fluorescent labels are: A = 6-FAM; B = HEX; C = ATTO550. Multiplex reaction products were diluted 30x prior to capillary electrophoresis. The LIZ600 dye standard was used during capillary electrophoresis. Raw data was analyzed by the peak analysis software Osirus identifying potential peaks between 60 and 400 bp. Several PCR artifacts are off-scale peaks that cause fluorescence bleeding, stutter peaks and N-1 peaks(C). Abbreviations: 6-FAM = 6-carboxyfluorescein; HEX = hexachlorofluorescein; STR = short tandem repeats; RFU = relative fluorescence units; BPS = base pairs

The genetic variation present between *A. fumigatus* STR genotypes can be visualized using the R package *poppr*. The R script *bruvo.msn* creates a pairwise Bruvo's genetic distances matrix between each pair of genotypes. This matrix is then used to generate a minimum spanning network (MSN). A high-quality MSN can then be generated using the R script *plot_poppr_msn* or *imsn* (Figure 2.6). A discriminatory analysis of principal components (DAPC) is another method to visualize the genetic relationships among strains (Figure 2.7). The R script *dapc* in the R package *adegenet* is used to perform DAPC and can be used with known or unknown group priors. With unknown group priors, it uses K-means clustering to identify the likely number of groups of individuals.

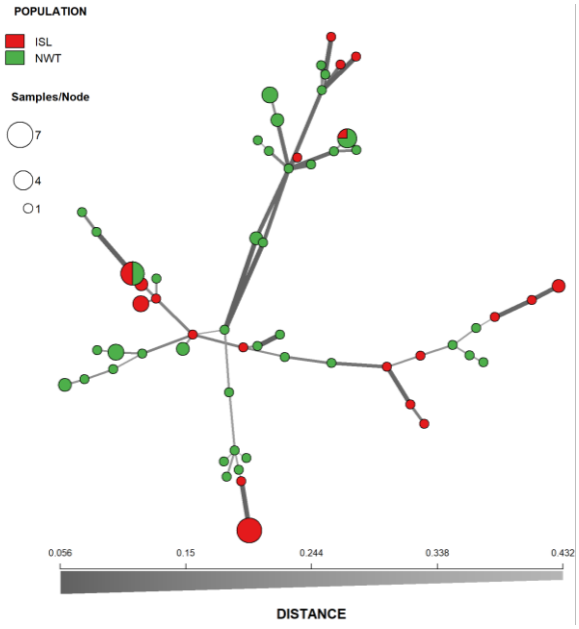

Figure 2.6**:** Minimum-spanning network showing the genetic relationship between MLGs of *A. fumigatus* from Iceland (ISL) and Northwest Territory in Canada (NWT). Each node represents one or more identical MLGs, where node size corresponds to the number of strains for each MLG. Nodes that are more genetically similar have darker and thicker edges, whereas nodes genetically distant have lighter and thinner edges. This figure was adapted from (Korfanty et al., 2021). Abbreviations: ISL = Iceland; NWT = Northwest Territories in Canada; MLG = multilocus genotype.

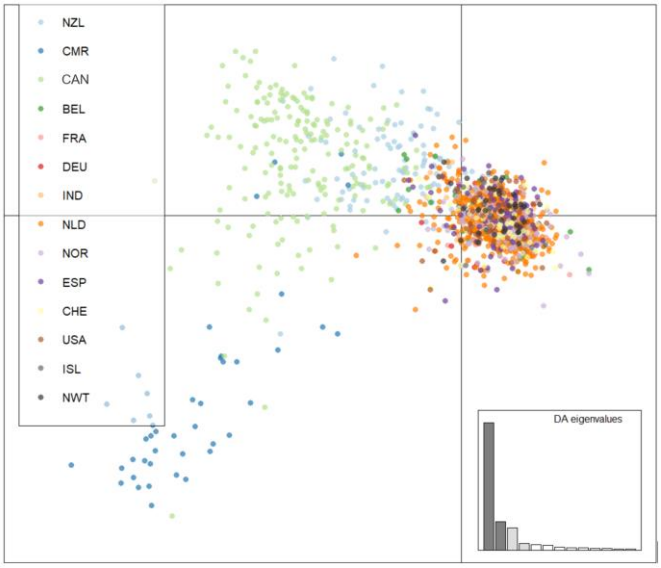

Figure 2.7: Genetic clustering using Discriminant analysis of principal components (DAPC) of Iceland, NWT, Eurasian, North American, and Oceanian *A. fumigatus* populations. Isolates were genotyped at nine microsatellite loci and clone corrected, totaling 1703 unique multilocus genotypes. Genotypes were colored according to geographic origins. This figure was adapted from (Korfanty et al., 2021).. NWT—Northwest Territories, ISL—Iceland, CMR—Cameroon, CAN—Hamilton, Ontario, Canada, BEL—Belgium, FRA—France, DEU—Germany, IND—India, NLD—Netherlands, NOR—Norway, NZL—New Zealand, ESP—Spain, CHE—Switzerland, and USA—United States.

2.4 Discussion

The protocol developed for isolating yeasts and *A. fumigatus* from soil is a fast and efficient method for high-throughput soil processing and fungal isolation. The protocol only requires a small amount of soil (0.1-0.2 g) per sample, allowing for more sites to be sampled with similar effort. The quick turnaround time ensures that results can be obtained within a short timeframe and allows time for troubleshooting and repeating experiments if necessary. This protocol can be easily replicated across many laboratory settings using standard microbiology and cell culturing equipment. However, when isolating yeast or molds from international soil, extra precautionary measures are required. All non-disposable plastic equipment, such as plastic trays and cell spreaders, should be sterilized by submersion in 10% bleach, followed by autoclaving. The used bench coat should be sealed in a plastic bag and sterilized in an autoclave prior to discarding. To note, the number and identity of yeasts isolated using the protocol above can be limited by the incubating conditions and media used. For example, 24 h incubation in the roller drum can favor the isolation of fast-growing

aerobic yeasts over slow-growing species. In addition, the use of nutrient rich YEPD medium for yeast isolation may have excluded yeast species with different nutrient requirements and preferences. Furthermore, most locations sampled here experience seasonal variations in temperature and other climatic conditions throughout the year. If time and resources permit, the same soil samples can be processed under a range of different temperatures to allow for isolation of a broader range of yeasts that inhabit these soils.

While culture-independent methods are crucial for elucidating large-scale patterns in environmental fungal diversity, they fail to be sufficiently informative for targeted groups of fungi such as yeasts. The use of culture-dependent isolation allowed for a comprehensive investigation of global soil yeast diversity and its predictors (Samarasinghe et al., 2021). While the metagenomics study conducted by Tedersoo and colleagues identified global predictors and patterns in soil fungal diversity, the extent to which these findings apply specifically to yeast diversity could not be elucidated (Tedersoo et al., 2014). Tedersoo and colleagues identified mean annual precipitation as a major climatic driver of soil fungal diversity worldwide (Tedersoo et al., 2014). This study found a similar correlation between mean annual precipitation and culturable yeast diversity in global soils, highlighting that culture-dependent methods can complement and expand on findings of high-throughput sequencing approaches (Samarasinghe et al., 2021).

The addition of chloramphenicol is an important step in the preparation of both solid and liquid media to prevent fungal growth interference by bacteria. The addition of chloramphenicol to liquid media is crucial as the lack of antibiotics will allow the bacteria present in the soil to ferment. This will lead to the production of gases that will forcibly open microcentrifuge tubes or 13 mL culture tubes used during soil incubation in the protocol. If bacterial contamination in chloramphenicol containing agar/broth is an issue, chloramphenicol may be substituted or supplemented with stronger antibiotics. When isolating *A. fumigatus* from soil, SD broth may be substituted with a Tween 20 solution (0.2 M NaCl with 1% Tween 20) to help suspend the hydrophobic *A. fumigatus* conidia present

within the soil (Snelders et al., 2009; Wang et al., 2018). Following suspension, 100 µL can be plated onto SD agar and incubated at 50 °C.

Aspergillus fumigatus grows quickly and sporulates abundantly when incubated alone on both SD agar and MEA media between 22 °C and 50 °C. However, depending on what other thermotolerant species are present in the soil sample, *A. fumigatus* growth and sporulation may be hindered (Figure 2.3A, D). Under such a situation, one to several subculturing steps may be required to obtain a pure colony for subsequent harvest and characterization.

The fragment analysis of *A. fumigatus* strains in Figure 2.5 was conducted using the program Osiris. Several PCR artifacts have been highlighted in Figure 2.5C and are discussed in detail by (De Valk et al., 2007). B-1 stutter peaks that have shorter repeat values are caused by strand slippage during the synthesis of the antisense strand by the DNA polymerase. N-1 peaks occur if the DNA concentration is too high during PCR. The recommended DNA concentration is 0.1 ng as stated in the protocol above. Another artifact is dye bleeding that can be remediated using fluorescent labels with non-overlapping absorbance wavelengths. For example, the fluorescent labels 6-FAM, HEX, and ATTO550, as well as the LIZ600 dye standard, generate distinct fragment peaks (Figure 2.5). Lastly, to prevent off-scale peaks, dilute each PCR reaction (in this case, it was ~50x dilution) prior to capillary electrophoresis. To further reduce fluorescence of the unused forward primers in the reaction mixture, halve the forward primer concentrations relative to the reverse primers when creating the PCR master mix.

The high throughput and conservative nature of this protocol allows for a relatively quick and easy acquisition of many yeasts and molds from soils. However, there are two main limitations present with the sampling methodology. First, the morphological characteristics of yeast colonies grown from soil were used to select for unique species. These were then subcultured and used for species identification via ITS sequencing. This was done to maximize the representation of yeast species present. However, yeast species that shared similar or identical morphologies to the selected colonies may fail to be subcultured. Second,

during *A. fumigatus* isolation, as only one individual colony is selected per soil sample, the presence of multiple individuals within the soil sample will be missed. This may lead to an underrepresentation of the true genetic diversity present within the sample population, as unique genotypes present within the same soil sample will not be collected. To mitigate this issue, during the streak for single colony step following the first culturing on solid media, several single colonies can be collected to obtain additional genotypes. The small volume of soil used per sample helps minimize this sampling limitation when compared to methods that used larger quantities of soil per sample.

The use of this high-throughput and labor-efficient protocol for the isolation of yeast and mold will increase the number of individuals within soil population while using less effort per sample. The increase in statistical power will provide a better picture of culturable yeast communities within the soil and help characterize soil populations of *A. fumigatus*.

2.5 Disclosures

The authors have no conflicts of interest to declare.

2.6 Acknowledgements

This research was supported by grants from the Natural Sciences and Engineering Research Council of Canada (Grant No. ALLRP 570780-2021) and McMaster University.

2.7 References

Alcazar-Fuoli, L., Mellado, E., Alastruey-Izquierdo, A., Cuenca-Estrella, M., & Rodriguez-Tudela, J. L. (2008). *Aspergillus* section *Fumigati*: Antifungal susceptibility patterns and sequence-based identification. *Antimicrobial Agents and Chemotherapy*, *52*(4), 1244–1251. https://doi.org/10.1128/AAC.00942-07

Aljohani, R., Samarasinghe, H., Ashu, T., & Xu, J. (2018). Diversity and relationships among strains of culturable yeasts in agricultural soils in Cameroon. *Scientific Reports 2018 8:1*, *8*(1), 1–11. https://doi.org/10.1038/s41598-018-34122-2

Ashu, Eta E., Korfanty, G. A., & Xu, J. (2017). Evidence of unique genetic diversity in

Aspergillus fumigatus isolates from Cameroon. *Mycoses*, *60*(11), 739–748. https://doi.org/10.1111/myc.12655

Ashu, Eta Ebasi, Hagen, F., Chowdhary, A., Meis, J. F., & Xu, J. (2017). Global population genetic analysis of *Aspergillus fumigatus*. *MSphere*, *2*(1), e00019-17. https://doi.org/10.1128/mSphere.00019-17

Bates, D., Mächler, M., Bolker, B. M., & Walker, S. C. (2015). Fitting linear mixed-effects models using *lme4*. *Journal of Statistical Software*, *67*(1), 1–48. https://doi.org/10.18637/JSS.V067.I01

Bongomin, F., Gago, S., Oladele, R., & Denning, D. (2017). Global and multi-national prevalence of fungal diseases—Estimate precision. *Journal of Fungi*, *3*(4), 57. https://doi.org/10.3390/jof3040057

Botha, A. (2011). The importance and ecology of yeasts in soil. In *Soil Biology and Biochemistry* (Vol. 43, Issue 1, pp. 1–8). Pergamon. https://doi.org/10.1016/j.soilbio.2010.10.001

Brakhage, A. A., & Langfelder, K. (2002). Menacing mold: The molecular biology of *Aspergillus fumigatus*. *Annual Review of Microbiology*, *56*(1), 433–455. https://doi.org/10.1146/annurev.micro.56.012302.160625

Calhelha, R. C., Andrade, J. V., Ferreira, I. C., & Estevinho, L. M. (2006). Toxicity effects of fungicide residues on the wine-producing process. *Food Microbiology*, *23*(4), 393–398. https://doi.org/10.1016/J.FM.2005.04.008

Camacho Christiam, Madden Thomas, Tao Tao, Agarwala Richa, & Morgulis Aleksandr. (2022). *BLAST ® Command Line Applications User Manual* (pp. 1–95). National Library of Medicine.

Carini, P., Marsden, P. J., Leff, J. W., Morgan, E. E., Strickland, M. S., & Fierer, N. (2016). Relic DNA is abundant in soil and obscures estimates of soil microbial diversity. *Nature Microbiology 2016 2:3*, *2*(3), 1–6. https://doi.org/10.1038/nmicrobiol.2016.242

Chowdhary, A., Kathuria, S., Xu, J., Sharma, C., Sundar, G., Singh, P. K., Gaur, S. N., Hagen, F., Klaassen, C. H., & Meis, J. F. (2012). Clonal expansion and emergence of environmental multiple-triazole-resistant *Aspergillus fumigatus* strains carrying the TR34/L98H mutations in the *cyp51A* gene in India. *PLoS ONE*, *7*(12), e52871.

https://doi.org/10.1371/journal.pone.0052871

Connell, L., Redman, R., Craig, S., Scorzetti, G., Iszard, M., & Rodriguez, R. (2008). Diversity of soil yeasts isolated from South Victoria Land, Antarctica. *Microbial Ecology*, *56*(3), 448–459. https://doi.org/10.1007/s00248-008-9363-1

de Valk, H. A., Meis, J. F. G. M., Curfs, I. M., Muehlethaler, K., Mouton, J. W., & Klaassen, C. H. W. (2005). Use of a novel panel of nine short tandem repeats for exact and high-resolution fingerprinting of *Aspergillus fumigatus* isolates. *Journal of Clinical Microbiology*, *43*(8), 4112–4120. https://doi.org/10.1128/JCM.43.8.4112-4120.2005

De Valk, H. A., Meis, J. F. G. M., De Pauw, B. E., Donnelly, P. J., & Klaassen, C. H. W. (2007). Comparison of two highly discriminatory molecular fingerprinting assays for analysis of multiple *Aspergillus fumigatus* isolates from patients with invasive aspergillosis. *Journal of Clinical Microbiology*, *45*(5), 1415–1419. https://doi.org/10.1128/JCM.02423-06

Egidi, E., Delgado-Baquerizo, M., Plett, J. M., Wang, J., Eldridge, D. J., Bardgett, R. D., Maestre, F. T., & Singh, B. K. (2019). A few Ascomycota taxa dominate soil fungal communities worldwide. *Nature Communications*, *10*(1), 1–9. https://doi.org/10.1038/s41467-019-10373

Frac, M., Hannula, S. E., Belka, M., & Jędryczka, M. (2018). Fungal biodiversity and their role in soil health. In *Frontiers in Microbiology* (Vol. 9, Issue APR, p. 707). Frontiers Media S.A. https://doi.org/10.3389/fmicb.2018.00707

Heo, S. T., Tatara, A. M., Jiménez-Ortigosa, C., Jiang, Y., Lewis, R. E., Tarrand, J., Tverdek, F., Albert, N. D., Verweij, P. E., Meis, J. F., Mikos, A. G., Perlin, D. S., & Kontoyiannis, D. P. (2017). Changes in in vitro ausceptibility patterns of *Aspergillus* to triazoles and correlation with aspergillosis outcome in a tertiary care cancer center, 1999–2015. *Clinical Infectious Diseases*, *65*(2), 216–225. https://doi.org/10.1093/cid/cix297

Korfanty, G. A., Dixon, M., Jia, H., Yoell, H., & Xu, J. (2021). Genetic diversity and dispersal of *Aspergillus fumigatus* in Arctic soils. *Genes 2022, Vol. 13, Page 19*, *13*(1), 19. https://doi.org/10.3390/GENES13010019

Kurtzman, C., Fell, J. W., & Boekhout, T. (2011). *The Yeasts A Taxonomic Study* (C. Kurtzman, J. W. Fell, & T. Boekhout (eds.); 5th editio). Elsevier.

Kwon-Chung, K. J., & Sugui, J. A. (2013). *Aspergillus fumigatus*--what makes the species a ubiquitous human fungal pathogen? *PLoS Pathogens*, *9*(12), e1003743. https://doi.org/10.1371/journal.ppat.1003743

Paoletti, M., Rydholm, C., Schwier, E. U., Anderson, M. J., Szakacs, G., Lutzoni, F., Debeaupuis, J.-P., Latgé, J.-P., Denning, D. W., & Dyer, P. S. (2005). Evidence for sexuality in the opportunistic fungal pathogen *Aspergillus fumigatus*. *Current Biology*, *15*(13), 1242–1248. https://doi.org/10.1016/J.CUB.2005.05.045

Rocchi, S., Godeau, C., Scherer, E., Reboux, G., & Millon, L. (2021). One year later: The effect of changing azole-treated bulbs for organic tulips bulbs in hospital environment on the azole-resistant *Aspergillus fumigatus* rate. *Medical Mycology*, *59*(7), 741–743. https://doi.org/10.1093/mmy/myab007

Samarasinghe, H., Aljohani, R., Jimenez, C., & Xu, J. (2019). Fantastic yeasts and where to find them: the discovery of a predominantly clonal *Cryptococcus deneoformans* population in Saudi Arabian soils. *FEMS Microbiology Ecology*, *95*, 122. https://doi.org/10.1093/femsec/fiz122

Samarasinghe, H., Lu, Y., Aljohani, R., Al-Amad, A., Yoell, H., & Xu, J. (2021). Global patterns in culturable soil yeast diversity. *IScience*, *24*(10), 103098. https://doi.org/10.1016/J.ISCI.2021.103098

Sewell, T. R., Zhu, J., Rhodes, J., Hagen, F., Meis, J. F., Fisher, M. C., & Jombart, T. (2019). Nonrandom distribution of azole resistance across the global population of *Aspergillus fumigatus*. *MBio*, *10*(3), e00392-19. https://doi.org/10.1128/mBio.00392-19

Snelders, E., Huis In 't Veld, R. A. G., Rijs, A. J. M. M., Kema, G. H. J., Melchers, W. J. G., & Verweij, P. E. (2009). Possible environmental origin of resistance of *Aspergillus fumigatus* to medical triazoles. *KorApplied and Environmental Microbiology*, *75*(12), 4053–4057. https://doi.org/10.1128/AEM.00231-09

Tedersoo, L., Bahram, M., Põlme, S., Kõljalg, U., Yorou, N. S., Wijesundera, R., Ruiz, L. V., Vasco-Palacios, A. M., Thu, P. Q., Suija, A., Smith, M. E., Sharp, C., Saluveer, E., Saitta, A., Rosas, M., Riit, T., Ratkowsky, D., Pritsch, K., Põldmaa, K., … Abarenkov, K. (2014). Global diversity and geography of soil fungi. *Science*, *346*(6213), 1256688. https://doi.org/10.1126/SCIENCE.1256688

Thomas, J. H., Neff, N. F., & Botstein, D. (1985). Isolation and characterization of mutations in the β-tubulin gene of *Saccharomyces cerevisiae*. *Genetics*, *111*(4).

Vishniac, H. S. (2006). A multivariate analysis of soil yeasts isolated from a latitudinal gradient. *Microbial Ecology*, *52*, 90–103. https://doi.org/10.1007/s00248-006-9066-4

Wang, H.-C., Huang, J.-C., Lin, Y.-H., Chen, Y.-H., Hsieh, M.-I., Choi, P.-C., Lo, H.-J., Liu, W.-L., Hsu, C.-S., Shih, H.-I., Wu, C.-J., & Chen, Y.-C. (2018). Prevalence, mechanisms and genetic relatedness of the human pathogenic fungus *Aspergillus fumigatus* exhibiting resistance to medical azoles in the environment of Taiwan. *Environmental Microbiology*, *20*(1), 270–280. https://doi.org/10.1111/1462-2920.13988

Xu, J. (2016). Fungal DNA barcoding. In *Genome* (Vol. 59, Issue 11, pp. 913–932). Canadian Science Publishing. https://doi.org/10.1139/gen-2016-0046

Xu, J. (2020). Fungal species concepts in the genomics era. *Genome*, *63*(9), 459–468. https://doi.org/10.1139/GEN-2020-0022

Xu, J., Ramos, A. R., Vilgalys, R., & Mitchell, T. G. (2000). Clonal and spontaneous origins of fluconazole resistance in *Candida albicans*. *Journal of Clinical Microbiology*, *38*(3), 1214. https://doi.org/10.1128/JCM.38.3.1214-1220.2000

Yurkov, A. M., Kemler, M., & Begerow, D. (2012). Assessment of yeast diversity in soils under different management regimes. *Fungal Ecology*, *5*(1), 24–35. https://doi.org/10.1016/J.FUNECO.2011.07.004

Yurkov, Andrey M. (2018). Yeasts of the soil - obscure but precious. *Yeast*, *35*(5), 369–378. https://doi.org/10.1002/yea.3310

Chapter 3

Genetic Diversity and Dispersal of *Aspergillus fumigatus* in Arctic Soils

Abstract *Aspergillus fumigatus* is a saprophytic mold and an opportunistic pathogen with a broad geographic and ecological distribution. *A. fumigatus* is the most common etiological agent of aspergillosis, affecting over 8,000,000 individuals worldwide. Due to the rising number of infections and increasing reports of resistance to antifungal therapy, there is an urgent need to understand *A. fumigatus* populations from local to global levels. However, many geographic locations and ecological niches remain understudied, including soil environments from arctic regions. In this study, we isolated 32 and 52 *A. fumigatus* strains from soils in Iceland and the Northwest Territories of Canada (NWT), respectively. These isolates were genotyped at nine microsatellite loci and the genotypes were compared with each other and with those in other parts of the world. Though significantly differentiated from each other, our analyses revealed that *A. fumigatus* populations from Iceland and NWT contained evidence for both clonal and sexual reproductions and shared many alleles with each other and with those collected from across Europe, Asia, and the Americas. Interestingly, we found one triazole-resistant strain containing the TR_{34}/L98H mutation in the *cyp51A* gene from NWT. This strain is closely related to a triazole-resistant genotype broadly distributed in India. Together, our results suggest that the northern soil populations of *A. fumigatus* are significantly influenced by those from other geographic regions.

I was the first author for the study in this chapter. This chapter is reprinted from following published paper:

Korfanty, G. A., Dixon, M., Jia, H., Yoell, H., & Xu, J. (2021). Genetic diversity and dispersal of *Aspergillus fumigatus* in Arctic soils. *Genes 2022, Vol. 13, Page 19*, *13*(1), 19. https://doi.org/10.3390/genes13010019

3.1 Introduction

Aspergillus fumigatus is a thermotolerant ascomycete mold with a ubiquitous presence around the world. Its primary ecological niche is within decaying plant matter and soil. However, it is also a common opportunistic fungal pathogen capable of infecting both immunocompetent and immunocompromised humans. Over the past three decades, there have been a rising number of reports of antifungal-resistant *A. fumigatus* strains, which have significantly impacted the treatment of patients with *A. fumigatus* infections (Abdolrasouli et al., 2018; Bueid et al., 2010; Resendiz Sharpe et al., 2018; Verweij et al., 2020; Zhang et al., 2017). *A. fumigatus* infections, collectively known as aspergillosis, encompass a range of illnesses from asthma to invasive aspergillosis. Invasive aspergillosis, the most severe form of aspergillosis, is estimated to occur at over 200,000 cases annually worldwide (Bongomin et al., 2017). Depending on the underlying conditions of patients and the effectiveness of antifungal management, the mortality of invasive aspergillosis ranges from 40% to 90%. For both treatment and prophylaxis, triazole antifungals such as itraconazole, voriconazole, posaconazole, and isavuconazole are often used for frontline therapy. Triazole antifungals target the enzyme lanosterol 14α-demethylase encoded by the gene *cyp51A*. This enzyme is required for the biosynthesis of ergosterol, an essential sterol in the cytoplasmic membrane of fungal cells. Resistance to triazoles is commonly conferred by mutations within the *cyp51A* gene, inhibiting triazole binding and/or causing overexpression of the enzyme (Liu et al., 2016). However, non-*cyp51A* mediated triazole-resistance mechanisms also exist, such as the overexpression of *abc* and *cdr* efflux pumps (Moye-Rowley, 2015). Aside from the triazoles, two other antifungal classes, the polyene amphotericin B and the echinocandins, are used for salvage therapy of aspergillosis, especially in the case of triazole-resistance (Dockrell, 2008).

Over the past 30 years, there have been rising incidences of triazole resistant *A. fumigatus* infections worldwide, including the identifications of triazole-resistant strains in triazole naïve patients (Astvad et al., 2014; Berger et al., 2017; Dauchy et al., 2018; Pelaez et al., 2015). These results suggest the importance of environmental populations of *A. fumigatus* to patients and to the clinical populations of this species. Consequently, it is extremely

important to understand the environmental populations of *A. fumigatus*. Indeed, an increasing number of environmental populations from different geographic regions have been surveyed to aid in monitoring drug resistance rates and identifying/tracking resistant *A. fumigatus* genotypes. The results so far suggest that agricultural use of triazole fungicides can contribute to the development of triazole resistant strains, which subsequently infect patients (Ashu, Korfanty, et al., 2017; Chowdhary et al., 2013; Ren et al., 2017; Stensvold et al., 2012). In these and other studies, a panel of nine highly polymorphic short tandem repeat (STR) loci are often used to analyze the relationships among strains and populations. Based on genotype information at these nine loci on thousands of *A. fumigatus* isolates, divergent lineages as well as high levels of gene flow between geographic populations have been identified (Ashu, Hagen, et al., 2017; Ashu, Korfanty, et al., 2017; Sewell et al., 2019). For example, Ashu, Hagen, et al., (2017) revealed eight genetic populations in their global sample with all eight genetic populations being broadly distributed across multiple countries and continents. However, the samples from Cameroon in central western Africa was genetically unique, different from those analyzed so far from Eurasia, Oceania, and the Americas (Ashu, Korfanty, et al., 2017).

Among the currently analyzed geographic populations of *A. fumigatus*, almost all have come from tropical, subtropical, and temperate regions. Little is known about geographic populations of *A. fumigatus* from cold climates. In this study, we isolated and analyzed strains of *A. fumigatus* from two high latitude regions: Iceland and the Northwest Territories (NWT) in Canada. Due to their long-distance separation, we hypothesized that populations of *A. fumigatus* from these two geographic regions should be genetically different from each other. In addition, due to their unique climates, we expect that these two *A. fumigatus* geographic populations would be genetically different from those reported from other geographic regions in temperate, subtropical, and tropical climates. Finally, since both geographic regions have very limited agriculture and no history of agricultural fungicide usage, we expected that all isolates from the soil in both regions should be susceptible to the common clinical triazole drugs itraconazole and voriconazole. Our results showed that some of the expectations were met. However, unexpected results were also identified.

3.2 Materials and Methods

3.2.1 Soil collection, *A. fumigatus* isolation, and STR genotyping

Soil samples were obtained from Iceland and the Northwest Territories in Canada. All soil samples were obtained from at least 1 cm below the soil surface. In Iceland, a total of 314 soil samples were collected from the following six sites: Dimmuborgir (60), Thingvellir (51), Skaftafell (52), Myvatn Lake (42), Landbrotalaug (60), and Reykjavik University (49). In Northwest Territories (NWT) in Canada, 220 soil samples were obtained from the following four sites within and near Yellowknife: Yellowknife Downtown (80), 30 km North of Yellowknife (50), 30 km Northwest of Yellowknife (60), and in Yellowknife Old Town (30). The numbers in parenthesis represent the number of soil samples taken from each site.

To isolate *A. fumigatus*, approximately 0.2 g of soil from each soil sample was put in 1 mL of Sabouraud dextrose (SD) broth containing 50 mg/L chloramphenicol within a 1.5 mL microcentrifuge tube. The soil suspension was mixed through vertexing and incubated at 50 °C for 3 days to select for *A. fumigatus* growth. For the soil samples that failed the initial attempt, two additional attempts were made, each with a different incubation temperature, at 42 °C and 30 °C, respectively. After incubation, mycelia grown on the surface of the broth from each incubation temperature was then transferred to SD agar containing 50 mg/L chloramphenicol and incubated at 37 °C for 3 days. Colonies resembling *A. fumigatus* were sub-cultured to a new agar medium and their conidia were harvested with sterile 30% glycerol and stored at −80 °C. To confirm their identity, these putative *A. fumigatus* isolates were genotyped at the mating type locus using *A. fumigatus* species-specific and mating-type specific primer pairs (Paoletti et al., 2005). Strains confirmed as *A. fumigatus* were then analyzed for their genotypes at nine highly polymorphic short tandem repeat (STR) loci specific for *A. fumigatus*, following protocols previously described by de Valk et al., (2005).The only modification was the fluorescent tag for primers STRAf2C, STRAf 3C, and STRAf 4C that was changed from the TET probe to ATTO550 (IDT) to provide better fragment size detection and scoring. STR fragments at the nine loci were separated using capillary electrophoresis at McMaster University's MoBix Lab and analyzed using the STR analysis software Osiris (Goor et al., 2011).

3.2.2 Allelic and genotypic diversities

Allelic diversity was calculated for each of the nine STR loci within both the Iceland and NWT populations using the Excel add-in *GenAlEx 6.5* (Peakall & Smouse, 2006, 2012). *GenAlEx 6.5* was also used to compute unbiased haploid genetic diversity (uh). The uh diversity measures the probability that two individuals will be different within the population using the sum of allele frequencies within the populations and adjusts for differences in sample size. Additionally, the number of effective alleles (Ne) was calculated. To determine whether the Iceland and NWT populations differ significantly in their mean uh and mean Ne, two-tailed Student's *T*-tests were conducted.

3.2.3 Clonality and recombination

To assess the potential evidence for clonality and/or recombination in these two regional populations, we conducted two tests. The first test was the overall linkage disequilibrium within each of the two geographic populations using the standardized index of association ($\bar{r}_d$) and the second was the proportion of loci that are phylogenetically compatible. The null hypothesis of the index of association test is random recombination. The function *poppr* from the R package *poppr* was used to calculate $\bar{r}_d$ (Kamvar et al., 2014). Statistical significance was determined through 999 permutations. To account for the influence of clonal genotypes on $\bar{r}_d$, both populations were clone-corrected using the *poppr* function *clonecorrect* and the $\bar{r}_d$ was recalculated. The proportion of phylogenetically compatible pairs of loci was calculated using the software MULTILOCUS v1.3b (Agapow & Burt, 2001). Two loci are phylogenetically compatible if all observed genotypes can be accounted for by mutation alone without inferring homoplasy or recombination. This test is also called the four-gamete test. Statistical significance was determined through 1000 randomizations.

3.2.4 Genetic relationships among strains from the two Arctic populations

To assess the proportion of genetic variation present within and between the two arctic populations, analysis of molecular variance (AMOVA) was conducted using *GenAlEx 6.5* (Peakall & Smouse, 2006, 2012). In a panmictic population, most of the variance observed will arise within the samples. In contrast, a high-level among-sample variance would suggest

the presence of genetically differentiated populations. The null hypothesis for AMOVA is that there is no genetic difference between the populations tested. For genetic distance calculation among strains, the parameter haploid-SSR was used to incorporate the stepwise mutation model. The smaller the difference between allele repeat numbers at each locus, the smaller the genetic distance between the alleles and consequently, their multilocus genotypes (MLGs) would be more similar to each other. Genetic differentiation between the two arctic populations was calculated using ϕ_{pt}, an analogue of F_{st}. Significance was determined through 999 permutations.

To visualize genetic distance between MLGs from Iceland and NWT, a minimum spanning network (MSN) was generated by calculating Bruvo's genetic distance between strains using the R package *poppr* (Kamvar et al., 2014). Bruvo's genetic distance is specific for STR genotypes and incorporates the stepwise mutation model. Genetic distance was calculated for each pair of MLGs, and the resulting matrix is visualized in the MSN. Minimum edge genetic distance was set to 0.05. In addition, a multivariate analysis, Discriminant Analysis of Principal Components (DAPC), implemented by *adegenet* package in R, was used to cluster MLGs genotypes in relation to their geographic origins (Jombart & Ahmed, 2011). In this analysis, DAPC first transforms the data using principal component analysis (PCA) to reduce the number of variables and allowing retention of the variables that have the greatest contribution to the variation within the dataset. This is followed by discriminate analysis (DA) to cluster the MLGs by optimizing the between-group variation and reducing within-group variation.

3.2.5 Genetic relationships between Arctic samples and those from other regions

To compare our arctic STR dataset with those from other geographic and climatic regions, STR data from 12 populations within Eurasia, North America, and Oceania, were included, totaling 2339 MLGs (Ashu, Hagen, et al., 2017; Korfanty et al., 2019). Specifically, the number of MLGs within these 12 populations were: Belgium (108), Hamilton, Canada (195), Cameroon (51), France (66), Germany (85), India (94), Netherlands (1082), Norway (203), New Zealand (104), Spain (180), Switzerland (70), and USA (101).

In our comparisons, the number of private alleles that were present only in Iceland and NWT populations but were absent in these 12 populations was determined. To analyze the level of differentiation between these two arctic populations and those from other geographic regions, we used the same parameters and AMOVA function as described above. In addition to the overall AMOVA, pairwise population ϕ_{pt} was estimated among the 14 geographic populations within this dataset. Statistical significance was determined through 999 permutations. An MSN was generated and DAPC was conducted as described in the above section.

3.2.6 Triazole susceptibility testing

Antifungal susceptibility testing was conducted following the reference protocols described in the Clinical and Laboratory Standards Institute (CLSI) document "M38 Reference Method for Broth Dilution Antifungal Susceptibility Testing of Filamentous Fungi" 3rd edition (Alexander et al., 2017). Here, two triazoles, itraconazole and voriconazole, were used. Two *Candida* strains, *C. parapsilosis* ATCC® 22019 and *C. krusei* ATCC® 6258, were used as references. Briefly, spore suspensions were adjusted to an optical density between 0.09 and 0.13 at 530 nm. The adjusted spore suspensions were then diluted 50× into RPMI 1640 at pH 7 ± 0.1. The two triazole antifungals were dissolved to 200 mg/L in DMSO. A two-fold serial dilution series was conducted for each antifungal to create a 3 to 200 mg/L concentration range in addition to a DMSO only control. Each concentration was then diluted 50× in RPMI 1640. Lastly, 100 µL from both the spore suspension and triazole solutions were added to 96-well cell culture plates to test the susceptibility of each isolate from NWT and Iceland at the final drug concentrations 0.03 to 2 mg/L. The 96-well cell culture plates were then incubated at 35 °C without agitation. The minimum inhibitory concentrations (MIC) for both antifungals were visually determined after 48 h. Strains that grew at 2 mg/L were further tested at the antifungal concentrations between 0.25 to 16 mg/L.

3.2.7. Cyp51A sequencing

The *cyp51A* gene was sequenced for a strain that had an itraconazole and/or voriconazole MIC of 2 or higher to identify putative triazole resistance mutation(s) in this gene. Following

the PCR protocol described by Mellado et al., (2001), five pairs of primers were used to amplify the *cyp51A* region and its 5′UTR. Amplified PCR products were sent for Sanger sequencing at McMaster University's MoBix Lab. To identify mutations within the *cyp51A* gene, the obtained sequences were aligned to the *cyp51A* gene from the *A. fumigatus* reference strain Af293 using the program MEGA-X (Kumar et al., 2018).

3.3 Results

3.3.1 Isolation rates of *A. fumigatus* from Arctic soils

In total, 52 (23.6%) and 32 (10.2%) *A. fumigatus* isolates were obtained from 220 NWT and 314 Iceland soils samples, respectively. In both regions, there were considerable variations among sites in their isolation rates of *A. fumigatus* (Table 3.1). Following isolation, all isolates were genotyped at nine microsatellite loci.

Table 3.1: Soil samples and *A. fumigatus* isolates obtained from Iceland and Northwest Territories (NWT).

Country/Territory	Local Site	Number of Soil Samples	Number of Isolates (*MAT1-1*:*MAT1-2*)*
Iceland	Dimmuborgir	60	1 (0:1)
	Thingvellir	51	8 (3:5)
	Skaftafell	52	6 (4:2)
	Myvatn Lake	42	10 (7:3)
	Landbrotalaug	60	1*
	Reykjavik University	49	6 (4:2)
	Total	312	32 (18:14)
Canada/NWT	Yellowknife Downtown	80	41 (24:17)*
	30km North of Yellowknife	50	0
	30Km Northwest of Yellowknife	60	3 (0:3)
	Yellowknife Old Town	30	6 (1:5)
	Total	220	52 (25:25)

* 1 isolate from Iceland and 2 from NWT were unable to be genotyped at the MAT locus

3.3.2 Local genetic diversity within Iceland and Northwest Territories

The STR genotypes were obtained for isolates from both Iceland and NWT *A. fumigatus* populations. Because of the small sample sizes and unequal sample size distributions among

local populations from within both Iceland and NWT (Table 3.1), we elected to not compare the local populations within each of the two regions but instead focused on comparing the two arctic populations. We found that the two regional populations had similar *uh* between Iceland and NWT where no significant difference was observed (Table 3.2; p = 0.36). For the effective number of alleles, the NWT population had a higher value than that from Iceland, but the difference was statistically nonsignificant ($p = 0.13$). Similarly, the number of observed alleles was higher in the NWT population but after being adjusted for sample size effects, the difference was statistically nonsignificant ($p = 0.08$). Together, the results indicated similar levels of allelic and genotypic diversities between the Iceland and NWT soil populations of *A. fumigatus*.

Table 3.2: Number of alleles and allelic diversity for the nine microsatellite loci of 32 and 52 *A. fumigatus* isolates from Iceland and Northwest Territories respectively.

Population	Locus	N[1]	Na[2]	Ne[3]	Uh[4]
Iceland	2A	32	7	4.92	0.82
	2B	32	5	4.70	0.81
	2C	32	8	6.10	0.86
	3A	32	13	6.02	0.86
	3B	32	6	4.66	0.81
	3C	32	10	6.24	0.87
	4A	29	5	2.87	0.68
	4B	32	6	2.94	0.68
	4C	30	10	5.63	0.85
	Mean	31.44	7.78	4.90	0.81
	Standard Error	0.38	0.91	0.43	0.03
Northwest Territories	2A	51	14	4.43	0.79
	2B	52	10	3.99	0.76
	2C	52	11	6.93	0.87
	3A	50	19	13.74	0.95
	3B	50	11	4.63	0.80
	3C	50	19	12.89	0.94
	4A	52	9	3.25	0.71
	4B	52	8	3.22	0.70
	4C	52	14	5.88	0.85
	Mean	51.22	12.78	6.55	0.82
	Standard Error	0.32	1.35	1.34	0.03

[1]N = number of alleles; [2]Na = number of unique alleles; [3]Ne = number of effective alleles = 1 / (Σ pi2) where pi is the frequency of the ith allele for the population; [4]uh = unbiased diversity = (N / (N-1)) (1 - Σ pi2)

3.3.3 Clonality and recombination within Iceland and Northwest Territories

To investigate evidence for clonality and recombination within the two arctic *A. fumigatus* populations, the $\bar{r}_d$ and the proportion of phylogenetically compatible loci were calculated for each population. The $\bar{r}_d$ values of Iceland and NWT were 0.36 (p = 0.001) and 0.16 (p = 0.001), respectively, rejecting the null hypothesis of random mating. The hypothesis of random mating was rejected even after clonal corrections where only 20 and 40 unique MLGs within Iceland and NWT populations, respectively, were retained for analyses. Specifically, after clone-correction, the $\bar{r}_d$ values of the Iceland and NWT populations were 0.19 (p = 0.001) and 0.13 (p = 0.001), respectively. However, phylogenetic compatibility analyses revealed that 55.6% (p = 0.001) and 5.6% (p = 0.001) pairs of loci within Iceland and NWT were phylogenetically compatible. The high proportions of phylogenetically incompatible pairs of loci, at 44.4% and 94.4%, respectively, for the Iceland and NWT populations, are consistent with recombination. Overall, these results indicate that both the Iceland and NWT soil populations of *A. fumigatus* contain signatures of both clonal and recombining modes of reproduction.

3.3.4 Relationships between Iceland and Northwest Territories samples

We analyzed the relationships among *A. fumigatus* isolates from Iceland and NWT. Bruvo's genetic distance was calculated between isolates of both populations and visualized through an MSN (Figure 3.1). Overall, while we observed some geographic clustering among MLGs, isolates from the two arctic populations were intermixed. For example, two different MLGs were shared between Iceland and NWT populations. One of these two MLGs was shared among six strains with three isolates from each of the two regional populations. The other was shared among four isolates (one from Iceland and three from NWT). A DAPC of the Iceland and NWT samples yielded comparable results, which both showed some geographic clustering as well as overlaps between these two regions (Figure 3.2). Results from AMOVA indicated that while the majority (86.8%) of the genetic variations were found within the two regional populations, 13.2% of the total observed genetic variance was found between these two populations (ϕ_{pt} = 0.132, p = 0.001). Together, these results are consistent with an overall statistically significant genetic differentiation between these two arctic populations.

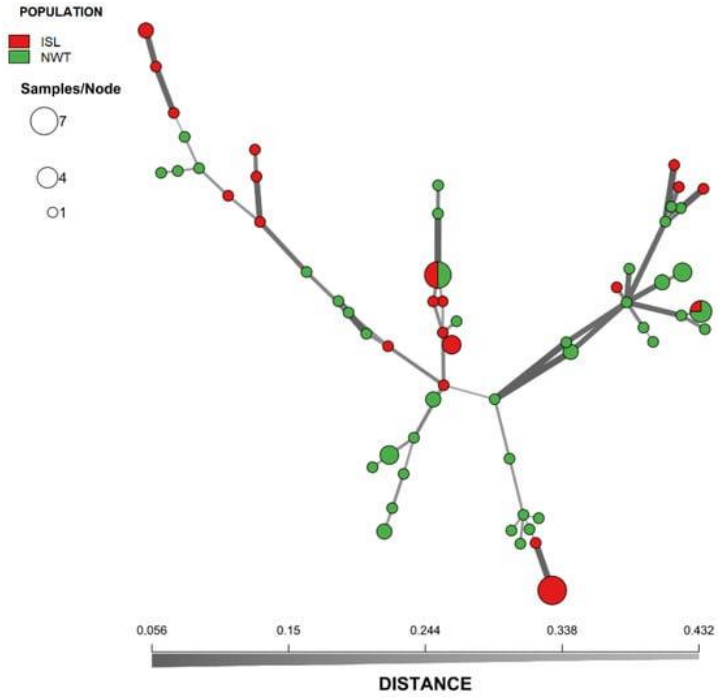

Figure 3.1: Minimum-spanning network showing the genetic relationship between MLGs of *A. fumigatus* from Iceland and Northwest Territory in Canada. The genetic distance between MLGs was calculated using Bruvo's genetic distance from the nine microsatellite loci that incorporates the stepwise mutation model. Each node represents one or more identical MLGs, where node size corresponds to the number of strains for each MLG. Nodes that are more genetically similar have darker and thicker edges, whereas nodes genetically distant have lighter and thinner edges.

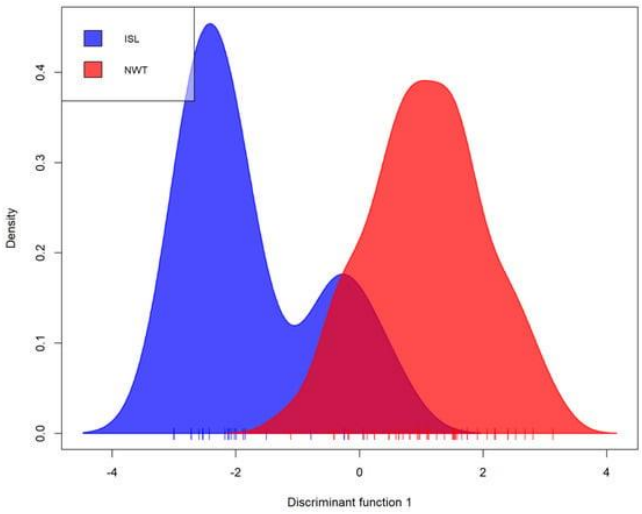

Figure 3.2: Discriminant analysis of principal components (DAPC) of Iceland and NWT *A. fumigatus* populations representing the first discriminant function in an individual density plot. Isolates were genotyped at nine microsatellite loci and clone corrected, totaling 60 multilocus genotypes. NWT—Northwest Territories, ISL—Iceland.

3.3.5 Relationship between the Arctic populations to additional global *A. fumigatus* populations

To determine how the arctic populations fit in the global context, the allelic and genotypic diversities of 12 other geographic populations totaling 2339 *A. fumigatus* MLGs were compared to the Iceland and NWT *A. fumigatus* populations. Within the 2423 MLGs, the number of private alleles present only within Iceland and NWT was 2 and 1 respectively. In Iceland, these two private alleles were #116 and #117 at the 3A locus. In NWT, the private allele was #57 at the 3B locus. Together, the allelic distribution results suggest limited novel genetic diversity in the arctic soil samples.

To determine the genetic relationships between the 2 arctic populations and the 12 other geographic populations, ϕpt was calculated between all pairwise population combinations (Table 3.3). For this analysis, the dataset was also clone-corrected to remove the influence of multiple clonal MLGs in determining genetic differentiation between populations. Overall, our analyses revealed that the two arctic populations of *A. fumigatus* were significantly different from most other geographic populations (Table 3.3). Specifically, before clonal correction, only the Belgian and French populations showed nonsignificant difference to the Iceland population. After clonal correction, only the Indian and French populations were not significantly differentiated from the Iceland population while the Norwegian and New Zealand populations were not significantly different from the NWT population.

Table 3.3: Pairwise differentiations between Iceland and Northwest Territories *A. fumigatus* populations to each other and 12 *A. fumigatus* populations from Eurasia, Oceania, and North America. NWT/ISL row represents the Iceland or Northwest Territories population being compared to the other. NWT—Northwest Territories, ISL—Iceland, CMR—Cameroon, CAN—Hamilton, Ontario, Canada, BEL—Belgium, FRA—France, DEU—Germany, IND—India, NLD—Netherlands, NOR—Norway, NZL—New Zealand, ESP—Spain, CHE—Switzerland, and USA—United States.

Pairwise ϕ_{pt}				
	Iceland		Northwest Territories	
Country	Original Dataset	Clone Corrected	Original Dataset	Clone Corrected
NWT/ISL	0.132**	0.083*	0.132**	0.083*
CMR	0.580***	0.629***	0.598***	0.588***
CAN	0.412***	0.439***	0.337***	0.327***
BEL	0.020	0.048*	0.178***	0.041**
FRA	0.028	0.012	0.070**	0.050*
DEU	0.170***	0.192***	0.285***	0.206***
IND	0.130***	0.052	0.213***	0.056*
NLD	0.054**	0.069*	0.088***	0.062**
NOR	0.152***	0.050*	0.037**	0.014
NZL	0.067**	0.123**	0.051**	0.024
ESP	0.082**	0.074*	0.122***	0.069***
CHE	0.089**	0.100**	0.063***	0.036*
USA	0.162***	0.146**	0.129***	0.051**

* p-value = 0.05, ** p-value = 0.01, *** p-value = 0.001

We also analyzed the genotypic similarities among individual MLGs from the 14 geographic populations. An MSN of all 2416 strains was generated to visualize the genetic distance among the MLGs (Figure 3.3). To highlight the distribution of the arctic isolates, the 12 previously surveyed *A. fumigatus* populations were coloured white. Overall, while the MLGs from the arctic regions showed some geographic clustering, these arctic genotypes were broadly embedded in the global genotype network. This overall pattern was similarly supported by DAPC analyses (Figure 3.4) where MLGs from Iceland and NWT clustered with those from Eurasia and the United States but were different from the Hamilton, Ontario, Canada population as well as from the Cameroonian population.

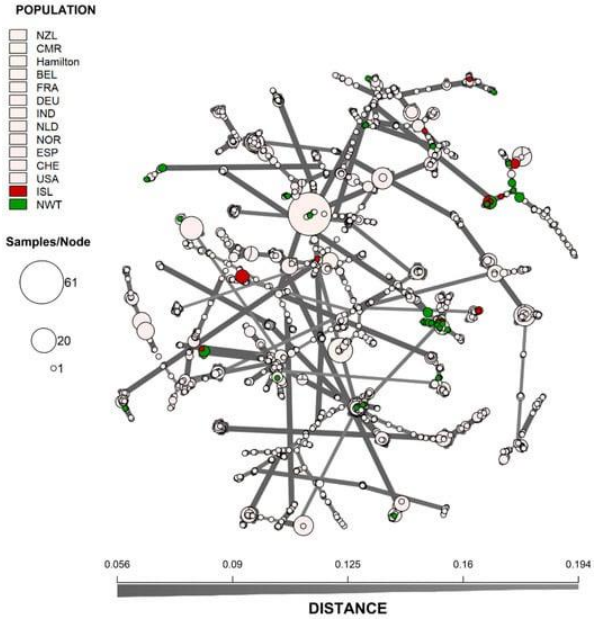

Figure 3.3: Minimum-spanning network showing the genetic relationship between MLGs from Iceland and Northwest Territory to 12 other *A. fumigatus* geographic populations. The genetic distance between MLGs was calculated using Bruvo's genetic distance based on the nine microsatellite loci that incorporates the stepwise mutation model. Each node represents one or more identical MLGs, where the node size corresponds to the number of identical MLGs. Nodes that are more genetically similar have darker and thicker edges, whereas nodes genetically distant have lighter and thinner edges. NWT—Northwest Territories, ISL—Iceland, CMR—Cameroon, CAN—Hamilton, Ontario, Canada, BEL—Belgium, FRA—France, DEU—Germany, IND—India, NLD—Netherlands, NOR—Norway, NZL—New Zealand, ESP—Spain, CHE—Switzerland, and USA—United States.

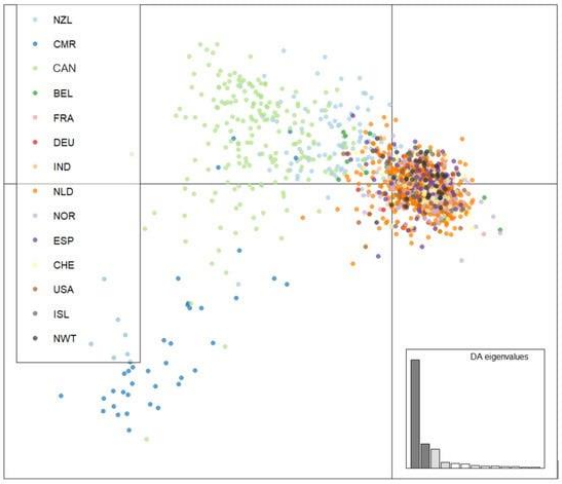

Figure 3.4**:** Genetic clustering using discriminant analysis of principal components (DAPC) of Iceland, NWT, Eurasian, North American, and Oceanian *A. fumigatus* populations. Isolates were genotyped at nine microsatellite loci and clone corrected, totaling 1703 unique multilocus genotypes. Populations were clustered according to population of origin. NWT—Northwest Territories, ISL—Iceland, CMR—Cameroon, CAN—Hamilton, Ontario, Canada, BEL—Belgium, FRA—France, DEU—Germany, IND—India, NLD—Netherlands, NOR—Norway, NZL—New Zealand, ESP—Spain, CHE—Switzerland, and USA—United States.

3.3.6 Susceptibility testing

Antifungal susceptibility testing using voriconazole and itraconazole was conducted for all isolates from the two arctic populations (Table 3.4). One isolate resistant to both triazoles was identified within NWT but no resistant strain was identified from Iceland (Figure 3.5). Our sequence analysis revealed that this triazole-resistant strain NCY6_13_2 had the TR_{34}/L98H mutation within the *cyp51A* gene. Interestingly, this strain had a near identical genotype at the nine STR loci to a clonal population of triazole-resistant strains discovered from India in 2012, differing by only one repeat unit at the 3A locus and with identical alleles at the other eight STR loci (Table 3.5) (Chowdhary et al., 2012). Furthermore, all the *A. fumigatus* isolates in this Indian clone contained the identical TR_{34}/L98H mutation within the *cyp51A* gene as the strain from NWT in our sample.

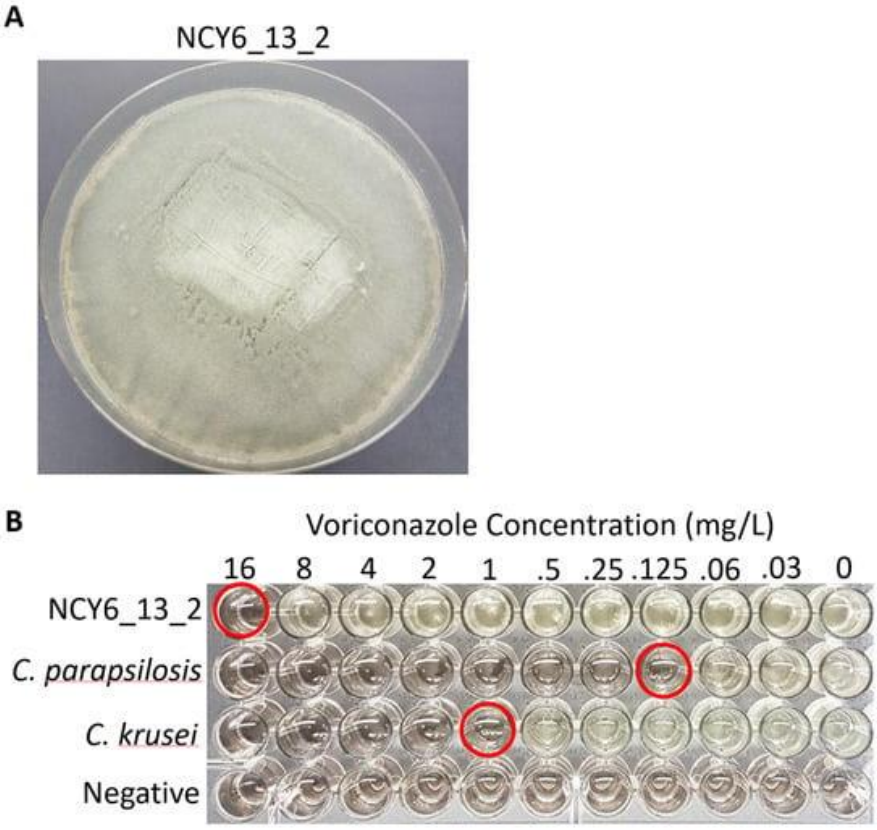

Figure 3.5: Radial growth and voriconazole susceptibility of triazole resistant *A. fumigatus* strain NCY6_13_2. (A) Growth morphology of *A. fumigatus* strain NCY6_13_2 on Malt extract agar after 5-day incubation at 35°C. (B) Voriconazole susceptibility of NCY6_13_2. Two control strains, *Candida parapsilosis* ATCC® 22019 and *C. krusei* ATCC® 6258, were used to verify the susceptibility results. A negative control that was not inoculated with any microbial strain was included in the bottom row. Susceptibility endpoints are circled in red for each strain.

Table 3.4: Triazole antifungal susceptibility of the 32 and 52 *A. fumigatus* isolates from Iceland and NWT, respectively, to itraconazole and voriconazole. Numbers in the table refer to the number of strains with the respective minimum inhibitory concentrations for each of the two drugs in each geographic population.

Country/Territory	Triazole	Minimum inhibitory concentration (mg/L)					
		0.125	0.25	0.5	1	2	16
Iceland	Itraconazole	0	0	24	8	0	0
	Voriconazole	2	29	1	0	0	0
Canada/NWT	Itraconazole	0	0	35	16	0	1
	Voriconazole	0	27	24	0	0	1

Table 3.5: Short tandem repeat genotype of the *A. fumigatus* strain with the TR_{34}/L98H mutation in the triazole-target gene *cyp51A* obtained from Northwest Territories in Canada. Alleles at eight of the nine STR loci in this strain were identical to those of the large Indian triazole-resistant clonal population as reported by Chowdhary et al. (2012).

Strain	Region	2A	2B	2C	3A	3B	3C	4A	4B	4C
NCY6-13_2	NWT	14	20	9	31	8	10	8	10	28
1042/09	India	14	20	9	31	9	10	8	10	28

3.4 Discussion

In this study, we obtained and genotyped *A. fumigatus* isolates from two northern climatic regions, Iceland and Northwest Territories, Canada. This is the first study to investigate *A. fumigatus* population structures at high latitudes and cold climates. A total of 32 (20 unique MLGs) and 52 isolates (40 unique MLGs) were obtained from Iceland and NWT, respectively. Both populations contained abundant allelic and genotypic diversities at the nine microsatellite loci, with evidence of recombination within both populations. However, the observed recombination was not due to random mating. Our analyses demonstrated that while Iceland and NWT shared several identical/similar multilocus genotypes, the two regional populations were significantly differentiated from each other. Similarly, while many alleles were shared, these two arctic soil populations were significantly differentiated from geographic samples from other parts of the world. Interestingly, one triazole resistant strain was identified from NWT and this strain had a near identical MLG as the clonal triazole-resistant population previously identified in India. Below we discuss the implications and relevance of this work to previous studies.

The high level of allelic and genotypic diversity observed within both the Iceland and NWT populations resemble that seen within most regional *A. fumigatus* populations (Ashu, Korfanty, et al., 2017; Ashu et al., 2018; Korfanty et al., 2019; Zhou, Korfanty, et al., 2021; Zhou, Wang, et al., 2021). The high allelic and genotypic diversities within both populations (Table 3.2) suggested that either these two populations were ancient or that there had been multiple migrations from other regions to these two arctic regions. Indeed, the high allelic and genotypic diversities in both regions suggested no evidence of recent selective sweep in either Iceland or NWT. In comparison, a large and broadly distributed MLG within India was found to be caused by a selective sweep of a highly drug-resistant genotype (Chowdhary et al., 2012). However, several MLG were over-represented by two or more isolates in both arctic samples, suggesting that local selection could happen in both populations. At present, due to the relatively small and uneven population sizes among local populations within each of these two regions, it is difficult to determine what selective force(s) might be responsible for their over-representation. The over-representation of certain genotypes is consistent with clonal reproduction of *A. fumigatus* in nature. However, evidence for recombination was also found in both regional populations. Our results are similar to those reported previously for other regional populations of *A. fumigatus* (Ashu et al., 2018; Ashu, Korfanty, et al., 2017; Korfanty et al., 2019; Zhou, Korfanty, et al., 2021; Zhou, Wang, et al., 2021) as well as other human pathogenic and non-pathogenic fungi (Xu, 2021).

Within individual fungal species, both latitudinal differences and geographic distances have been found to correlate with population genetic differences (Barrès et al., 2008; Diao et al., 2015). For example, a latitudinal gradient-based differentiation was observed among populations of the chili pepper anthracnose pathogen *Colletotrichum acutatum* (Diao et al., 2015). In the rust fungus *Melampsora laricipopulina*, a gradual dispersal of genetic elements across the European populations was observed, which led to higher genetic variations between populations at greater geographic distances (Barrès et al., 2008). In contrast, the significant genetic differentiation of the Canadian and Icelandic populations of *M. laricipopulina* was likely caused by founder effects (Barrès et al., 2008). Regarding *A. fumigatus*, geographic *A. fumigatus* populations have been shown to be shaped by both

historical differentiation and high contemporary gene flow due to anthropogenic influences (Ashu, Hagen, et al., 2017; Korfanty et al., 2019). Our results from the Icelandic and NWT samples of *A. fumigatus* are consistent with previous findings. Specifically, we observed both allele and genotype-sharing between these two regions but also found an overall significant genetic differentiation both between these two arctic samples as well as between the arctic samples and the geographic populations from other regions of the world.

At present, while the close relationship between the NWT and Norwegian samples might be due to similar selection pressure, the reasons for the low/nonsignificant level of differentiation between Icelandic *A. fumigatus* population and those from Belgium, France, and Indian populations as well as between the NWT *A. fumigatus* population and the New Zealand population are unknown. As previously discussed by Korfanty et al. (2019), two types of factors may contribute to gene flow between distant countries. The first type is natural factors such as wind. However, given the geographic distance between most of these areas, while possible, direct wind-aided dispersal of *A. fumigatus* conidia is unlikely, especially across hemispheres such as between New Zealand and NWT in Canada (~12,694 km). The second type is anthropogenic factors such as human travel and commercial trade. For both Iceland and NWT, the European Union is a major exporter and importer of goods to and from both regions, contributing to 30% of exports from NWT and 53% of Iceland's total trade in goods in 2019 (Library of Parliament, accessed on 21 November 2021; European Commission, accessed on 21 November 2021). Similarly, India was the top importer of NWT goods in 2019, where Asian specific exports from NWT began to increase in 2011. Within Iceland in 2019, 682,700 tourists (34.4%) originated from the European Union (Iceland Tourist Board, accessed on 21 November 2021). Similarly, Yellowknife in NWT has been a popular destination for observing northern lights, which have attracted tourists from around the world, including from many Asian countries such as China and India. However, the number of tourists from all destinations declined substantially since the start of the SARS-Covid-19 pandemic. Given the resilience of *A. fumigatus* spores to a variety of environmental stressors and their abundance within the atmosphere (Kwon-Chung

& Sugui, 2013), spores could have followed these anthropogenic routes and migrated to and from Iceland and NWT.

One triazole resistant *A. fumigatus* strain was identified in the NWT population. This triazole-resistant strain contained the TR_{34}/L98H mutation in the *cyp51A* gene. This mutation has been reported from environmental and clinical samples from many countries (Berger et al., 2017; Etienne et al., 2021; Fan et al., 2020; Wu et al., 2015), including the selective sweep observed in a widespread Indian genotype of *A. fumigatus* in 2012 (Chowdhary et al., 2012). The resistant strain identified in our study had a near identical MLG to the Indian population. However, how the strain migrated into the NWT region is unclear. A recent long distance dispersal event may have occurred, which introduced this strain to NWT from India, potentially by an anthropogenic event. Unfortunately, the lack of clinical research on *A. fumigatus* and aspergillosis within both Iceland and Northern regions in Canada makes it difficult to determine the clinical significance of triazole-resistant aspergillosis in both northern regions and the potential relationship between the triazole-resistant strain isolated here from the soil and the clinical strains of *A. fumigatus* in NWT. Systematic analyses of clinical aspergillosis and susceptibility testing of the strains responsible for such infections in both regions are needed in order to assess the frequency of triazole-resistant aspergillosis and the relationship between environmental and clinical populations of *A. fumigatus* in both Iceland and Northern Canada.

3.5 Conclusions

This study investigated the population structure of the opportunistic fungal pathogen *A. fumigatus* obtained from northern climates above 60° latitude. Prior to this study, limited isolation and genotypic data has been described from soil environments in these northern regions (Land et al., 1989; Schuerger & Lee, 2015; Viegas et al., 2020). Here we characterized *A. fumigatus* diversity present within Iceland and Northwest Territories in Canada. Our study revealed significant genetic diversity with evidence of both clonal and sexual reproduction within both regional populations. While evidence for gene flow was found between these two regional arctic populations as well as between them and other

geographic populations, unique alleles and genotypes were also found in both arctic populations. The finding of a triazole-resistant strain from the arctic with a nearly identical genotype to strains in India demonstrates the complexity of managing drug resistance in *A. fumigatus*. Our study highlights the importance of both genetically characterizing *A. fumigatus* populations from a diversity of geographic and ecological niches and identifying the level of triazole susceptibility within these populations to help track the spread of drug-resistant strains. Indeed, the discovery of high genetic diversity in cold environments coupled with the known high-temperature tolerance of *A. fumigatus* calls for greater effort for understanding the thermo-adaptability of this organism, with implications even for space travel and contamination of Mars from the Mars missions (Schuerger & Lee, 2015; Wong Sak Hoi et al., 2012).

3.6 Author Contributions

Conceptualization, J.X.; methodology, G.A.K.; software, G.A.K.; formal analysis, G.A.K.; investigation, G.A.K. and M.D.; resources, H.J., H.Y. and J.X.; writing—original draft preparation, G.A.K.; writing—review and editing, G.A.K., M.D., H.J., H.Y. and J.X.; visualization, G.A.K.; supervision, J.X.; project administration, J.X.; funding acquisition, J.X. and G.A.K. All authors have read and agreed to the published version of the manuscript.

3.7 Funding

This research was supported by grants from the Natural Sciences and Engineering Research Council of Canada (Grant No. CRDPJ 474638-14), and by the Institute of Infectious Diseases Research (IIDR) Antibiotic Resistance Initiative and the Faculty of Science's Global Science Initiative of McMaster University. The APC was funded by IIDR. G.A.K. is supported by MITACS and NSERC PGS-D Scholarships.

3.8 Conflicts of Interest

The authors declare no conflict of interest. The funders had no role in the design of the study; in the collection, analyses, or interpretation of data; in the writing of the manuscript, or in the decision to publish the results.

3.9 References

Abdolrasouli, A., Petrou, M. A., Park, H., Rhodes, J. L., Rawson, T. M., Moore, L. S. P., Donaldson, H., Holmes, A. H., Fisher, M. C., & Armstrong-James, D. (2018). Surveillance for azole-resistant *Aspergillus fumigatus* in a centralized diagnostic mycology service, London, United Kingdom, 1998–2017. *Frontiers in Microbiology*, *9*(SEP), 2234. https://doi.org/10.3389/fmicb.2018.02234

Agapow, P.-M., & Burt, A. (2001). Indices of multilocus linkage disequilibrium. *Molecular Ecology Notes*, *1*(1–2), 101–102. https://doi.org/10.1046/j.1471-8278.2000.00014.x

Alexander, B. D., Procop, G. W., Dufresne, P., Espinel-Ingroff, A., Fuller, J., Ghannoum, M. A., Hanson, K. E., Holliday, D., Holliday, N. M., Ostrosky-Zeichner, L., Schuetz, A. N., Wiederhold, N. P., & Zelazny, A. M. (2017). Reference method for broth dilution antifungal susceptibility testing of filamentous fungi. 3rd ed. *Clinical and Laboratory Standards Institute*, *37*(15).

Ashu, E. E., Hagen, F., Chowdhary, A., Meis, J. F., & Xu, J. (2017). Global population genetic analysis of *Aspergillus fumigatus*. *MSphere*, *2*(1), e00019-17. https://doi.org/10.1128/mSphere.00019-17

Ashu, E. E., Kim, G. Y., Roy-Gayos, P., Dong, K., Forsythe, A., Giglio, V., Korfanty, G., Yamamura, D., & Xu, J. (2018). Limited evidence of fungicide-driven triazole-resistant *Aspergillus fumigatus* in Hamilton, Canada. *Canadian Journal of Microbiology*, *64*(2), 119–130. https://doi.org/10.1139/cjm-2017-0410

Ashu, E. E., Korfanty, G. A., & Xu, J. (2017). Evidence of unique genetic diversity in *Aspergillus fumigatus* isolates from Cameroon. *Mycoses*, *60*(11), 739–748. https://doi.org/10.1111/myc.12655

Astvad, K. M. T., Jensen, R. H., Hassan, T. M., Mathiasen, E. G., Thomsen, G. M., Pedersen, U. G., Christensen, M., Hilberg, O., & Arendrup, M. C. (2014). First detection of TR46/Y121F/T289A and TR34/L98H alterations in *Aspergillus fumigatus* isolates from azole-naive patients in Denmark despite negative findings in the environment. *Antimicrobial Agents and Chemotherapy*, *58*(9), 5096–5101. https://doi.org/10.1128/AAC.02855-14

Barrès, B., Halkett, F., Dutech, C., Andrieux, A., Pinon, J., & Frey, P. (2008). Genetic

structure of the poplar rust fungus *Melampsora larici-populina*: Evidence for isolation by distance in Europe and recent founder effects overseas. *Infection, Genetics and Evolution*, *8*(5), 577–587. https://doi.org/10.1016/J.MEEGID.2008.04.005

Berger, S., El Chazli, Y., Babu, A. F., & Coste, A. T. (2017). Azole resistance in *Aspergillus fumigatus*: A consequence of antifungal use in agriculture? *Frontiers in Microbiology*, *8*, 1024. https://doi.org/10.3389/fmicb.2017.01024

Bongomin, F., Gago, S., Oladele, R., & Denning, D. (2017). Global and multi-national prevalence of fungal diseases—Estimate precision. *Journal of Fungi*, *3*(4), 57. https://doi.org/10.3390/jof3040057

Bueid, A., Howard, S. J., Moore, C. B., Richardson, M. D., Harrison, E., Bowyer, P., & Denning, D. W. (2010). Azole antifungal resistance in *Aspergillus fumigatus*: 2008 and 2009. *Journal of Antimicrobial Chemotherapy*, *65*(10), 2116–2118. https://doi.org/10.1093/jac/dkq279

Chowdhary, A., Kathuria, S., Xu, J., & Meis, J. F. (2013). Emergence of azole-resistant *Aspergillus fumigatus* strains due to agricultural azole use creates an increasing threat to human health. *PLoS Pathogens*, *9*(10). https://doi.org/10.1371/journal.ppat.1003633

Chowdhary, A., Kathuria, S., Xu, J., Sharma, C., Sundar, G., Singh, P. K., Gaur, S. N., Hagen, F., Klaassen, C. H., & Meis, J. F. (2012). Clonal expansion and emergence of environmental multiple-triazole-resistant *Aspergillus fumigatus* strains carrying the TR34/L98H mutations in the *cyp51A* gene in India. *PLoS ONE*, *7*(12), e52871. https://doi.org/10.1371/journal.pone.0052871

Dauchy, C., Bautin, N., Nseir, S., Reboux, G., Wintjens, R., Le Rouzic, O., Sendid, B., Viscogliosi, E., Le Pape, P., Arendrup, M. C., Gosset, P., Fry, S., & Fréalle, E. (2018). Emergence of *Aspergillus fumigatus* azole resistance in azole-naïve patients with chronic obstructive pulmonary disease and their homes. *Indoor Air*, *28*(2), 298–306. https://doi.org/10.1111/INA.12436

de Valk, H. A., Meis, J. F. G. M., Curfs, I. M., Muehlethaler, K., Mouton, J. W., & Klaassen, C. H. W. (2005). Use of a novel panel of nine short tandem repeats for exact and high-resolution fingerprinting of *Aspergillus fumigatus* isolates. *Journal of Clinical Microbiology*, *43*(8), 4112–4120. https://doi.org/10.1128/JCM.43.8.4112-4120.2005

Diao, Y., Zhang, C., Xu, J., Lin, D., Liu, L., Mtung'e, O. G., & Liu, X. (2015). Genetic differentiation and recombination among geographic populations of the fungal pathogen *Colletotrichum truncatum* from chili peppers in China. *Evolutionary Applications*, *8*(1), 108–118. https://doi.org/10.1111/EVA.12233

Dockrell, D. H. (2008). Salvage therapy for invasive aspergillosis. *Journal of Antimicrobial Chemotherapy*, *61*(Supplement 1), i41–i44. https://doi.org/10.1093/jac/dkm426

Etienne, K. A., Berkow, E. L., Gade, L., Nunnally, N., Lockhart, S. R., Beer, K., King Jordan, I., Rishishwar, L., & Litvintseva, A. P. (2021). Genomic diversity of azole-resistant *Aspergillus fumigatus* in the united states. *MBio*, *12*(4). https://doi.org/10.1128/MBIO.01803-21

European Commission. (2021, 21 November). *EU trade by country/region*. https://ec.europa.eu/trade/policy/countries-and-regions/countries/iceland/.

Fan, Y., Wang, Y., & Xu, J. (2020). Comparative genome sequence analyses of geographic samples of *Aspergillus fumigatus*—Relevance for Amphotericin B Resistance. *Microorganisms*, *8*(11), 1673. https://doi.org/10.3390/microorganisms8111673

Goor, R. M., Neall, L. F., Hoffman, D., & Sherry, S. T. (2011). A mathematical approach to the analysis of multiplex DNA profiles. *Bulletin of Mathematical Biology*, *73*(8), 1909. https://doi.org/10.1007/S11538-010-9598-0

Iceland Tourist Board. (2021, November 21). *Numbers of foreign visitors*. https://www.ferdamalastofa.is/en/recearch-and-statistics/numbers-of-foreign-visitors.

Jombart, T., & Ahmed, I. (2011). adegenet 1.3-1: new tools for the analysis of genome-wide SNP data. *Bioinformatics*, *27*(21), 3070–3071. https://doi.org/10.1093/bioinformatics/btr521

Kamvar, Z. N., Tabima, J. F., & Grünwald, N. J. (2014). *Poppr* : an R package for genetic analysis of populations with clonal, partially clonal, and/or sexual reproduction. *PeerJ*, *2*, e281. https://doi.org/10.7717/peerj.281

Korfanty, G. A., Teng, L., Pum, N., & Xu, J. (2019). Contemporary gene flow is a major force shaping the *Aspergillus fumigatus* population in Auckland, New Zealand. *Mycopathologia*, *184*(4), 479–492. https://doi.org/10.1007/s11046-019-00361-8

Kumar, S., Stecher, G., Li, M., Knyaz, C., & Tamura, K. (2018). MEGA X: Molecular

evolutionary genetics analysis across computing platforms. *Molecular Biology and Evolution*, *35*(6), 1547. https://doi.org/10.1093/molbev/msy096

Kwon-Chung, K. J., & Sugui, J. A. (2013). *Aspergillus fumigatus*--what makes the species a ubiquitous human fungal pathogen? *PLoS Pathogens*, *9*(12), e1003743. https://doi.org/10.1371/journal.ppat.1003743

Land, C. J., Sostaric, B., Fuchs, R., Lundstrom, H., & Hult, K. (1989). Intratracheal exposure of rats to *Aspergillus fumigatus* spores isolated from sawmills in Sweden. *Applied and Environmental Microbiology*, *55*(11), 2856–2860. https://doi.org/10.1128/aem.55.11.2856-2860.1989

Library of Parliament. (2021, November 21) *Northwest Territories' Merchandise Trade with the World*. https://lop.parl.ca/sites/PublicWebsite/default/en_CA/ResearchPublications/TradeAndInvestment/2020517E

Liu, M., Zheng, N., Li, D., Zheng, H., Zhang, L., Ge, H., & Liu, W. (2016). *cyp51A* based mechanism of azole resistance in *Aspergillus fumigatus* : Illustration by a new 3D Structural Model of *Aspergillus fumigatus* CYP51A protein. *Medical Mycology*, *54*(4), 400–408. https://doi.org/10.1093/mmy/myv102

Mellado, E., Diaz-Guerra, T. M., Cuenca-Estrella, M., & Rodriguez-Tudela, J. L. (2001). Identification of two different 14-α sterol demethylase- related genes (cyp51A and cyp51B) in *Aspergillus fumigatus* and other *Aspergillus* species. *Journal of Clinical Microbiology*, *39*(7), 2431–2438. https://doi.org/10.1128/JCM.39.7.2431-2438.2001/

Moye-Rowley, W. S. (2015). Multiple mechanisms contribute to the development of clinically significant azole resistance in *Aspergillus fumigatus*. *Frontiers in Microbiology*, *6*, 70. https://doi.org/10.3389/fmicb.2015.00070

Paoletti, M., Rydholm, C., Schwier, E. U., Anderson, M. J., Szakacs, G., Lutzoni, F., Debeaupuis, J.-P., Latgé, J.-P., Denning, D. W., & Dyer, P. S. (2005). Evidence for sexuality in the opportunistic fungal pathogen *Aspergillus fumigatus*. *Current Biology*, *15*(13), 1242–1248. https://doi.org/10.1016/J.CUB.2005.05.045

Peakall, R., & Smouse, P. E. (2006). genalex 6: genetic analysis in Excel. Population genetic software for teaching and research. *Molecular Ecology Notes*, *6*(1), 288–295.

https://doi.org/10.1111/j.1471-8286.2005.01155.x

Peakall, R., & Smouse, P. E. (2012). GenAlEx 6.5: genetic analysis in Excel. Population genetic software for teaching and research--an update. *Bioinformatics (Oxford, England)*, *28*(19), 2537–2539. https://doi.org/10.1093/bioinformatics/bts460

Pelaez, T., Monteiro, M. C., Garcia-Rubio, R., Bouza, E., Gomez-Lopez, A., & Mellado, E. (2015). First detection of *Aspergillus fumigatus* azole-resistant strain due to Cyp51A TR46/Y121F/T289A in an azole-naive patient in Spain. *New Microbes and New Infections*, *6*, 33–34. https://doi.org/10.1016/J.NMNI.2015.04.005

Ren, J., Jin, X., Zhang, Q., Zheng, Y., Lin, D., & Yu, Y. (2017). Fungicides induced triazole-resistance in *Aspergillus fumigatus* associated with mutations of TR46/Y121F/T289A and its appearance in agricultural fields. *Journal of Hazardous Materials*, *326*, 54–60. https://doi.org/10.1016/j.jhazmat.2016.12.013

Resendiz Sharpe, A., Lagrou, K., Meis, J. F., Chowdhary, A., Lockhart, S. R., & Verweij, P. E. (2018). Triazole resistance surveillance in *Aspergillus fumigatus*. *Medical Mycology*, *56*(suppl_1), S83–S92. https://doi.org/10.1093/mmy/myx144

Schuerger, A. C., & Lee, P. (2015). Microbial ecology of a crewed rover traverse in the arctic: Low microbial dispersal and implications for planetary protection on human mars missions. *Astrobiology*, *15*(6), 478–491. https://doi.org/10.1089/AST.2015.1289

Sewell, T. R., Zhu, J., Rhodes, J., Hagen, F., Meis, J. F., Fisher, M. C., & Jombart, T. (2019). Nonrandom distribution of azole resistance across the global population of *Aspergillus fumigatus*. *MBio*, *10*(3), e00392-19. https://doi.org/10.1128/mBio.00392-19

Stensvold, C. R., Jørgensen, L. N., & Arendrup, M. C. (2012). Azole-Resistant invasive aspergillosis: Relationship to agriculture. *Current Fungal Infection Reports*, *6*(3), 178–191. https://doi.org/10.1007/s12281-012-0097-7

Verweij, P. E., Lucas, J. A., Arendrup, M. C., Bowyer, P., Brinkmann, A. J. F., Denning, D. W., Dyer, P. S., Fisher, M. C., Geenen, P. L., Gisi, U., Hermann, D., Hoogendijk, A., Kiers, E., Lagrou, K., Melchers, W. J. G., Rhodes, J., Rietveld, A. G., Schoustra, S. E., Stenzel, K., … Fraaije, B. A. (2020). The one health problem of azole resistance in *Aspergillus fumigatus*: current insights and future research agenda. In *Fungal Biology Reviews* (Vol. 34, Issue 4, pp. 202–214). Elsevier Ltd.

https://doi.org/10.1016/j.fbr.2020.10.003

Viegas, C., Almeida, B., Aranha Caetano, L., Afanou, A., Straumfors, A., Veríssimo, C., Gonçalves, P., & Sabino, R. (2020). Algorithm to assess the presence of *Aspergillus fumigatus* resistant strains: The case of Norwegian sawmills. *Https://Doi.Org/10.1080/09603123.2020.1810210*. https://doi.org/10.1080/09603123.2020.1810210

Wong Sak Hoi, J., Beau, R., & Latgé, J. P. (2012). A novel dehydrin-like protein from *Aspergillus fumigatus* regulates freezing tolerance. *Fungal Genetics and Biology*, *49*(3), 210–216. https://doi.org/10.1016/J.FGB.2012.01.005

Wu, C.-J., Wang, H.-C., Lee, J.-C., Lo, H.-J., Dai, C.-T., Chou, P.-H., Ko, W.-C., & Chen, Y.-C. (2015). Azole-resistant *Aspergillus fumigatus* isolates carrying TR_{34}/L98H mutations in Taiwan. *Mycoses*, *58*(9), 544–549. https://doi.org/10.1111/myc.12354

Xu, J. (2021). Is natural population of *Candida tropicalis* sexual, parasexual, and/or asexual? *Frontiers in Cellular and Infection Microbiology*, *0*, 1066. https://doi.org/10.3389/FCIMB.2021.751676

Zhang, M., Feng, C.-L., Chen, F., He, Q., Su, X., & Shi, Y. (2017). Triazole resistance in *Aspergillus fumigatus* clinical isolates obtained in Nanjing, China. *Chinese Medical Journal*, *130*(6), 665–668. https://doi.org/10.4103/0366-6999.201609

Zhou, D., Korfanty, G. A., Mo, M., Wang, R., Li, X., Li, H., Li, S., Wu, J.-Y., Zhang, K.-Q., Zhang, Y., & Xu, J. (2021). Extensive genetic diversity and widespread azole resistance in greenhouse populations of *Aspergillus fumigatus* in Yunnan, China. *MSphere*, *6*(1). https://doi.org/10.1128/

Zhou, D., Wang, R., Li, X., Peng, B., Yang, G., Zhang, K. Q., Zhang, Y., & Xu, J. (2021). Genetic Diversity and azole resistance among natural *Aspergillus fumigatus* populations in Yunnan, China. *Microbial Ecology*, 1–17. https://doi.org/10.1007/S00248-021-01804-W/

Chapter 4

What in Earth? Analyses of a Global Soil Population of *Aspergillus fumigatus*

Abstract *Aspergillus fumigatus* is a globally distributed mold and a major cause of opportunistic infections in humans. Each year, over 200,000 people die from *A. fumigatus* infections and the number is increasing mainly due to the increasing numbers of susceptible hosts and drug-resistant infections. Because most infections are from environmental exposure, it's critical to understand environmental populations of *A. fumigatus*. Soil is a major ecological niche for *A. fumigatus*. In this study, we analyzed 1303 soil isolates from 69 locations in 11 countries on 6 continents. All isolates were genotyped using nine microsatellite markers. Our results indicated high genotypic diversities within most local and national soil populations. Comparisons with clinical isolates at national and continental levels revealed that overall, the soil population of *A. fumigatus* had a higher genetic diversity than those from patients. Similar to those found among clinical populations of *A. fumigatus*, low but statistically significant genetic differentiations were found among soil populations from different geographic regions, with relatively similar proportions of strains and genotypes belonging to two large genetic clusters. However, differences were found among geographic regions in the relationships between soil and clinical populations of *A. fumigatus*. Of the 1303 soil isolates analyzed here, 63 were resistant to triazole antifungals. Most triazole-resistant soil isolates in this study were from India and Europe, with few or no triazole-resistant isolates recovered from most other geographic regions. We discuss the implications of our results to the evolution and epidemiology of *A. fumigatus*.

Importance Aspergillosis is an opportunistic infection predominately caused by the ubiquitous mold *Aspergillus fumigatus*. Aspergillosis primarily occurs in immunocompromised patients, where treatment involves the use of antifungal drugs, however, resistance has been increasingly reported. Almost all *A. fumigatus* infections occur

as a result of the inhalation of spores from the environment. Therefore, it's important to understand the environmental populations of this species. Here, we analyzed 1303 *A. fumigatus* strains from natural, agricultural, and urban soils obtained from 11 countries on 6 continents, and when possible, compared with corresponding clinical populations of *A. fumigatus*. Our analyses several broad features of soil populations of *A. fumigatus*, including high genetic diversity and evidence of gene flow within and among most local populations. Our results highlight the extraordinary nature of *A. fumigatus* populations to quickly spread and adapt across diverse regions.

This chapter has been submitted to mSphere. The format of the chapter therefore follows the mSphere format. I am the first author of this work.

4.1 Introduction

Aspergillus fumigatus is a saprophytic mold distributed ubiquitously around the world. The global presence of *A. fumigatus* can be attributed to this mold's many morphological characteristics and adaptations. These traits include (i) its broad thermo-adaptability, including growth at temperatures above 50°C; (ii) its small and abundant asexual spores, the conidia; and (iii) its ability to grow in many natural niches such as soil, plant wastes such as compost heaps (Kwon-Chung & Sugui, 2013; Xu, 2022). Within these niches, *A. fumigatus* can propagate through both sexual and asexual reproduction. Through asexual means, millions of highly volatile conidia are released into the atmosphere, capable of spreading to remote geographic areas around the world (Kwon-Chung & Sugui, 2013). Through sexual means, highly fit strains may be produced and quickly spread adaptive mutations through local populations (Auxier et al., 2022; Barber et al., 2021; Lofgren et al., 2022; O'Gorman et al., 2009). The high atmospheric prevalence, small conidial size, and thermophilicity aid *A. fumigatus* strains in causing opportunistic infections in humans. These infections, collectively termed aspergillosis, impact eight million people worldwide each year and led to *A. fumigatus* being recently classified into the critical priority group of fungal pathogens by the WHO (WHO, 2022). Aspergillosis primarily occur in individuals with immunodeficiencies or with previous lung abnormalities caused by asthma, cystic fibrosis,

or tuberculosis. The most serious form, invasive aspergillosis has a mortality rate between 40-95% (Kwon-Chung & Sugui, 2013; Xu, 2022). Treatment and prophylaxis against aspergillosis infections mainly involve triazole antifungal drugs, however triazole resistant strains are increasingly burdening medical centres around the world (Meis et al., 2016).

In recent years, triazole-resistant strains of *A. fumigatus* have been observed within both clinical and environmental niches around the world. Compounding this, triazole naïve patients have become more likely to be infected with a triazole-resistant *A. fumigatus* strain. At present, there is limited evidence for person-to-person transmission of *A. fumigatus* as most infections originate from environmental sources (Burks et al., 2021). Thus, understanding environmental sources of triazole resistance is very important for limiting clinical triazole resistance. Many studies have investigated the structure of *A. fumigatus* populations to identify prevalence of drug-resistant genotypes with clinical and environmental populations, as well as determine the level of geneflow within and among these populations. These populations include medical centres, sawmills, and plant bulb cultivation facilities where triazole are commonly used and/or where bioaccumulation of triazoles occur (Abdolrasouli et al., 2018; Alvarez-Moreno et al., 2017; Barber et al., 2020; Chowdhary, et al., 2012a; Jeanvoine et al., 2017; Rocchi et al., 2021). Within these populations, triazole-resistant strains have been detected, likely due to independent selection pressures exerted by triazoles in their respective environments. Concerningly, mutations conferring resistance are very diverse but with certain mutations highly prevalent within environmental populations. For example, a TR_{34} L98H mutation in the lanosterol 14α-demethylase is observed to manifest in niches with high triazole use (Burks et al., 2021). Furthermore, triazole-resistant strains with highly similar or identical genotypes have been found in distant geographic locations, suggesting long-distance gene flow between populations (Korfanty et al., 2021; Sharma et al., 2015).

Given the ability for *A. fumigatus* to thrive in many ecological niches and its propensity to spread across distant geographic areas, it's surprising that *A. fumigatus* populations often show significant genetic differentiation (Ashu, et al., 2017a; Korfanty et al., 2019; Zhou et

al., 2021). Normally, the ancestral population of an organism is expected to contain higher genotypic diversity than recently derived populations. For example, in the study by Simwami et al., (2011), a migrant Asian population of *Cryptococcus neoformans* had lower allelic and genotypic diversity compared to Africa, the center of origin of *C. neoformans*. This pattern is also seen in other fungal pathogens such as the wheat yellow rust pathogen *Puccinia striiformis* f.sp. *tritici* (Ali et al., 2014). For opportunistic human pathogens with extensive environmental reservoirs, the environmental population often serve as the source of the clinical population causing human infections. Therefore, the clinical population likely represents a subpopulation of the environmental population and with reduced allelic and genotypic diversities (Firacative et al., 2016; Muller & McCusker, 2009). However, depending on the mode of reproduction, environmental populations may have a higher proportion of clonal genotypes which may contribute to lower estimates of allelic and genotypic diversities. In addition, clinical and environmental populations may experience different selection pressures, such as differential antibiotic usages between clinics and environmental settings, could influence the observed diversities between these two niches.

In population genetic and epidemiological studies of *A. fumigatus*, a panel of nine highly polymorphic short tandem repeat (STR) loci are commonly used to compare and analyze the genotypic relationships among *A. fumigatus* strains and populations. These nine loci have helped reveal genetic differentiation and gene flow among *A. fumigatus* populations (Ashu et al., 2018; Ashu, et al., 2017a; Chowdhary, et al., 2012b; Korfanty et al., 2019, 2021). These analyses identified two large *A. fumigatus* genetic clusters, with one cluster having a higher abundance of triazole resistant strains and the other containing more triazole susceptible strains (Sewell et al., 2019). The presence of such distinct genetic clusters and the biased distributions of triazole-resistant strains between clusters were also observed based on whole-genome sequence analyses (Fan et al., 2020; Rhodes et al., 2022).

Soil is a significant ecological niche for *A. fumigatus* and several previous studies have reported the genetic diversity of *A. fumigatus* from a few geographic locations, including Cameroon, Auckland (New Zealand), Iceland, Yunnan (China), and Hamilton and the

Northwest Territories (Canada) (Ashu et al., 2018; Korfanty et al., 2019, 2021; Zhou et al., 2021). These studies revealed both shared and unique alleles and genotypes within each geographic population. However, a global analysis of soil populations of *A. fumigatus* from multiple continents have not been performed. In addition, how the global soil population of *A. fumigatus* might differ from the global clinical populations remains to be determined. To address these issues, we obtained 826 new *A. fumigatus* isolates from 4357 soil samples from six countries on four continents. These new soil populations were combined with our previously published 477 soil isolates from six countries on four continents for a global analysis. Given the different ecological niches in patient's body vs in soil, we hypothesize that populations of *A. fumigatus* may differ between these two niches. However, given that patients acquire pathogens from environmental sources and soil being a major source of *A. fumigatus*, we hypothesize that the soil population may have a higher allelic and genotypic diversities than clinical population.

4.2 Results

4.2.1 Isolation of *A. fumigatus* from global soils

The *A. fumigatus* isolates obtained and analyzed in this study are summarized in Table 5.1. In total, this study obtained 822 new *A. fumigatus* isolates from 4176 soil samples from across 37 locations spread among 6 countries. Each new isolate was genotyped at nine STR loci. In addition, we included 481 soil isolates previously reported from our lab. Those 481 isolates were from Hamilton and Northwest Territories in Canada, Auckland in New Zealand, Iceland, various locations in India, the Netherlands, and Cameroon (Ashu et al., 2018; Ashu, et al., 2017a; Korfanty et al., 2019, 2021). Overall, our analyzed global soil population of *A. fumigatus* contained a total of 1303 isolates belonging to 978 multilocus genotypes (MLGs), of which 91 were each represented by two or more isolates and 887 were each represented by a single isolate (Table 5.2).

Table 4.1: The number of soil samples and *A. fumigatus* isolates collected across 6 continents and 11 countries.

Continent	Country	Region	Soil Samples	*A. fumigatus* isolated	reference
Africa	Cameroon	Northwest	201	7 †	(Ashu, et al., 2017b)
		Litoral	47	1 †	
		Centre	246	42 †	
		Total	494	51	
Asia	China	Ailao Mountain	100	17 *	(Samarasinghe et al., 2021)
		Fenyi	100	34 *	
		Taihang Mountains	32	15 *	
		Pangquangou	32	12 *	
		Total	264	78	
	India		NA	74 *†	(Ashu, et al., 2017a)
	Saudi Arabia	West	346	68 *	(Aljohani et al., 2018)
		East	56	0 *	
		South	32	0 *	
		Total	434	68	
	Continental Total		698	220	
Europe	France	Nice	250	51 *	(Samarasinghe et al., 2021)
		Hyeres	100	18 *	
		Total	350	69	
	Iceland	Dimmuborgir	60	1 †	(Korfanty et al., 2021)
		Thingvellir	51	8 †	
		Skaftafell	52	6 †	
		Myvatn Lake	42	10 †	
		Landbrotalaug	60	1 †	
		Reykjavik University	49	6 †	
		Total	314	32	
	Netherlands		NA	44 *†	(Ashu, et al., 2017a)
	Continental Total		664	145	
North/Central America	Canada	Central	1381	235 *†	(Ashu et al., 2018)
		Eastern	310	124	
		Northwest Territories	220	52 †	
		Western	1340	337	
		Total	3251	748	

	Costa Rica	Alajuela	154	4 *	(Samarasinghe et al., 2021)
		Guanacaste	101	0 *	
		Puntarenas	133	2 *	
		Total	388	6	
	Continental Total		3639	754	
Oceania	New Zealand	Auckland Domain	100	20 †	(Korfanty et al., 2019)
		Mount Eden	110	13 †	
		Trusts Arena	100	14 †	
		Millenium Field	100	20 †	
		University of Auckland	100	17 †	
		Auckland Rail station	100	20 †	
		Total	610	104	
South America	Peru	Rainbow Mountain	110	6 *	(Samarasinghe et al., 2021)
		Lima	100	7 *	
		Sacred Valley	100	16 *	
		Amazon	100	0 *	
		Machu Pichu	20	0 *	
		Cusco	60	0 *	
		Total	490	29	
Grand Total			6595	1303	

Table 4.2: Summary of soil-derived *A. fumigatus* multilocus genotypes (MLGs) among continents and countries

Continent	Country	Subpopulation	Number of isolates	Number of MLGs	MLGs represented by 2 or more isolates
Africa	Cameroon		51	45	4
Asia	China		78	23	2
	India		74	16	4
	Saudi Arabia		68	19	6
	Total		220	58	12
Europe	France		69	68	1
	Iceland		32	21	4
	Netherlands		44	39	2
	Total		145	128	7
North/Central America	Canada	Central	235	188	9
		Eastern	124	92	14
		Northern	52	40	8

		Western	337	300	26
		Total	748	620	64
	Costa Rica		6	6	0
	Total		754	626	64
Oceania	New Zealand		104	100	4
South America	Peru		29	27	2
World Total			1303	978	91

4.2.2 Allelic diversity and private alleles among the soil populations

To compare our soil populations of *A. fumigatus* to one another, we stratified the soil populations first by continent and second by country. Additionally, due to the size and geographic diversity of the Canadian samples in our collection that spanned across the country, we compared the regional populations across Canada, with isolates grouped into four regional subpopulations: Western (British Columbia and Alberta), Northern (Northwest Territories), Central (Ontario and Quebec), and Eastern (New Brunswick and Prince Edward Island).

Allelic diversities for the nine loci varied among national and continental populations stratified (Table 4.3). Using ANOVA, we identified significant differences between the haploid diversity across the 9 loci among both continents and countries (p-value = 1.86×10^{-8} and 4.31×10^{-37} respectively). Among continents, Asia and Europe were observed to have the lowest and highest haploid diversity respectively (uh = 0.731 and 0.899 respectively). Haploid diversity among countries was considerably more variable than among continents. China, Saudi Arabia, and India had lower haploid diversity (0.387, 0.416, and 0.478 respectively) than other countries, where New Zealand had the highest (0.887). After clone correction, where each STR genotype within each stratified population was reduced to one representative strain, ANOVA identified that continents maintained significant differentiation in haploid diversity, however, no significant difference was seen among countries (p-value = 0.008 and 0.173 respectively). Among the four Canadian regional populations, there was no significant difference in haploid diversity in either the full or the clone-corrected dataset (p-value = 0.236 and 0.124 respectively).

Table 4.3: Summary of haploid diversity and private alleles among continental and national soil populations of *A. fumigatus* across nine STR loci. In addition, four Canadian regional populations were also included.

Continent	Country	Region	Shannon's Index	Na[1] (NP[2])	Uh[3] (± SE[4])	Clone Corrected Uh (± SE)
Africa	Cameroon		0.95	96 (3)	0.755 (0.025)	0.787 (0.029)
Asia	China		0.45	96 (4)	0.387 (0.014)	0.879 (0.017)
	India		0.52	77 (2)	0.478 (0.015)	0.861 (0.037)
	Saudi Arabia		0.501	78 (0)	0.416 (0.038)	0.838 (0.027)
	Total		0.83	157 (6)	0.731 (0.023)	0.883 (0.019)
Europe	France		0.997	147 (3)	0.875 (0.019)	0.875 (0.019)
	Iceland		0.935	70 (2)	0.804 (0.025)	0.818 (0.046)
	Netherlands		0.988	118 (4)	0.866 (0.018)	0.881 (0.017)
	Total		0.995	199 (9)	0.899 (0.013)	0.9 (0.017)
North America	Canada	Central	0.975	258 (69)	0.888 (0.015)	0.916 (0.016)
		Eastern	0.997	157 (3)	0.852 (0.027)	0.850 (0.029)
		Northern	0.988	115 (2)	0.819 (0.030)	0.837 (0.029)
		Western	0.999	231 (42)	0.795 (0.050)	0.815 (0.046)
		Total	0.996	323 (73)	0.870 (0.022)	0.882 (0.021)
	Costa Rica		1	39 (1)	0.874 (0.042)	0.874 (0.042)
	Total		0.996	324 (76)	0.874 (0.023)	0.900 (0.014)
Oceania	New Zealand		0.997	177 (6)	0.887 (0.021)	0.889 (0.021)
South America	Peru		0.995	104 (1)	0.896 (0.013)	0.897 (0.014)
World Total			0.993	362	0.840 (0.012)	0.868 (0.010)

[1] Na = number of unique alleles across 9 loci; [2] NP = Number of private alleles; [3] Uh = unbiased diversity = $(N/(N-1)) \times (1-\Sigma p_i^2)$ where p_i is the frequency of the ith allele for the population; [4] SE = Standard error

4.2.3 Linkage disequilibrium among the soil populations

To investigate the clonality and recombination across the *A. fumigatus* soil populations, we calculated the phylogenetic compatibility and standardised index of association ($\bar{r}_d$) respectively among continents and countries (Table 4.4). From our initial observations, China, Saudi Arabia, and the Quebec region in the central Canadian subpopulation were dominated by clonal MLGs (21, 15, and 7 unique MLGs were present respectively) where the most prevalent MLG was represented by 57, 48, and 38 isolates within China, Saudi Arabia, and Quebec respectively. The dominant clonal MLGs were unique to each region.

Across the non-clone corrected continental and country populations, $\bar{r}_d$ values and linkage disequilibrium tests rejected the null hypothesis of random recombination among alleles at different loci in all populations. The $\bar{r}_d$ values ranged from 0.065 for the Peruvian and French populations to 0.851 for the Indian population. The departure from random recombination was maintained in the clone-corrected dataset, except for India (p-value = 0.137). In this clone-corrected dataset, the $\bar{r}_d$ values ranged from 0.025 within India to 0.258 within Cameroon. However, all populations, except for Costa Rica, showed evidence of phylogenetic incompatibility, consistent with some level of recombination within each national population. With regards to the Canadian subpopulations, $\bar{r}_d$ values ranged from 0.098 (Eastern) to 0.241 (Central) and 0.051 (Central) to 0.117 (Northern) within the full and clone corrected datasets respectively, all rejecting the null hypothesis of random recombination within individual populations (Table 4.4). Similar to other national populations, across all Canadian subpopulations, the hypothesis for complete clonality was also rejected. Overall, these results indicate that soil populations of *A. fumigatus* across the global contains signatures of both clonal and recombining modes of reproduction, and the balance between these modes varied among the geographic populations.

Table 4.4: Modes of reproduction across continental and national soil populations of *A. fumigatus* estimated using standardized index of association ($\bar{r}_d$) and phylogenetic compatibility.

Continent	Country	Subpopulation	$\bar{r}_d$	Clone Corrected $\bar{r}_d$	Phylogenetic compatibility
Africa	Cameroon		0.410***	0.258***	0.111***
Asia	China		0.802***	0.149***	0.722***
	India		0.851***	0.025	0.833***
	Saudi Arabia		0.650***	0.101***	0.639***
	Total		0.619***	0.062***	0
Europe	France		0.065***	0.050***	0.000
	Iceland		0.350***	0.143***	0.556***
	Netherlands		0.165***	0.115***	0.028
	Total		0.085***	0.051***	0
North America	Canada	Central	0.241***	0.051***	0
		Eastern	0.098***	0.055***	0

		Northern	0.156***	0.117***	0.056***
		Western	0.127***	0.100***	0
		Total	0.110***	0.078***	0
	Costa Rica		0.200*	0.200*	1.000
	Total		0.108***	0.078***	0
Oceania	New Zealand		0.090 ***	0.079 ***	0
South America	Peru		0.065 ***	0.030 **	0.139 *
World Total			0.114 ***	0.058 ***	0

* p-value < 0.05, ** p-value < 0.01, *** p-value < 0.001.

4.2.4 Global soil populations are genetically differentiated

We investigated the level of genetic differentiation among geographic populations of *A. fumigatus* from soil using AMOVA (Supplementary Tables 4.1). Among continents, we observed significant genetic differentiation in both the full and the clone-corrected datasets (ϕ_{pt} = 0.110, p-value = 0.001 and ϕ_{pt} = 0.119, p-value = 0.001 respectively). Results from AMOVA indicated that the majority of observed genetic variation was found within continental populations (89.0% and 88.1% for the full and clone-corrected respectively), with the remaining variation (~11%) from among continental populations. Similarly, significant genetic differentiations were observed among countries (ϕ_{pt} = 0.165, p-value = 0.001 in the full dataset; and ϕ_{pt} = 0.115, p-value = 0.001 in the clone-corrected dataset). Again, most of the variation was found within countries (83.5% in the full dataset and 88.5% the clone-corrected dataset), with the remaining variation (~11.5-16.5%) found among countries.

Within Canada, we observed significant genetic differentiation among the four regional populations (ϕ_{pt} = 0.108, p-value = 0.001 in the full dataset and ϕ_{pt} = 0.104, p-value = 0.001 in the clone-corrected dataset), with the regional separation contributing about 10% of the total genetic variance. In our previous work, the strains isolated from Hamilton within the central subpopulation were consistently differentiated from populations from other geographic areas outside of Canada that contained A. fumigatus isolates mostly from clinical sources (Ashu et al., 2018; Ashu, et al., 2017b; Korfanty et al., 2019, 2021). Therefore, to investigate the impact of these strains on our analysis, we removed this subset of 124 MLGs

from the central soil population. Upon removal, a decreased yet still significant level of genetic differentiation was maintained across the four Canadian soil subpopulations (ϕ_{pt} = 0.043, p-value = 0.001 in the full dataset, ϕ_{pt} = 0.047, p-value = 0.002 in the clone-corrected dataset). Taken together, soil populations of *A. fumigatus* from different geographic regions in Canada were overall significantly differentiated from each other. However, most local and regional populations contained abundant genetic diversity, with a mixture of sexual and clonal reproductions.

4.2.5 Broad geographic clustering among soil *A. fumigatus* isolates

Following the analysis of population relationships, we next investigated the relationships among the *A. fumigatus* isolates. We visualized strains relationships using three different methods: neighbor joining (NJ) tree, minimum spanning network (MSN), and through discriminant analysis of principal components (DAPC). The NJ tree was generated using Bruvo's genetic distance values between pairs of strains (Figure 4.1). Here, strains from each continent were seen dispersed across the NJ tree, however, certain strains showed geographic clustering. Interestingly, the 3 clonal genotypes from China, India, and Saudi Arabia were in different parts of the tree, with the Chinese MLG being similarly distant from the other two. A similar pattern was observed based on MSN analysis (Supplementary Figure 4.1).

As we were interested in highlighting the genetic diversity between strains at the different geographic levels, DAPC was used to maximize the genetic variation between strains obtained from different countries and continents (Figure 4.2). Here, DAPC revealed three large clusters: one large compact cluster contained the majority isolates from Canada, Iceland, Netherlands, Peru, Costa Rica, and a portion of the non-clonal Indian strains. Slightly overlapping the first large cluster, the second cluster mainly contained isolates from France, New Zealand, Saudi Arabia, and China. The last isolated cluster is comprised of only strains from Cameroon.

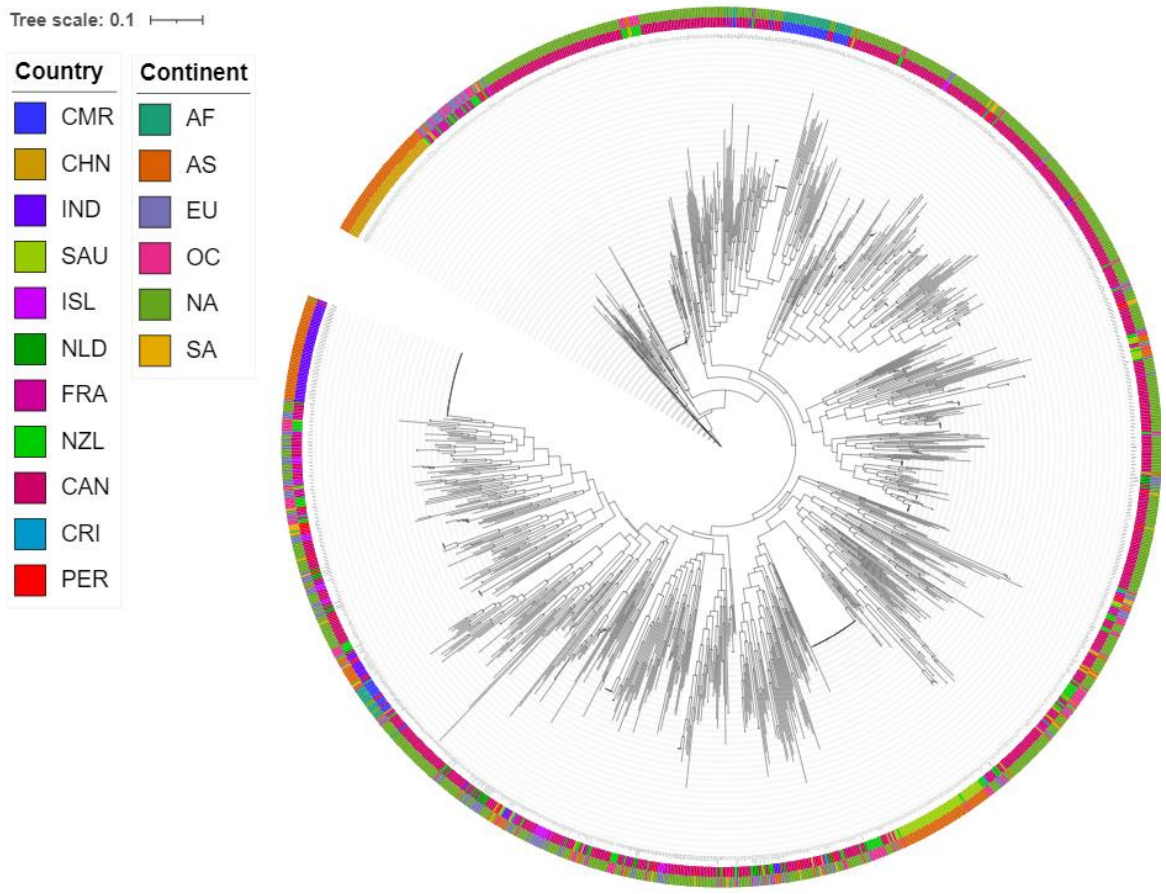

Figure 4.1: Neighbor joining tree of *A. fumigatus* strains obtained from soil around the world. The phylogram was constructed using the Bruvo's genetic distances at nine microsatellite loci. Color strips at each individual node represent the country and continent of origin (inner and outer ring respectively). AF = Africa, AS = Asia, EU = Europe, OC = Oceania, NA = North America, SA = South America, CMR = Cameroon, CAN = Canada, CHN = China, CRI = Costa Rica, FRA = France, ISL = Iceland, IND = India, NLD = Netherlands, NZL = New Zealand, PER = Peru, SAU = Saudi Arabia.

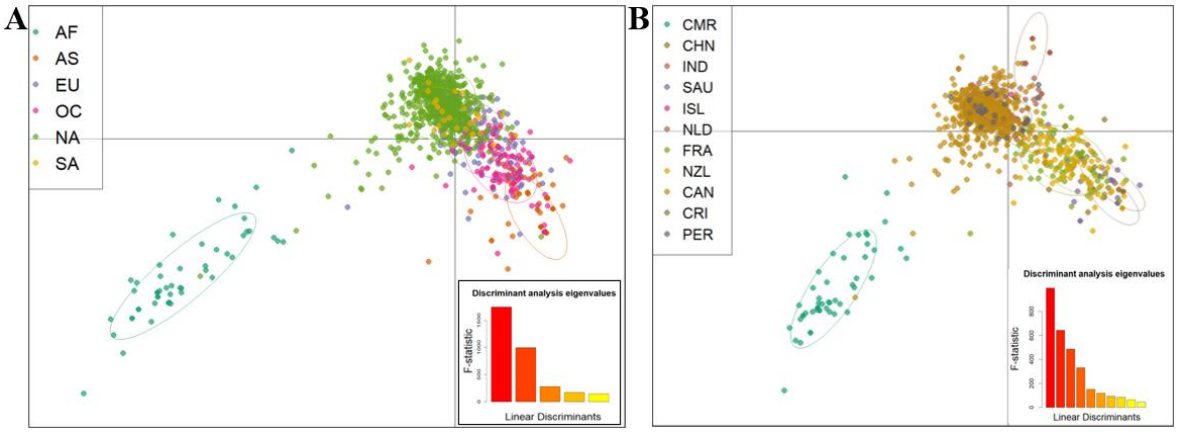

Figure 4.2: Discriminant analysis of principal components (DAPC) of *A. fumigatus* global soil populations grouped by (A) country and (B) continent. The x and y axes describe the first and second discriminant functions highlighted in the barplot of DA eigenvalues (bottom right). Populations are distinguished by colours and 67% inertia ellipses. AF = Africa, AS = Asia, EU = Europe, OC = Oceania, NA = North America, SA = South America, CMR = Cameroon, CAN = Canada, CHN = China, CRI = Costa Rica, FRA = France, ISL = Iceland, IND = India, NLD = Netherlands, NZL = New Zealand, PER = Peru, SAU = Saudi Arabia.

4.2.6 Soil populations of *A. fumigatus* are divided into 2 genetic clusters and 5 subclusters.

Our analyses above revealed a moderate contribution of geographic separation to the total genetic variation within our global *A. fumigatus* soil population. However, other population genetic pattern may exist among strains within our dataset. To investigate this possibility, we first analyzed and assigned the 1303 soil isolates into genetic populations using the Bayesian clustering analysis implemented in the software STRUCTURE. Using the Evanno method, the optimal number of genetic clusters was identified as two, however the ΔK for other values of K between 3-20 were similar to that of K=2. In the clone-corrected data of 984 MLGs, the optimal number of clusters was two, however the ΔK for this dataset was significantly higher than all other K populations (ΔK = 90.1). In the clone-corrected dataset, 91.1% MLGs had an assignment probability above 80% to one of the two clusters (Figure 4.3). The remaining 8.9% (88 isolates) were classified as having mixed ancestry. Of the 896 MLGs with assignment probability above 80%, 485 and 411 were assigned to genetic clusters #1 and #2 respectively. All geographic populations excluding Cameroon and Saudia Arabia contained isolates assigned to both clusters, however, most of these geographic populations had different degrees of uneven distributions of isolates between the two genetic clusters (Supplementary Figure 4.2).

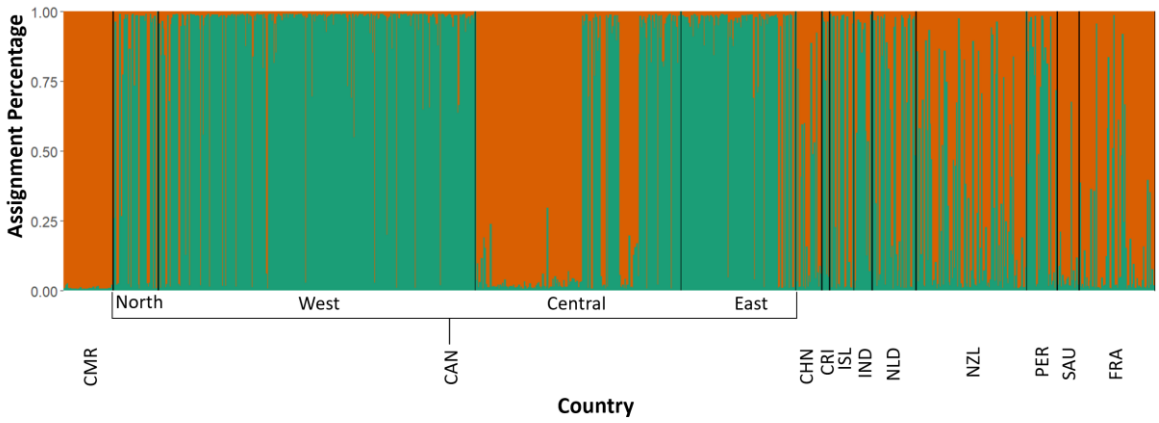

Figure 4.3: Genetic structure bar plot inferred by STRCUTURE for the 11 soil populations of *A. fumigatus*. Isolates were assigned into one of two genetic populations based on nine microsatellite loci. Isolates were clone corrected prior to STRUCTURE analysis. CMR = Cameroon, CAN = Canada, CHN = China, CRI = Costa Rica, FRA = France, ISL = Iceland, IND = India, NLD = Netherlands, NZL = New Zealand, PER = Peru, SAU = Saudi Arabia.

Following the recommendation by Evanno et al., (2005), we conducted a hierarchal STRUCTURE analysis on the strains assigned to the two genetic clusters revealed whether there were subclusters nested within each of the two clusters. Our analysis revealed that Cluster 1, which contained most *A. fumigatus* strains from North America, was further divided into two genetic subclusters ($\Delta K = 98.2$). Cluster 2, which contained all strains from Cameroon and Saudi Arabia as well as strains from other regions, was divided into three genetic subclusters ($\Delta K = 20.3$). In the original genetic cluster analyses, 89.1% and 92.9% of MLGs had an assignment probability above 80% to either Cluster 1 or 2 respectively, while the remaining strains were considered admixed (53 and 29 MLGs from clusters 1 and 2 respectively) (Figure 4.4). For the two subclusters within Cluster 1a, using the >80% assignment probability criteria, 198 and 234 MLGs were assigned to subclusters 1 and 1b respectively. For the three nested subclusters within Cluster 2, 102, 229, and 51 MLGs were assigned to subclusters 2a, 2b, and 2c respectively. The nested subcluster 1a of Cluster 1 was broadly distributed in nine countries. However, the majority of subcluster 1b of Cluster 1 came from north and western Canada (Supplementary Figure 4.3). In cluster 2, Cameroon contained >70% of strains assigned to nested subcluster 2a (Supplementary Figure 4.4); subcluster 2b was broadly distributed; and subcluster 2c was mainly found in northern,

central, and eastern Canada, Peru, and Iceland.

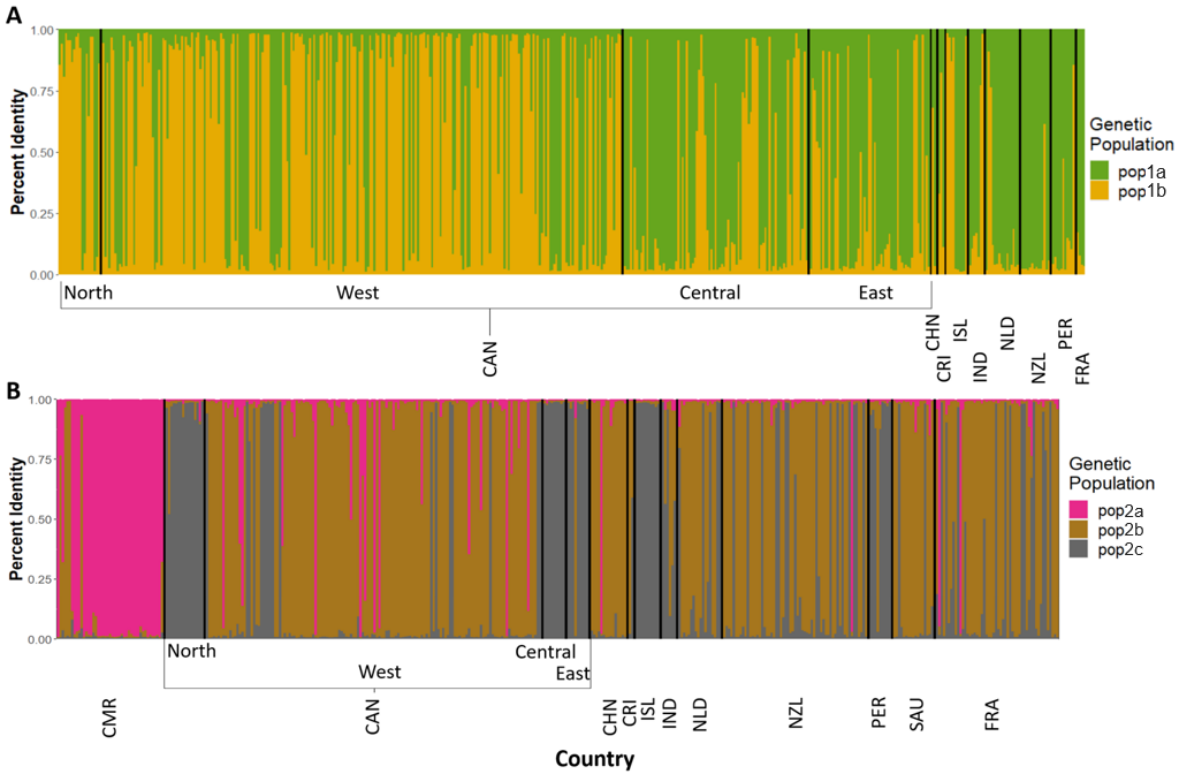

Figure 4.4: Genetic structure bar plot inferred by STRCUTURE for the *A. fumigatus* isolates assigned to genetic populations 1 and 2. Isolates were assigned into genetic populations based on nine microsatellite loci. (A) STRUCTURE assignment of strains assigned to genetic population one. Strains were assigned into one of two genetic clusters. (B) STRUCTURE assignment of strains assigned to genetic population two. Strains were assigned into one of three genetic clusters. CMR = Cameroon, CAN = Canada, CHN = China, CRI = Costa Rica, FRA = France, ISL = Iceland, IND = India, NLD = Netherlands, NZL = New Zealand, PER = Peru, SAU = Saudi Arabia.

4.2.7 Novel soil isolates of *A. fumigatus* are susceptible to itraconazole and voriconazole antifungals.

Antifungal susceptibility testing for itraconazole and voriconazole was conducted on the 826 new isolates obtained in this study. Among these, one strain from Western Canada presented an MIC of greater than 2 (µg/mL) to voriconazole. Overall, of the 1303 soil isolates, 63 were resistant to itraconazole and/or voriconazole. (Tables 4.5)

Table 4.5: Itraconazole and voriconazole susceptibility of *A. fumigatus* isolates.

		Number of isolates in each MIC category of itraconazole/voriconazole (µg/ml)							
Continent	Country	0.03	0.06	0.13	0.25	0.5	1	2	>2
Africa	Cameroon	0/0	0/0	13/1	12/42	2/8	24/0	0/0	0/0
Asia	China	0/0	0/0	0/0	4/9	70/66	3/2	0/0	0/0
	Saudi Arabia	0/0	0/0	0/0	0/5	63/63	5/0	0/0	0/0
	Total	0/0	0/0	0/0	4/14	133/129	8/2	0/0	0/0
Europe	France	0/0	0/0	0/10	0/51	25/6	43/2	0/0	0/0
	Iceland	0/0	0/0	0/2	0/29	24/1	8/0	0/0	0/0
	Total	0/0	0/0	0/12	0/80	49/7	51/2	0/0	0/0
North/Central America	Canada	0/1	1/0	5/44	184/234	332/370	223/84	2/13	1/2
	Costa Rica	0/0	0/0	0/0	0/1	0/4	6/1	0/0	0/0
	Total	0/1	1/0	5/44	184/235	332/374	229/85	2/13	1/2
Oceania	New Zealand	0/0	0/0	8/0	12/11	62/72	20/19	1/1	1/1
South America	Peru	0/0	0/0	0/0	0/1	29/23	0/5	0/0	0/0
World Total		0/1	1/0	26/57	212/383	607/613	332/113	3/14	2/3

4.2.8 Higher allelic diversity in soil populations than in clinical populations

To test the hypothesis that there is greater genetic diversity in the global soil population than in the clinical population, we compared the two populations in several diversity indicators: genotypic diversity, allelic richness, and allelic diversity at global, continental, and country levels. The diversity, LD and AMOVA results of the clinical population can be found in Supplementary data. Between soil and clinical populations, a greater proportion of unique MLGs were found within the soil population (76.5% unique) compared to the clinical population (71.4% unique). Within the soil and clinical populations, 91 (9.12%) and 142 (16.8%) MLGs respectively were represented by two or more isolates. Of the 1809 MLGs in the combined clinical and soil populations, 11 MLGs were shared between the clinical and soil populations (Table 4.6). However, the global clinical population had a lower proportion of clonal genotypes compared to the soil population.

We then compared both allelic richness and diversity between the global soil and clinical populations (Table 4.7). Overall, no significant difference in allelic richness was observed between the two ecological populations at the global level. However, in regional comparisons

where both clinical and soil populations were present, soil populations had significantly higher allelic richness in four of six countries and 2 of the 3 continents. In contrast, higher allelic richness was observed in the Netherlands clinical population than in its soil population, likely due to sample size effect.

Next, haploid diversity was calculated for both the soil and clinical *A. fumigatus* populations on global and regional levels. At the global level, higher allelic diversity for the nine loci was observed within the soil population compared to the clinical population (p-value = 0.043, Table 4.7). After clone correction, the higher allelic diversity within soil population was maintained (p-value = 0.010). At the country level, allelic diversity was statistically higher only within the French soil population. In contrast, the clinical populations in China and India had statistically higher diversity that their corresponding soil populations. After clone correction, only the Chinese soil population had a higher diversity compared to its clinical population. No significant difference was observed between the two populations within any continent.

Table 4.6: Shared multilocus genotypes (MLGs) within continents and countries between soil and clinical *A. fumigatus* populations.

Continent	Country	Soil Isolates (MLGs)	Clinical Isolates (MLGs)	Shared MLGs
Asia	China	78 (23)	8 (8)	0
	India	74 (16)	22 (14)	1
	Total	151 (38)	30 (22)	1
Europe	France	69 (68)	30 (14)	0
	Netherlands	44 (39)	673 (500)	7
	Total	113 (107)	703 (514)	10
North America	Canada	748 (620)	71 (68)	0
	Total	754 (626)	116 (98)	0
World Total		1303 (997)	1197 (843)	11

Table 4.7: Summary of haploid diversity and private alleles among soil and clinical populations and subpopulations of *A. fumigatus* across nine STR loci.

Continent	Country	Niche	Na[1] (NP[2])	Mean Na (SD)	Shannon's Index	Uh[3] (± SE[4])	Clone Corrected Uh (± SE)
Africa	Cameroon	Soil	96 (2)	10.67 (4.42)	0.950	0.755 (0.025)	0.787 (0.029)
Asia	China	Clinical	36 (0)	4.00 (2.12)	1.000	0.687 (0.076)	0.687 (0.076)
		Soil	96 (4)	10.67 (3.04)	0.450	0.387 (0.014)	0.879 (0.017)
		Total	108 (3)	12.00 (4.15)***	0.593	0.489 (0.012)**	0.885 (0.015)*
	India	Clinical	75 (0)	8.33 (2.96)	0.844	0.760 (0.024)	0.881 (0.030)
		Soil	71 (1)	7.89 (2.32)	0.520	0.478 (0.015)	0.861 (0.037)
		Total	107 (1)	11.89 (4.04)	0.599	0.548 (0.013)***	0.876 (0.036)
	Saudi Arabia	Soil	78 (0)	8.67 (2.35)	0.501	0.416 (0.038)	0.838 (0.027)
	Total	Clinical	93 (0)	10.33 (3.91)	0.917	0.818 (0.028)	0.868 (0.028)
		Soil	152 (4)	16.89 (6.29)	0.830	0.731 (0.023)	0.883 (0.019)
		Total	175 (4)	19.44 (7.92)*	0.869	0.764 (0.019)*	0.908 (0.014)
Europe	Belgium	Clinical	148 (3)	16.44 (5.48)	0.994	0.857 (0.016)	0.859 (0.016)
	France	Clinical	69 (1)	7.67 (1.73)	0.910	0.795 (0.019)	0.846 (0.031)
		Soil	147 (1)	16.33 (6.75)	0.997	0.875 (0.019)	0.875 (0.019)
		Total	171 (2)	19.00 (7.14)**	0.992	0.894 (0.015)**	0.892 (0.015)
	Iceland	Soil	70 (0)	7.78 (2.73)	0.935	0.804 (0.025)	0.818 (0.046)
	Italy	Clinical	19 (0)	2.11 (0.60)	0.600	0.378 (0.071)	0.556 (0.100)
	Netherlands	Clinical	263 (23)	29.22 (16.35)	0.995	0.855 (0.021)	0.863 (0.020)
		Soil	118 (0)	13.11 (6.01)	0.988	0.866 (0.018)	0.881 (0.017)
		Total	267 (27)	29.67 (17.32)*	0.998	0.856 (0.021)	0.866 (0.020)
	Norway	Clinical	146 (0)	16.22 (7.08)	0.991	0.805 (0.032)	0.811 (0.029)
	Spain	Clinical	80 (0)	8.89 (3.62)	0.882	0.759 (0.031)	0.799 (0.030)
	Switzerland	Clinical	155 (5)	17.22 (6.36)	0.995	0.866 (0.022)	0.869 (0.022)
	Total	Clinical	293 (40)	32.56 (17.66)	0.998	0.862 (0.022)	0.864 (0.020)
		Soil	199 (1)	22.11 (9.29)	0.995	0.899 (0.013)	0.900 (0.017)
		Total	313 (48)	34.78 (18.31)	0.998	0.871 (0.020)	0.879 (0.018)
Oceania	New Zealand	Soil	177 (4)	19.67 (7.31)	0.997	0.887 (0.021)	0.889 (0.021)
North America	Canada	Clinical	154 (3)	17.11 (5.93)	0.997	0.890 (0.019)	0.892 (0.018)
		Soil	323 (37)	35.89 (16.08)	0.996	0.870 (0.022)	0.882 (0.021)
		Total	329 (52)	36.56 (16.09)**	0.998	0.881 (0.019)	0.892 (0.018)
	Costa Rica	Soil	39 (1)	4.33 (1.22)	1.000	0.874 (0.042)	0.874 (0.042)

	USA	Clinical	110 (1)	12.22 (4.21)	0.960	0.855 (0.023)	0.878 (0.021)
	Total	Clinical	201 (4)	22.33 (7.7)	0.995	0.909 (0.015)	0.912 (0.016)
		Soil	324 (38)	36 (15.96)	0.996	0.874 (0.023)	0.900 (0.014)
		Total	331 (55)	36.78 (15.84)*	0.998	0.882 (0.019)	0.893 (0.018)
South America	Peru	Soil	104 (1)	11.56 (3.36)	0.995	0.896 (0.013)	0.897 (0.014)
		Clinical	362 (45)	37.22 (17.22)	0.997	0.874 (0.020)	0.881 (0.018)
		Soil	335 (72)	40.22 (18.65)	0.993	0.900 (0.012)	0.909 (0.014)
		Total	407	45.22 (22.02)	0.998	0.887 (0.012)*	0.895 (0.012)**

* p-value < 0.05, ** p-value < 0.01, *** p-value < 0.001.
[1]Na = number of unique alleles across 9 loci; [2]NP = Number of private alleles; [3] Uh = unbiased diversity = $(N/(N-1)) \times (1-\Sigma p_i^2)$ where p_i is the frequency of the ith allele for the population; [4] SE = Standard error

4.2.9 Genetic differentiation between the soil and clinical populations of *A. fumigatus*

Similar to the analysis on soil populations, we quantified genetic differentiation between the soil and clinical populations within selected countries and continents where both sample types are available. Overall, a statistically significant genetic differentiation was observed between the soil and clinical populations at the global, continental, and country levels (Table 4.8). However, the majority genetic variation was observed within the soil and clinical populations compared to the variation between the two ecological niche populations (95.8% and 4.2% respectively). After clone-correction, the two ecological niche populations in most geographic regions remained significantly differentiated. Again, most of the variations were observed within individual ecological niche populations with the remainder present among the populations (Table 4.8).

Table 4.8: Genetic differentiation between soil and clinical populations of *A. fumigatus* at country, continental, and global levels.

Continent	Country	Sample Size	ϕ_{pt} pt	Clone Corrected Sample Size	Clone Corrected ϕ_{pt}
Asia	China	86	0.356**	34	0.032
	India	96	0.143**	29	0.071
	Total†	249	0.069**	79	0.014
Europe	France	99	0.053**	82	0.093*
	Netherlands	717	0.050***	539	0.056***

	Total†	1196	0.016**	852	0.021***
North America	Canada	819	0.185***	688	0.164***
	Total†	870	0.060***	724	0.070***
World Total		2500	0.042***	1820	0.047***

* p-value < 0.05, ** p-value < 0.01, *** p-value < 0.001.
† Note: Total data has countries without a clinical or soil population included in the continental analysis

4.2.10 Genotypic and genetic clustering of global *A. fumigatus* strains

Following the analyses comparing the two *A. fumigatus* ecological populations, we again investigated the genetic relationships among strains from both clinical and soil *A. fumigatus* populations. We visualized these strains relationships again using a NJ tree, MSN, and conducted a DAPC. On the NJ tree, strains from both clinical and soil populations were dispersed across the tree (Figure 4.5). Several small strain clusters were observed containing a high proportion of strains from one of the two niche populations. Strain clusters containing approximately even proportions of strains from both niche populations were also observed. A similar pattern was also seen when visualizing genetic distances on an MSN (Supplementary Figure 4.5). Lastly, DAPC analysis revealed some separation among isolates from the two ecological niches but with significant overlaps between them (Supplementary Figure 4.6).

Given the soil populations were separated into two genetic populations, we therefore used STRUCTURE on our *A. fumigatus* strains from both clinical and soil populations to determine if strains would be similarly assigned. The likelihoods of 1 to 20 genetic clusters were tested for both full and clone corrected datasets. Using the Evanno method for both datasets, we were not able to identify an optimum number of clusters, as all ΔK values across all tested values of K were low and similar.

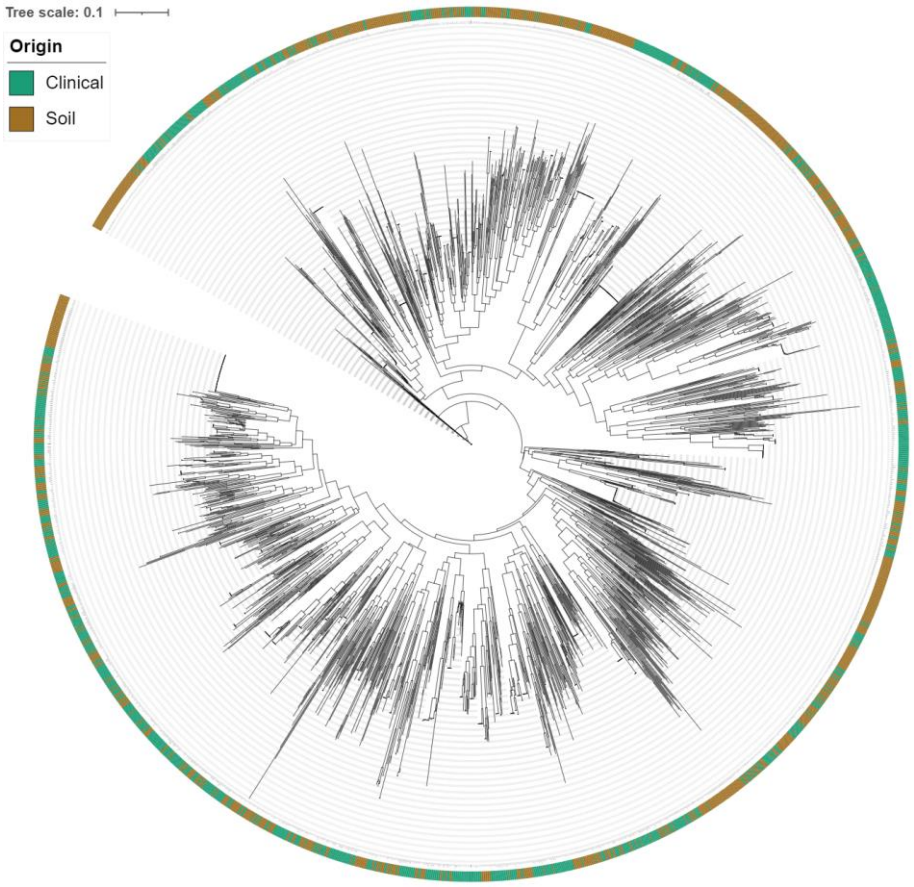

Figure 4.5: Neighbor joining tree of *A. fumigatus* strains from global soil and clinical populations. The phylogram was constructed using the Bruvo's genetic distances at nine microsatellite loci.

4.3 Discussion

In this study, we obtained 826 new *A. fumigatus* isolates from six countries on four continents. Combined with soil populations obtained in our previous studies, we analyzed a combined total of 1303 soil isolates from eleven countries on six continents. The geographic structures of the soil populations were analyzed and when possible, compared with their corresponding clinical population at global, continental, and country levels. Soil populations contained high allelic and genotypic diversities. At the nine microsatellite loci, the soil populations had an overall higher allelic diversity than their corresponding clinical populations, except for Asian countries. Interestingly, geographic soil populations varied in the level of recombination. However, random recombination was not observed in any population sample. Soil populations of *A. fumigatus* from different countries and continents

were differentiated from each other, with a relatively small but statistically significant proportion of the total genetic variation present among populations. With the exception of Asian populations, countries containing both clinical and soil populations were also significantly differentiated. Lastly, STURCTURE analysis separated soil strains into two large genetic clusters, where countries differed in their strains' distributions between these two clusters. Below, we discuss the relevance and implications of our results.

In our previous work, *A. fumigatus* soil populations from several geographic regions showed high genotypic and allelic diversities and with evidence of genetical differentiation among some of them (Ashu, et al., 2017b; Korfanty et al., 2019, 2021). Here, three *A. fumigatus* populations from Asia showed relatively low allelic and genotypic diversities. The low diversity within the Chinese and Saudi Arabian populations in this study was largely caused by the high abundance of a single clonal genotype in each population, similar to what was observed in the Indian *A. fumigatus* populations previously described (Chowdhary, et al., 2012b). In India, a clonal expansion of a triazole-resistant genotype occurred that caused a hard selective sweep and reduced both allelic and genotypic diversities. By contrast, strains from both Chinese and Saudi Arabian populations were not resistant to the triazoles tested. It is possible that a selective sweep(s) occurred within these two geographic populations. Selective sweeps have been observed to occur across multiple regions within *A. fumigatus* genomes (Rhodes et al., 2022). The clonal Chinese genotype was found in both southern and northern China, approximately 870 km apart. Given the lack of triazole resistant strains within both populations, the nature of the clonal expansion was unlikely due to triazole drug selection pressure. It should be noted that this clonal genotype in our Chinese sample was not reported from Yunnan province, southwestern China (Zhou et al., 2021, 2023).

Similar to results from previous studies (Auxier et al., 2022; Etienne et al., 2021; Lofgren et al., 2022; Rhodes et al., 2022; Sewell et al., 2019), evidence for non-random recombination was observed within soil populations of *A. fumigatus* at all geographic scales. The observed evidence for recombination, including many isolates with admixture ancestry, is consistent with dispersal and genetic exchange among genetic populations. In this study, we showed

that *A. fumigatus* populations based on their geographic origins at the regional, country, or continental levels were statistically significantly differentiations. The relatively high proportion of among-group genetic variation suggests that each continent and country contained unique allelic and genotypic frequencies. However, evidence for gene flow, including allele and genotype sharing, was observed between populations at all three geographic levels. These results are consistent with previous studies on *A. fumigatus* populations, where genetic differentiation was observed at all analyzed geographic levels yet evidence for gene flow was also found (Ashu et al., 2018; Korfanty et al., 2019, 2021; Zhou et al., 2021). At smaller geographic levels, genetic differentiation between populations is expected to be lower (Araujo et al., 2010; Zhou et al., 2021). For example, in the study by Araujo et al., (2010), *A. fumigatus* samples obtained from multiple sites within a hospital found no evidence of genetic differentiation at eight microsatellite markers. However, among sites within a region such as among three subpopulations in Vancouver in western Canada revealed fine-scale genetic differentiations (data not shown). Altogether, though evidence for gene flow was found across geographic scales, *A. fumigatus* soil populations can be genetically differentiated at all geographic levels.

STRUCTURE analysis of the global soil population separated the *A. fumigatus* genotypes into two genetic clusters and five subclusters. Our two cluster results correlated with the two dominant *A. fumigatus* clades reported in previous studies (Rhodes et al., 2022; Sewell et al., 2019). These two clades were found to differ in their triazole susceptibility patterns, where *A. fumigatus* strains with environmental azole resistance mostly belonged to one clade, and azole- susceptible strains comprised the other clade. However, the differential distributions of azole-resistant and azole-susceptible strains between the two clades were not found in our soil samples. This was likely due to the small number of azole-resistant multilocus genotypes in our samples. Further hierarchal analysis identified two genetic subclusters within Cluster 1 and three subclusters within Cluster 2. Geographic clustering was observed at the subcluster level, most prominently with the Cameroon *A. fumigatus* populations. This population is highly genetically differentiated from all other geographic *A. fumigatus* populations, in line with what we observed in this and previous studies (Ashu, et al., 2017b). Apart from

Cameroon, the extent of the geographic clustering for other populations is less clear, as populations at all geographic levels contained strains from multiple genetic clusters and subclusters. We note that even though our analyzed soil population has a relatively large sample size, they likely represent only a small proportion of the true global *A. fumigatus* diversity. Using different geographic/ecological samples could yield different estimates of genetic clusters (Fan et al., 2021; Lofgren et al., 2022).

In recent environmental *A. fumigatus* population surveys, high-frequency triazole-resistance was reported in several ecological niches, including greenhouses and tulip flower bulb wastes, where up to 83.7% of *A. fumigatus* strains were triazole resistant (Chowdhary et al., 2014; Gómez Londoño & Brewer, 2023; Rocchi et al., 2021; Shelton et al., 2022; Zhang et al., 2022; Zhou et al., 2021, 2023). By contrast, some environmental studies focused on natural soil populations found low proportions or no resistant strains within the surveyed *A. fumigatus* population (Fraaije et al., 2020; Jeanvoine et al., 2017; Kano et al., 2015). Our soil samples were mostly from parks and natural forests and strains from these ecological niches had low to no triazole resistance. Interestingly, in the literature review by Burks et al., (2021) that investigated the effect of sampling origins of antifungal resistant *A. fumigatus,* 56.7% of all triazole resistant strains among the 52 studies originated from soils. Given the high variation of triazole-resistance prevalence among soil populations of *A. fumigatus*, further research is required to identify how azole resistant genotypes are maintained within certain soil populations and not others as well whether resistance was introduced into or evolved within these populations.

We compared the *A. fumigatus* soil population to their corresponding clinical populations at the global, continental, and country levels. Globally, soil populations of *A. fumigatus* had a greater allelic diversity than their corresponding clinical populations. Overall, the soil populations had fewer clonal genotypes, and the soil and clinical populations shared relatively few genotypes in most geographic regions. Interestingly, the Chinese and Indian clinical *A. fumigatus* populations showed higher allelic diversity than their soil counterparts, mainly due to the large clonal soil populations in our samples from these two countries.

Studies analyzing genetic differences between clinical and soil populations in other pathogenic species have been performed and showed results similar to ours (Muller & McCusker, 2009; Pirnay et al., 2009; Simwami et al., 2011). In general, the source population is expected to have a higher genetic diversity than the derived populations (Litvintseva et al., 2006; Simwami et al., 2011). In opportunistic pathogens with significant environmental reservoirs, clinical isolates often contain lower allelic and genotypic diversities of those found within the natural reservoir of the species (Muller & McCusker, 2009; Simwami et al., 2011). Our results are largely consistent with the previously reported pattern. Recently, conidia have been found aerosolized from patient coughs and such conidia could be inhaled by another host nearby (Engel et al., 2019; Lemaire et al., 2018). If this person-to-person transmission of *A. fumigatus* plays an important role in causing patient infection, coupled with microevolution of the infecting strains within patients, novel genetic diversity is also expected in clinical samples that may not be found in environmental samples (Ballard et al., 2018).

We observed statistically significant genetic differentiation between soil and clinical populations at all three geographic levels. Our results are similar to what was observed in previous studies of *A. fumigatus* at regional and national scales (Ashu, et al., 2017b; Korfanty et al., 2019, 2021). Similar results have also been obtained for several other human pathogens (Chen et al., 2015; Durigan et al., 2017; Muller & McCusker, 2009). Interestingly, unlike the global soil population, STRUCTURE was unable to resolve the combined clinical and soil *A. fumigatus* populations into genetic clusters. The lack of distinct clusters may have resulted from two possibilities. First, the total number of clusters K may be above 20. However, given that previous studies reported eight or fewer clusters for both microsatellite and genomic data (Ashu, et al., 2017a; Rhodes et al., 2022; Sewell et al., 2019; Zhou et al., 2021), it is therefore unlikely that there are more than 20 genetic clusters in our global dataset. Second, as STRUCTURE uses allelic association patterns to separate reproductively isolated strains into genetic clusters, the increased sample size may have revealed the admixture genotypes among geographic and ecological populations, eroding signatures of reproductive isolations among genetic clusters in nature, resulting in one global metapopulation in this species. We

note that one major drawback in this comparison is that our compared soil and clinical populations of *A. fumigatus* were often from different locations within individual countries or continents and thus their geographic differences could have caused over-estimation of niche contributions. Further analyses of *A. fumigatus* strains from under-sampled regions and from diverse but comparable geographic and ecological origins are required to reveal the extent of genetic mixing among geographic and ecological populations of *A. fumigatus*.

4.4 Conclusion

This study analyzed the largest number of soil isolates of *A. fumigatus* from many geographic and climatic regions around the world. Additionally, we compared the *A. fumigatus* soil populations with the clinical populations analyzed previously. Within both the soil analysis and the comparison of clinical and soil populations, we found extensive genetic and allelic diversity as well as evidence for both clonal and sexual reproduction present among soil populations. Despite the significant genetic differentiation, evidence for gene flow and genetic exchange was also found. Interestingly, both the Chinese and Saudi Arabian soil populations contained a widely dispersed but different clonal genotype. At present, the mechanism(s) for their high prevalence is unknown but should be closely monitored for clinical significance. In contrast to the increasing prevalence of triazole-resistant strains of *A. fumigatus* within clinical samples, greenhouses, and agricultural wastes, relatively few isolates from natural soil samples from most countries investigated here were resistant to triazoles. As *A. fumigatus* is a ubiquitously distributed mold, found in the air, aquatic systems, and at home and workplaces, additional analyses should target *A. fumigatus* from diverse ecological niches to identify their relationships with each other and with those from clinics. Together, such understanding could help develop better prevention and control strategies against aspergillosis.

4.5 Methods

4.5.1 Soil collection, *A. fumigatus* isolation, and STR genotyping

The soil samples used to isolate *A. fumigatus* for this study were obtained from 6 countries (Table 4.1). In total, 4357 soil samples were processed for this study. Soil samples obtained

from part of Canada (Northwest Territories), China, Costa Rica, France, Peru, and Saudi Arabia have been described previously, with a small portion of each used to isolate yeast species by Samarasinghe et al., (2021), totalling 2907 soil samples. An additional 1450 soil samples were collected from five Canadian provinces that included Alberta (300), British Columbia (1040), New Brunswick (260) Ontario (500), Quebec (100), and Prince Edward Island (50).

Each isolate was also genotyped at nine highly polymorphic short tandem repeat (STR) loci that used primers specific to *A. fumigatus*, following a protocol previously described by de Valk et al., (2005) and Korfanty et al., (2021). The generated *A. fumigatus* STR dataset was then combined with STR datasets obtained previously from soil samples in seven countries that contained 481 strains (Ashu, et al., 2017b; Korfanty et al., 2019, 2021).

To compare our soil samples with those from clinics, we included a clinical STR dataset containing 1197 STR genotypes from 11 countries from Europe, Asia, and North America (Ashu, et al., 2017a). Specifically, the number of MLGs within these 11 populations were: Belgium (66), Hamilton, Canada (71), China (8), France (30), India (94), Italy (6), Netherlands (673), Norway (93), Spain (115), Switzerland (68), and USA (45). These clinical isolates were obtained from patients suffering cystic fibrosis, undergoing corticosteroid immunosuppression, or were immunocompromised from a variety of other reasons.

4.5.2 Allelic and genotypic diversities

Allelic diversity was calculated across the nine STR loci using the STR datasets grouped by continent, country, and soil or clinical origin. Haploid diversity was calculated using the Excel add-in GenAlEx 6.5 (Peakall & Smouse, 2006, 2012). The unbiased haploid (uh) diversity measures the probability that two individuals will be different within the population using the sum of allele frequencies within the populations and adjusts for differences in sample size. Additionally, the number of unique alleles (Na) was determined. To determine whether the datasets grouped by continent, country, and soil or clinical origin contained

statistically significant differentiation, an ANOVA and Bonferroni post hoc tests were conducted.

4.5.3 Clonality and recombination within the global *A. fumigatus* populations

To investigate the potential evidence of clonality and/or recombination present within each stratum of our global *A. fumigatus* dataset, we measured two metrics. The first test evaluated the overall linkage disequilibrium (LD) that is present within each stratum. The overall LD was measured using the standardized index of association ($\bar{r}_d$), where the null hypothesis states that random recombination is occurring across individuals within the dataset. The $\bar{r}_d$ was calculated using the R package *poppr* (Kamvar et al., 2014). Statistical significance was determined using our observed population and a sample of 999 permutations. The second test evaluated the proportion of loci that are phylogenetically compatible across strains within each geographic level. Using Multilocus (version 1.3b), two loci are phylogenetically compatible if all observed genotypes can be accounted for by mutation alone without inferring homoplasy or recombination. Statistical significance was determined through 1000 randomizations. Lastly, the Shannon's index was used to calculate the probability of selecting two identical genotypes. To account for the influence of clonal individuals on our analyses, both $\bar{r}_d$ and phylogenetic compatibility was recalculated using a clone corrected version of each stratum.

4.5.4 Genetic relationships among populations

The proportion of genetic variation present within and among populations was assessed similarly to our previous work (Korfanty et al., 2021). In brief, the analysis of molecular variance (AMOVA) was conducted using GenAlEx 6.5 using the haploid-SSR parameter (Peakall & Smouse, 2006, 2012). The total genetic variance was partitioned among populations based on continent, country, and soil or clinical origin groupings. Genetic differentiation between the defined populations was calculated using ϕpt, an analogue of Fst (Meirmans, 2006). Statistical significance was determined through 999 permutations. To account for the influence of clonal individuals on our analyses, a repeat analysis was conducted on a clone corrected dataset.

To visualize genetic distance between all isolates within our dataset, first the pairwise genetic distance between strains was calculated using Bruvo's genetic distance, implemented by the R package *poppr* (Bruvo et al., 2004; Kamvar et al., 2014). Bruvo's distance measure is specific to STR MLGs and incorporates the stepwise mutation model, where genotypes with smaller allele differences will be considered more genetically similar than MLGs with larger allele difference across their loci. The genetic distances between strains were visualized using a minimum spanning network (MSN) and a neighbor joining tree. Multiple MSNs were generated for each of the four strata as well as the four genetic clusters.

4.5.5 Genetic structure of the global *A. fumigatus* populations

To identify genetic clusters within our *A. fumigatus* dataset, the Bayesian algorithm as implemented in STURCTURE version 2.3 was used (Pritchard et al., 2000). Default parameters were used for each STRUCTURE run. Specifically, the admixture model was used as the ancestry model, where an individual can have mixed ancestry to multiple genetic populations, therefore an individual may share genetic elements obtained from multiple k populations. The correlated allele frequencies model was used as the allele frequency model. This model states that alleles frequencies present within a given K population are more likely to be similar than allele frequencies between K populations. This model uses a (multidimensional) vector, P_A, that is assumed to have a Dirichlet prior. The vector P_A, records the allele frequencies in a hypothetical "ancestral" population, where the K populations represented in our soil populations each undergone independent drift away from these ancestral frequencies.

For our *A. fumigatus* dataset, Markov chain Monte Carlo (MCMC) simulations were run for K populations 1 to 20. The burn-in period as well as the MCMC sampling was run for 30,000 iterations each. A stationary distribution of the alpha values was observed for almost all the 300 repetitions after the burn-in period. After the 30,000 sampling iterations the summary statistics values (Alpha, Fst, and likelihood) maintained a stationary distribution, validating the run length. Fifteen replicates were run for each K population. Repetitions where MCMC alpha values did not achieve a stationary distribution after the burn-in period were removed.

These removed repetitions from the global soil STRUCTURE analysis were 1 replicate from each K value equaling 12, 15, 18 and 20. From the nested clusters STUCTURE analysis of Cluster 2, following STRUCTURE, the Evanno method was used to identify the optimal number of K populations, as implemented in STRUCTURE HARVESTER v. 0.6.93 (Earl & vonHoldt, 2012; Evanno et al., 2005). Using this method, the optimal number clusters was inferred as the K population with the highest ΔK value.

Additionally, the multivariate analysis Discriminant Analysis of Principal Components (DAPC), implemented by *adegenet* package in R, was used (Jombart & Ahmed, 2011). Samples were analyzed according to their geographic/ecological origins. The three origins used were: continent, country, and soil or clinical. In DAPC analysis, the data is first transformed using principal component analysis (PCA) to reduce the number of variables and allowing retention of the variables that have the greatest contribution to the variation within the dataset. This is followed by discriminate analysis (DA) to cluster the MLGs by optimizing the between-group variation and reducing within-group variation.

4.5.6 Triazole susceptibility testing

Antifungal susceptibility testing was conducted on the 826 *A. fumigatus* isolates following the reference protocols for non-dermatophyte molds described in the Clinical and Laboratory Standards Institute (CLSI) document "M38 Reference Method for Broth Dilution Antifungal Susceptibility Testing of Filamentous Fungi" 3rd edition (Alexander et al., 2017). Two triazoles, itraconazole and voriconazole, were used to test all novel strains obtained in this study. Two Candida strains, *C. parapsilosis* ATCC® 22019 and *C. krusei* ATCC® 6258, were used as references.

4.5.7 Comparison between soil and clinical populations

The allelic and genotypic diversities as well as geographic structures of the clinical *A. fumigatus* populations from around the globe based on data published previously were similarly calculated using the approaches described above. The population genetic parameters for the clinical samples were then compared with those of the soil samples.

4.6 Acknowledgements

This research was supported by the Institute of Infectious Diseases Research (IIDR) Antibiotic Resistance Initiative, the Faculty of Science's Global Science Initiative of McMaster University, and Natural Science and Engineering Research Council of Canada. The funders had no role in study design, data collection and interpretation, or the decision to submit the work for publication.

Conceptualization, J.X.; methodology, G.A.K.; software, G.A.K.; formal analysis, G.A.K.; investigation, G.A.K., A.K., M.D., M.T., and P.G.; resources, A.K. and J.X.; writing—original draft preparation, G.A.K.; writing—review and editing, G.A.K., A.K., M.D., M.T., P.G., and J.X.; visualization, G.A.K.; supervision, J.X., G.A.K.; project administration, J.X.; funding acquisition, J.X. and G.A.K. All authors have read and agreed to the published version of the manuscript.

4.7 Supplementary Material

4.7.1 Supplementary data

Clinical *A. fumigatus* population data set analyses

Genotypic and allelic diversity of clinical *A. fumigatus* populations

The global clinical population is composed of *A. fumigatus* strains from 11 countries and three continents (Ashu et al., 2018; Ashu, et al., 2017a). The allelic richness, allelic diversity, and genotypic diversity for the 1197 global clinical *A. fumigatus* strains are presented in Supplementary Table 4.2 and 4.3.

Linkage disequilibrium of the global *A. fumigatus* population

We investigated the level of recombination and clonality present among clinical *A. fumigatus* populations. Of the clinical subpopulations, 10 of the 11 subpopulations had $\overline{r_d}$ values that departed from the null hypothesis of random recombination (Supplementary Table 4.4). Upon clone correction, 9 of the 11 subpopulations departed from the null hypothesis of random recombination. All subpopulations were phylogenetic incompatibility with the exception of the Italy subpopulation that failed to reject the hypothesis for complete clonality.

Clinical populations are genetically differentiated

An AMOVA was conducted on the clinical populations. Across continents, we observed statistically significant genetic differentiation present across the clinical dataset (ϕ_{pt} = 0.156, p-value = 0.001 and ϕ_{pt} = 0.181, p-value = 0.001 clone corrected). The majority of the variation was observed within populations (84.4% and 81.9% clone corrected) with the remainder present among the populations (15.5% and 18.1% clone corrected). Across countries, we again observed statistically significant genetic differentiation present across the clinical dataset (ϕ_{pt} = 0.148, p-value = 0.001 and ϕ_{pt} = 0.155, p-value = 0.001 clone corrected). The majority of the variation was observed within populations (85.2% and 84.5% clone corrected) with the remainder present among the populations (14.8% and 15.5% clone corrected).

4.7.2 Supplementary figures

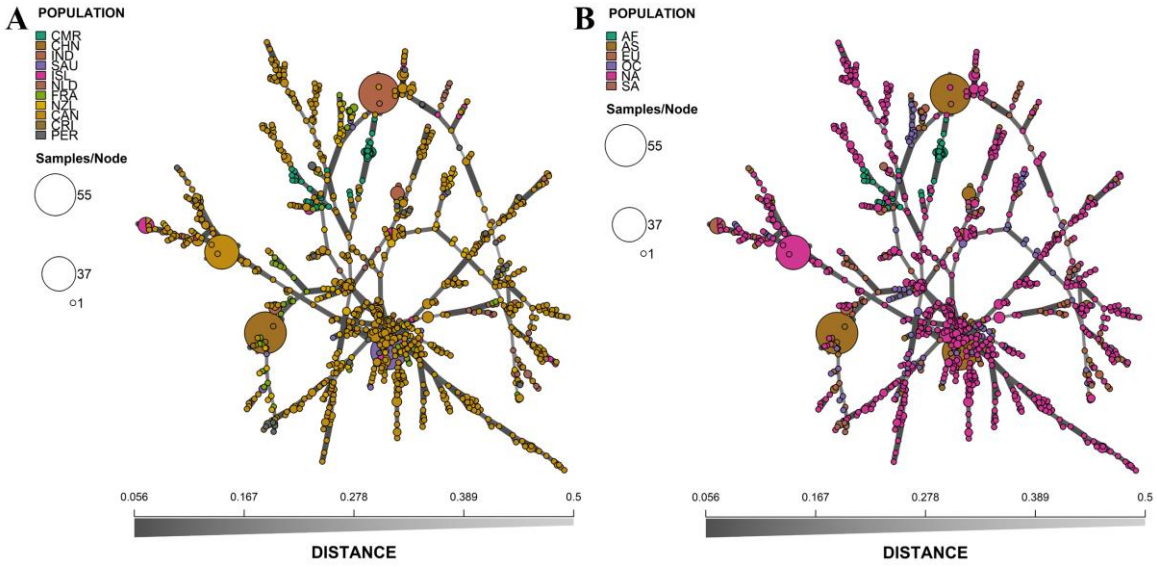

Supplementary Figure 4.1: Minimum-spanning network showing the genetic relationship between MLGs from *A. fumigatus* isolates grouped by geographic origin. The genetic distance between MLGs was calculated using Bruvo's genetic distance. Each node represents one or more identical MLGs, where the node size corresponds to the number of identical MLGs. Nodes that are more genetically similar have darker and thicker edges, whereas nodes genetically distant have lighter and thinner edges. Geographic origin grouped *A. fumigatus* isolates by (A) country and (B) continent. AF = Africa, AS = Asia, EU = Europe, OC = Oceania, NA = North America, SA = South America, CMR = Cameroon, CAN = Canada, CHN = China, CRI = Costa Rica, FRA = France, ISL = Iceland, IND = India, NLD = Netherlands, NZL = New Zealand, PER = Peru, SAU = Saudi Arabia.

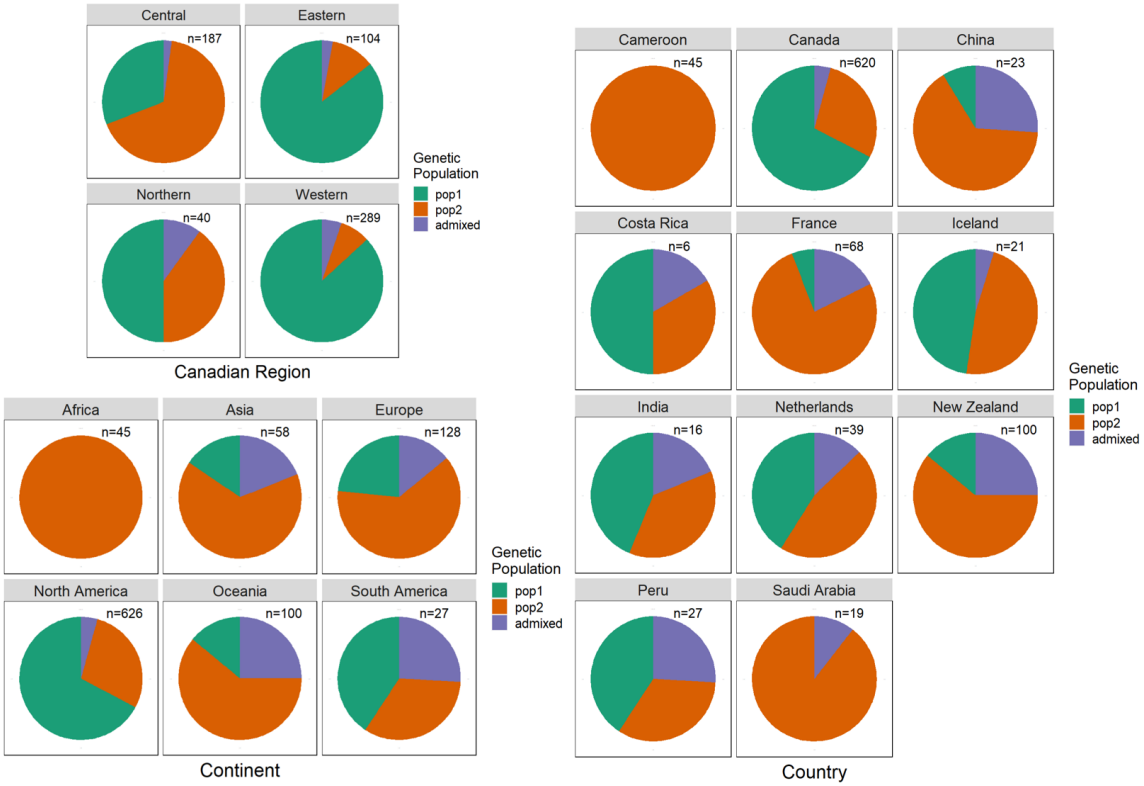

Supplementary Figure 4.2: Proportion of clone-corrected *A. fumigatus* isolates assigned by STRUCTURE into two genetic populations among Canadian regions, countries, and continents. Admixed strains with assignment identity less than 0.800 are coloured purple. n = the number of MLGs per population.

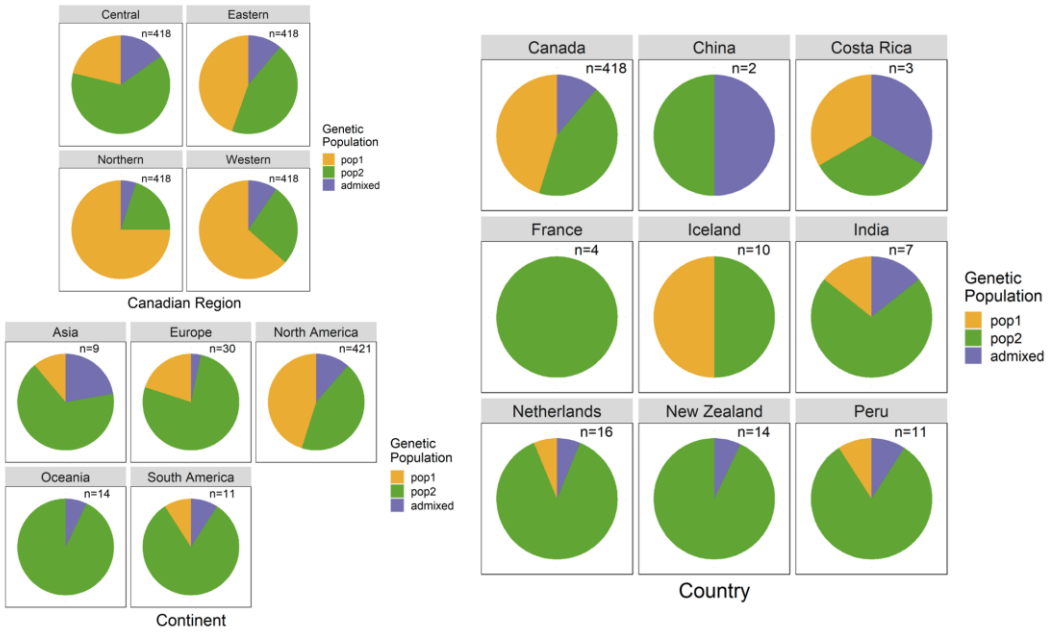

Supplementary Figure 4.3: Proportion of *A. fumigatus* isolates from genetic population one assigned by STRUCTURE into two nested genetic populations among Canadian regions, countries, and continents. Admixed strains with assignment identity less than 0.800 are coloured purple. n = the number of MLGs per population.

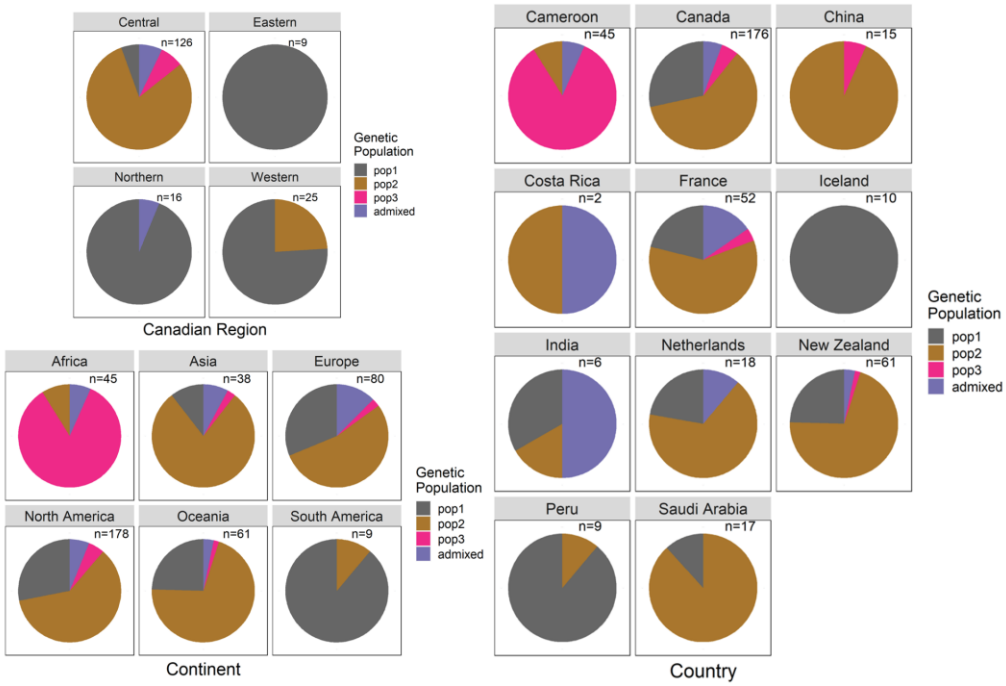

Supplementary Figure 4.4: Proportion of *A. fumigatus* isolates from genetic population 2 assigned by STRUCTURE into three nested genetic populations among Canadian regions, countries, and continents. Admixed strains with assignment identity less than 0.800 are coloured purple. n = the number of MLGs per population.

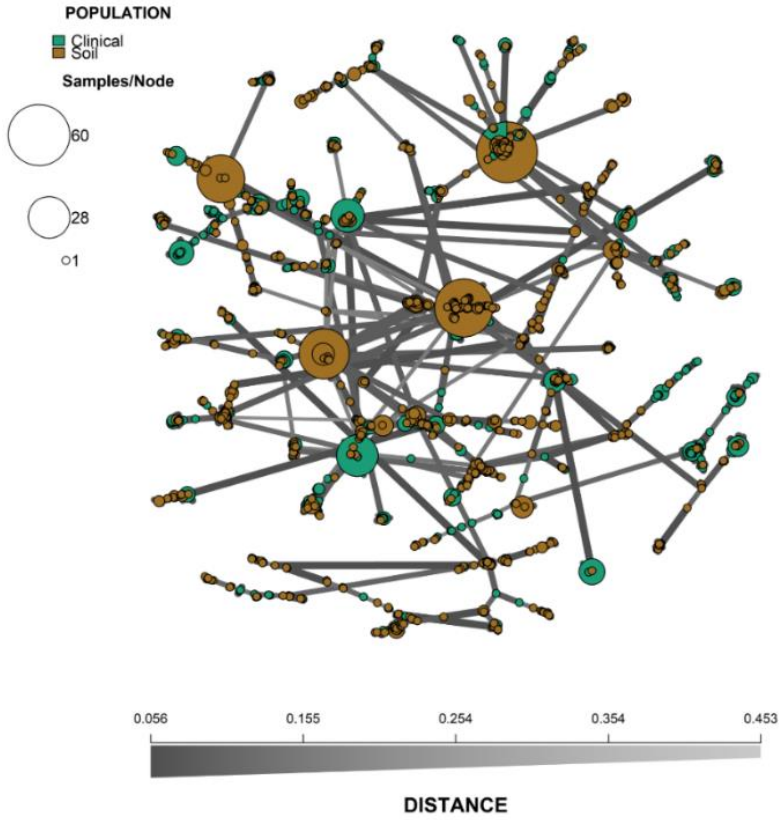

Supplementary Figure 4.5: Minimum-spanning network showing the genetic relationship between MLGs from *A. fumigatus* isolates grouped by clinical or soil origin. The genetic distance between MLGs was calculated using Bruvo's genetic distance. Each node represents one or more identical MLGs, where the node size corresponds to the number of identical MLGs.

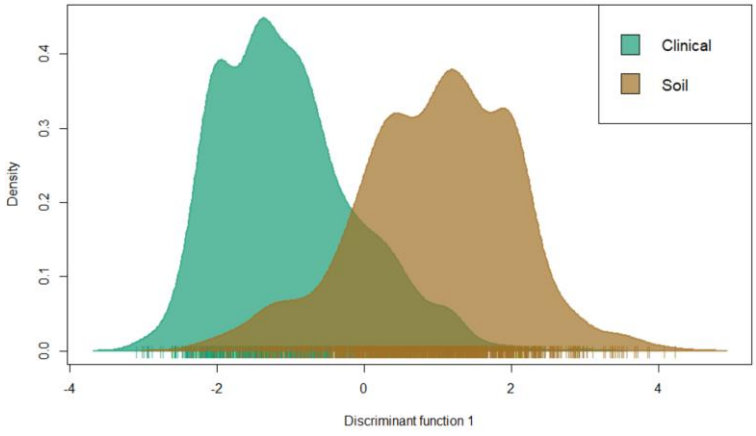

Supplementary Figure 4.6: Discriminant analysis of principal components (DAPC) of the clinical and soil *A. fumigatus* populations representing the first discriminant function in an individual density plot. All *A. fumigatus* isolates were genotyped at nine microsatellite loci.

4.7.3 Supplementary tables

Supplementary Tables 4.1: AMOVA outputs and pairwise ϕpt between full and clone-corrected *A. fumigatus* populations at country and continental levels.

Please click on the following link to access the table.
https://docs.google.com/spreadsheets/d/1eJ6WCvWhEvnWc1HfGJQlrtkFZjVTi8HVw6MIQbzEpvA/edit?usp=sharing

Supplementary Table 4.2: Summary of clinically derived *A. fumigatus* multilocus genotypes (MLGs) among continents and countries

Continent	Country	Number of isolates	Number of MLGs	MLGs represented by 2 or more isolates	Reference
Asia	China	8	8	8	Ashu et al. 2017a
	India	22	14	1	
	Total	30	22	1	
Europe	Belgium	66	58	6	
	France	30	14	6	
	Italy	6	4	1	
	Netherlands	673	500	84	
	Norway	93	83	9	
	Spain	115	28	15	
	Switzerland	68	62	5	
	Total	1051	724	131	
North America	Canada	71	68	3	Ashu et al. 2017b
	USA	45	30	7	Ashu et al. 2017a
	Total	116	98	10	
World Total		1197	843	142	

Supplementary Table 4.3: Summary of haploid diversity and private alleles among continents and country of *A. fumigatus* clinical populations of across nine STR loci.

Continent	Country	Na[1] (NP[2])	Uh[3] (± SE[4])	Clone Corrected Uh (± SE)
Asia	China	36 (0)	0.687 (0.076)	0.687 (0.076)
	India	75 (1)	0.760 (0.024)	0.881 (0.030)
	Total	93 (1)	0.818 (0.028)	0.868 (0.028)
Europe	Belgium	148 (7)	0.857 (0.016)	0.859 (0.016)
	France	69 (1)	0.795 (0.019)	0.846 (0.031)

	Italy	19 (0)	0.378 (0.071)	0.556 (0.100)
	Netherlands	263 (56)	0.855 (0.021)	0.863 (0.020)
	Norway	146 (2)	0.805 (0.032)	0.811 (0.029)
	Spain	80 (1)	0.759 (0.031)	0.799 (0.030)
	Switzerland	155 (8)	0.866 (0.022)	0.869 (0.022)
	Total	293 (116)	0.862 (0.022)	0.864 (0.020)
North America	Canada	154 (37)	0.890 (0.019)	0.892 (0.018)
	USA	110 (2)	0.855 (0.023)	0.878 (0.021)
	Total	201 (40)	0.909 (0.015)	0.912 (0.016)
World Total		335	0.863 (0.014)	0.813 (0.016)

[1] Na = number of unique alleles across 9 loci; [2] NP = Number of private alleles; [3] Uh = unbiased diversity = $(N/(N-1)) \times (1-\Sigma p_i^2)$ where p_i is the frequency of the ith allele for the population; [4] SE = Standard error

Supplementary Table 4.4: Modes of reproduction across continental and country Clinical populations of *A. fumigatus* estimated using standardized index of association ($\bar{r}_d$) and phylogenetic compatibility. Data was previously analyzed by (Ashu et al., 2018; Ashu, et al., 2017a).

Continent	Country	$\bar{r}_d$	Clone Corrected $\bar{r}_d$	Phylogenetic compatibility
Asia	China	0.027	0.027	0.805
	India	0.726 ***	0.039 *	0.694 ***
	Total	0.414 ***	0.030 *	0.250 ***
Europe	Belgium	0.145 ***	0.107 ***	0.000
	France	0.377 ***	-0.017	0.694 ***
	Italy	0.726 ***	0.667 ***	1.000
	Netherlands	0.140 ***	0.137 ***	0.000
	Norway	0.125 ***	0.124 ***	0.000
	Spain	0.440 ***	0.196 ***	0.388 ***
	Switzerland	0.098 ***	0.073 ***	0.000
	Total	0.136 ***	0.135 ***	0.000
North America	Canada	0.115 ***	0.101 ***	0.083 ***
	USA	0.265 ***	0.102 ***	0.166 ***
	Total	0.131 ***	0.086 ***	0.000
World Total		0.144 ***	0.144 ***	0.000

* p-value < 0.05, ** p-value < 0.01, *** p-value < 0.001.

4.8 References

Abdolrasouli, A., Petrou, M. A., Park, H., Rhodes, J. L., Rawson, T. M., Moore, L. S. P., Donaldson, H., Holmes, A. H., Fisher, M. C., & Armstrong-James, D. (2018). Surveillance for azole-resistant *Aspergillus fumigatus* in a centralized diagnostic mycology service, London, United Kingdom, 1998–2017. *Frontiers in Microbiology*, *9*(SEP), 2234. https://doi.org/10.3389/fmicb.2018.02234

Alexander, B. D., Procop, G. W., Dufresne, P., Espinel-Ingroff, A., Fuller, J., Ghannoum, M. A., Hanson, K. E., Holliday, D., Holliday, N. M., Ostrosky-Zeichner, L., Schuetz, A. N., Wiederhold, N. P., & Zelazny, A. M. (2017). Reference method for broth dilution antifungal susceptibility testing of filamentous fungi. 3rd ed. *Clinical and Laboratory Standards Institute*, *37*(15).

Ali, S., Gladieux, P., Leconte, M., Gautier, A., Justesen, A. F., Hovmøller, M. S., Enjalbert, J., & de Vallavieille-Pope, C. (2014). Origin, migration routes and worldwide population genetic structure of the wheat yellow rust pathogen *Puccinia striiformis f.sp. tritici*. *PLOS Pathogens*, *10*(1), e1003903. https://doi.org/10.1371/journal.ppat.1003903

Aljohani, R., Samarasinghe, H., Ashu, T., & Xu, J. (2018). Diversity and relationships among strains of culturable yeasts in agricultural soils in Cameroon. *Scientific Reports 2018 8:1*, *8*(1), 1–11. https://doi.org/10.1038/s41598-018-34122-2

Alvarez-Moreno, C., Lavergne, R. A., Hagen, F., Morio, F., Meis, J. F., & Le Pape, P. (2017). Azole-resistant *Aspergillus fumigatus* harboring TR 34 /L98H, TR 46 /Y121F/T289A and TR 53 mutations related to flower fields in Colombia. *Scientific Reports*, *7*, 45631. https://doi.org/10.1038/srep45631

Araujo, R., Amorim, A., & Gusmão, L. (2010). Genetic diversity of *Aspergillus fumigatus* in indoor hospital environments. *Medical Mycology*, *48*(6), 832–838. https://doi.org/10.3109/13693780903575360

Ashu, E. E., Hagen, F., Chowdhary, A., Meis, J. F., & Xu, J. (2017a). Global population genetic analysis of *Aspergillus fumigatus*. *MSphere*, *2*(1), e00019-17.

https://doi.org/10.1128/mSphere.00019-17

Ashu, E. E., Kim, G. Y., Roy-Gayos, P., Dong, K., Forsythe, A., Giglio, V., Korfanty, G. A., Yamamura, D., & Xu, J. (2018). Limited evidence of fungicide-driven triazole-resistant *Aspergillus fumigatus* in Hamilton, Canada. *Canadian Journal of Microbiology*, *64*(2), 119–130. https://doi.org/10.1139/cjm-2017-0410

Ashu, E. E., Korfanty, G. A., & Xu, J. (2017b). Evidence of unique genetic diversity in *Aspergillus fumigatus* isolates from Cameroon. *Mycoses*, *60*(11), 739–748. https://doi.org/10.1111/myc.12655

Auxier, B., Becker, F., Nijland, R., Debets, A. J. M., Heuvel, J. van den, & Snelders, E. (2022). Meiosis in the human pathogen *Aspergillus fumigatus* has the highest known number of crossovers. *BioRxiv*, 2022.01.14.476329. https://doi.org/10.1101/2022.01.14.476329

Ballard, E., Melchers, W. J. G., Zoll, J., Brown, A. J. P., Verweij, P. E., & Warris, A. (2018). In-host microevolution of *Aspergillus fumigatus*: A phenotypic and genotypic analysis. *Fungal Genetics and Biology*, *113*, 1–13. https://doi.org/10.1016/j.fgb.2018.02.003

Barber, A. E., Riedel, J., Sae-Ong, T., Kang, K., Brabetz, W., Panagiotou, G., Deising, H. B., & Kurzai, O. (2020). Effects of agricultural fungicide use on *Aspergillus fumigatus* abundance, antifungal susceptibility, and population structure. *MBio*, *11*(6). https://doi.org/10.1128/mbio.02213-20

Barber, A. E., Sae-Ong, T., Kang, K., Seelbinder, B., Li, J., Walther, G., Panagiotou, G., & Kurzai, O. (2021). *Aspergillus fumigatus* pan-genome analysis identifies genetic variants associated with human infection. *Nature Microbiology 2021 6:12*, *6*(12), 1526–1536. https://doi.org/10.1038/s41564-021-00993-x

Bruvo, R., Michiels, N. K., D'Souza, T. G., & Schulenburg, H. (2004). A simple method for the calculation of microsatellite genotype distances irrespective of ploidy level. *Molecular Ecology*, *13*(7), 2101–2106. https://doi.org/10.1111/J.1365-294X.2004.02209.X

Burks, C., Darby, A., Londoño, L. G., Momany, M., & Brewer, M. T. (2021). Azole-resistant *Aspergillus fumigatus* in the environment: Identifying key reservoirs and hotspots of antifungal resistance. *PLOS Pathogens*, *17*(7), e1009711. https://doi.org/10.1371/journal.ppat.1009711

Chen, Y., Litvintseva, A. P., Frazzitta, A. E., Haverkamp, M. R., Wang, L., Fang, C., Muthoga, C., Mitchell, T. G., & Perfect, J. R. (2015). Comparative analyses of clinical and environmental populations of *Cryptococcus neoformans* in Botswana. *Molecular Ecology*, *24*(14), 3559–3571. https://doi.org/10.1111/MEC.13260

Chowdhary, A., Kathuria, S., Randhawa, H. S., Gaur, S. N., Klaassen, C. H., & Meis, J. F. (2012a). Isolation of multiple-triazole-resistant *Aspergillus fumigatus* strains carrying the TR/L98H mutations in the cyp51A gene in India. *Journal of Antimicrobial Chemotherapy*, *67*(2), 362–366. https://doi.org/10.1093/jac/dkr443

Chowdhary, A., Kathuria, S., Xu, J., Sharma, C., Sundar, G., Singh, P. K., Gaur, S. N., Hagen, F., Klaassen, C. H., & Meis, J. F. (2012b). Clonal expansion and emergence of environmental multiple-triazole-resistant *Aspergillus fumigatus* strains carrying the TR34/L98H mutations in the *cyp51A* gene in India. *PLoS ONE*, *7*(12), e52871. https://doi.org/10.1371/journal.pone.0052871

Chowdhary, A., Sharma, C., van den Boom, M., Yntema, J. B., Hagen, F., Verweij, P. E., & Meis, J. F. (2014). Multi-azole-resistant *Aspergillus fumigatus* in the environment in Tanzania. *Journal of Antimicrobial Chemotherapy*, *69*(11), 2979–2983. https://doi.org/10.1093/jac/dku259

de Valk, H. A., Meis, J. F. G. M., Curfs, I. M., Muehlethaler, K., Mouton, J. W., & Klaassen, C. H. W. (2005). Use of a novel panel of nine short tandem repeats for exact and high-resolution fingerprinting of *Aspergillus fumigatus* isolates. *Journal of Clinical Microbiology*, *43*(8), 4112–4120. https://doi.org/10.1128/JCM.43.8.4112-4120.2005

Durigan, M., Ciampi-Guillardi, M., Rodrigues, R. C. A., Greinert-Goulart, J. A., Siqueira-Castro, I. C. V., Leal, D. A. G., Yamashiro, S., Bonatti, T. R., Zucchi, M. I., Franco, R. M. B., & de Souza, A. P. (2017). Population genetic analysis of *Giardia duodenalis*:

genetic diversity and haplotype sharing between clinical and environmental sources. *MicrobiologyOpen*, *6*(2), e00424. https://doi.org/10.1002/MBO3.424

Earl, D. A., & vonHoldt, B. M. (2012). STRUCTURE HARVESTER: A website and program for visualizing STRUCTURE output and implementing the Evanno method. *Conservation Genetics Resources*, *4*(2), 359–361. https://doi.org/10.1007/S12686-011-9548-7

Engel, T. G. P., Erren, E., Vanden Driessche, K. S. J., Melchers, W. J. G., Reijers, M. H., Merkus, P., & Verweij, P. E. (2019). Aerosol transmission of *Aspergillus fumigatus* in cystic fibrosis patients in the Netherlands. *Emerging Infectious Diseases*, *25*(4), 797. https://doi.org/10.3201/EID2504.181110

Etienne, K. A., Berkow, E. L., Gade, L., Nunnally, N., Lockhart, S. R., Beer, K., King Jordan, I., Rishishwar, L., & Litvintseva, A. P. (2021). Genomic diversity of azole-resistant *Aspergillus fumigatus* in the united states. *MBio*, *12*(4). https://doi.org/10.1128/MBIO.01803-21

Evanno, G., Regnaut, S., & Goudet, J. (2005). Detecting the number of clusters of individuals using the software structure: a simulation study. *Molecular Ecology*, *14*(8), 2611–2620. https://doi.org/10.1111/J.1365-294X.2005.02553.X

Fan, Y., Wang, Y., Korfanty, G. A., Archer, M., & Xu, J. (2021). Genome-wide association analysis for triazole resistance in *Aspergillus fumigatus*. *Pathogens*, *10*(6), 701. https://doi.org/10.3390/pathogens10060701

Fan, Y., Wang, Y., & Xu, J. (2020). Comparative genome sequence analyses of geographic samples of *Aspergillus fumigatus*—relevance for amphotericin B resistance. *Microorganisms*, *8*(11), 1673. https://doi.org/10.3390/microorganisms8111673

Firacative, C., Roe, C. C., Malik, R., Ferreira-Paim, K., Escandón, P., Sykes, J. E., Castañón-Olivares, L. R., Contreras-Peres, C., Samayoa, B., Sorrell, T. C., Castañeda, E., Lockhart, S. R., Engelthaler, D. M., & Meyer, W. (2016). MLST and whole-genome-based population analysis of *Cryptococcus gattii* VGIII links clinical, veterinary and

environmental strains, and reveals divergent serotype specific sub-populations and distant ancestors. *PLOS Neglected Tropical Diseases*, *10*(8), e0004861. https://doi.org/10.1371/JOURNAL.PNTD.0004861

Fraaije, B., Atkins, S., Hanley, S., Macdonald, A., & Lucas, J. (2020). The multi-fungicide resistance status of *Aspergillus fumigatus* populations in arable soils and the wider european environment. *Frontiers in Microbiology*, *11*, 3199. https://doi.org/10.3389/fmicb.2020.599233

Gómez Londoño, L. F., & Brewer, M. T. (2023). Detection of azole-resistant *Aspergillus fumigatus* in the environment from air, plant debris, compost, and soil. *PLOS ONE*, *18*(3), e0282499. https://doi.org/10.1371/journal.pone.0282499

Jeanvoine, A., Rocchi, S., Reboux, G., Crini, N., Crini, G., & Millon, L. (2017). Azole-resistant *Aspergillus fumigatus* in sawmills of Eastern France. *Journal of Applied Microbiology*, *123*(1), 172–184. https://doi.org/10.1111/jam.13488

Jombart, T., & Ahmed, I. (2011). adegenet 1.3-1: new tools for the analysis of genome-wide SNP data. *Bioinformatics*, *27*(21), 3070–3071. https://doi.org/10.1093/bioinformatics/btr521

Kamvar, Z. N., Tabima, J. F., & Grünwald, N. J. (2014). *Poppr* : an R package for genetic analysis of populations with clonal, partially clonal, and/or sexual reproduction. *PeerJ*, *2*, e281. https://doi.org/10.7717/peerj.281

Kano, R., Kohata, E., Tateishi, A., Murayama, S. Y., Hirose, D., Shibata, Y., Kosuge, Y., Inoue, H., Kamata, H., & Hasegawa, A. (2015). Does farm fungicide use induce azole resistance in *Aspergillus fumigatus*? *Medical Mycology*, *53*(2), 174–177. https://doi.org/10.1093/mmy/myu076

Korfanty, G. A., Dixon, M., Jia, H., Yoell, H., & Xu, J. (2021). Genetic diversity and dispersal of *Aspergillus fumigatus* in Arctic soils. *Genes 2022, Vol. 13, Page 19*, *13*(1), 19. https://doi.org/10.3390/GENES13010019

Korfanty, G. A., Teng, L., Pum, N., & Xu, J. (2019). Contemporary gene flow is a major

force shaping the *Aspergillus fumigatus* population in Auckland, New Zealand. *Mycopathologia*, *184*(4), 479–492. https://doi.org/10.1007/s11046-019-00361-8

Kwon-Chung, K. J., & Sugui, J. A. (2013). *Aspergillus fumigatus*--what makes the species a ubiquitous human fungal pathogen? *PLoS Pathogens*, *9*(12), e1003743. https://doi.org/10.1371/journal.ppat.1003743

Lemaire, B., Normand, A. C., Forel, J. M., Cassir, N., Piarroux, R., & Ranque, S. (2018). Hospitalized patient as source of *Aspergillus fumigatus*, 2015. *Emerging Infectious Diseases*, *24*(8), 1524–1527. https://doi.org/10.3201/EID2408.171865

Litvintseva, A. P., Thakur, R., Vilgalys, R., & Mitchell, T. G. (2006). Multilocus Sequence Typing Reveals Three Genetic Subpopulations of *Cryptococcus neoformans* var. *grubii* (Serotype A), Including a Unique Population in Botswana. *Genetics*, *172*(4), 2223. https://doi.org/10.1534/genetics.105.046672

Lofgren, L. A., Ross, B. S., Cramer, R. A., & Stajich, J. E. (2022). The pan-genome of *Aspergillus fumigatus* provides a high-resolution view of its population structure revealing high levels of lineage-specific diversity driven by recombination. *PLOS Biology*, *20*(11), e3001890. https://doi.org/10.1371/journal.pbio.3001890

Meirmans, P. G. (2006). Using the amova framework to estimate a standardized genetic differentiation measure. *Evolution*, *60*(11), 2399–2402. https://doi.org/10.1111/J.0014-3820.2006.TB01874.X

Meis, J. F., Chowdhary, A., Rhodes, J. L., Fisher, M. C., & Verweij, P. E. (2016). Clinical implications of globally emerging azole resistance in *Aspergillus fumigatus*. *Philosophical Transactions of the Royal Society of London. Series B, Biological Sciences*, *371*(1709), 20150460. https://doi.org/10.1098/rstb.2015.0460

Muller, L. A. H., & McCusker, J. H. (2009). Microsatellite analysis of genetic diversity among clinical and nonclinical *Saccharomyces cerevisiae* isolates suggests heterozygote advantage in clinical environments. *Molecular Ecology*, *18*(13), 2779–2786. https://doi.org/10.1111/J.1365-294X.2009.04234.X

O'Gorman, C. M., Fuller, H. T., & Dyer, P. S. (2009). Discovery of a sexual cycle in the opportunistic fungal pathogen *Aspergillus fumigatus*. *Nature*, *457*(7228), 471–474. https://doi.org/10.1038/nature07528

Peakall, R., & Smouse, P. E. (2006). genalex 6: genetic analysis in Excel. Population genetic software for teaching and research. *Molecular Ecology Notes*, *6*(1), 288–295. https://doi.org/10.1111/j.1471-8286.2005.01155.x

Peakall, R., & Smouse, P. E. (2012). GenAlEx 6.5: genetic analysis in Excel. Population genetic software for teaching and research--an update. *Bioinformatics (Oxford, England)*, *28*(19), 2537–2539. https://doi.org/10.1093/bioinformatics/bts460

Pirnay, J. P., Bilocq, F., Pot, B., Cornelis, P., Zizi, M., Van Eldere, J., Deschaght, P., Vaneechoutte, M., Jennes, S., Pitt, T., & De Vos, D. (2009). *Pseudomonas aeruginosa* population structure revisited. *PLOS ONE*, *4*(11), e7740. https://doi.org/10.1371/journal.pone.0007740

Pritchard, J. K., Stephens, M., & Donnelly, P. (2000). Inference of Population Structure Using Multilocus Genotype Data. *Genetics*, *155*(2), 945–959. https://doi.org/10.1093/genetics/155.2.945

Rhodes, J., Abdolrasouli, A., Dunne, K., Sewell, T. R., Zhang, Y., Ballard, E., Brackin, A. P., van Rhijn, N., Chown, H., Tsitsopoulou, A., Posso, R. B., Chotirmall, S. H., McElvaney, N. G., Murphy, P. G., Talento, A. F., Renwick, J., Dyer, P. S., Szekely, A., Bowyer, P., … Fisher, M. C. (2022). Population genomics confirms acquisition of drug-resistant *Aspergillus fumigatus* infection by humans from the environment. *Nature Microbiology 2022 7:5*, *7*(5), 663–674. https://doi.org/10.1038/s41564-022-01091-2

Rocchi, S., Godeau, C., Scherer, E., Reboux, G., & Millon, L. (2021). One year later: The effect of changing azole-treated bulbs for organic tulips bulbs in hospital environment on the azole-resistant *Aspergillus fumigatus* rate. *Medical Mycology*, *59*(7), 741–743. https://doi.org/10.1093/mmy/myab007

Samarasinghe, H., Lu, Y., Aljohani, R., Al-Amad, A., Yoell, H., & Xu, J. (2021). Global

patterns in culturable soil yeast diversity. *IScience*, *24*(10), 103098. https://doi.org/10.1016/J.ISCI.2021.103098

Sewell, T. R., Zhu, J., Rhodes, J., Hagen, F., Meis, J. F., Fisher, M. C., & Jombart, T. (2019). Nonrandom distribution of azole resistance across the global population of *Aspergillus fumigatus*. *MBio*, *10*(3), e00392-19. https://doi.org/10.1128/mBio.00392-19

Sharma, C., Hagen, F., Moroti, R., Meis, J. F., & Chowdhary, A. (2015). Triazole-resistant *Aspergillus fumigatus* harbouring G54 mutation: Is it de novo or environmentally acquired? *Journal of Global Antimicrobial Resistance*, *3*(2), 69–74. https://doi.org/10.1016/J.JGAR.2015.01.005

Shelton, J. M. G., Collins, R., Uzzell, C. B., Alghamdi, A., Dyer, P. S., Singer, A. C., & Fisher, M. C. (2022). Citizen science surveillance of triazole-resistant *Aspergillus fumigatus* in United Kingdom residential garden soils. *Applied and Environmental Microbiology*, *88*(4). https://doi.org/10.1128/aem.02061-21

Simwami, S. P., Khayhan, K., Henk, D. A., Aanensen, D. M., Boekhout, T., Hagen, F., Brouwer, A. E., Harrison, T. S., Donnelly, C. A., & Fisher, M. C. (2011). Low diversity *Cryptococcus neoformans* Variety *grubii* multilocus sequence types from Thailand are consistent with an ancestral African origin. *PLOS Pathogens*, *7*(4), e1001343. https://doi.org/10.1371/journal.ppat.1001343

WorldHealthOrganization. (2022). *WHO fungal priority pathogens list to guide research, development and public health action*. World Health Organization. https://www.who.int/publications/i/item/9789240060241

Xu, J. (2022). Assessing global fungal threats to humans. *MLife*, *1*(3), 223–240. https://doi.org/10.1002/MLF2.12036

Zhang, J., Verweij, P. E., Rijs, A. J. M. M., Debets, A. J. M., & Snelders, E. (2022). Flower bulb waste material is a natural niche for the sexual cycle in *Aspergillus fumigatus*. *Frontiers in Cellular and Infection Microbiology*, *11*. https://doi.org/10.3389/fcimb.2021.785157

Zhou, D., Gong, J., Duan, C., He, J., Zhang, Y., & Xu, J. (2023). Genetic structure and triazole resistance among *Aspergillus fumigatus* populations from remote and undeveloped regions in Eastern Himalaya. *MSphere, 8*. https://doi.org/10.1128/msphere.00071-23

Zhou, D., Korfanty, G. A., Mo, M., Wang, R., Li, X., Li, H., Li, S., Wu, J.-Y., Zhang, K.-Q., Zhang, Y., & Xu, J. (2021). Extensive genetic diversity and widespread azole resistance in greenhouse populations of *Aspergillus fumigatus* in Yunnan, China. *MSphere, 6*(1). https://doi.org/10.1128/msphere.00066-21.

Chapter 5

Variations in Sexual Fitness among Natural Strains of the Opportunistic Human Fungal Pathogen *Aspergillus fumigatus*

Abstract *Aspergillus fumigatus* is a ubiquitous ascomycete fungus, naturally inhabiting the soil and compost piles. Its conidia readily disperse into the atmosphere and cause opportunistic infections known as aspergillosis. With the emerging resistance to many antifungal drugs, our understanding of *A. fumigatus* epidemiology has become increasingly important for developing effective control and treatment strategies. As a pathogen capable of both sexual and asexual reproduction, mutations causing drug resistance and increased virulence could be spread rapidly in *A. fumigatus* populations. However, relatively little is known about the distributions of sexual reproductive fitness among natural strains of *A. fumigatus*. Here we investigated the formation of sexual reproductive structure (i.e. cleistothecia) and sexual spore viability among 60 natural strains of *A. fumigatus*. These strains were from six geographically distant countries (India, China, Canada, Cameroon, Saudi Arabia, and New Zealand), with 10 strains (including five *MAT1-1* strains and five *MAT1-2* strains) from each country. These strains were crossed in all combinations with strains of the opposite mating type. In addition, all 60 strains were crossed with either AFB62-1 (*MAT1-1*) or AFIR928 (*MAT1-2*), two reference supermater strains. Of the 900 crosses among the 60 natural strains, 136 crosses (15.1%) produced cleistothecia. Our analyses revealed that strains from China had the highest average ability to form cleistothecia, followed by those from New Zealand, Saudi Arabia, India, Canada, and Cameroon. Among the crosses that produced cleistothecia, about 40% produced viable ascospores, with the rate of ascospore germination varied significantly among crosses. Interestingly, neither the ability to form cleistothecia nor ascospore germination rate showed any distinct relationships with either geographic or genetic distance between parental strains. Our results suggest that genetic exchange among geographically and genetically divergent

strains of *A. fumigatus* are possible. However, the rates of genetic exchange likely vary among strains and populations in nature.

I was the first author for the study in this chapter, the following paper has been published:

Korfanty, G., Stanley, K., Lammers, K., Fan, Y. Y., & Xu, J. (2021). Variations in sexual fitness among natural strains of the opportunistic human fungal pathogen *Aspergillus fumigatus*. *Infection, Genetics and Evolution,* 87, 104640. https://doi.org/10.1016/j.meegid.2020.104640

5.1 Introduction

Sexual reproduction is a fundamental feature of most eukaryotes. Through sexual reproduction, alleles from diverse sources can be combined into the same individual offspring. The ability to undergo sexual reproduction among strains and populations of organisms is also the hallmark of the biological species concept. In contrast, the formations of barriers leading to the inability to undergo sexual reproduction among strains and populations of organisms are the hallmarks of speciation, the evolutionary process of forming distinct species. Speciation is among the main drivers of biodiversity and is considered one of the fundamental issues in evolutionary biology. At the genetic level, speciation occurs when a population separates from other members of its species and accumulates independent genetic changes, leading to reproductive isolation. Mechanisms of reproductive isolation can be grouped into two broad categories, pre-zygotic and post-zygotic reproductive isolation. Pre-zygotic reproductive barriers refer to those that prevent fertilization from occurring while post-zygotic reproductive barriers reduce the viability or fertility of hybrid offspring. For several reasons, fungi can be excellent models for studying reproductive isolation and speciation: (i) many fungi can be cultured and crossed in vitro, (ii) they are amenable to experimental manipulations, (iii) they have relatively small genomes, and (iv) they often have broad geographical and ecological ranges (Giraud et al., 2008; Vogan & Xu, 2014). There are several known fungal examples of pre-zygotic reproductive barriers [e.g. sexual and heterokaryon (vegetative) incompatibilities] and post-zygotic reproductive barriers (e.g.

meiotic mutants and spore killer mutants). However, despite these potential advantages, little is known about the distributions of sexual reproductive fitness among strains and populations for most fungi, including the medically important species *Aspergillus fumigatus*.

Aspergillus fumigatus is a cosmopolitan saprophytic fungus found worldwide, playing an important role in decomposing organic materials and in nutrient cycling. Its natural niche is soil, growing on organic debris and sporulating abundantly into asexual spores, conidia, that readily become airborne. These spores are frequently inhaled by humans and in healthy individuals, are eliminated by pulmonary defense mechanisms. However, in immunocompromised hosts, the host immune system can fail to clear the inhaled conidia, which leads to a group of diseases generally termed as aspergillosis. As such, *A. fumigatus* is a common opportunistic pathogen. The fungus was long considered an asexual fungus until 2009 when its sexual cycle was reported (O'Gorman et al., 2009). Specifically, strains of *A. fumigatus* belong to one of two mating types, *MAT1-1* and *MAT1-2*. When strains of these two different mating types are crossed with each other, cleistothecia, the typical sexual reproductive structure of ascomycete species, may be observed. In the original experiment by O'Gorman et al., (2009), it took about six months for two strains to mate and generate viable offspring, the ascospores. A subsequent study identified a more suitable condition as well as two strains, AFB62-1 and AFIR928, that were capable of completing the sexual cycle much faster than originally reported by O'Gorman et al., (2009) (Sugui et al., 2011). Strain AFB62-1 was isolated from a patient with invasive aspergillosis in San Antonio, Texas, United States (AFB62-1) and it has the *MAT1-1* mating type. Strain AFIR928 was isolated from an environmental sample in Dublin, Ireland and it has the alternative mating-type *MAT1-2*. These two strains could mate and produce mature cleistothecia with an abundance of viable ascospores in four weeks (Sugui et al., 2011). As a result of their high fertility and efficient reproduction, strains AFB62-1 and AFIR928 have been used as reference strains (supermaters) for genetic studies of *A. fumigatus*.

Sexual reproduction in *A. fumigatus* is similar to those in other filamentous ascomycetes. Specifically, contact between the hyphae of parental strains with different mating-types

(*MAT1-1* and *MAT1-2*) leads to cell fusion and the generation of heterokaryotic hyphae. The nuclei of the two mating partners then fuse, followed by meiosis to generate four recombinant haploid nuclei. Each of these haploid nuclei then undergo one round of mitosis to produce eight haploid ascospores within each ascus. These asci and ascospores are contained within spherical fruiting bodies, known as cleistothecia, and they are typically found in the contact zones between the two mating partner colonies (O'Gorman et al., 2009).

Owing to increases in the number of immunocompromised patients and in the severity of immunosuppressive therapies over recent years, there has been a dramatic rise in sufferers of aspergillosis (Kosmidis & Denning, 2015). Approximately 10% of the time, this infection becomes invasive and causes death in up to 90% of cases (Chowdhary et al., 2013). The presence of a sexual cycle in *A. fumigatus* suggests mutations originated in one strain could be passed onto another strain with a different genotype, enabling the potential creation of strains that are resistant to multiple drugs and/or with new virulence properties. In addition, sexual recombination may confound diagnostic tests to track the spread of *A. fumigatus* genotypes and drug-resistance genes (Alvarez-Perez et al., 2010). However, there is currently limited information on sexual reproductive fitness among natural strains of *A. fumigatus.* As a result, the potential rates of spread of antifungal drug resistance genes and virulence properties within and among populations of this species are unknown.

The objectives of this study were to assess sexual reproductive ability among 60 strains of *A. fumigatus* obtained from six geographically distinct populations. Here, sexual reproductive ability between pairs of strains were assayed based on whether they were able to form cleistothecia and whether their ascospores are viable. The ability to form cleistothecia between mating partners in *A. fumigatus* was considered a successful mating, with the number of cleistothecia representing a quantitative estimate of their mating ability. In contrast, the inability to form cleistothecia represented one form of reproductive isolation between those strains. For strain pairs that formed cleistothecia, the viability of their ascospores represents the second feature of their sexual reproductive fitness, with a high rate of ascospore germination signifying a high post-zygotic reproductive fitness while a low

germination rate indicating the presence of a post-zygotic reproductive barrier. With data on those two traits, we were interested in whether geographically closely located strains were more likely to be sexually compatible with each other (i.e., having a greater ability to produce cleistothecia and producing more viable ascospores) than those from geographically distant regions. In addition, we obtained multilocus microsatellite genotypes from all strains. The relationships between genetic distance of the parental strains and their sexual fitness will also be analyzed.

5.2 Materials and Methods

5.2.1 *Aspergillus fumigatus* strains

The two reference supermater strains AFB62-1 and AFIR928 were obtained from Dr. June Kwon-Chung at NIAID, NIH, USA. The 60 *A. fumigatus* strains assayed here were collected from either environmental or clinical sources from geographically distant regions in the following six countries: Canada, Cameroon, China, India, New Zealand, and Saudi Arabia. From each country, we randomly selected ten strains total, with five representing mating-type *MAT1-1* and five representing the alternative mating-type *MAT1-2* (The strain mating types were determined following the procedure described below). Strains from Canada, Cameroon, India, and New Zealand have been reported previously (Ashu, Korfanty, et al., 2017; Ashu, Kim, et al., 2018; Chang et al., 2016; Korfanty et al., 2019). The strains from China and Saudi Arabia were recently isolated from soil samples of these two countries, following procedures described in Ashu et al., (2017). All strains were genotyped at nine highly polymorphic microsatellite loci as described below. Information about all 62 strains, including their strain codes, geographic locations, mating types, and multilocus microsatellite genotypes are presented in Table 5.1. It should be noted that the 60 analyzed strains were obtained from limited locations in each of the six countries. Thus, while the 10 strains from each country were randomly selected for this study, they are unlikely representative of the genotypes and sexual fitness features of *A. fumigatus* population from each of the six countries.

Table 5.1: *Aspergillus fumigatus* strains used within this study. Five *MAT1-1* strains and five *MAT1-2* strains were selected from each of New Zealand, Saudi Arabia, Cameroon, Hamilton (Canada), India and China. Two supermater strains, AFB62-1 and AFIR928, were also included, to give a total of sixty-two strains. Listed in the table are strain ID, country of origin, specific region within the country, approximate latitude (Lat) and longitude (Lon) coordinates, ecological origin (either environmental or clinical source), and their microsatellite genotype at nine loci.

ID	Mating Type	Region, Country	Lat/long	Source	2A	2B	2C	3A	3B	3C	4A	4B	4C
C158	*MAT1-2*	Makepe, Cameroon	9.741/4.064	Enviro.	14	33	8	6	12	36	6	6	10
C304	*MAT1-2*	Eloundem, Cameroon	11.437/3.838	Enviro.	8	27	10	35	7	30	3	3	4
C308	*MAT1-1*	Eloundem, Cameroon	11.437/3.838	Enviro.	8	27	10	14	11	34	4	3	4
C322	*MAT1-2*	Eloundem, Cameroon	11.437/3.838	Enviro.	5	24	7	15	8	31	3	3	4
C372	*MAT1-1*	Mbalgong, Cameroon	11.468/3.803	Enviro.	9	28	2	6	11	34	6	6	10
C428	*MAT1-2*	Simbock, Cameroon	11.475/3.821	Enviro.	5	24	7	14	6	50	3	3	4
C44	*MAT1-1*	Mbingo, Cameroon	10.29/6.164	Enviro.	5	24	7	25	7	31	3	3	4
C480	*MAT1-1*	Mbandoumou, Cameroon	11.453/3.791	Enviro.	9	28	11	20	15	38	8	9	10
C65	*MAT1-1*	Bambui, Cameroon	10.232/6.015	Enviro.	9	28	11	20	13	38	8	9	10
C79	*MAT1-2*	Bambui, Cameroon	10.232/6.015	Enviro.	11	30	3	1	9	32	8	8	8
CF10	*MAT1-1*	St. George, Canada	-80.25/43.271	Agri.	23	41	25	19	5	34	7	9	10
CM16	*MAT1-1*	St. George, Canada	-80.25/43.271	Agri.	13	32	15	10	3	25	8	8	9
CM58	*MAT1-2*	St. George, Canada	-80.25/43.271	Agri.	10	28	12	32	11	6	7	8	9
Hclin-09	*MAT1-2*	Hamilton, Canada	-79.856/43.263	Clinical	13	31	15	20	10	33	8	9	10
Hclin-21	*MAT1-1*	Hamilton, Canada	-79.856/43.263	Clinical	10	29	12	20	12	32	11	8	9
Hclin-34	*MAT1-2*	Hamilton, Canada	-79.856/43.263	Clinical	10	29	12	10	10	33	5	5	6
Hclin-42	*MAT1-1*	Hamilton, Canada	-79.856/43.263	Clinical	23	41	25	6	2	25	14	6	10
M14	*MAT1-2*	Hamilton, Canada	-79.919/43.261	Urban	17	36	19	26	10	51	7	7	15
M16	*MAT1-2*	Hamilton, Canada	-79.919/43.261	Urban	23	31	14	30	14	33	9	9	6
P20	*MAT1-1*	Hamilton, Canada	-79.786/43.277	Urban	11	29	13	10	28	21	15	7	8
AC10-2	*MAT1-2*	Ailao mountains, China	101.37/24.206	Enviro.	18	25	16	27	11	26	21	10	4
AC3-3	*MAT1-1*	Ailao mountains, China	101.37/24.206	Enviro.	21	17	11	36	22	25	9	9	9
AC3-4	*MAT1-1*	Ailao mountains, China	101.37/24.206	Enviro.	8	14	8	23	12	9	6	4	4
AC6-5	*MAT1-1*	Ailao mountains, China	101.37/24.206	Enviro.	16	10	13	41	10	26	33	9	7
AC7-1	*MAT1-2*	Ailao mountains, China	101.37/24.206	Enviro.	9	10	11	21	13	21	10	7	4
AC8-4	*MAT1-1*	Ailao mountains, China	101.37/24.206	Enviro.	21	15	20	27	12	25	12	10	7
C2-5	*MAT1-2*	Fenyi, China	114.687/27.828	Enviro.	16	10	14	24	10	21	7	7	6
C4-1	*MAT1-2*	Fenyi, China	114.687/27.828	Enviro.	16	10	14	24	10	21	7	7	6
C4-2	*MAT1-2*	Fenyi, China	114.687/27.828	Enviro.	16	10	14	24	10	21	7	7	6
C5-10	*MAT1-1*	Fenyi, China	114.687/27.828	Enviro.	16	20	26	30	12	17	11	7	7
I1268	*MAT1-2*	New Delhi, India	77.222/28.598	Clinical	20	26	17	28	9	20	18	10	5

I1272	*MAT1-2*	New Delhi, India	77.222/28.598	Clinical	25	23	11	0	9	7	7	10	8
I1591	*MAT1-2*	New Delhi, India	77.222/28.598	Clinical	0	0	0	0	0	0	0	0	0
I162	*MAT1-1*	New Delhi, India	77.222/28.598	Enviro.	14	20	9	31	9	10	8	10	28
I245	*MAT1-1*	New Delhi, India	77.222/28.598	Clinical	14	20	9	31	9	10	8	10	28
I2581	*MAT1-1*	New Delhi, India	77.222/28.598	Clinical	19	12	8	13	9	22	18	11	15
I384	*MAT1-2*	New Delhi, India	77.222/28.598	Enviro.	11	21	8	24	10	10	12	4	5
I388	*MAT1-2*	New Delhi, India	77.222/28.598	Enviro.	18	12	15	52	25	19	15	9	5
I437	*MAT1-1*	New Delhi, India	77.222/28.598	Enviro.	14	20	9	31	9	10	8	10	28
I591	*MAT1-1*	New Delhi, India	77.222/28.598	Clinical	14	20	9	31	9	10	8	10	28
A3-4	*MAT1-2*	Trusts Arena, New Zealand	174.636/-36.866	Enviro.	18	10	14	31	10	9	14	8	9
A6-6	*MAT1-1*	Trusts Arena, New Zealand	174.636/-36.866	Enviro.	17	25	16	30	10	26	10	10	9
D2-6	*MAT1-2*	Auckland Domain, New Zealand	174.776/-36.859	Enviro.	19	10	13	24	24	19	7	7	4
D6-5	*MAT1-1*	Auckland Domain, New Zealand	174.776/-36.859	Enviro.	17	20	21	27	42	20	7	8	7
M3-8	*MAT1-2*	Millennium Field, New Zealand	174.731/-36.743	Enviro.	19	10	13	24	24	19	6	7	4
M4-8	*MAT1-1*	Millennium Field, New Zealand	174.731/-36.743	Enviro.	11	18	8	29	8	9	7	9	19
R5-6	*MAT1-2*	Auckland Rail, New Zealand	174.765/-36.849	Enviro.	18	10	19	29	12	21	9	8	4
U5-1	*MAT1-1*	Auckland University, New Zealand	174.77/-36.85	Enviro.	15	22	19	25	12	20	11	8	6
V6-1	*MAT1-2*	Mount Eden, New Zealand	174.765/-36.877	Enviro.	11	18	9	26	8	9	14	8	9
V8-8	*MAT1-1*	Mount Eden, New Zealand	174.765/-36.877	Enviro.	15	10	9	13	8	15	7	8	7
AML22	*MAT1-2*	Al-Madinah East, Saudi Arabia	39.61/24.473	Enviro.	19	10	13	24	24	19	7	7	4
AML81	*MAT1-1*	Al-Madinah East, Saudi Arabia	39.61/24.473	Enviro.	16	22	13	35	10	19	9	8	7
Jed22	*MAT1-2*	Jeddah, Saudi Arabia	39.171/21.606	Enviro.	19	10	13	24	25	19	7	7	4
Jed47	*MAT1-1*	Jeddah, Saudi Arabia	39.171/21.606	Enviro.	16	16	10	22	10	32	9	13	4
Jed57	*MAT1-2*	Jeddah, Saudi Arabia	39.171/21.606	Enviro.	19	10	13	24	24	19	7	7	4
Jed70	*MAT1-1*	Jeddah, Saudi Arabia	39.171/21.606	Enviro.	17	10	14	24	8	19	14	7	7
Jed71	*MAT1-1*	Jeddah, Saudi Arabia	39.171/21.606	Enviro.	12	8	6	36	8	6	8	9	13
Jed75	*MAT1-2*	Jeddah, Saudi Arabia	39.171/21.606	Enviro.	9	10	13	11	18	59	15	9	4
Yan179	*MAT1-2*	Yanbu, Saudi Arabia	38.067/24.088	Enviro.	19	10	13	24	24	19	7	7	4
Yan67	*MAT1-1*	Yanbu, Saudi Arabia	38.067/24.088	Enviro.	19	13	11	18	10	7	6	4	5
AFB62	*MAT1-1*	San Antonio, United States	-98.492/29.425	Clinical	16	14	11	23	16	24	4	10	NA
AFIR928	*MAT1-2*	Dublin, Ireland	-6.313/53.324	Enviro.	16	10	14	24	10	21	7	7	4

5.2.2 Mating-type identification and strain genotyping

For strains from Canada, Cameroon, India, and New Zealand that were previously published by our lab (Ashu, Korfanty, et al., 2017; Ashu, Kim, et al., 2018; Chang et al., 2016; Korfanty et al., 2019), their mating types and multilocus microsatellite genotypes were obtained from those reports. For strains from China and Saudi Arabia, their mating types and microsatellite genotypes were determined following protocols described in Korfanty et al., (2019). Briefly, the mating type of each strain was identified through PCR using a 11.5 µL reaction volume that contained 5 µL 2x GoTaq Master Mix (Promega), 0.32 µL AFM1 (5′-CCTTGACGCGATGGGGTGG-3′) and AFM2 (5′-CGCTCCTCATCAGAACAACTCG-3′) forward primers, 0.64 µl AFM3 (5′-CGGAAATCTGATGTCGCCACG-3′) reverse primer, 3.72 µL nuclease free H_2O, and 1.5 µL diluted genomic DNA. The PCR protocol involved a denaturation step of 95°C for 5 min, followed by 35 cycles of 95°C for 30 seconds, 60°C for 30 seconds, and 72°C for 1 min, and concluded with a final elongation step at 72°C for 5 min. For microsatellite genotyping at nine loci, we followed the protocol described by de Valk et al. (2005). In brief, PCR on three separate multiplex reactions were conducted where each contained three primer pairs each. Capillary electrophoresis was conducted on the amplified products to obtain fragment lengths, and repeat lengths were determined for each of the nine loci., following that described earlier (de Valk et al., 2005; Korfanty et al., 2019). Only one strain, Indian strain I1591, was not able to be genotyped in this study.

5.2.3 Mating and cleistothecia formation

The sixty natural strains belonged to two mating types, with 30 belonging to the *MAT1-1* type and the remaining 30 belonging to the *MAT1-2* type. Each strain was mated with 30 strains of the opposite mating type. Together, 900 crosses (30 x 30) were made among the 60 strains (Table 5.1). In addition, each of the 60 strains were mated with either of the two supermaters, AFIR928 or AFB62-1. As a positive control, the two supermaters AFIR928 and AFB62-1 were crossed with each other. For a negative control, each of the 62 strains were crossed with itself. In total, this yielded 1023 crosses, including 62 self crosses (negative controls), 900 non-self crosses involving only our natural strains, and 61 crosses involving at least one supermater.

Crosses were conducted on oatmeal agar (12g/L agar, 60g/L Quaker oatmeal), a medium shown to be the most conducive for mating in *A. fumigatus* by previous studies (O'Gorman et al., 2009; Sugui et al., 2011). For each cross, two drops of conidia (5 µL each, ~1000 conidia) of each parental strain were pipetted onto opposing ends of an oatmeal agar plate. A strain with an opposing mating type was then pipetted similarly such that both strains are perpendicular to one another (a representative set up is shown in Figure 5.1). These plates were sealed with parafilm and wrapped in stacks of five with aluminum foil. The stacks were incubated at 30°C in the dark. The strains would then grow to cover the plate and produce cross-like junction zones where sexual mating may occur. The plates were inspected twice in the initial month, and four times during each subsequent month up to seven months. The colony morphology, presence of junction or barrage zones, and the presence and number of cleistothecia for each plate were recorded. The cleistothecia formation rate for each population was calculated as the ratio of successful crosses over the total number of crosses performed. In contrast to the method outlined by O'Gorman et al. (2009), the mating plates were not hoovered prior to inspection but instead were scraped with the insulin needle to expose cleistothecia. Mating success rates were calculated for within and between pairs of countries. In addition, the mating success rates were separately calculated for those involving the supermaters and those without supermaters. Sexual fertility in this study was assessed in two ways: the presence or absence of cleistothecia and the number of cleistothecia formed per cross.

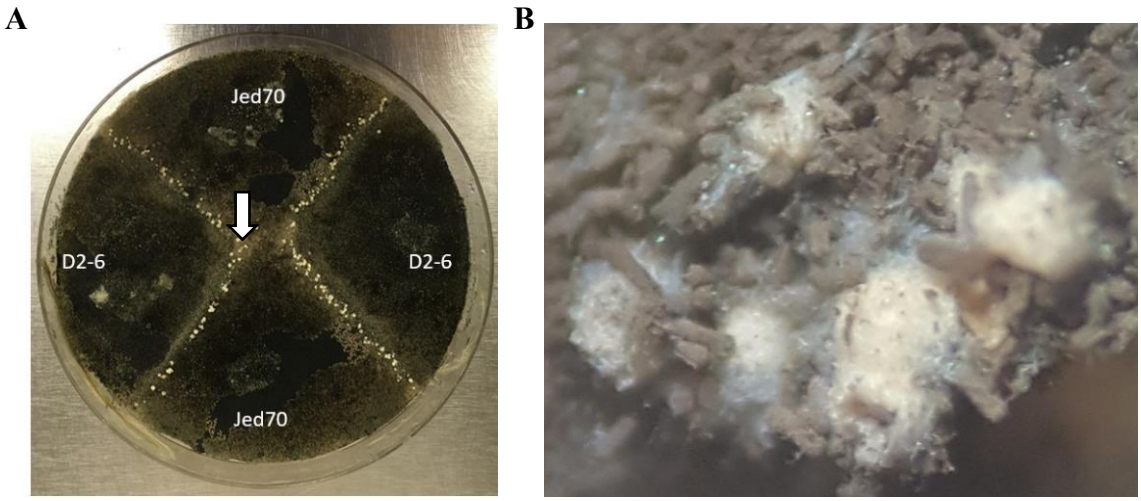

Figure 5.1: A representative cross showing successful mating. (A) Here, the cross was between *A. fumigatus* strain Jed70 (*MAT1-1* from Saudi Arabia) and strain D2-6 (*MAT1-2* from New Zealand). 10 µL of spore solution was inoculated on oatmeal agar medium, wrapped in parafilm and incubated at 30 °C in the dark. A dark green lawn of conidia covered the surface of the plate. Arrow indicates a cleistothecium (a white dot) formed along the junction of two intersecting colonies of opposite mating types after four weeks of incubation. (B) 48× magnification image of cleistothecia.

5.2.4 Ascospore germination

Crosses that successfully produced cleistothecia were examined for their ascospore germinations. Approximately three weeks after cleistothecia were first observed, three to five cleistothecia were harvested using an insulin needle from successful crosses and suspended in 0.05% TWEEN 20 solution. Cleistothecia suspensions were then vortexed for 10 min to release ascospore from cleistothecia. Ascospore concentrations were adjusted to 2.00×10^3 cfu using the Countess™ II Automated Cell Counter from Thermo Fisher Scientific. Vegetative cells such as hyphae and conidia incidentally attached to the cleistothecia and the needles were killed via heating the cell suspensions at 70°C for 60 min. 100 µL of each ascospore suspension was plated on Sabouraud dextrose agar (SDA) supplemented with chloramphenicol and incubated at 37°C for 2-3 days. The percentage of viable ascospores germinated was calculated as the ratio of germinated spores over the total number of plated spores.

5.2.5 Data analysis

The numbers of successful crosses were compared among those from within and between countries. Similarly, the ascospore germination rates were compared among successfully mated crosses from different countries. The statistical significances of the differences in mating success and in spore germination were obtained based on Fisher's Exact test using the R package *rcompanion* (R Core Team, 2020).

Aside from the above pairwise tests, we also investigated whether geographic distance and genetic distance (as estimated based on microsatellite genotypes) between mating partners might impact mating success and/or ascospore germination rates. Pearson's correlation coefficients were calculated for each of the comparisons. Here, the geographic distance between each pair of strains was calculated in kilometers based on approximate latitude and longitude coordinates of each strain, using the R package *geosphere* (R Core Team, 2020). The genetic distance between each pair of mating partners used the Bruvo's distance. The Bruvo's distance incorporates repeat size into the distance algorithm and assumes a stepwise mutation model for microsatellite markers. The script *bruvo.dist* within the R package *poppr* created a distance matrix between all pairwise strains (Kamvar et al., 2014; R Core Team, 2020). The distance matrix contained values ranging from 0 to 1, where 0 indicated an identical genotype between the two parental strains and 1 indicated a theoretical maximum distance if all alleles from one strain differed by an infinite number of repeats from all alleles at the nine loci in the second strain. The values generated from *bruvo.dist* were used to create a neighbor joining tree for all 61 genotyped isolates using the R package *ape* (Paradis & Schliep, 2019). Kruskal-Wallace tests were conducted between geographic and genetic distance groups using the R package *ggpubr* (R Core Team, 2020).

5.3 Results

5.3.1 Genetic similarity among strain populations

Among the 60 natural strains analyzed in this study, 40 from India, New Zealand, Canada, and Cameroon have been reported in previously published studies. The remaining 20 were newly isolated, with 10 from China and 10 from Saudi Arabia. We successfully obtained the

microsatellite genotypes of these 20 strains. Based on the genotypes of these strains, a neighbor-joining tree using Bruvo's genetic distances among the strains were constructed shown in Figure 5.2. Our analyses showed that the Cameroonian and Canadian strains formed a cluster different from those in four other countries. The four other countries were generally inter-dispersed with each other across the remainder of the tree. Similarly, both mating types were inter-dispersed with each other across the neighbor-joining tree.

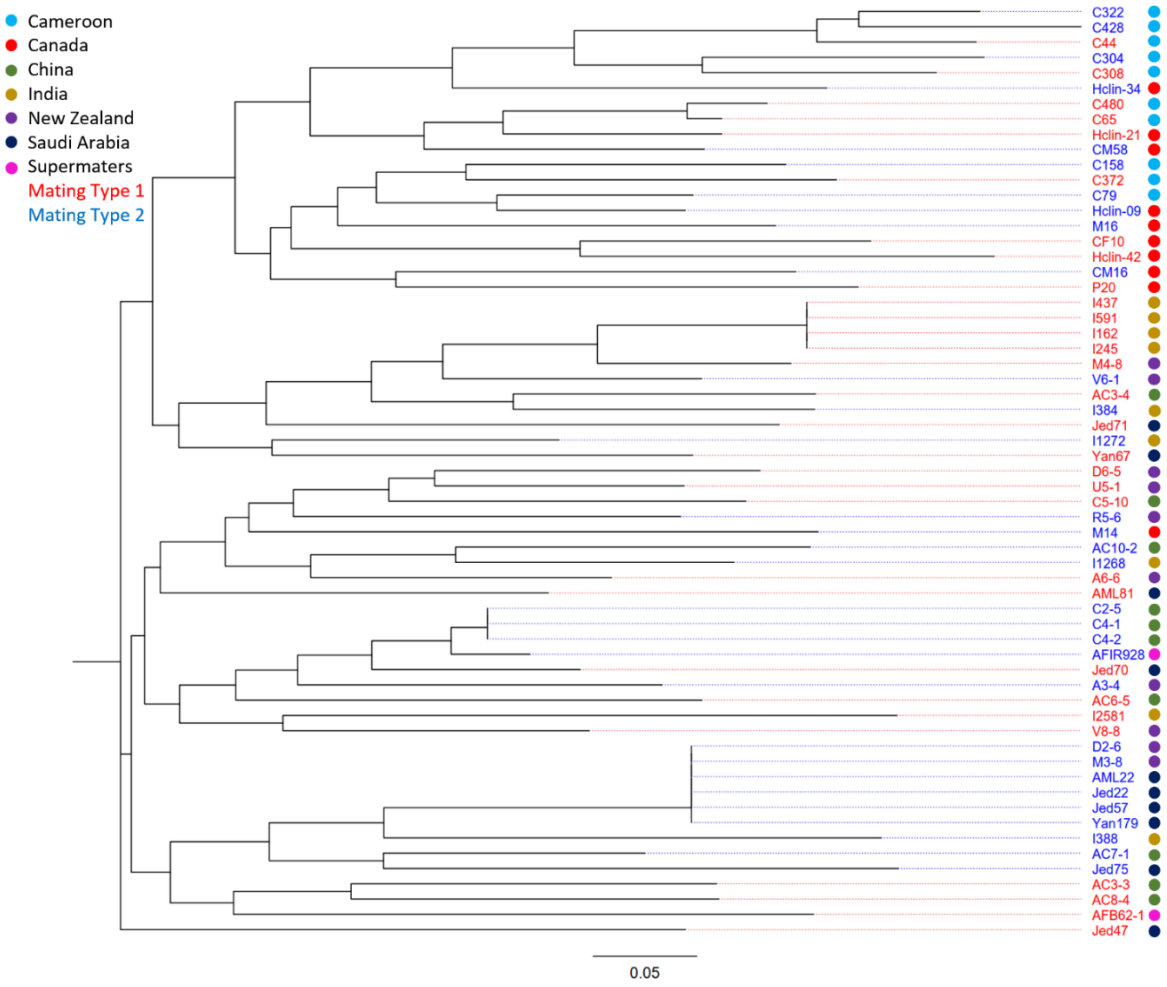

Figure 5.2: Neighbor joining tree of *A. fumigatus* strains used in this study. Bruvo's genetic distance between all the parental strains was calculated using the short tandem repeat (STR) genotypes of each strain. *MAT1-1* strains IDs are red, *MAT1-2* strain IDs are blue. Country of origin for each strain is represented by a coloured circle. Scale bar represents 5% genetic variation. Indian strain I1591 was not included as its STR genotype was not determined.

5.3.2 Mating and cleistothecia formation

Of the 900 crosses involving the 60 natural strains, 136 (15.1%) produced cleistothecia. For the 61 crosses that involved at least one supermater strain, 38 (62.3%) produced cleistothecia. The cross between the two supermaters AFIR928 and AFB62-1 produced cleistothecia within the expected four to five weeks as shown previously (Sugui et al., 2011). Also as expected, none of the 62 self crosses produced any cleistothecia. Aside from cleistothecia formation along the junction zone for successfully mated crosses, several other colony phenotypes were also observed. For example, crosses that did not produce any cleistothecia had several phenotypes, the most common being a fairly homogeneous lawn of hyphae and conidia without cleistothecia. Other phenotypes included the presence of barrages at the junction zones of two mated strains or an altered coloration of conidial colour. A few representative colony phenotypes of select crosses are shown in Supplementary Figure 5.1. Among the crosses that produced cleistothecia, the number of cleistothecia varied widely, from less than five to over 100, depending on the cross (Figure 5.3). Within most crosses, the majority of cleistothecia were distributed across junction zones between the two parental strains. Less commonly, cleistothecia were present along the edges and/or in the center of the plate. Overall, the number of observed cleistothecia depended on the specific strains and/or strain combinations (Figure 5.3).

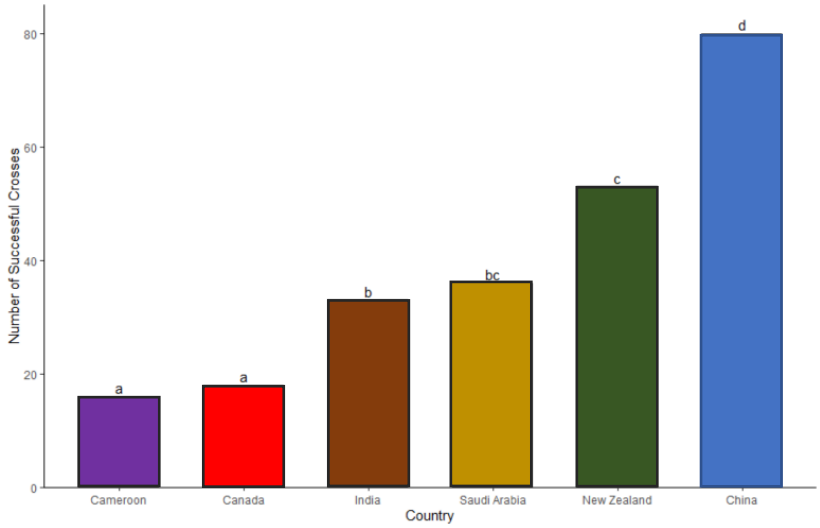

Figure 5.3: The number of successful crosses for each of the six countries. For each country, 285 crosses were performed involving at least one strain from that country. Successful crosses were designated by the presence of cleistothecia. Fisher's Exact test was conducted for each of the 15 pairwise combinations. Different letters represent that their differences are statistically significant at $p < 0.05$ between countries.

Large variations in mating success were observed among individual strains originating from the same country and between strains originating from different countries. Of the 60 strains, 4 failed to mate with any of the 30 strains of the opposite mating type, with the remaining 56 strains successfully mated with at least one strain. However, upon inclusion of the supermater strains, all strains successfully mated with at least one strain. The strain with the highest mating success was C2-5 that produced cleistothecia when crossed with 19 of the 31 strains of opposite mating type (61%). Interestingly, crosses involving strains from within the same country had an overall higher mating success rate than those involving strains from different countries (Table 5.2). Specifically, of the 136 crosses that produced cleistothecia, 36 were from intranational crosses (out of 150 total intranational crosses, or an overall mating success rate of 24%). The remaining 100 successful crosses were between strains from different countries (out of 750 total international crosses, or a mating success rate of 13.3%). The intranational mating success rate was significantly higher than that of the international crosses (p-value = 0.0016).

Table 5.2: Mating success rate (%) between strains from within and between the six different countries. The total number of crosses performed within each country is 25 while that between any two countries is 50. Significant difference, obtained through Fisher's Exact Test, was denoted when *p*-value <0.05. Intranational crosses are shown across diagonal with different superscripts have significantly different mating success. International crosses in their mating success rates are shown below diagonal. Statistically significant differences between both intranational and international crosses are denoted above the diagonal line at top right side.

	Canada	China	Cameroon	India	New Zealand	Saudi Arabia
Canada	0[a]	*			*	*
China	14	64[b]	#	*#		#
Cameroon	0	20	4[a]		*	
India	12	32	0	4[a]	*	
New Zealand	10	38	4	6	56[b]	*
Saudi Arabia	0	24	6	14	20	16[a]
Supermaters	40	80	10	20	80	90

* = significance only with one intranational rate with the countries listed in the row,

= significance only with one intranational rate with the countries listed in the column,

*# = significance was obtained with both intranational rates.

Of the six intranational cross groups, China showed the highest mating success (64%), followed by New Zealand (56%), Saudi Arabia (16%), and India and Cameroon (both at 4%) (Table 5.2). None of the 25 intranational crosses between strains from within Canada produced cleistothecia. However, several Canadian strains mated successfully with strains from China, India, and New Zealand. Furthermore, crosses that involved at least one Chinese strain had the highest mating success rate (28.7%), accounting for over 50% (79/136) of the successful crosses. In contrast, crosses involving the Cameroonian strains had the lowest mating success rate (5.8%), with a total of 16 successful crosses.

Mating success rates were further compared between crosses involving and crosses not involving the supermater strains (Table 5.2). As expected, at the population level, the supermater strains had an overall significantly higher mating success than those not involving supermater strains (p-value < 0.001). Interestingly, two strains from southern China of the *MAT1-2* type, strains C2-5 and C4-2 had more successful crosses than the reference supermater of the *MAT1-2* type, AFIR928. Specifically, out of the 31 crosses involving each of these three strains C2-5, C4-2, and AFIR928, 19, 17, and 15 crosses respectively produced

cleistothecia. However, the observed differences among the three strains were not statistically significant.

Aside from mating success (as defined based on whether any cleistothecia was produced), we also noted the number of cleistothecia produced in each successful cross. Our results showed large variations among the 136 crosses (Figure 5.4). In general, across all countries, the majority of crosses had few cleistothecia, falling into the one to five and six to ten cleistothecia per plate. However, only eight successful crosses produced between 50 and 100 cleistothecia. These crosses involved strains from China, New Zealand, and India. This pattern of cleistothecia production parallels the observed mating success rates of the different geographic populations.

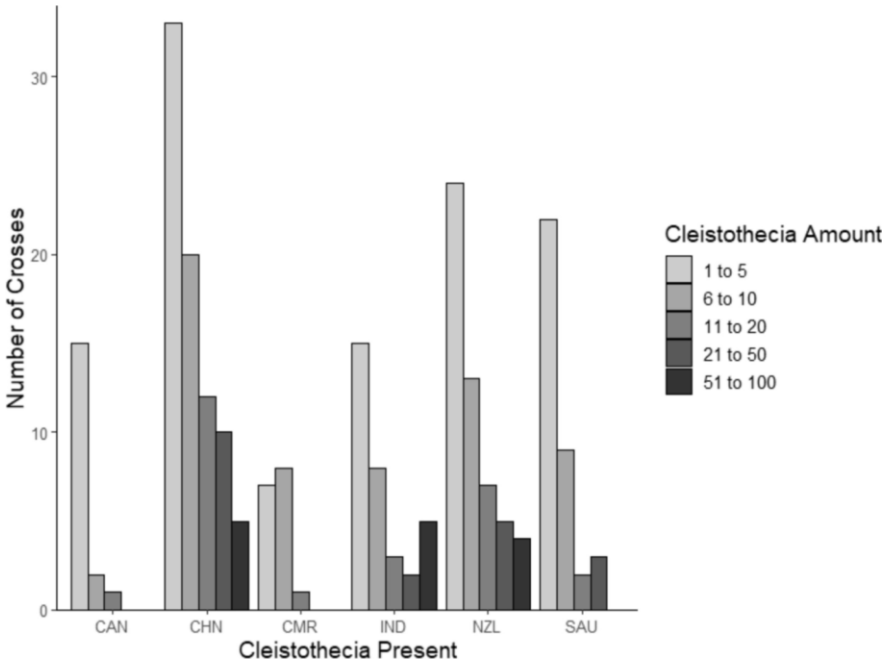

Figure 5.4: The number of cleistothecia developed per cross separated based on the country of origin. To be counted toward a country, at least one of the parental strains in the cross needs to come from that country. Cleistothecia from successful crosses were counted and were grouped into 5 ranges (1 to 5, 6 to 10, 11 to 20, 21 to 50, and 51 to 100). CAN = Canada, CHN = China, CMR = Cameroon, IND = India, NZL = New Zealand, SAU = Saudi Arabia.

5.3.3 Effect of genetic and geographic distance on mating success

We investigated the relationship between geographic distance between parental strains and mating success. The geographic distance between parental isolates ranged from approximately 0 to 1391 km (for intranational crosses) to a max of 16 248 km (Cameroon C79 and New Zealand D6-5 parental strains) and was binned into seven ranges of 2500 km intervals. The mating success rate was determined for all crosses that fell into their respective distance range (Figure 5.5A). Geographic distance was found to significantly impact mating success rate (p-value = 0.0385). However, upon adjustment for the number of populations, no significant differences were observed within the pairwise comparisons among the different geographic distance ranges. The effect of geographic distance on cleistothecia production was then investigated (Figure 5.6A). Successful crosses were classified on the number of cleistothecia they produced. These cleistothecial ranges were: 1 to 5, 6 to 10, 11 to 20, 21 to 50 and 51 to 100. Overall, crosses that produced one to five cleistothecia had parental isolates with a significantly greater geographic distance than those crosses that produced six to ten or eleven to twenty cleistothecia (p-value < 0.001 and p-value < 0.05 respectively). However, no other significant relationships were observed between other cleistothecial ranges (detailed analyses not shown).

Similarly, the effect of genetic distance on mating success was investigated. The genetic distance between parental strains was determined and binned into seven ranges (Figure 5.5B). Genetic distance significantly influenced mating success rate (p-value = 0.0035). However, few significant differences were observed among the seven bins of genetic distances. The only one showing significant difference with others was the group of parental strains that were binned into the 0.565 to 0.678 genetic distance range. This group had a significantly lower mating success than those binned into the other ranges. The effect of genetic distance on cleistothecia production was also investigated (Figure 5.6B). However, unlike the significance obtained with geographic distance on cleistothecia production, no significant relationships were present between any of the five cleistothecial ranges (p-value = 0.14).

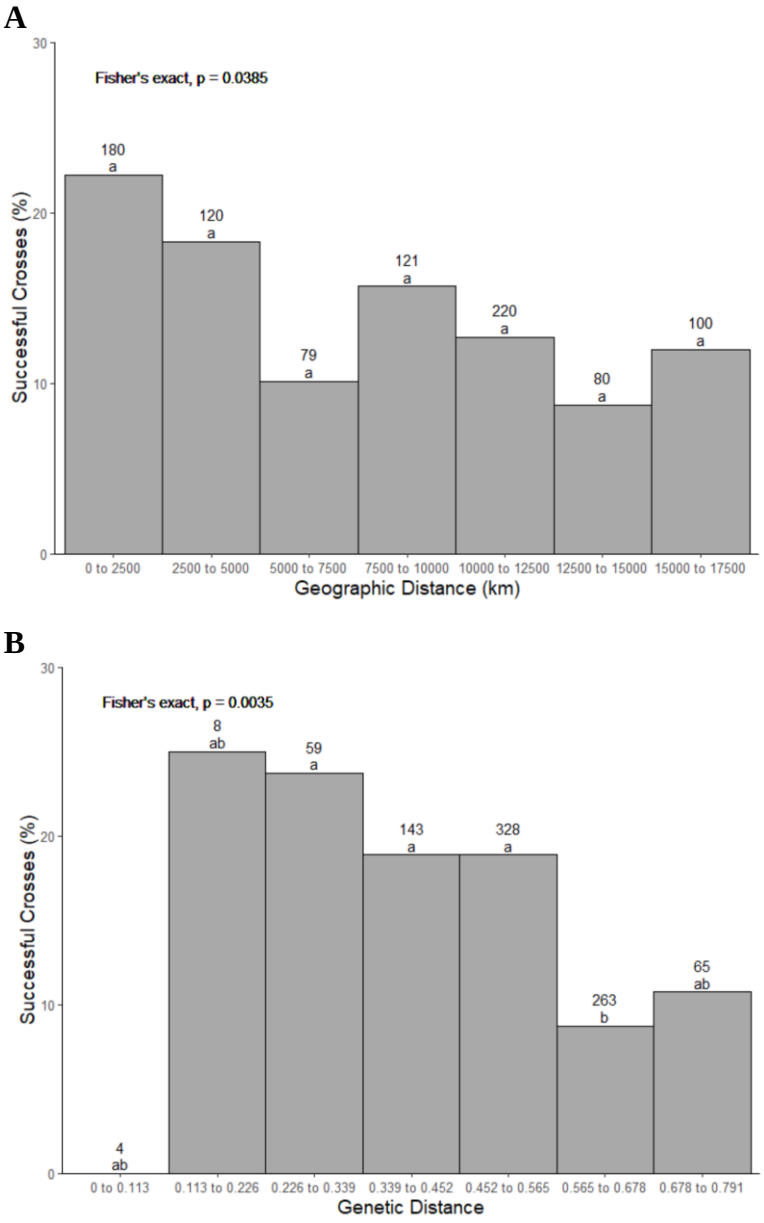

Figure 5.5: The effect of geographic and genetic distance between parental strains on mating success and cleistothecia formation. Genetic distance between parental strains was calculated as Bruvo's distance. Fisher's exact test was conducted for both the overall and the pairwise comparisons between the seven distance groups (bins). The number above each bar represents the total number of crosses within each bin. Different letters above each bar represent statistically significant difference at $p < 0.05$ between distance bins. (A) The percentage of successful crosses within each of the seven binned geographic distances. (B) The percentage of successful crosses within each of the seven binned Bruvo's genetic distances.

A

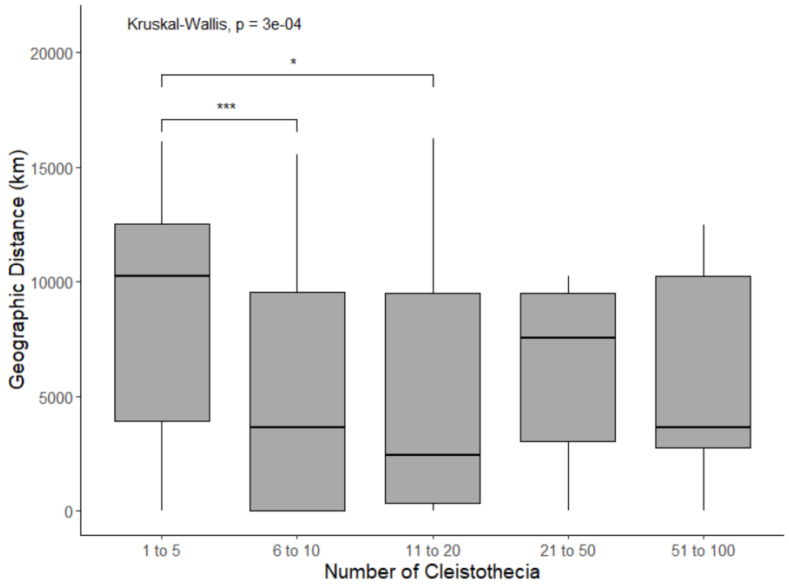

B

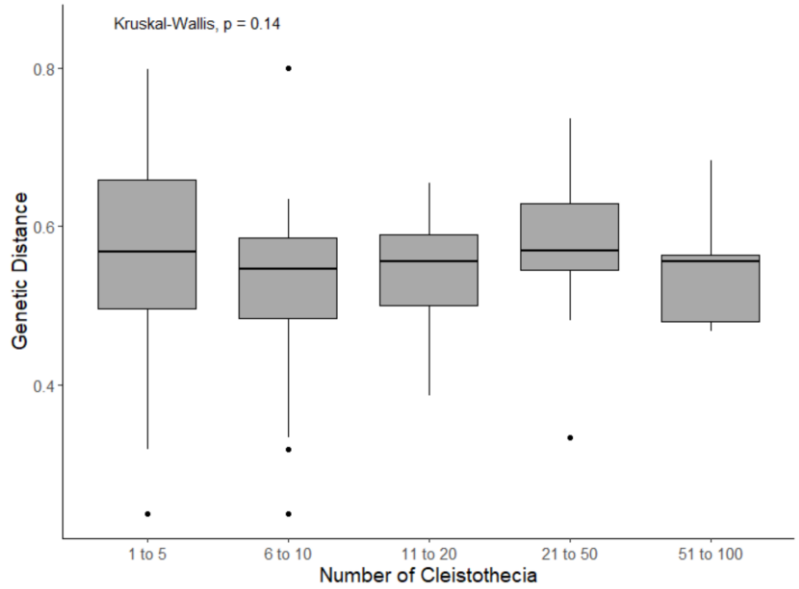

Figure 5.6: Effect of geographic and genetic distances on cleistothecial number in successful crosses. Successful crosses were separated into five groups based on cleistothecial number. Kruskal-Wallis test for significance was conducted between groups. Wilcoxon signed-rank test determined pairwise significance between groups. *Represents a *p*-value <0.05, ***Represents a *p*-value <0.001. (A) Cleistothecial number compared to geographic distance. (B) Cleistothecial number compared to genetic distance.

5.3.4 Rates of germination success among successful crosses

Crosses that produced cleistothecia were tested for ability to produce viable ascospores on SDA medium (Table 5.3). Variable ascospore germination rates were observed among crosses. Of the 136 successful crosses, ascospores that were harvested from 55 of them (40.4%) successfully germinated. Of these 55 crosses, 22 were intranational crosses (out of 36 total intranational crosses that produced cleistothecia, for an overall rate of 61.1% that produced any viable ascospore). The remaining 33 were international crosses (out of 100 total international crosses that produced cleistothecia, for an overall rate of 33% that produced any viable ascospore). The ascospore germination rates among the 55 crosses ranged from 0.17% to 21.1%, with an average of 3.9% (± 4.78%). Similar to cleistothecial development, there was a significant proportional difference between intranational and international crosses that produced viable ascospores (p-value = 0.0052) (Figure 5.7). Here, successful crosses involving strains obtained from China, India and New Zealand had a significantly higher average germination success rate than those involving strains from Canada, Saudi Arabia, and Cameroon. None of the crosses with a Canadian parental strain produced viable ascospores.

Table 5.3: Germination rate, in descending order, of the 55 crosses with viable ascospores. Geographic and genetic distance between parental strains is listed in addition to the germination rate of each cross. CHN = China, CMR = Cameroon, IND = India, NZL = New Zealand, SAU = Saudi Arabia.

MAT1-1	*MAT1-2*	Cross type	Germination Rate	Bruvo's Distance	Geographic Distance (km)
AC6-5	AC7-1	CHN X CHN	21.1 (±23.26)	0.655	0
M4-8	A3-4	NZL X NZL	17.33 (±15.53)	0.556	16.06
A6-6	AC7-1	NZL X CHN	16.4 (±19.84)*	0.556	10223.8
AC3-4	C4-1	CHN X CHN	14.33 (±11.73)	0.546	1391.22
Jed_70	AML_22	SAU X SAU	11.1 (±15.02)*	0.722	320.71
AC3-4	C2-5	CHN X CHN	8.9 (±8.8)*	0.616	1391.22
AC3-4	Jed_57	CHN X SAU	8.7 (±9.13)*	0.523	6334.24
U5-1	C4-2	NZL X CHN	8.67 (±7.57)	0.533	9523.59
C5-10	Jed_75	CHN X SAU	7.5 (±12.99)	0.318	7553.5
I591	C2-5	IND X CHN	7.5 (±2.29)	NA	3663.63
I2581	AC7-1	IND X CHN	7 (±12.09)*	0.276	2453.44
M4-8	R5-6	NZL X NZL	7 (±1.32)	0.533	12.11
I2581	C4-2	IND X CHN	6.9 (±7.79)*	0.557	3663.63
C44	C2-5	CMR X CHN	6.17 (±1.04)	0.583	11098.3

U5-1	V6-1	NZL X NZL	5.8 (±8.4)*	0.479	3
M4-8	C2-5	NZL X CHN	4.67 (±1.04)	0.561	9513.35
I591	C4-1	IND X CHN	4.5 (±4.3)*	0.557	3663.63
M4-8	C4-1	NZL X CHN	4.4 (±4.66)*	0.556	9513.35
I162	A3-4	IND X NZL	4.33 (±1.76)	0.5	12468.58
AC6-5	C4-2	CHN X CHN	3.83 (±0.58)	0.375	1391.22
C5-10	C4-2	CHN X CHN	3.67 (±0.76)	0.62	0
I2581	C2-5	IND X CHN	3.5 (±2.18)	0.71	3663.63
AC3-3	C4-2	CHN X CHN	3.3 (±3.9)*	0.59	1391.22
C5-10	Jed_57	CHN X SAU	2.67 (±4.62)	0.484	7553.5
U5-1	R5-6	NZL X NZL	2.33 (±2.25)	0.556	0.44
U5-1	A3-4	NZL X NZL	2.3 (±1.96)*	0.563	12.11
C5-10	AC10-2	CHN X CHN	2.13 (±2.17)	0.637	1391.22
C44	C4-2	CMR X CHN	1.67 (±1.61)	0.622	11098.3
AC6-5	C2-5	CHN X CHN	1.33 (±2.31)	0.72	1391.22
M4-8	AC7-1	NZL X CHN	1.33 (±1.04)	0.524	10224.7
A6-6	A3-4	NZL X NZL	1.3 (±2.08)*	0.556	0
AC3-3	C4-1	CHN X CHN	1.17 (±0.29)	0.59	1391.22
AML_81	A3-4	SAU X NZL	1.17 (±0.29)	NA	15547.1
A6-6	C2-5	NZL X CHN	1 (±0.87)	0.552	9515.48
AC3-3	C2-5	CHN X CHN	0.83 (±1.44)	0.236	1391.22
C5-10	C428	CHN X CMR	0.83 (±1.44)	0.606	11110.77
I437	A3-4	IND X NZL	0.83 (±0.58)	0.375	12468.58
M4-8	V6-1	NZL X NZL	0.83 (±1.04)	0.358	15.13
C5-10	AC7-1	CHN X CHN	0.67 (±0.76)	0.461	1391.22
I162	AC7-1	IND X CHN	0.67 (±0.76)	0.582	2453.44
M4-8	D2-6	NZL X NZL	0.67 (±1.15)	0.484	13.49
I591	C4-2	IND X CHN	0.5 (±0.5)	0.453	3663.63
Jed_70	A3-4	SAU X NZL	0.5 (±0.87)	0.359	15425.61
M4-8	M3-8	NZL X NZL	0.5 (±0.87)	0.285	0
U5-1	AC7-1	NZL X CHN	0.5 (±0.5)	0.453	10233.46
D6-5	A3-4	NZL X NZL	0.33 (±0.29)	0.318	12.51
I162	C4-1	IND X CHN	0.33 (±0.29)	0.8	3663.63
I245	AC7-1	IND X CHN	0.33 (±0.58)	0.586	2453.44
M4-8	AC10-2	NZL X CHN	0.33 (±0.29)	0.644	10224.7
M4-8	C4-2	NZL X CHN	0.33 (±0.58)	0.656	9513.35
U5-1	C2-5	NZL X CHN	0.33 (±0.58)	0.434	9523.59
AC3-3	Jed_57	CHN X SAU	0.17 (±0.29)	0.194	6334.24
AC3-4	A3-4	CHN X NZL	0.17 (±0.29)	0.385	10223.8
AC3-4	AML_22	CHN X SAU	0.17 (±0.29)	0.538	6210.75
C5-10	C2-5	CHN X CHN	0.17 (±0.29)	0.561	0

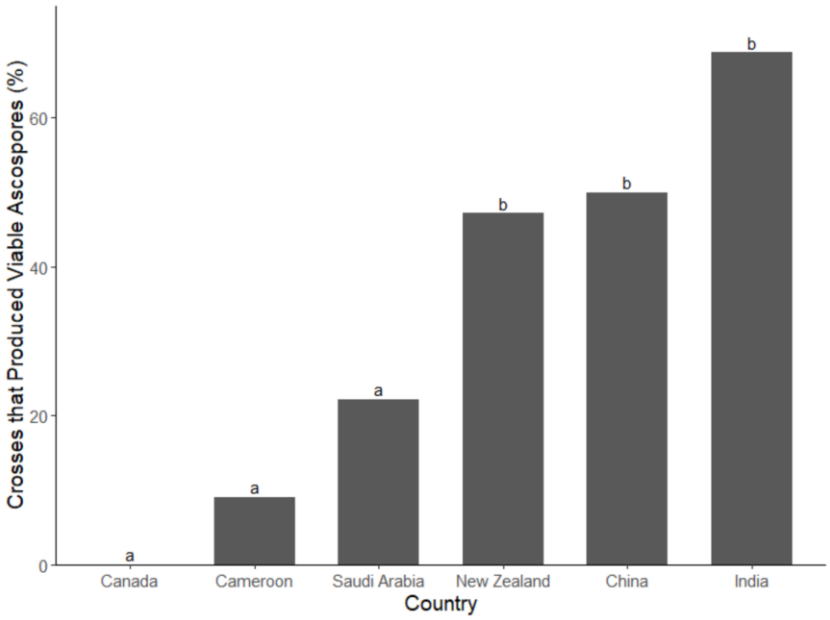

Figure 5.7: Percentage of viable ascospores based on geographic origins of parental strains. *A. fumigatus* strains originated from six countries: China, New Zealand, Saudi Arabia, India, Canada, and Cameroon. A total of 55 crosses contained viable ascospores as determined based on their ability to germinate on SDA media. Fisher's Exact test was conducted for each of the 15 pairwise combinations. Different letters represent statistically significant difference of $p < 0.05$ between countries.

Among the 56 strains that produced cleistothecia with at least one other parental strain, only 30 of these had viable ascospore progeny when crossed. Interestingly, strain C2-5 to be involved in the highest number of crosses that produced viable progeny. Along with the *MAT1-1* strain M4-8, strains C2-5 and M4-8 each produced viable progeny in 10 different crosses. The supermaters AFIR928 and AFB62-1 parented viable progeny in 11 and 15 crosses respectively. The supermater control had a germination rate of 9.83% (± 4.04%). Indeed, the germination rates were quite variable between crosses, where only 5 (9.09%) crosses had above 10% germination. Within a cross, ascospores from different cleistothecia also showed highly variable spore germination rates. Among the top five crosses with the highest ascospore germination rates, four were intranational and only one was an international cross. Of these intranational crosses, two involved Chinese strains, one involved New Zealand strains and the last involved Saudi Arabian strains. The only international cross producing highly viable ascospores was between a New Zealand strain and a Chinese strain.

5.3.5 Effect of genetic and geographic distance on germination success

Parallel to our investigation on the relationship between geographic/genetic distance and mating success, the relationships between these two-distance metrics and ascospore germination rates were also investigated. Here, the geographic distance was similarly binned into seven ranges of 2500 km intervals and the crosses that produced any viable ascospores were placed in their respective bins (Figure 5.8A). Similar to mating success, geographic distance between parental strains were found to be significantly correlated with their progeny ascospore germination success (p = 0.005). Specifically, ascospores from parents located between 12,500 km to 15,000 km apart had no germination success, which was significantly different than intranational crosses (0 to 2500 km range). This suggests that parental isolates that were geographically closer to each other were more likely to produce viable ascospore progeny. However, no correlation was observed between genetic distance of the parental strains and the germination success of their ascospore progeny (p = 0.647) (Figure 5.8B).

A

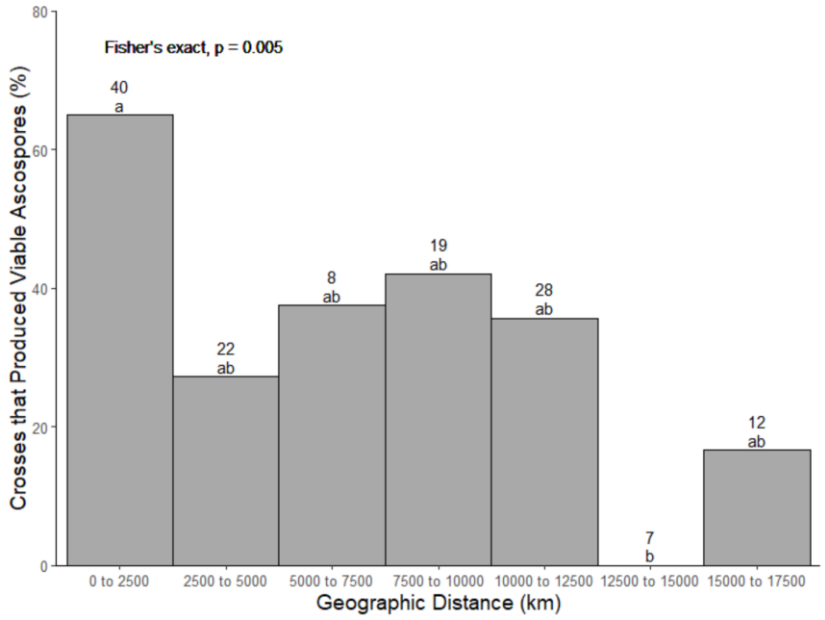

B

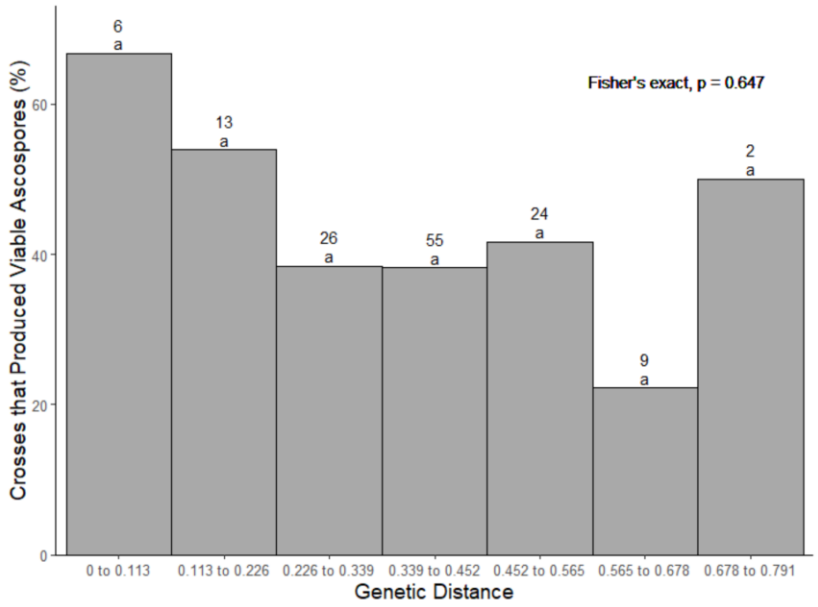

Figure 5.8: The effect of genetic and geographic distance on ascospore germination success. Fisher's exact test was conducted for both overall and pairwise between the seven distance groups (bins). The number above each bar represents the total number of crosses within each bin. Different letters represent statistically significant differences at $p < 0.05$ between distance bins. (A) The percentage of germination success within each of the seven binned geographic distances. (B) The percentage of germination success within each of the seven binned genetic distances.

We also investigated the potential relationship between geographic/ genetic distance of the parental strains and the ascospore germination rate for only the 55 crosses that produced viable ascospores. Figure 5.9 shows the negative correlation between the geographic distance of the parental strains and ascospore germination rate of these 55 crosses. However, the relationship was statistically not significant (*p*-value = 0.2023). By contrast, a positive correlation was observed between the genetic distance of the parental isolates and ascospore germination rate (Figure 5.10). Again, this correlation was statistically not significant (*p*-value = 0.1427).

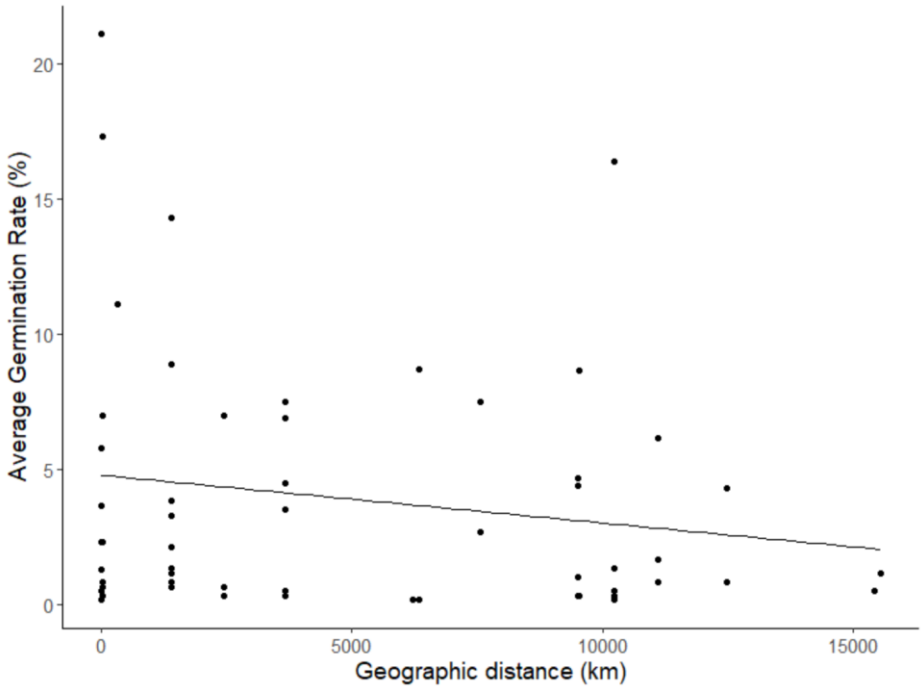

Figure 5.9: Relationship between geographic distance of parental strains and their progeny ascospore germination rate. The geographic distance (km) between the 55 parental strain pairs was calculated using the latitudinal and longitudinal coordinates of each strain. This distance is plotted against the germination rate of the offspring ascospore. Each data point represents the average of 3 to 5 repeats. Linear model *p*-value = 0.202.

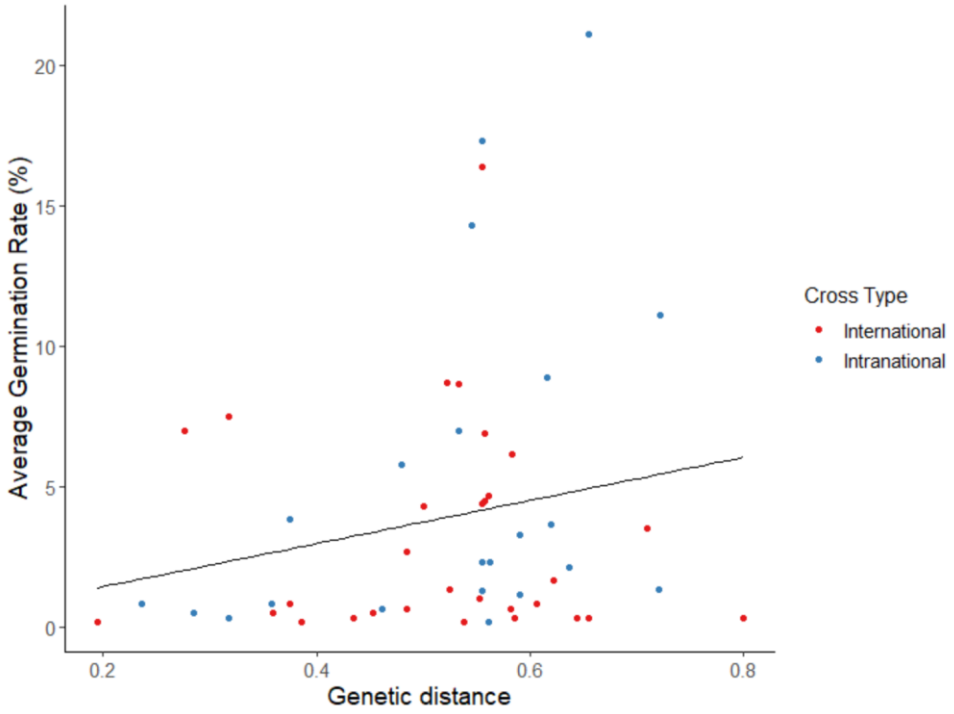

Figure 5.10: The relationship between genetic distance between parental strain pairs and their offspring ascospore germination rate. Bruvo's genetic distance between parental strain pairs in each of the 55 crosses that produced ascospores was calculated using the short tandem repeat (STR) genotypes of each strain. The genetic distance was plotted against the germination rate of the offspring ascospore, calculated from an average of 3–5 repeats. Red and blue circles are international and intranational crosses respectively. Linear model *p*-value = 0.1427.

5.3.6 Correction for the low sexually fertility present within distant populations

Our results suggested that there was high variability in sexual fertility within and among our study populations. This variability was particularly obvious within the Canadian population, as crosses involving Canadian strains exhibited much lower fitness in terms of both mating success and ascospore germination than isolates from other populations. As the Canadian population was the most geographically distant population used in our study, the low mating success of the strains in this populations could have contributed disproportionally to some of the observed correlations. To correct for this potential bias, we analyzed a subset of strains that produced 6 to 10 cleistothecia (Figure 5.4) from each study population and performed the correlational analysis with both geographic and genetic distances. The 6 to 10 cleistothecial range was chosen as it represented a low to moderate mating success and contained enough crosses for analysis.

The relationship between geographic/genetic distance for crosses that produced 6 to 10 cleistothecia was initially investigated (Supplementary Figure 5.2). Similar to Figure 5.5A, geographic distance was significantly correlated with mating success (*p*-value = 0.0350). However, no significant differences were observed among the seven bins. In addition, similar to Figure 5.5B**,** genetic distance was significantly correlated with mating success rate (p-value = 0.0005). Furthermore, the bin with parental strain genetic distance between 0.565 and 0.678 showed lower mating success than the bins with closer genetic distances (0.226 to 0.339 and 0.452 to 0.565).

Next, we investigated the relationship between geographic/genetic distance for crosses that produced 6 to 10 cleistothecia and the percentages of viable ascospores that they produced (Supplementary Figure 5.3). Again, similar patterns to Figure 5.8A and B, geographic distance was significantly correlated with ascospore germination success (*p*-value = 0.005). The 0 to 2500 km range had significantly more crosses that produced viable ascospores than the 2500 to 5000 km range. No significant differences between the remaining ranges were observed. With regards to genetic distances, no significant relation between genetic distance and the production of viable ascospores was observed (*p*-value = 0.2024).

Lastly, we investigated whether geographic or genetic distance was correlated with ascospore germination rate for crosses that produced 6 to 10 cleistothecia (Supplementary Figures 5.4 and 5.5). Similar to both Figures 5.9 and 5.10, significant correlations were observed for both geographic and genetic distance with ascospore germination rate (Supplementary Figures 5.4 and 5.5; *p*-value = 0.3454 and *p*-value = 0.1217 respectively). In summary, the subset of crosses that produced 6 to 10 cleistothecia showed similar correlations to geographic and genetic distances as those based on the total sample. Both types of analyses revealed potential effects of geographic and genetic distances of their parental strains on sexual fitness in our crosses.

5.4 Discussion

This study investigated the potential presence of pre- and post-zygotic isolation between geographically distant *A. fumigatus* strains and populations. Sixty isolates that contained an even distribution of both *MAT1-1* and *MAT1-2* were analyzed, ten from each of the six countries, and crossed in all 900 combinations. Two supermater controls were additionally crossed with each parental strain. Crosses that involved Chinese strains demonstrated the highest average mating success in terms of cleistothecial development. By contrast, crosses involving Canadian and Cameroonian strains had the lowest mating success. Additionally, the potential effects of geographic and genetic distance between parental strains on both mating success and ascospore germination rate were investigated. Our analyses identified that the origin of a parental strain could significantly influence both mating and ascospore germination successes. Overall, an increase of geographic or genetic distance between parental strains generally led to a decrease in both mating and ascospore germination success. Below we will discuss our results.

A large proportion of crosses (84.9%) did not produce any cleistothecia. The phenotypes associated with these crosses ranged from a standard green suede-like lawn of mycelia and conidia to growth inhibition along the junction zones and altered conidial pigments for both parental strains. Vegetative incompatibility has been studied and shown previously in fungal and *Aspergillus* literature (Bruggeman et al., 2003; Glass & Kaneko, 2003). The phenotypes observed within our study had characteristic elements of vegetative incompatibility. These include hyphal repulsion or deadlock across the junction zone (Falconer et al., 2008; Glass et al., 2000), suggested by the lack of mycelia across the junction between the parental strains. In some of the crosses, increased mycelial growth at the junction zone was found, forming a barrage, where mycelia from the parental strains developed into an elevated ridge at the junction zone. The biological significance of the morphological changes observed here are not known. In nature, mycelia of different fungal species are known to compete regularly for resources by either outgrowing or inhibiting competitor species (Ujor et al., 2018). These mechanisms include pigmentation, mycelial production, sealing of septa, up-regulation of hydrophobic compounds, and the release of secondary metabolites. Interestingly, the colony

morphological changes were observed in both intranational and international crosses. The broad distributions for these phenomena suggest potentially shared genetic bases that contribute to their development.

Within this study, relatively few crosses mated successfully to produce viable sexual offspring. Similar observations in low mating success rate have been found in other fungi (Barrett et al., 2009; Yan et al., 2002). One possibility for the limited success may be related to our sampling and to the reproductive history of individual strains. For example, the plant pathogen *Melampsora lini* consisted of two lineages, where one was predominantly asexual and the other was sexual and asexual (Barrett et al., 2009). Recombinant and clonal populations of the yellow rust fungus *Puccinia striiformis* f. sp. *tritici* have also been identified in different continents (Ali et al., 2010). Clonal strains of *A. fumigatus* strains have been observed in both clinical and environmental populations (Chowdhary et al., 2012; Guinea et al., 2011). Thus, it's possible that many strains of *A. fumigatus* used in our tests had been reproducing asexually and lost the ability to mate. The loss of sexual reproduction ability has been experimentally demonstrated in the human pathogenic yeast *Cryptococcus neoformans* (Xu, 2002). Specifically, in experimental populations of this yeast subjected to 600 generations of asexual reproduction, severe reductions in sexual reproductive ability were observed (Xu, 2002). The loss of sexual reproduction was also seen in *Magnaporthe oryzae* after 10 to 19 asexual generations (Saleh et al., 2012).

Within our analyzed samples, the Chinese strains had the greatest propensity to develop cleistothecia compared to all other populations, whereas the fewest successful crosses involved parental strains from, Canada and Cameroon (Figure 5.2). Interestingly, both the Canadian and Cameroonian *A. fumigatus* populations were previously shown to have a distinct genetic makeup when compared to other geographic populations (Ashu, Korfanty, et al., 2017; Ashu, Kim, et al., 2018). Additionally, the Canadian population was shown to contain strains that are amphotericin B tolerant, possibly due to historical selection or genetic drift of the Canadian population.

It is tempting to speculate that the observed genetic differentiations of these two geographic populations from other populations based on microsatellite markers also reflect their sexual reproductive isolations. Indeed, these two geographic populations may be close to complete their speciation process. However, despite the limited mating success and low ascospore germination rates, genetic exchange between strains from Canada and Cameroon with strains from other geographic areas are still possible.

Our results indicated low levels of ascospore germination between successful crosses. In total, 81 of the 136 crosses that produced cleistothecia yielded no viable ascospores, suggesting some form of post-zygotic reproductive isolation. In addition, for crosses that produced viable ascospores, the ascospore germination rates among cleistothecia of the same cross can differ greatly. Overall, the germination rate of *A. fumigatus* ascospores in our study differed from those from previous studies. For example, O'Gorman et al., (2009), found that offspring from an AfRB2/AfIR956 cross germinated at a rate of approximately 50.5% (± 3.4%). This was considerably higher and less variable than what was observed in our study. When characterizing the supermater pair, Sugui et al., (2011) found that the proportion of viable ascospores increased with the age of the cross. In our study, cleistothecia from the supermater cross were observed after four weeks and harvested three weeks later, similar to that reported previously by Sugui et al., (2011). However, while a 40% ascospore germination rate from the supermater pair was observed by Sugui et al., (2011), only a 9.83% (± 4.04%) germination rate was observed in our analysis of this cross. Other *Aspergillus* species also have shown variable germination rates. *A. lentulus* strains, upon discovery of its sexual cycle, had low mating success among, where only 4 of 14 (28.6%) crosses produced cleistothecia after 3 weeks. An additional 4 weeks of incubation increased the success rate to 35% (Swilaiman et al., 2013). In addition, a low fertility rate has been noted in *A. terreus*, where only 8.3% of crosses were viable (Arabatzis & Velegraki, 2013). At present, the mechanisms underlying these differences are unknown. However, several factors might have contributed to the discrepancy and the low ascospore germination rates in our study.

Depending on the species, the germination of sexual fungal spores can be initiated by subjecting the spores to specific environmental conditions. Within the current study, as suggested (O'Gorman et al., 2009; Sugui et al., 2011), 70 °C heat shock for one hour was used to stimulate ascospore germination. However, heat shock temperature used in other ascomycete species vary, and 70 °C may not be the most optimal temperature for some of the crosses in *A. fumigatus*. For example, in *Neosartorya fischeri* and *Talaromyces macrosporus*, the heat shock temperature and duration required to germinate ascospores varied depending on the structure and compounds within the cell wall (Wyatt et al., 2015), with a recommended heat shock of 85 °C for 2 min that resulted in ~94% of ascospore germination rates within both species. Another ascomycete, *Monosporascus cannonballus*, is present in the soil rhizosphere and required actinomycetes to prompt ascospore germination in 25 °C to 35 °C (Stanghellini et al., 2000). In basidiomycetes, lower temperatures are used to germinate basidiospores. The study by Forsythe et al., (2016) investigated the basidiospore germination rates in six *C. neofomans* and *C. deneoformans* intraspecific and interspecific crosses. They found that overall, greater genetic differences between parental strains were related to decreased offspring basidiospore germination rate. Interestingly, the lowest basidiospore germination rate was observed the highest temperature of 37 °C compared to both 23 °C and 30 °C. The variations in spore germination rate among crosses at different temperatures and other conditions could have contributed to the low ascospore germination observed in this study. At present, studies on *A. fumigatus* sexual cycle used 70 °C as the optimal heat shock temperature to germinate ascospores (Losada et al., 2015; O'Gorman et al., 2009; Sugui et al., 2011). However, parental strains of *A. fumigatus* from different geographic and ecological populations may produce ascospores that germinate under different optimal conditions.

Secondly, the low and variable germination rate may be associated with our specific experimental procedure. When extracting cleistothecia from mating junctions, the asexual conidia spores may stick to the surface of cleistothecia. While treatment at 70 °C for one hour can effectively destroy all contaminating conidia, some of the conidia may be included in cell counts. In our study, after heat shock, the concentration of ascospores was determined

by a cell counter. Because ascospores are larger than conidia (4–5 μm and 2–3 μm respectively) (Kwon-Chung & Sugui, 2013; O'Gorman et al., 2009), the identification parameter of the cell counter was set between the 4–5 μm range. However, it is possible that clumped conidia were counted and therefore artificially inflated the concentration of the ascospore solutions, thus leading to decreased germination counts. While the contaminating conidia might decrease our estimates of spore germination rates, some conidia might also survive the 70 °C heat shock treatment and lead to increased spore germination. In our preliminary pilot experiment, the 70 °C heat shock of a conidia solution containing thousands of conidia yielded no to very few colonies on SDA medium. However, as a 0% germination rate was seen in three replicates for many crosses that produced cleistothecia, it is highly unlikely that any viable conidia contributed positively to the observed spore germinations. This result is consistent with the observation that heat treatment at 70 °C for 30 min resulted in 100% conidial inactivation, without affecting the viability of ascospores (Sugui et al., 2011).

Third, variable ascospore germination rate may also be impacted by meiosis and ascospore development. In *A. fumigatus*, ascospores originate from an ascus mother cell that underwent meiosis followed by one round of mitosis. The eight ascospores within an ascus therefore originate from the same meiotic event and different asci undergo independent meiosis. If the parental strains had different chromosomal structures such as inversions and translocations, different meiotic events would produce progeny spores with different chromosomal complements with some of the combinations not viable (Sun & Xu, 2009; Vogan & Xu, 2014). The proportions of inviable ascospores depend on where crossing-overs happen and how different chromosomes re-assort with each other (Kassim et al., 2016). Chromosomal structural polymorphisms have been frequently reported in fungi (Zolan, 1995). However, the chromosomal structures of the 60 *A. fumigatus* strains analyzed here are not known at present.

Overall, our analyses showed that geographic distance had relatively low but significant influence on ascospore germination rate. This result is consistent with results from recent

population genetic studies that showed recent global migration of *A. fumigatus* among many geographic populations. Recent gene flows make the current geographic distances among strains not an informative feature of their historical geographic isolation (Ashu, Hagen, et al., 2017; Korfanty et al., 2019). Other genera of fungi that are more limited in global gene flow have contrasting results, as demonstrated by Dettman et al., (2003) in a parallel paradigm work. Here the authors investigated the sexual divergence within species of the fungal genus *Neurospora* using 929 crosses. The authors used two species of *Neurospora, N. crassa* and *N. intermedia,* and crossed both within and between species to test their ability to recognize species. They assessed the relationship between the biological species recognition (BSR) and phylogenetic species recognition (PSR). The parental strains were obtained from distant geographical regions and had high genetic variability. The authors identified that both increased genetic and geographic distance between parental strains significantly yielded both lower mating success and reduced progeny viability. Parental strains that were classified into different species by the authors also yielded very low sexual fertility.

Several strains within this study, particularly those from China, were capable of mating with both geographically and genetically distant strains. The presence of viable offspring suggests reproductive compatibility and a lack of reproductive barriers between those strains. Given the high level of gene flow and recombination between both genetic and geographic *A. fumigatus* populations (Ashu, Hagen, et al., 2017), the sexual compatibility at least between certain strains suggest that virulence and drug resistance genes originated in one region could be spread to other geographic regions. For example, within our study, the Canadian strain CM16 successfully mated with the Indian strain I1272. Amphotericin B resistance is widespread in the Hamilton population (Ashu, Korfanty, et al., 2018) and high-level triazole resistance is prevalent within the Indian population (Chowdhary et al., 2012). Successful offspring between these two population could produce offspring that are resistant to both classes of drugs. In another study, Camps et al., (2012) demonstrated that *A. fumigatus* strains containing the TR34/L98H mutation, which confers azole resistance, are able to outcross to azole susceptible strains. Considering that the resistant strains used were genetically similar and less diverse, the resistant strains were still capable of crossing into different genetic

backgrounds. The authors also demonstrated that the TR34/L98H mutation was capable of being transferred to the progeny of a cross involving a susceptible and resistant strain. Continuous monitoring is needed in order to evaluate these and other possibilities in nature.

5.5 Conclusions

This study investigated the extent of both pre- and post-zygotic isolation between geographically distant populations of *A. fumigatus*. In total, of the 900 crosses involving 60 strains from six different countries, 136 crosses successfully produced cleistothecia. Overall, intranational crosses developed more cleistothecia than international crosses, with strains from China and Cameroon producing the most and least average number of cleistothecia respectively. Viable offspring were obtained from 55 of the 136 successful mated crosses. The parental strains capable of mating and producing viable offspring span broad geographic regions. Our analyses revealed that the germination rates were highly variable among crosses and among repeats of the same cross. Though the observed ascospore germination rates were overall low, our results indicated that genetic exchanges between strains from diverse geographic and genetic backgrounds are possible. Furthermore, we would like to note that only 10 strains were randomly selected from each of the six countries for this study, thus, our observations might not accurately represent all *A. fumigatus* populations from these six countries. Expanded analyses and active surveillance are needed in order to examine the extent of genetic exchange among geographic populations and genetic clusters in this important human fungal pathogen at the global level.

5.6 Funding

This study was supported by grants from the Natural Sciences and Engineering Research Council (NSERC) of Canada, by the Ontario Graduate Scholarship, and by the Institute of Infectious Diseases Research at McMaster University

5.7 Declaration of Competing Interest

We declare that we have no competing interest associated with this study, commercial or otherwise.

5.8 Acknowledgements

We would like to thank Dr. Eta Ashu for the acquisition of *A. fumigatus* isolates from Cameroon and Canada, Renad Aljohani for the soil acquisition from Saudi Arabia and Dr. Anu Chowdhary for the strains originating from India. We would like to thank all members of the Jianping Xu lab for their help and support during this project.

5.9 Supplementary Figures

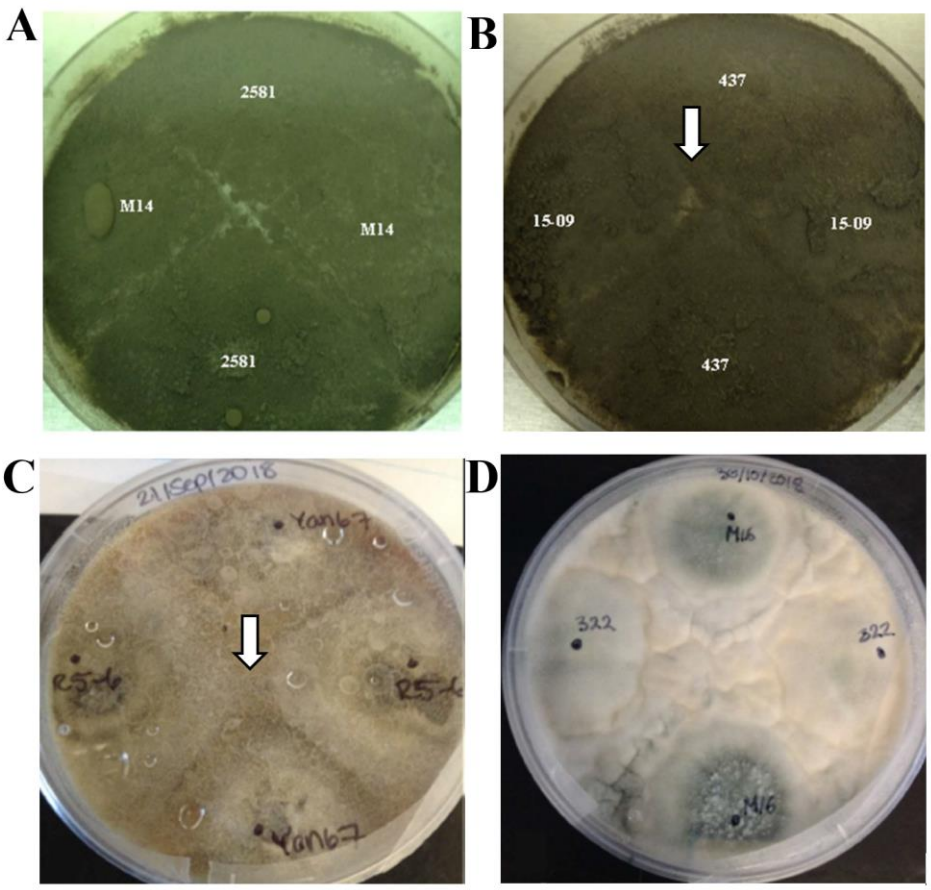

Supplementary Figure 5.1: Representative junction zone phenotypes that produced no cleistothecia. (A) Cross between the Indian strain I2581 and the Canadian strain M14. (B) Barrage formation in the cross between C437 and Hclin-09. Arrow designates position of the elevated ridge of the barrage. (C) Altered colony pigmentation in the cross between the Saudi Arabian strain Yan67 and the New Zealand strain R5-6. Arrow designates area of no conidial production. (D) Lack of conidial growth between the Canadian strain M16 and the Cameroonian strain C322.

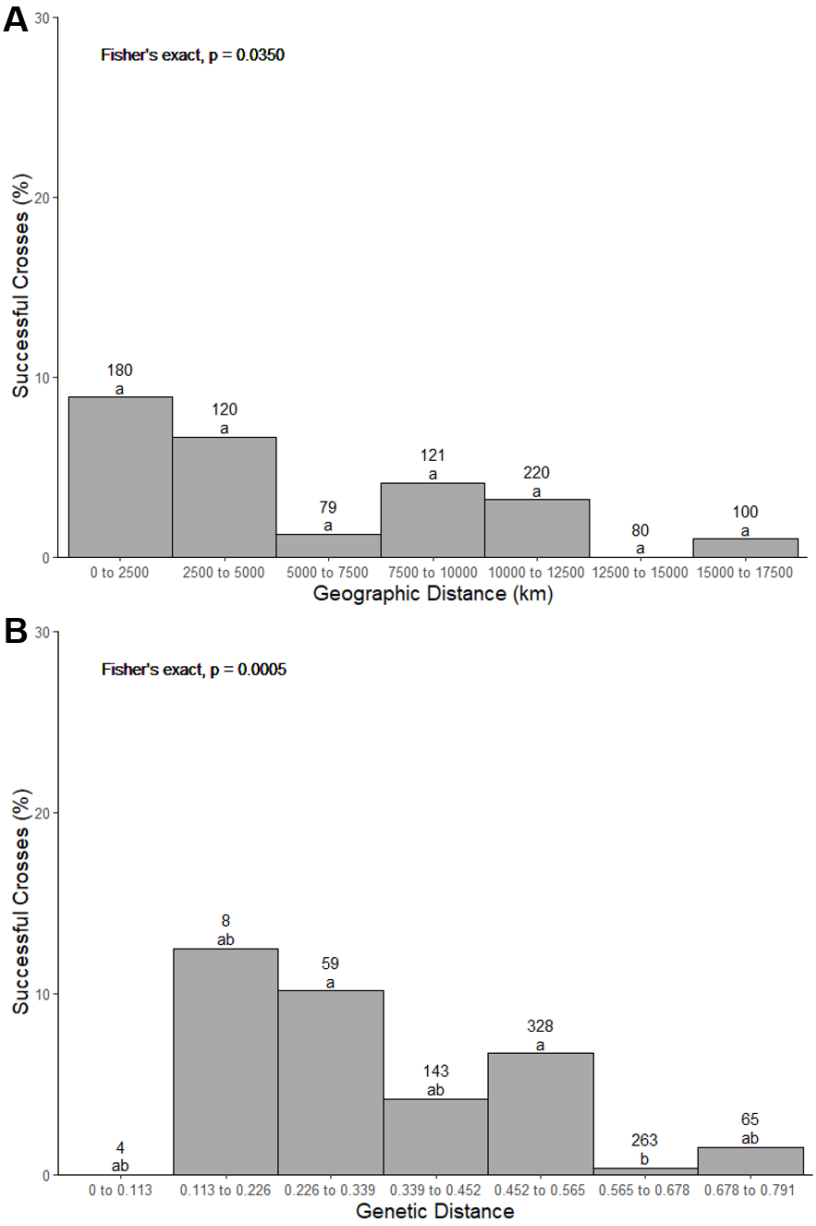

Supplementary Figure 5.2**:** The effect of geographic and genetic distance between parental strains on mating success and cleistothecia formation for crosses that produced 6 to 10 cleistothecia. Fisher's exact test was conducted for both the overall and the pairwise comparisons between the 7 distance groups. The number represents total amount of crosses within each bin. (A) The percentage of successful crosses within 7 binned geographic distances. (B) The percentage of successful crosses within 7 binned genetic distances.

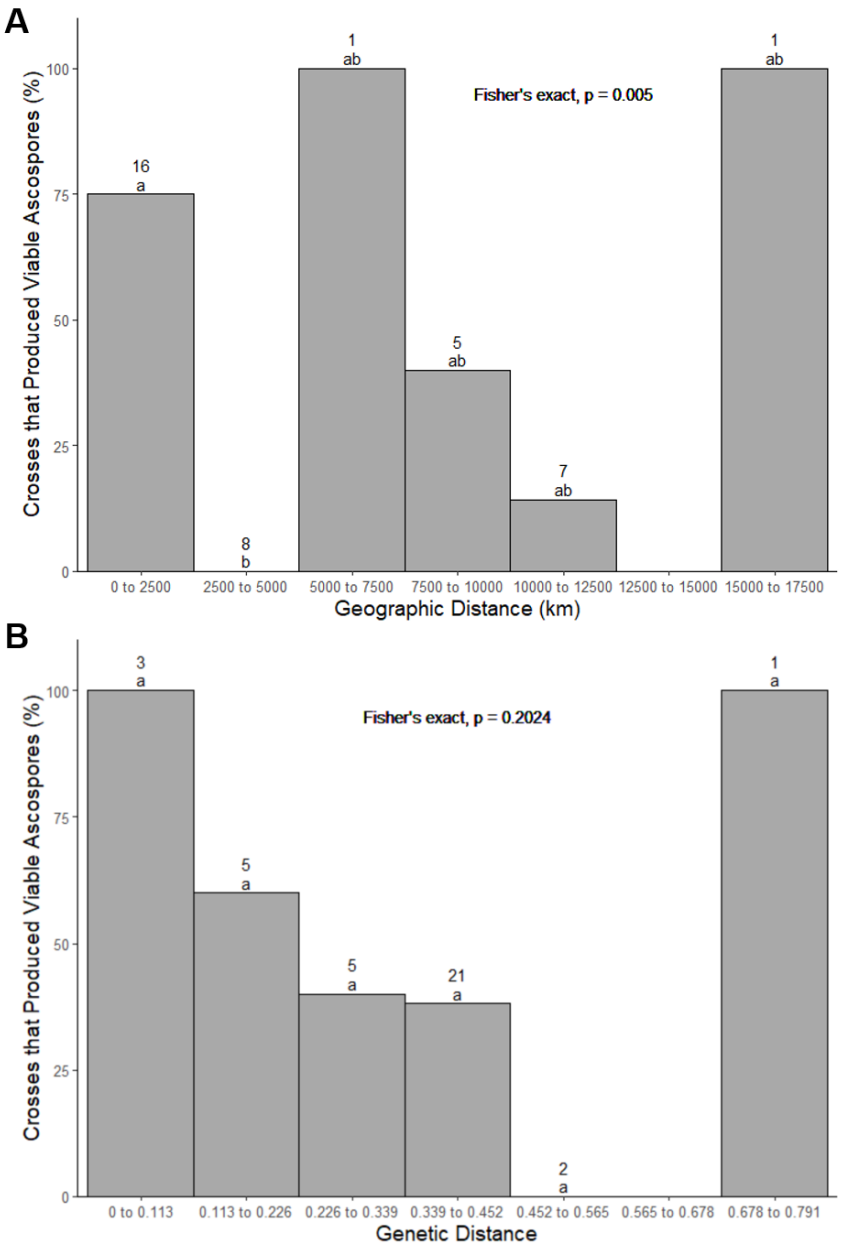

Supplementary Figure 5.3: The effect of genetic and geographic distance on ascospore germination success for crosses that produced 6 to 10 cleistothecia. Fisher's exact test was conducted for both overall and pairwise between the 7 distance groups. The number represents total amount of crosses within each bin. Letters represent statistical significance of $p < 0.05$ between countries. (A) The percentage of germination success within 7 binned geographic distances. (B) The percentage of germination success within 7 binned genetic distances.

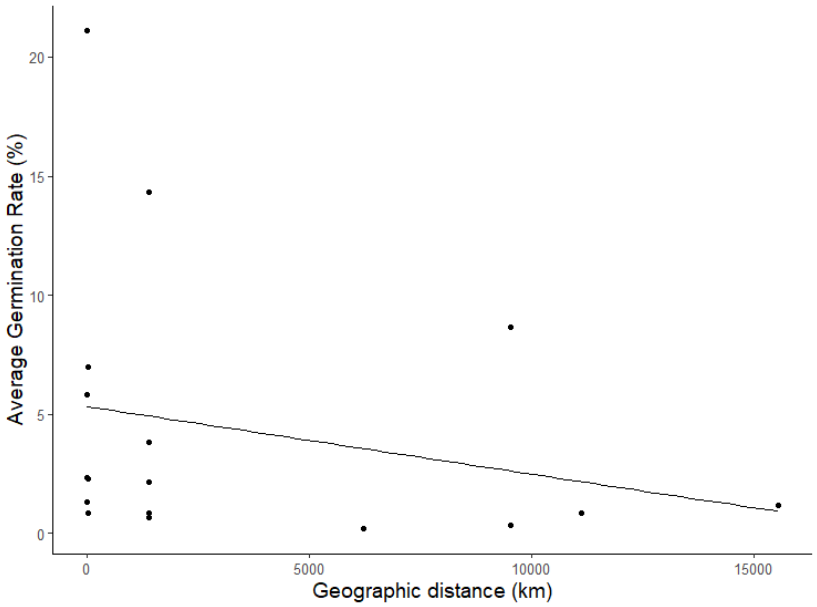

Supplementary Figure 5.4: Geographic distance effects on ascospore germination rate of crosses that produced 6 to 10 cleistothecia. The geographic distance (km) between the 55 parental strains was calculated using the latitudinal and longitudinal coordinates of each strain. This distance is plotted against the germination rate of the hybrid offspring, calculated from an average of 3 or 5 repeats. Linear model p-value = 0.3454.

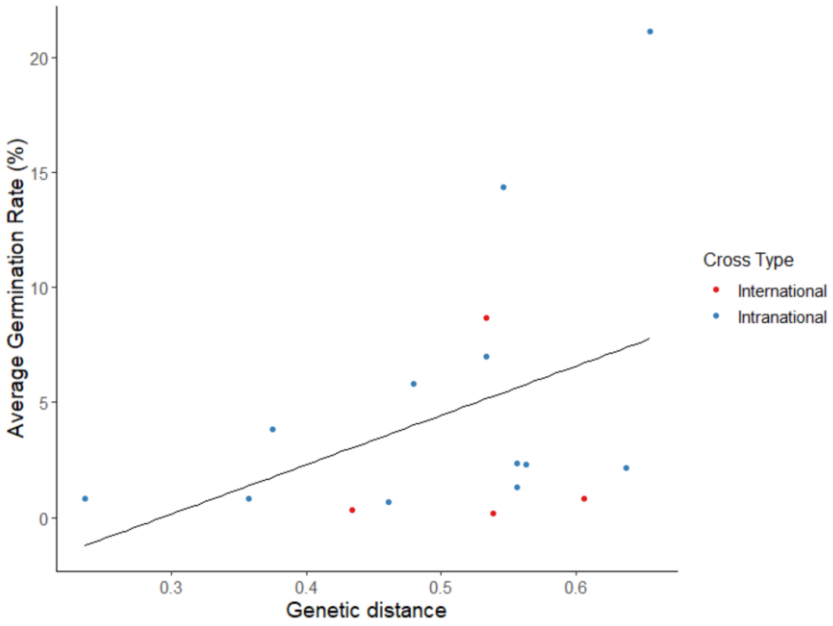

Supplementary Figure 5.5: Genetic distance and ascospore germination rate of crosses that produced 6 to 10 cleistothecia. Bruvo's genetic distance between the two parental strains involved in each of the 55 crosses that produced ascospores analyzed was calculated using the STR genotypes of each strain. The genetic distance was plotted against the germination rate of the hybrid offspring, calculated from an average of 3-5 repeats. Red and blue circles are international and intranational crosses, respectively. Linear model p-value = 0.1217.

5.10 References

Ali, S., Leconte, M., Walker, A. S., Enjalbert, J., & de Vallavieille-Pope, C. (2010). Reduction in the sex ability of worldwide clonal populations of *Puccinia striiformis* f.sp. *tritici*. *Fungal Genetics and Biology*, *47*(10), 828–838. https://doi.org/10.1016/j.fgb.2010.07.002

Alvarez-Perez, S., Blanco, J., Alba, P., & Garcia, M. (2010). Mating type and invasiveness are significantly associated in *Aspergillus fumigatus*. *Medical Mycology*, *48*(2), 273–277. https://doi.org/10.1080/13693780903095414

Arabatzis, M., & Velegraki, A. (2013). Sexual reproduction in the opportunistic human pathogen *Aspergillus terreus*. *Mycologia*, *105*(1), 71–79. https://doi.org/10.3852/11-426

Ashu, E. E., Hagen, F., Chowdhary, A., Meis, J. F., & Xu, J. (2017). Global population genetic analysis of *Aspergillus fumigatus*. *MSphere*, *2*(1), e00019-17. https://doi.org/10.1128/mSphere.00019-17

Ashu, E. E., Kim, G. Y., Roy-Gayos, P., Dong, K., Forsythe, A., Giglio, V., Korfanty, G., Yamamura, D., & Xu, J. (2018). Limited evidence of fungicide-driven triazole-resistant *Aspergillus fumigatus* in Hamilton, Canada. *Canadian Journal of Microbiology*, *64*(2), 119–130. https://doi.org/10.1139/cjm-2017-0410

Ashu, E. E., Korfanty, G. A., Samarasinghe, H., Pum, N., You, M., Yamamura, D., & Xu, J. (2018). Widespread amphotericin B-resistant strains of *Aspergillus fumigatus* in Hamilton, Canada. *Infection and Drug Resistance*, *11*, 1549–1555. https://doi.org/10.2147/IDR.S170952

Ashu, E. E., Korfanty, G. A., & Xu, J. (2017). Evidence of unique genetic diversity in *Aspergillus fumigatus* isolates from Cameroon. *Mycoses*, *60*(11), 739–748. https://doi.org/10.1111/myc.12655

Barrett, L. G., Thrall, P. H., Dodds, P. N., van der Merwe, M., Linde, C. C., Lawrence, G. J., & Burdon, J. J. (2009). Diversity and evolution of effector loci in natural populations of the plant pathogen *Melampsora lini*. *Molecular Biology and Evolution*, *26*(11), 2499–2513. https://doi.org/10.1093/molbev/msp166

Bruggeman, J., Debets, A. J. M., Swart, K., & Hoekstra, R. F. (2003). Male and female roles

in crosses of *Aspergillus nidulans* as revealed by vegetatively incompatible parents. *Fungal Genetics and Biology*, *39*(2), 136–141. https://doi.org/10.1016/S1087-1845(03)00016-1

Camps, S. M. T. T., Rijs, A. J. M. M. M. M., Klaassen, C. H. W. W., Meis, J. F., O'Gorman, C. M., Dyer, P. S., Melchers, W. J. G. G., & Verweij, P. E. (2012). Molecular epidemiology of *Aspergillus fumigatus* isolates harboring the TR34/L98H azole resistance mechanism. *Journal of Clinical Microbiology*, *50*(8), 2674–2680. https://doi.org/10.1128/JCM.00335-12

Chang, H., Ashu, E. E., Sharma, C., Kathuria, S., Chowdhary, A., & Xu, J. (2016). Diversity and origins of Indian multi-triazole resistant strains of *Aspergillus fumigatus*. *Mycoses*, *59*(7), 450–466. https://doi.org/10.1111/myc.12494

Chowdhary, A., Kathuria, S., Xu, J., & Meis, J. F. (2013). Emergence of azole-resistant *Aspergillus fumigatus* strains due to agricultural azole use creates an increasing threat to human health. *PLoS Pathogens*, *9*(10). https://doi.org/10.1371/journal.ppat.1003633

Chowdhary, A., Kathuria, S., Xu, J., Sharma, C., Sundar, G., Singh, P. K., Gaur, S. N., Hagen, F., Klaassen, C. H., & Meis, J. F. (2012). Clonal expansion and emergence of environmental multiple-triazole-resistant *Aspergillus fumigatus* strains carrying the TR34/L98H mutations in the *cyp51A* gene in India. *PLoS ONE*, *7*(12), e52871. https://doi.org/10.1371/journal.pone.0052871

de Valk, H. A., Meis, J. F. G. M., Curfs, I. M., Muehlethaler, K., Mouton, J. W., & Klaassen, C. H. W. (2005). Use of a novel panel of nine short tandem repeats for exact and high-resolution fingerprinting of *Aspergillus fumigatus* isolates. *Journal of Clinical Microbiology*, *43*(8), 4112–4120. https://doi.org/10.1128/JCM.43.8.4112-4120.2005

Dettman, J. R., Jacobson, D. J., Turner, E., Pringle, A., & Taylor, J. W. (2003). Reproductive isolation and phylogenetic divergence in *Neurospora* : Comparing methods of species recognition in a model eukaryote. *Evolution*, *57*(12), 2721–2741. https://doi.org/10.1111/j.0014-3820.2003.tb01515.x

Falconer, R. E., Bown, J. L., White, N. A., & Crawford, J. W. (2008). Modelling interactions in fungi. *Journal of the Royal Society Interface*, *5*(23), 603–615. https://doi.org/10.1098/rsif.2007.1210

Forsythe, A., Vogan, A., & Xu, J. (2016). Genetic and environmental influences on the germination of basidiospores in the *Cryptococcus neoformans* species complex. *Scientific Reports*, *6*(1), 1–12. https://doi.org/10.1038/srep33828

Giraud, T., Refrégier, G., Le Gac, M., de Vienne, D. M., & Hood, M. E. (2008). Speciation in fungi. *Fungal Genetics and Biology*, *45*(6), 791–802. https://doi.org/10.1016/j.fgb.2008.02.001

Glass, N. L., Jacobson, D. J., & Shiu, P. K. T. (2000). The genetics of hyphal fusion and vegetative incompatibility in filamentous Ascomycete fungi. *Annual Review of Genetics*, *34*(1), 165–186. https://doi.org/10.1146/annurev.genet.34.1.165

Glass, N. L., & Kaneko, I. (2003). Fatal attraction: Nonself recognition and heterokaryon incompatibility in filamentous fungi. In *Eukaryotic Cell* (Vol. 2, Issue 1, pp. 1–8). American Society for Microbiology Journals. https://doi.org/10.1128/EC.2.1.1-8.2003

Guinea, J., De Viedma, D. G., Peláez, T., Escribano, P., Muñoz, P., Meis, J. F., Klaassen, C. H. W., & Bouza, E. (2011). Molecular epidemiology of *Aspergillus fumigatus:* An in-depth genotypic analysis of isolates involved in an outbreak of invasive aspergillosis. *Journal of Clinical Microbiology*, *49*(10), 3498–3503. https://doi.org/10.1128/JCM.01159-11

Kamvar, Z. N., Tabima, J. F., & Grünwald, N. J. (2014). *Poppr* : an R package for genetic analysis of populations with clonal, partially clonal, and/or sexual reproduction. *PeerJ*, *2*, e281. https://doi.org/10.7717/peerj.281

Kassim, A., Omuse, G., Premji, Z., & Revathi, G. (2016). Comparison of clinical laboratory standards institute and European committee on antimicrobial susceptibility testing guidelines for the interpretation of antibiotic susceptibility at a university teaching hospital in Nairobi, Kenya: a cross-sectional study. *Annals of Clinical Microbiology and Antimicrobials*, *15*, 21. https://doi.org/10.1186/s12941-016-0135-3

Korfanty, G. A., Teng, L., Pum, N., & Xu, J. (2019). Contemporary gene flow is a major force shaping the *Aspergillus fumigatus* population in Auckland, New Zealand. *Mycopathologia*, *184*(4), 479–492. https://doi.org/10.1007/s11046-019-00361-8

Kosmidis, C., & Denning, D. W. (2015). The clinical spectrum of pulmonary aspergillosis. *Thorax*, *70*(3), 270–277. https://doi.org/10.1136/thoraxjnl-2014-206291

Kwon-Chung, K. J., & Sugui, J. A. (2013). *Aspergillus fumigatus*--what makes the species a ubiquitous human fungal pathogen? *PLoS Pathogens*, *9*(12), e1003743. https://doi.org/10.1371/journal.ppat.1003743

Losada, L., Sugui, J. A., Eckhaus, M. A., Chang, Y. C., Mounaud, S., Figat, A., Joardar, V., Pakala, S. S. B., Pakala, S. S. B., Venepally, P., Fedorova, N., Nierman, W. C., & Kwon-Chung, K. J. (2015). Genetic Analysis Using an Isogenic Mating Pair of *Aspergillus fumigatus* identifies azole resistance genes and lack of *MAT* locus's role in virulence. *PLOS Pathogens*, *11*(4), e1004834. https://doi.org/10.1371/journal.ppat.1004834

O'Gorman, C. M., Fuller, H. T., & Dyer, P. S. (2009). Discovery of a sexual cycle in the opportunistic fungal pathogen *Aspergillus fumigatus*. *Nature*, *457*(7228), 471–474. https://doi.org/10.1038/nature07528

Paradis, E., & Schliep, K. (2019). ape 5.0: an environment for modern phylogenetics and evolutionary analyses in R. *Bioinformatics*, *35*(3), 526–528. https://doi.org/10.1093/BIOINFORMATICS/BTY633

R Core Team. (2022). R: a language and environment for statistical computing. *R Foundation for Statistical Computing Vienna, Austria* (4.2.1). https://www.r-project.org/.

Saleh, D., Milazzo, J., Adreit, H., Tharreau, D., & Fournier, E. (2012). Asexual reproduction induces a rapid and permanent loss of sexual reproduction capacity in the rice fungal pathogen *Magnaporthe oryzae:* Results of in vitro experimental evolution assays. *BMC Evolutionary Biology*, *12*(1), 42. https://doi.org/10.1186/1471-2148-12-42

Stanghellini, M. E., Kim, D. H., & Waugh, M. (2000). Microbe-mediated germination of ascospores of *Monosporascus cannonballus*. *Phytopathology*, *90*(3), 243–247. https://doi.org/10.1094/PHYTO.2000.90.3.243

Sugui, J. A., Losada, L., Wang, W., Varga, J., Ngamskulrungroj, P., Abu-Asab, M., Chang, Y. C., O'Gorman, C. M., Wickes, B. L., Nierman, W. C., Dyer, P. S., & Kwon-Chung, K. J. (2011). Identification and characterization of an *Aspergillus fumigatus* "supermater" pair. *MBio*, *2*(6). https://doi.org/10.1128/mBio.00234-11

Sun, S., & Xu, J. (2009). Chromosomal rearrangements between serotype A and D strains in *Cryptococcus neoformans*. *PLoS ONE*, *4*(5), e5524. https://doi.org/10.1371/journal.pone.0005524

Swilaiman, S. S., O'Gorman, C. M., Balajee, S. A., & Dyera, P. S. (2013). Discovery of a sexual cycle in *Aspergillus lentulus*, a close relative of *A. fumigatus*. *Eukaryotic Cell*, *12*(7), 962–969. https://doi.org/10.1128/EC.00040-13

Ujor, V. C., Adukwu, E. C., & Okonkwo, C. C. (2018). Fungal wars: The underlying molecular repertoires of combating mycelia. In *Fungal Biology* (Vol. 122, Issue 4, pp. 191–202). Elsevier B.V. https://doi.org/10.1016/j.funbio.2018.01.001

Vogan, A. A., & Xu, J. (2014). Evidence for genetic incompatibilities associated with post-zygotic reproductive isolation in the human fungal pathogen *Cryptococcus neoformans*. *Genome*, *57*(6), 335–344. https://doi.org/10.1139/gen-2014-0077

Wyatt, T. T., van Leeuwen, M. R., Golovina, E. A., Hoekstra, F. A., Kuenstner, E. J., Palumbo, E. A., Snyder, N. L., Visagie, C., Verkennis, A., Hallsworth, J. E., Wösten, H. A. B., & Dijksterhuis, J. (2015). Functionality and prevalence of trehalose-based oligosaccharides as novel compatible solutes in ascospores of *Neosartorya fischeri* (*Aspergillus fischeri*) and other fungi. *Environmental Microbiology*, *17*(2), 395–411. https://doi.org/10.1111/1462-2920.12558

Xu, J. (2002). Estimating the spontaneous mutation rate of loss of sex in the human pathogenic fungus *Cryptococcus neoformans*. *Genetics*, *162*(3), 1157–1167. http://www.ncbi.nlm.nih.gov/pubmed/12454063

Yan, Z., Li, X., & Xu, J. (2002). Geographic distribution of mating type alleles of *Cryptococcus neoformans* in four areas of the United States. *Journal of Clinical Microbiology*, *40*(3), 965–972. https://doi.org/10.1128/JCM.40.3.965-972.2002

Zolan, M. E. (1995). Chromosome-length polymorphism in fungi. *Microbiological Reviews*, *59*(4), 686–698. https://doi.org/10.1128/mmbr.59.4.686-698.1995

Chapter 6

Assessing Thermal Adaptation of a Global Sample of *Aspergillus fumigatus*: Implications for Climate Change Effects

Abstract *Aspergillus fumigatus* is a common environmental mold and a major cause of opportunistic infections in humans. It's distributed among many ecological niches across the globe. A major virulence factor of *A. fumigatus* is its ability to grow at high temperatures. However, at present, little is known about variations among strains in their growth at different temperatures and how their geographic origins may impact such variations. In this study, we analyzed 89 strains from 12 countries (Cameroon, Canada, China, Costa Rica, France, India, Iceland, Ireland, New Zealand, Peru, Saudi Arabia, and USA) representing diverse geographic locations and temperature environments. Each strain was grown at four temperatures and genotyped at nine microsatellite loci. Our analyses revealed a range of growth profiles, with significant variations among strains within individual geographic populations in their growths across the temperatures. No statistically significant association was observed between strain genotypes and their thermal growth profiles. Similarly geographic separation contributed little to differences in thermal adaptations among strains and populations. The combined analyses among genotypes and growth rates at different temperatures in the global sample suggest that most natural populations of *A. fumigatus* are capable of rapid adaptation to temperature changes. We discuss the implications of our results to the evolution and epidemiology of *A. fumigatus* under increasing climate change.

I was the first author for the study in this chapter. The following paper has been published:

Korfanty, G. A., Heifetz, E., & Xu, J. (2023). Assessing thermal adaptation of a global sample of *Aspergillus fumigatus*: Implications for climate change effects. *Frontiers in Public Health*, *11*, 1059238. https://doi.org/10.3389/FPUBH.2023.1059238

6.1 Introduction

Among the vast diversity of biotic and abiotic factors that can impact the evolution of organisms, temperature has undoubtedly captured more than its share of attention. Biologists have linked variations in temperature to everything from temporal patterns of growth, survival, and reproduction of individual organisms to broad spatial patterns of population density and species distributions across a range of geographic scales. These studies have shown that the same change in temperature often affect different organisms differently. Even for the same organism, temperature does not affect all life stages equally. However, most thermal adaptation studies so far have focused on plants and animals. Relatively little is known about how temperature impact the spatial and temporal distributions of microbial populations, including populations of human fungal pathogens. With increasing climate change and global warming, there is a pressing need to understand the thermal adaptation of these organisms in order to better prepare for potential future epidemics and pandemics (Xu, 2022).

The ascomycete mold *Aspergillus fumigatus* is among the most common opportunistic human pathogens (Latgé & Chamilos, 2020; Xu, 2022). It's ubiquitously distributed in a diversity of ecological niches such as air, water, compost, and soil across the globe. *A. fumigatus* can cause a broad spectrum of opportunistic infections collectively termed aspergillosis that affects approximately 8 million individuals worldwide (Kwon-Chung & Sugui, 2013). Among aspergillosis infections, invasive aspergillosis is the most severe, responsible for ~250,000 deaths worldwide each year (Kwon-Chung & Sugui, 2013; Latgé & Chamilos, 2020; Xu, 2022). At risk-populations include immunocompromised patients such as patients receiving immunosuppressive drugs due to haematopoietic stem cell or solid organ transplants, patients with severe neutropenia, and as co-infections in patients with coronavirus disease 2019 (COVID-19) (Alanio et al., 2020; Latgé & Chamilos, 2020). Different from other human fungal pathogens, *A. fumigatus* can grow at temperatures above 50°C (Kwon-Chung & Sugui, 2013). However, the selective forces and genetic mechanisms govern its high thermotolerance remains largely unknown.

Population genetic surveys have shown that the global population of *A. fumigatus* consists of at least three distinct clades and multiple genetic clusters (Ashu et al., 2017; Etienne et al., 2021; Sewell et al., 2019). These genetic clusters were likely historically differentiated from each other due to geographic separations. However, evidence for gene flow and clonal dispersal have been found across countries and continents, resulting in most regional geographic populations containing strains of different clades and different genetic clusters (Ashu et al., 2017; Korfanty et al., 2019; Korfanty, Dixon, et al., 2021; Zhou et al., 2021). Some of these dispersals were most likely driven by contemporary anthropogenic activities, including human travel and commercial trade (Korfanty et al., 2019; Korfanty, Dixon, et al., 2021). In addition, agricultural fungicides are creating significant selective pressure where drug-resistant strains are rapidly spreading (Barber et al., 2020). The identification of successful recent migrants across broad geographic scales and ecological niches with different temperature spectra suggests that there might be little or no variation in thermal adaptation among strains of *A. fumigatus*. Alternatively, the individual genomes of *A. fumigatus* may have high adaptive potential and/or that immigrants may be readily recombining with local strains to acquire a thermal response profile adapted to local environments. At present, little is known about the geographic and ecological patterns of thermal adaptation of *A. fumigatus* populations.

With the effects of climate change in a diversity of areas being increasingly felt, an important question to consider is how climate change may affect natural *A. fumigatus* populations in different areas around the world. With increasing temperatures, potentially more thermotolerant strains will likely emerge and that *A. fumigatus* may further expand to colder regions. Indeed, global warming is the major suspected cause of the newly emerged and highly antifungal resistant pathogen *Candida auris* that has already caused many outbreaks across the world (Arora et al., 2021; Wang & Xu, 2022; Yadav et al., 2022). The emergence of *C. auris* occurred simultaneously across multiple continents and is hypothesized to be the first documented occurrence of a pathogen emerging due to global warming (Casadevall et al., 2019, 2021).

In this study, we aim to characterize the variations among strains in their growths at different temperatures and investigate how their geographic origins and genetic relationships may impact such variations. To achieve the goals, we selected strains that originated from 12 countries. The phenotypic plasticity of these strains to temperature, which we termed as strain thermal adaptation, was measured via growth in liquid media at four incubation temperatures. Elucidating the impact of temperature on strain growth variation will provide insights on how *A. fumigatus* may adapt to global climate change. Such knowledge should help us develop better understanding of *A. fumigatus* epidemiology and minimize the disease burden on humans.

6.2 Methodology

6.2.1 Geographic populations of *A. fumigatus*

In total, 89 *A. fumigatus* strains were analyzed in this study. These strains were obtained from a variety of ecological niches and geographic locations (Table 6.1). They were selected from our strain collections to represent different mating types, antifungal susceptibilities, and ecological and geographic origins. Among the 89 strains, 77 were isolated from soil samples collected from 11 countries: Cameroon (11 strains), Canada [Northwest Territories (NWT) (3 strains) and Hamilton, Ontario (11 strains)], China (10 strains), Costa Rica (6 strains), France (3 strains), India (4 strains), Iceland (3 strains), Ireland (1 strains), New Zealand (11 strains), Peru (3 strains), and Saudi Arabia (11 strains). Environmental strains from Cameroon, Canada, China, Costa Rica, France, Iceland, New Zealand, Peru and Saudi Arabia have been described in previous studies (Ashu et al., 2017; Korfanty et al., 2019; Korfanty, Dixon, et al., 2021). Environmental strains from soil samples were isolated following the procedures described in Samarasinghe et al., (2022). The remaining 12 strains were from patients in Hamilton, Ontario (5 strains), New Delhi, India (6 strains), and the US (1 strain) (Ashu et al., 2018; Chowdhary et al., 2012). Two strains, one from Ireland (environmental) and the other from US (clinical), represented two super-maters of this species and they were included in our study (Sugui et al., 2011). For additional strain information, please refer to Supplementary Table 6.1.

Table 6.1: Metadata about the 89 *A. fumigatus* strains used in this study.

ID	Country	Region	Average Temperature (°C)	Temperature Range of Monthly Averages (°C)	Latitude	Longitude	Source
C44	Cameroon	Mbingo	19.9	26.8 to 13.1	6.164	10.290	Envir.
C65	Cameroon	Bambui	19.9	26.8 to 13.1	6.015	10.232	Envir.
C79	Cameroon	Bambui	19.9	26.8 to 13.1	6.015	10.232	Envir.
C158	Cameroon	Makepe	26	30 to 23	4.064	9.741	Envir.
C304	Cameroon	Eloundem	23	29 to 18	3.838	11.437	Envir.
C308	Cameroon	Eloundem	23	29 to 18	3.838	11.437	Envir.
C322	Cameroon	Eloundem	23	29 to 18	3.838	11.437	Envir.
C372	Cameroon	Mbalgong	23	29 to 18	3.803	11.468	Envir.
C428	Cameroon	Simbock	23	29 to 18	3.821	11.475	Envir.
C443	Cameroon	Simbock	23	29 to 18	3.821	11.475	Envir.
C480	Cameroon	Mbandoumou	23	29 to 18	3.791	11.453	Envir.
AC10-2	China	Ailao mountains	14	25 to 2	24.206	101.370	Envir.
AC3-3	China	Ailao mountains	14	25 to 2	24.206	101.370	Envir.
AC3-4	China	Ailao mountains	14	25 to 2	24.206	101.370	Envir.
AC6-5	China	Ailao mountains	14	25 to 2	24.206	101.370	Envir.
AC7-1	China	Ailao mountains	14	25 to 2	24.206	101.370	Envir.
AC7-10	China	Ailao mountains	14	25 to 2	24.206	101.370	Envir.
C2-5	China	Fenyi	18.2	29.9 to 2.2	27.828	114.687	Envir.
C4-1	China	Fenyi	18.2	29.9 to 2.2	27.828	114.687	Envir.
C4-2	China	Fenyi	18.2	29.9 to 2.2	27.828	114.687	Envir.
C5-10	China	Fenyi	18.2	29.9 to 2.2	27.828	114.687	Envir.
EJ13	Costa Rica	El Jardin	21	30.2 to 18.2	10.016	-84.214	Envir.
EJ24	Costa Rica	El Jardin	21	30.2 to 18.2	10.016	-84.214	Envir.
MA28	Costa Rica	Manuel Antonio	25.8	33.4 to 19.1	9.392	-84.137	Envir.
MA31	Costa Rica	Manuel Antonio	25.8	33.4 to 19.1	9.392	-84.137	Envir.
LF18	Costa Rica	La Fotuna	21	30.2 to 18.2	10.468	-84.643	Envir.
LF25	Costa Rica	La Fotuna	21	30.2 to 18.2	10.468	-84.643	Envir.
DF29	France	Downtown Nice	16	27.7 to 5.3	43.710	7.262	Envir.
TF59	France	Oldtown Nice	16	27.7 to 5.3	43.710	7.262	Envir.
HF16	France	Hyeres	15.3	28.2 to 4.3	43.121	6.129	Envir.
AV88	Hamilton	St. George	7.9	26.5 to -9.3	43.271	-80.250	Envir.
CF10	Hamilton	St. George	7.9	26.5 to -9.3	43.271	-80.250	Envir.
CM11	Hamilton	St. George	7.9	26.5 to -9.3	43.271	-80.250	Envir.
CM16	Hamilton	St. George	7.9	26.5 to -9.3	43.271	-80.250	Envir.
CM21	Hamilton	St. George	7.9	26.5 to -9.3	43.271	-80.250	Envir.
CM38	Hamilton	St. George	7.9	26.5 to -9.3	43.271	-80.250	Envir.
CM58	Hamilton	St. George	7.9	26.5 to -9.3	43.271	-80.250	Envir.
15-1	Hamilton	Hamilton	7.9	26.5 to -9.3	43.263	-79.856	Clinical

15-09	Hamilton	Hamilton	7.9	26.5 to -9.3	43.263	-79.856	Clinical
15-21	Hamilton	Hamilton	7.9	26.5 to -9.3	43.263	-79.856	Clinical
15-34	Hamilton	Hamilton	7.9	26.5 to -9.3	43.263	-79.856	Clinical
15-42	Hamilton	Hamilton	7.9	26.5 to -9.3	43.263	-79.856	Clinical
M14	Hamilton	Hamilton	7.9	26.5 to -9.3	43.261	-79.919	Envir.
M16	Hamilton	Hamilton	7.9	26.5 to -9.3	43.261	-79.919	Envir.
P20	Hamilton	Hamilton	7.9	26.5 to -9.3	43.277	-79.786	Envir.
P80	Hamilton	Hamilton	7.9	26.5 to -9.3	43.277	-79.786	Envir.
T34	Iceland	Thingvellir	4	12 to -2	64.256	-21.130	Envir.
SF37	Iceland	Skaftafell	4	13 to -3	64.070	-16.975	Envir.
N9	Iceland	Nautholsvik	4	12 to -2	64.124	-21.927	Envir.
I1268	India	New Delhi	25	40.5 to 6.7	28.598	77.222	Clinical
I1272	India	New Delhi	25	40.5 to 6.7	28.598	77.222	Clinical
I1591	India	New Delhi	25	40.5 to 6.7	28.598	77.222	Clinical
I162	India	New Delhi	25	40.5 to 6.7	28.598	77.222	Envir.
I245	India	New Delhi	25	40.5 to 6.7	28.598	77.222	Clinical
I2581	India	New Delhi	25	40.5 to 6.7	28.598	77.222	Clinical
I384	India	New Delhi	25	40.5 to 6.7	28.598	77.222	Envir.
I388	India	New Delhi	25	40.5 to 6.7	28.598	77.222	Envir.
I437	India	New Delhi	25	40.5 to 6.7	28.598	77.222	Envir.
I591	India	New Delhi	25	40.5 to 6.7	28.598	77.222	Clinical
AFIR928	Ireland	Dublin	9.8	19.5 to 2.3	-6.313	53.324	Envir.
A3-4	New Zealand	Trusts Arena	15.5	23.6 to 7.5	-36.866	174.636	Envir.
A6-6	New Zealand	Trusts Arena	15.5	23.6 to 7.5	-36.866	174.636	Envir.
D2-6	New Zealand	Auckland Domain	15.5	23.6 to 7.5	-36.859	174.776	Envir.
D6-5	New Zealand	Auckland Domain	15.5	23.6 to 7.5	-36.859	174.776	Envir.
M3-8	New Zealand	Millenium Field	15.5	23.6 to 7.5	-36.743	174.731	Envir.
M4-8	New Zealand	Millenium Field	15.5	23.6 to 7.5	-36.743	174.731	Envir.
R5-6	New Zealand	Aukland Rail	15.5	23.6 to 7.5	-36.849	174.765	Envir.
U5-1	New Zealand	Auckland U.	15.5	23.6 to 7.5	-36.850	174.770	Envir.
V1-8	New Zealand	Mount Eden	15.5	23.6 to 7.5	-36.877	174.765	Envir.
V6-1	New Zealand	Mount Eden	15.5	23.6 to 7.5	-36.877	174.765	Envir.
V8-8	New Zealand	Mount Eden	15.5	23.6 to 7.5	-36.877	174.765	Envir.
1_18	NWT	Yellowknife	-4.3	21.3 to -29.5	62.454	-114.372	Envir.
5_4	NWT	Yellowknife	-4.3	21.3 to -29.5	62.454	-114.372	Envir.
6_13_2	NWT	Yellowknife	-4.3	21.3 to -29.5	62.454	-114.372	Envir.
RM7-10	Peru	Rainbow Mountain	12	20 to 1	-13.618	-71.844	Envir.
LP19-2	Peru	Lima	20	26 to 15	-12.046	-77.043	Envir.
SV28-4	Peru	Sacred Valley	12	20 to 1	-13.333	-72.085	Envir.
AML22	Saudi Arabia	Al-Madina East	27	38 to 12	24.473	39.610	Envir.
AML81	Saudi Arabia	Al-Madina East	27	38 to 12	24.473	39.610	Envir.
Jed22	Saudi Arabia	Jeddah	28	37 to 18	21.606	39.171	Envir.

Jed47	Saudi Arabia	Jeddah	28	37 to 18	21.606	39.171	Envir.
Jed57	Saudi Arabia	Jeddah	28	37 to 18	21.606	39.171	Envir.
Jed70	Saudi Arabia	Jeddah	28	37 to 18	21.606	39.171	Envir.
Jed71	Saudi Arabia	Jeddah	28	37 to 18	21.606	39.171	Envir.
Jed75	Saudi Arabia	Jeddah	28	37 to 18	21.606	39.171	Envir.
AML38	Saudi Arabia	Al-Madina East	27	38 to 12	24.525	39.569	Envir.
Yan179	Saudi Arabia	Yanbu	27	37 to 15	24.088	38.067	Envir.
Yan67	Saudi Arabia	Yanbu	27	37 to 15	24.088	38.067	Envir.
AFB62-1	United States	San Antonio	20.6	34.9 to 4.3	29.425	-98.492	Clinical

6.2.2 Experimental conditions

To identify variations in growth among *A. fumigatus* strains at different temperatures, strains were grown at the following five temperatures in triplicates per temperature, 4°C, 15°C, 22°C, 35°C, and 41°C. For each strain, an inoculum was created and used to assess growth at all temperatures. To prepare the inoculum, *A. fumigatus* strains were cultured on malt extract agar (MEA) for 2–3 days at 37°C. Conidia were then harvested by dispensing 1 ml of a sterile 0.85% saline solution onto the culture and aspirating the conidial suspension to a sterile 1.5 ml tube. Conidial density was measured using a Countess® II FL automated cell counter and adjusted to 1×10^8 conidia/ml in saline. Conidial suspensions were diluted in RPMI 1,640 to a concentration of 1×10^6 conidia/ml. In total 200 µL of this suspension was then aliquoted in triplicates into a 96 well microtiter plate for each temperature. Relative growth was estimated using the optical density (OD) values at 600 nm absorbance using the Biotek Epoch™ 2 Microplate Spectrophotometer. Growth measurements were taken at four time points: immediately after inoculation, and 24 h, 48 h, and 72 h post inoculation. For each 96-well microtiter plate, three wells with medium but without any fungal culture were used as negative controls.

6.2.3 Strain genotyping and geographic climate data

Each *A. fumigatus* strain was genotyped at nine highly polymorphic short tandem repeat (STR) loci (also called microsatellite loci) and at the mating type (MAT) locus. Strain genotyping at the nine STR loci followed the protocol described by de Valk et al., (2005).

The mating type of each strain was identified following the protocol described by Paoletti et al., (2005).

Atmospheric temperature profiles of the geographical locations where individual strains were isolated were obtained using the website Weatherbase (weatherbase.com). Specifically, the closest city to the sampling site with recorded data was used as a proxy of the temperature at each location. The average temperature, highest and lowest monthly average temperature across all months of a year, and the temperature range between the highest and lowest monthly average temperatures were collected.

6.2.4 Statistical analysis

The growth of each strain under each temperature condition was obtained at three time points. To identity differences in growth between strains and populations, pairwise *t*-tests were conducted. *Post hoc* corrections followed the Holm method. No growth was observed for any strain at 4°C. Thus, our analyses of growths were conducted on data at the remaining four temperatures 15°C, 22°C, 35°C, and 41°C. All analyses were conducted in *R* version 4.2.1 (R Core Team, 2022). Specifically, the following analyses were conducted.

In the first, we constructed reaction norm plots for all strains across four temperatures to show if there are strain x temperature interactions. The mean OD value of each strain at each temperature was used to construct the reaction norm plot.

Second, the broad sense heritability contributing to growth differences among strains was calculated using the below formula.

$$H^2 = \frac{V_G}{V_P} = \frac{(V_P - V_E)}{V_P}$$

where H^2 is the broad sense heritability, V_P is the phenotypic variance calculated as the total variance in growth across all strains, and V_G is the genotypic variance, calculated as the difference between V_P and environmental variance (V_E). V_E is calculated as the average of

the variances in growth between replicates over all strains. H^2 was calculated for each temperature on each of the 3 days.

Third, a mixed ANOVA was conducted to determine the contribution of country, temperature, and day post incubation on strain growth. The r package *rstatix* was used to conduct the ANOVA.

Forth, for each strain, we quantified the extent of variation in their growths among temperatures, using the measure of coefficient of variation. The coefficient of variation (CV), shown below,

$$CV = \frac{\sigma}{\mu}$$

is the ratio of standard deviation (σ) to the mean (μ). A large CV represents big differences in growth rates among temperatures. In contrast, a small CV represents relative uniformity in growths among temperatures for the specific strain. The CV was calculated for each *A. fumigatus* strain using growth values across all four temperatures.

Fifth, the contributions of mating type, temperature range and average temperature where strain came from on the CV of each strain on each day were estimated as follows. For each independent variable, the assumptions of normality were verified using Shapiro–Wilk's test and homoscedasticity using the Breusch–Pagan test. For mating type, we used both the parametric Student's *t*-test and the non-parametric Mann-Whitney test to compare the differences between them. For temperature range and average temperature, a linear regression model was generated to determine significance in the relationship between the temperature parameters in their native environments on CV.

Lastly, we tested whether the difference in CV among strains were related to their genotypic relationships as determined based on the nine STR loci. Specifically, we obtained two matrices and conducted non-parametric Mantel test between them. In one matrix, we calculated the absolute difference in CV between all pairs of strains. In the other matrix,

Bruvo's genetic distance between all pairwise combination of strains was calculated using *bruvo.dist* in the R package *poppr* (Kamvar et al., 2014). Bruvo's genetic distance is specific for STR loci as it incorporates the stepwise mutation model during genetic distance calculations. A Shapiro-Wilk's test was conducted on the residuals to determine whether the distributions of the two matrices were Gaussian. A linear regression model was used to determine the relationship between differences in genetic distance and in CV between pairs of strains. All 3,916 pairwise strain combinations were included in the analysis. Additionally, using the Bruvo's genetic distance matrix, a neighbor joining tree was generated using the R package *ape* (Paradis & Schliep, 2019). The tree was edited and visualized through the Interactive Tree of Life (iTOL) website (Letunic & Bork, 2016).

6.3 Results

6.3.1 Growth is significantly influenced by temperature but remains highly varied within four of the five tested temperatures

In this study, we determined the growths of 89 strains for 3 days at 5 different temperatures. No growth was found at the 4°C environment for any of the 89 strains. Thus, our analyses will be focused on the remaining four temperatures. The growth profiles for all strains at the four temperatures are shown in Figure 6.1 as the reaction norm plots. For better visualization and comparison among strains within each country, growth profiles of strains separated by country of origin were also generated (Supplementary Figure 6.1). Among the four temperatures, significant growth differences between temperatures were observed (Figure 6.1). Overall, among these four temperatures, limited growths were observed at 15°C for most strains over all 3 days. Similarly, there was limited growth within 24 h at 22°C. However, broad variations among strains were observed at both the 35°C and 41°C environments. Interestingly, many strains showed similar growths at 35°C and 41°C.

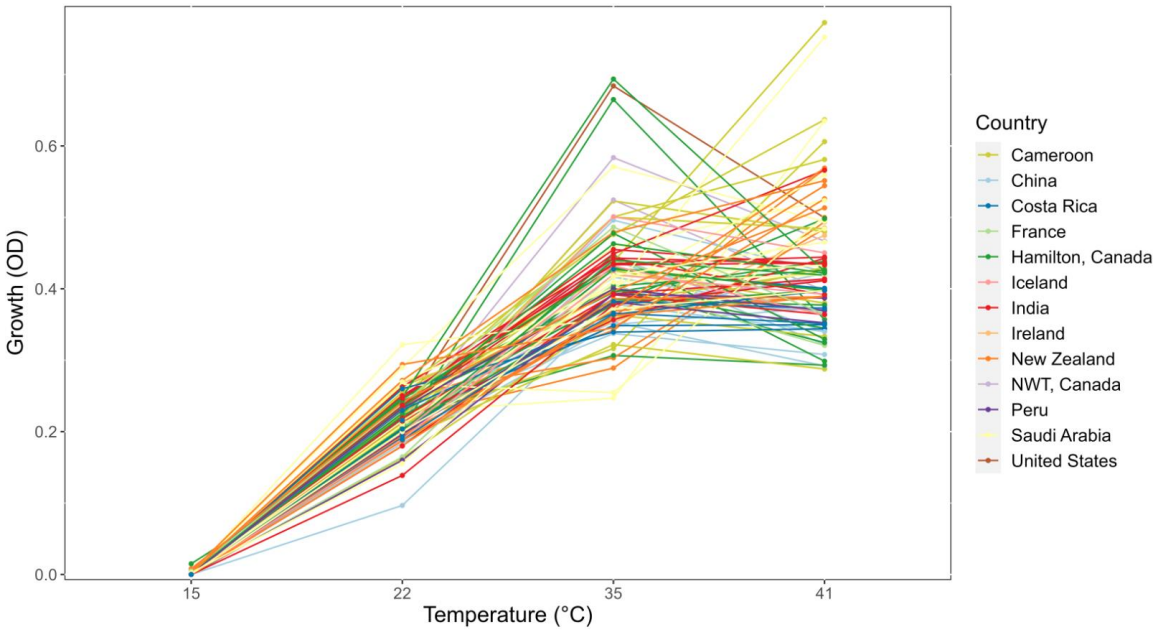

Figure 6.1: Reaction norm plot showing strain × temperature interactions in the day 3 growth profiles of 89 strains across four temperatures. NWT, Northwest Territories, Canada.

To investigate how much of the differences in growth at each temperature at each of the three time points were due to genetic differences among strains, we calculated the broad sense heritability (BSH) of the growth observed among our strains (Table 6.2). Our analyses revealed that in 10 of the 12 temperature × date combinations, their BSH values were all greater than 0.5. The only two combinations with BSH <0.5 were growths at 35°C during day 2 and day 3. Overall, at each of the 3 days, the 35°C environment showed the lowest BSH while the 22°C and 41°C showed the highest. However, there was no obvious pattern among the 3 days at each of the four temperatures.

Table 6.2: Broad sense heritability (BSH, H^2) calculated using the observed growth of the 89 *A. fumigatus* strains across the 3 days and four temperatures.

Day	Temperature			
	15°C	22°C	35°C	41°C
24h	0.454	0.675	0.514	0.749
48h	0.654	0.806	0.368	0.565
72h	0.652	0.703	0.355	0.701

At each temperature, we observed substantial variations in growth among strains (Figures 6.1, 6.2). As the temperature increases, the range of growth rates became wider among strains. Similarly, as time progresses, the growth differences among most strains became more obvious and the standard deviations correspondingly increased. To highlight some of the differences, Figure 6.3 shows the growths of the top six fastest growing and the bottom six slowest growing strains over the 3 days at each of the four temperatures. Further, to visualize the differences in growth between 72 and 24 h, we calculated the difference in growth of each *A. fumigatus* strain at each temperature between day 3 and day 1 (Figure 6.4). Within each temperature, strains showed high variability in growth difference between the days. Interestingly, except between 35°C and 41°C where no difference in change between growth at day 1 and day 3 was observed in our sample, the remaining pairwise temperature comparisons all showed statistically significant differences (p-value < 0.001). Together, our results indicate tremendous variations in growth profiles among strains across the four temperatures and among the 3 days.

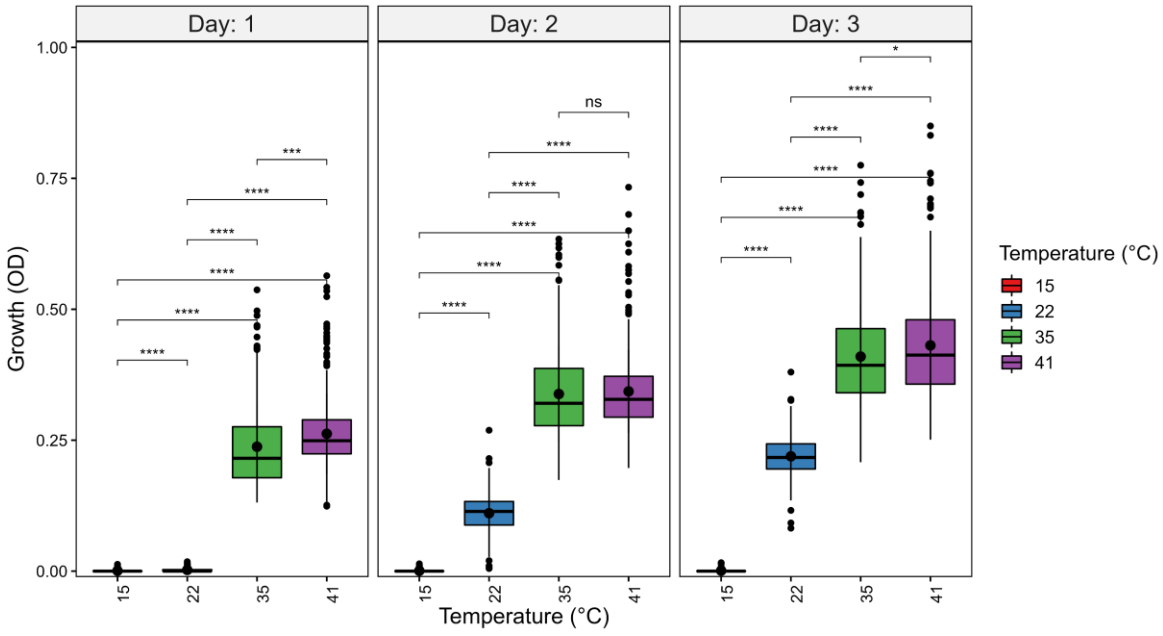

Figure 6.2: Temperature significantly contributes to growth differences among strains of *A. fumigatus*. *A. fumigatus* strains were grown at four temperatures: 15°C, 22°C, 35°C, and 41°C during a 3-day period. To quantify growth, the optical density (OD) at 600 nm of each strain was measured. Significance was determined through pairwise *t*-tests with *post hoc* correction via Holm's method. Boxplot center line represent the median and the top and bottom represent interquartile range. *p-value < 0.05, ***p-value < 0.001, ****p-value < 0.0001.

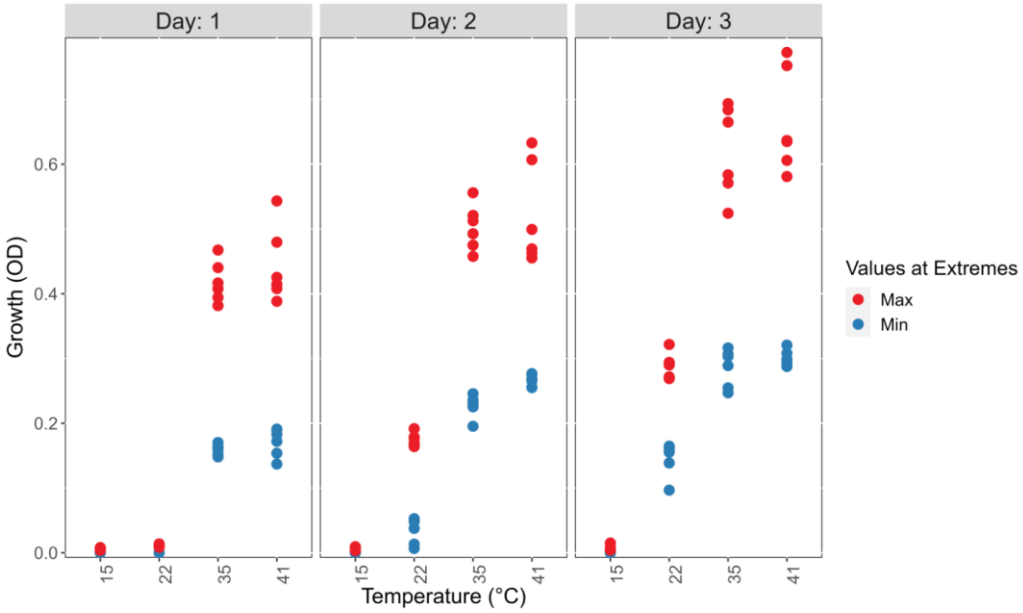

Figure 6.3: Visual representations of the top six fastest growing strains and the bottom six slowest growing ones at each of the four temperatures on 3 days to show the range of growth difference of *A. fumigatus* strains. The top 6 (Max) are shown in red and the bottom 6 (Min) are shown in blue.

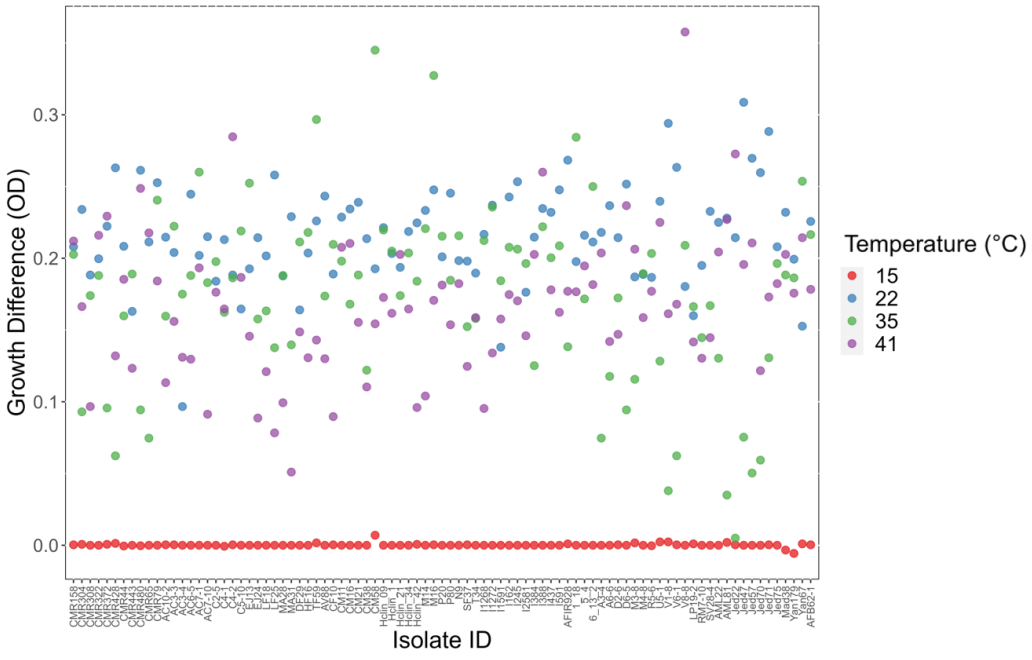

Figure 6.4: Difference in growth between day 3 and day 1 at each of four temperatures among 89 *A. fumigatus* strains. X-axis represents strain names. Y-axis represents in OD value differences between day 3 and day 1.

6.3.2 *A. fumigatus* strains demonstrate highly variable thermal adaptability to different temperatures

The broad range of growth between strains seen in Figures 6.1–6.4 suggest that there are high variations in growths between strains in their responses to different temperatures. To effectively analyze the broad variations and partition the observed variations to different contributors, we calculated the coefficient of variation (CV), a dimensionless and unitless measure for each strain for each of the 3 days (Figure 6.5). Our results showed overall highest CV values in Day 1, followed by those in Day 2 and with Day 3 being the lowest. The results suggest big differences in strains' initial responses to different temperatures. However, as time progresses and the strains adapt, the differences in growth among the temperatures decreased. Interestingly, most of the delayed growth occurred at 22°C where limited growths were seen for most strains during the first 24 h but significant growths were observed over the following 48 h at day 2 and day 3 (Figure 6.5A). Indeed, upon removal of the 22°C data from the dataset, the three-day data showed no significant contribution to differences in CV at the whole sample level (p-value = 0.722; Figure 6.5B). However, obvious variations in CVs among strains were observed (Day 1 range = 0.299, Day 2 range = 0.160, Day 3 range = 0.208).

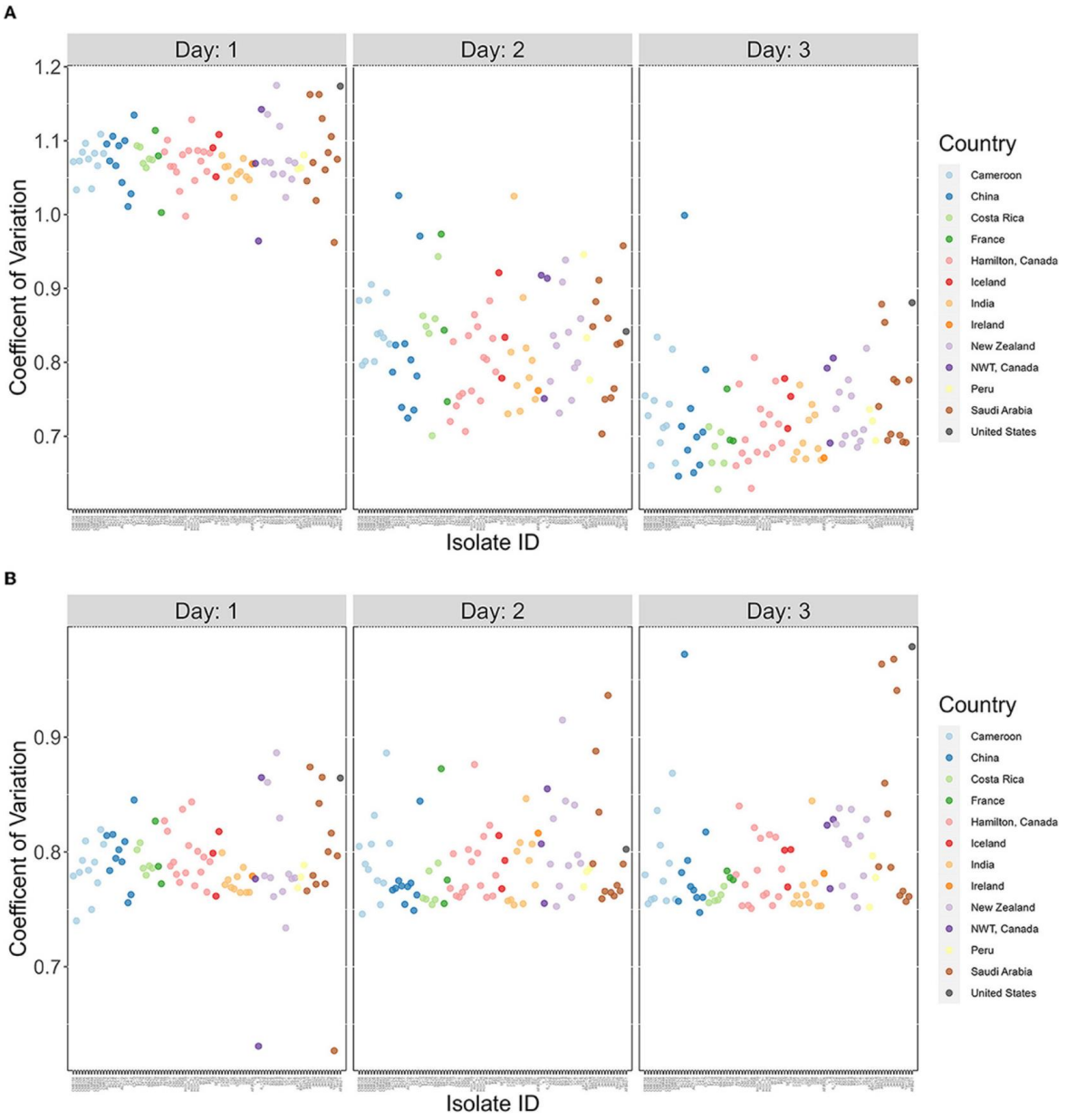

Figure 6.5: The coefficients of variation are highly variable among *A. fumigatus* strains but decreased over time. X-axis represents 89 *A. fumigatus*. Y-axis represents coefficient of variation (CV) values for each strain. (A) CV calculated based on all four temperatures (15°C, 22°C, 35°C, and 41°C). (B) CV calculated based on three temperatures (15°C, 35°C, and 41°C).

6.3.3 Geographic origin and the atmospheric temperature at isolation sites have no significant contribution to the high CV between strains

To determine the potential environmental factors that may contribute to the broad variability in growth and CV among strains, we investigated the impact of geographic origin, the average temperature present at each soil sample site, as well as the range between the highest and lowest temperatures at each sampling site (Table 6.3 and Figure 6.6). For geographic origin, strains were grouped by their country of origin. Countries that had < 3 strains were excluded from the analyses. We conducted a mixed ANOVA to determine the contributions of country of origin, temperature, and day post-incubation on strain growth as well as their interaction effects (Table 6.3). Our ANOVA analyses revealed a significant but relatively minor effect of country of origin on strain growth alone and in its interactions with day post-incubation and temperature. However, though an overall significant contribution based on country of origin was observed, none of the pairwise country comparisons showed significant difference in the growth (Figure 6.6A) and CV between their strains (Figure 6.6B).

Table 6.3: Mixed ANOVA on the contributions of country of origin, temperature, and day post incubation and their interactions on the growth of *A. fumigatus* strains. ges = generalized eta squared.

Effect	DF	F	p-value	ges
Country	12	2.773	4×10^{-3} **	0.118
Temperature	3	723.03	4.46×10^{-85} ****	0.836
Day	2	1581.055	1.87×10^{-102} ****	0.429
Country:Temperature	39	3.054	8×10^{-6} ****	0.206
Country:Day	26	2.079	4×10^{-3} **	0.012
Temperature:Day	6	163.871	8.02×10^{-61} ****	0.209
Country:Temperature:Day	72	3.16	3.11×10^{-8} ****	0.058

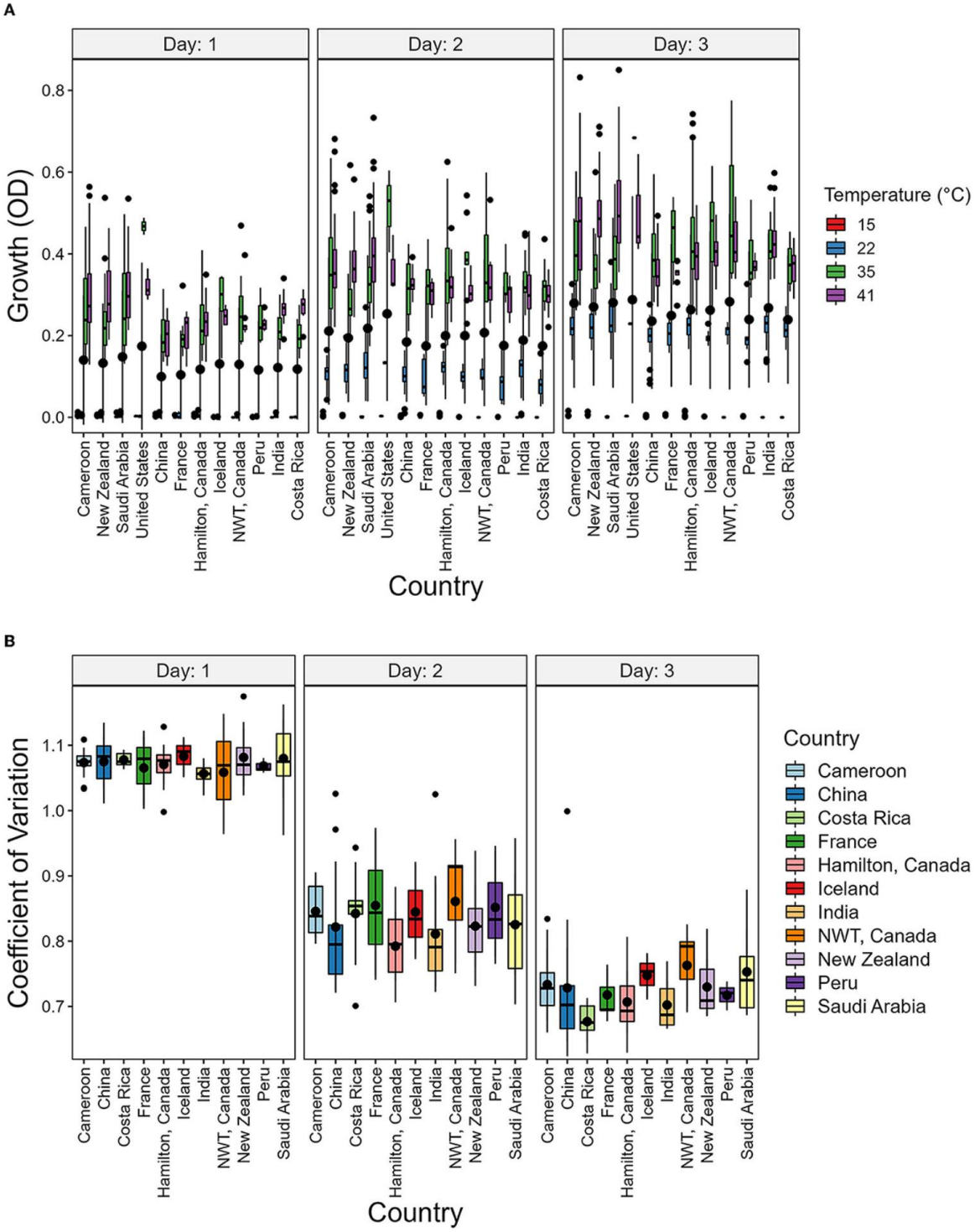

Figure 6.6 : Country of origin has no significant contribution to strain growth and to coefficient of variation (CV). (A) Boxplot showing the growth of strains grouped by country and temperature. (B) Boxplot showing the CV of strains grouped by country. The CV was calculated as the ratio of variance to the mean using the growth values of each temperature.

In our data, a low CV represents the ability of a strain to grow similarly at different temperatures. We hypothesized that strains from geographic regions with less varied temperature changes throughout the year will show greater CV than those experiencing more variable temperatures. To investigate this, we obtained atmospheric temperature near the geographic origin of each strain. The contribution of the average temperature and the range between the highest and lowest temperature at each geographic location on CV was analyzed (Figure 6.7). However, we found no support for this hypothesis.

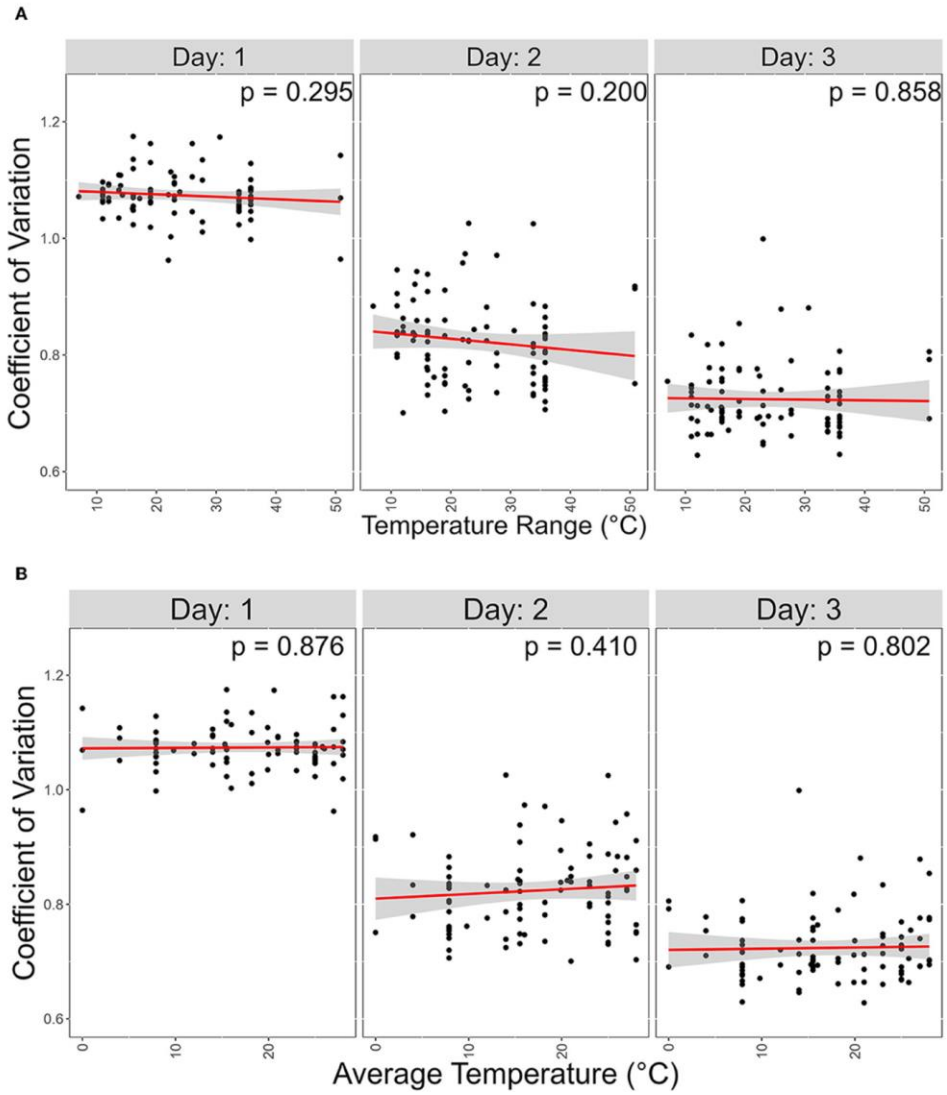

Figure 6.7: Atmospheric temperature at isolation sites has no significant contribution on coefficient of variation (CV). X-axis represents temperature range; Y-axis represents coefficient variations. Linear regression was used to determine significance between the two variables. (A) Scatter plot of the effect of the Average temperature of each isolation site on CV. (B) Scatter plot of the effect of the temperature range, which is the difference between the high and lowest monthly average temperature of each isolation site, on CV.

6.3.4 Strain mating type has minimal contribution to growth and no significant contribution to CV

We investigated the potential effects of mating type on growth and CV among temperatures and days post incubation. *A. fumigatus* has two mating type idiomorphs, *MAT1-1* and *MAT1-2*. Mating between strains of opposite idiomorphs are required for sexual reproduction. The details of our analyses results are shown in Figure 6.8. Overall, our comparisons showed limited difference between the two mating types, in either growth or CV (Figure 6.8). Except in one comparison, we observed no significant influence of mating type on either growth or CV. The only marginally significant difference observed here were growth at 35°C on day 3 where strains of *MAT1-2* overall grew slightly more and had higher CV than strains of *MAT1-1*.

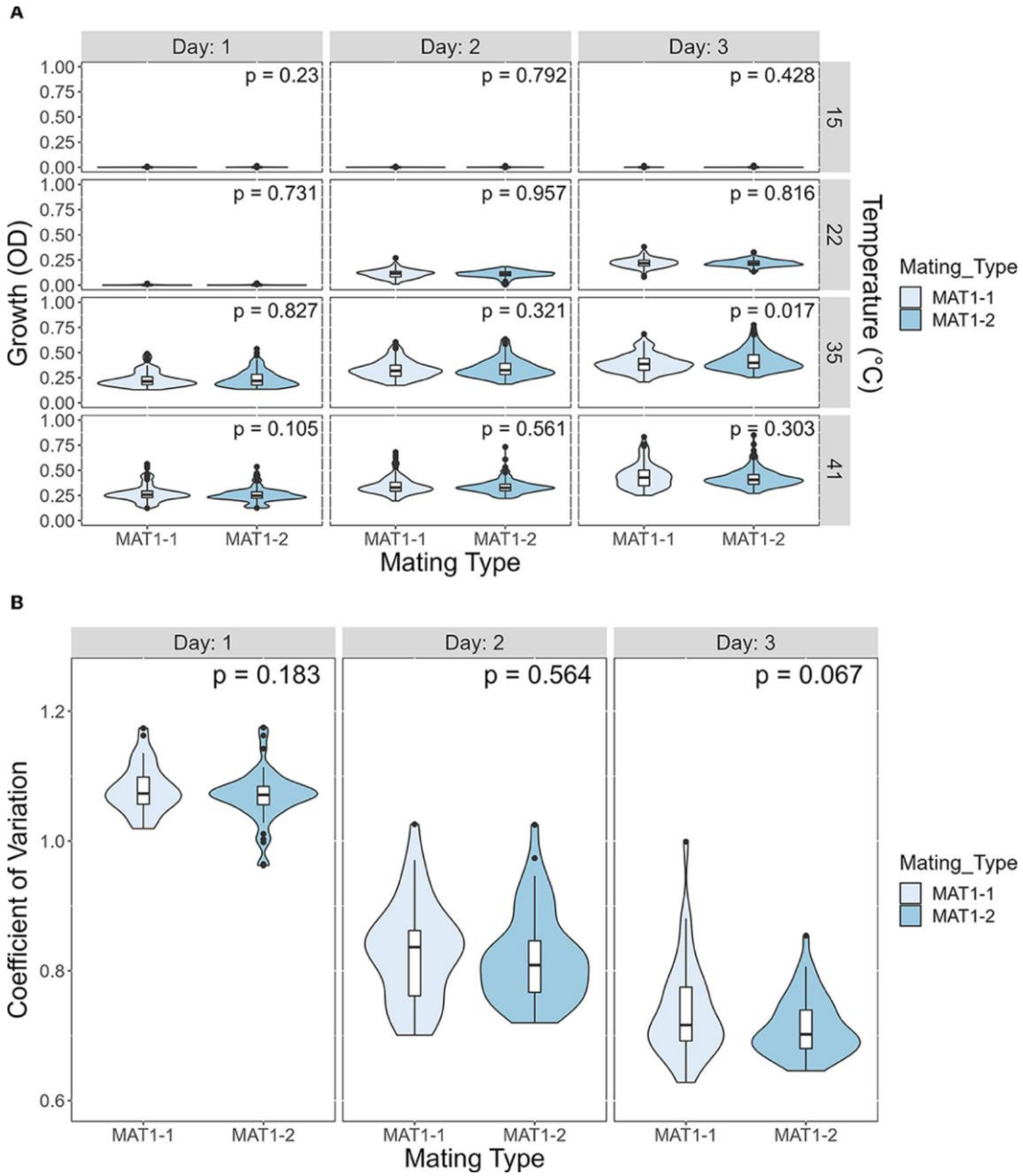

Figure 6.8: The mating type of *A. fumigatus* strains has a minimal contribution to growth difference and to coefficient of variation (CV). (A) Violin plot showing difference in growth between *MAT1-1* and *MAT1-2* at each temperature on each day. Significance was determined through Mann-Whitney test. (B) Violin plot showing difference in CV between *MAT1-1* and *MAT1-2* at each day. Significance was determined through Student's t-test.

6.3.5. Genetic distances between strains have no significant association to the pairwise difference in CV

We also tested the hypothesis that strains with similar STR genotypes would have similar CV. Specifically, we used a linear regression model to determine if the difference in CV between all pairwise combinations of strains grown for 72 h were correlated to their genetic distances. A cubic root transformation on the CV difference was done to achieve a Gaussian distribution among residuals. Our results indicate that the genetic distance between strains was not significantly correlated to CV difference between pairs of strains (Figure 6.9). Interestingly, the Chinese strain AC3-4 contributed to the top 64 CV difference values. The CV value of strain AC3-4 was 0.999 for day 3, the highest among all strains. Figure 6.10 shows the relationships among the 89 strains based on their genetic distances inferred from genotypes at nine STR loci.

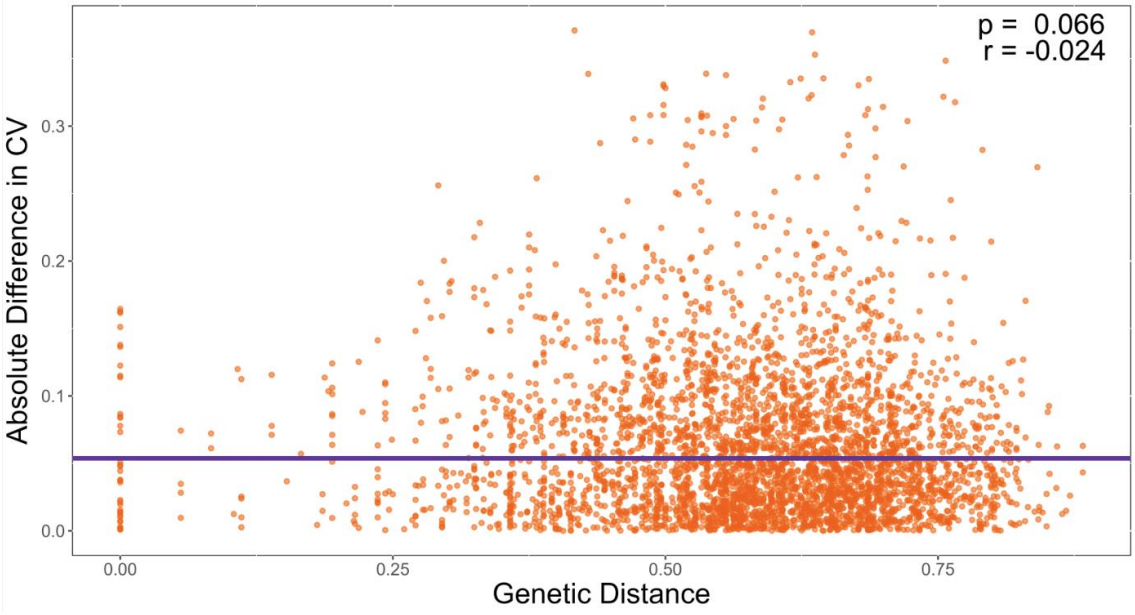

Figure 6.9: Genetic distance is not significantly correlated with the coefficient of variation (CV) in growths among temperatures. X-axis refers to pairwise genetic distance between strains based on Bruvo's genetic distance. Y-axis refers to pairwise absolute difference in CV on Day 3. Significance was determined through a linear regression model.

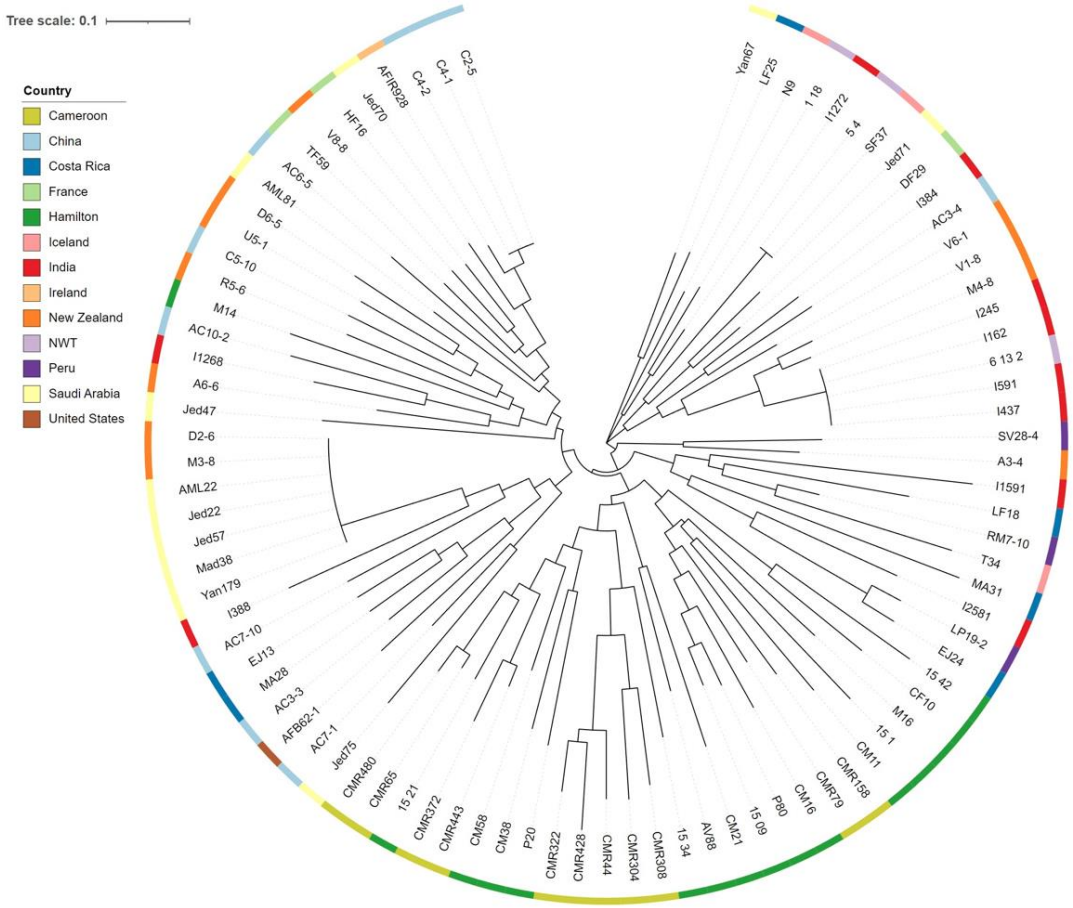

Figure 6.10: Neighbor joining tree among strains of *A. fumigatus* based on STR genotypes. The phylogram was constructed using the Bruvo's genetic distances at nine STR loci. Color strips at each individual node represent the country of origin.

6.4 Discussion

In our study, we characterized the thermal adaptation of 89 *A. fumigatus* strains from 12 countries representing different climatic areas. After incubation at four temperatures for 3 days, high variation in growth and CV was seen among *A. fumigatus* strains through all 3 days. We then investigated whether genetic and geographic factors contributed to the observed variations in growth and CV. We found that geographic factors such as country of origin, average temperature at isolation site, and the temperature range of the isolation site had no significant contribution to growth or to CV within and among each of the 3 days. Among genetic factors, the *MAT1-2* strains showed a slightly higher growth at 35°C on day 3 than the *MAT1-1* strains. However, genetic distances as determined based on nine STR loci

between strains showed no correlation with their CV differences. Our results highlight the remarkable variation in thermal adaptation displayed among *A. fumigatus* populations regardless of their genotypic similarity and geographic origin. Below we discuss the relevance of our findings to previous studies and their contributions to understanding the evolution and epidemiology of *A. fumigatus* in the future.

Growth differences among strains at different temperatures have been investigated in several fungi, including species of *Aspergillus, Penicillium, Paecilomyces,* and *Metarhizium* (Mattoon et al., 2021; Medina et al., 2015; Rangel et al., 2005; Sangamesh et al., 2018; Vidal et al., 1997). For filamentous fungi, previous studies measured the radial growth of colonies on solid media at different temperatures as indicators of their growths (Gibson & Hocking, 1997; Granade et al., 1985; Miyazawa et al., 2022). Larger colonies represent higher tolerance to the environmental conditions tested. However, radial growth measures two-dimensional growth via colony surface area or colony diameter (Gibson & Hocking, 1997). In comparison, relative optical densities measure three-dimensional growth in liquid media and therefore is likely a more accurate reflection of the total mycelial growth of *A. fumigatus* strains (Granade et al., 1985). Indeed, liquid culture and OD reading has been used as an indicator for measuring *A. fumigatus* growth for determining their susceptibilities to antifungal drugs (Miyazawa et al., 2022). In addition, liquid culturing and OD measurements provided us a high throughput method to measure the thermal adaptability of a large number of strains under diverse temperatures through multiple days. However, we note that the liquid culture in the lab can't reflect the dynamic environmental conditions of *A. fumigatus* in nature and that, despite efforts to maintain uniformity, variations among batches and among wells in microtiter plates likely existed that could have contributed to variations in OD among replicates within and among strains.

Aspergillus fumigatus is highly thermophilic and has been isolated from soil microenvironments from diverse geographic locations and climates. However, our growth and CV results suggested no significant association between the geographic origins of *A. fumigatus* strains and strain growth patterns at different temperatures. Our results contrast

those observed in several other fungal species that showed associations between geographic origin and growth pattern (Cordero et al., 2018; Kryukov et al., 2012; Rangel et al., 2005, 2010; Vidal et al., 1997). For example, *Paecilomyces fumosoroseusis* was shown to have intraspecific variability in growth at different temperatures, with increased radial growth at temperatures similar to their climate of origin (Vidal et al., 1997). The level of yeast pigmentation was also observed to be latitudinally distributed and associated with varying levels of thermal tolerance (Cordero et al., 2018). Dark pigmented yeasts were more commonly found in high latitude regions with lower temperatures whereas light pigmented yeasts were associated with equatorial regions with higher temperatures. Similar to the observed variability in radial growth among strains on solid medium in *P. fumosoroseusis*, we observed tremendous intraspecific variabilities in both growth and CV among our strains. However, in contrast to the growth patterns observed among *P. fumosoroseusis* populations, geographic origin had no significant contribution to the observed variations in our samples. This suggests the individual geographic populations of *A. fumigatus* contain strains with variable levels of adaptability to temperature.

At present, how individual populations of *A. fumigatus* maintain such variabilities is unknown. However, there are three possibilities that may explain the observed variability. In the first, the variabilities in thermal adaptations might be maintained in response to daily and seasonal temperature fluctuations. Within each country and at each site, the daily and seasonal air temperatures can vary widely (Feng et al., 2022; Lembrechts et al., 2022). Second, different ecological niches within a local site can also have different temperature patterns. For example, the inside of a compost pile consisting of decomposing dead organic matter can exceed 50°C while outside of the compost pile the temperature may be <20°C or even lower (Margesin et al., 2006). Third, gene flow could bring strains adapted at temperatures in other sites into new locations (Ashu et al., 2017; Korfanty et al., 2019; Korfanty, Dixon, et al., 2021; Sewell et al., 2019; Zhou et al., 2021). Indeed, strains with high CV may have originated from geographic regions with limited variability in temperature, such as regions closer to the equator. Gene flow has been observed between distant geographic populations of *A. fumigatus* and such gene flow could contribute to the

limited difference among geographic populations in their thermal response profiles (Ashu et al., 2017; Korfanty et al., 2019; Korfanty, Dixon, et al., 2021; Sewell et al., 2019; Zhou et al., 2021). These three possibilities are not mutually exclusive and all three could have contributed to the observed variabilities, with potentially different contributions to different geographic populations. Greater sampling of diverse ecological niches within specific geographic regions combined with temperature-based experimental evolution studies could help determine the extent of their contributions to *A. fumigatus* growth variations at different temperatures (Xu, 2004, 2022).

The genetic mechanisms underlying thermal tolerance have been examined in several fungal species. Though some genes and mutations can have major effects on thermal tolerance (Xu, 2004), most studies have shown that thermotolerance is a polyphyletic trait that emerged multiple times throughout the fungal phylogeny (Bhabhra & Askew, 2005; Mattoon et al., 2021). Our BSH results suggested genetic differences between strains contributed to variations in thermal growth profiles among strains of *A. fumigatus*. Therefore, we tested the contribution of strain mating type and STR genotype on strain thermal adaptivity. Our results suggested mating type had minimal effect on growth and no effect on CV, where the only significant association was for day 3 at 35°C. For ascomycete fungi, mating type idiomorphs predominantly function as transcription factors that regulate the sexual cycle (Wilson et al., 2019). However, in some fungi, genetic pathways influenced by mating type intersected with other pathways including those for conidiation, stress response, and pathogenicity (Nielsen et al., 2005; Yong et al., 2020). In *A. fumigatus*, a temperature around 65°C is required to germinate sexual ascospores (O'Gorman et al., 2009). Sexual reproduction within composting plant-waste material has recently been observed between *A. fumigatus* strains, where temperature above 65°C readily occur (Zhang et al., 2022). Given that the sexual reproductive pathways intersect with many other pathways and sexual reproduction requires elevated temperatures to occur in *A. fumigatus*, there may exist a possible link between sexual pathways and thermal adaptability. Although no signification correlation between mating type and thermal adaptability was observed in our study population, an association may exist in some strains. An example of this potential association was the Chinese strain AC3-4. In

our study, AC3-4 showed the highest CV and contributed to the highest CV differences between strains. Interestingly, our previous work showed that strain AC3-4 was among the most fertile in the samples we tested (Korfanty, Stanley, et al., 2021). Given the data we presented here, it's templating to speculate that there may be an association between high mating ability and high CV for growth at different temperatures for a subset of strains within many geographic populations of *A. fumigatus*. Interestingly, another supermater strain AFB62-1 also had a similarly high CV value (Korfanty, Stanley, et al., 2021; Sugui et al., 2011). Further investigation is required to identify if and how mating ability influences thermal adaptability.

Interestingly, the genetic distance between strains estimated through nine STR markers showed no relationship to their CV differences. This lack of association suggests that the STR markers were indeed neutral with regard to thermal growth profile differences among strains and therefore they were unable to explain the observed variance in CV among strains. Frequent recombination between strains within and between many *A. fumigatus* populations would erode any linkage disequilibrium between the nine STR markers and genes associated with growth at different temperatures (Ashu et al., 2017; Korfanty et al., 2019; Sewell et al., 2019). Indeed, a recent study by Auxier et al., (2022) found that *A. fumigatus* has the highest number of crossovers during meiosis among eukaryotic species, approximately 29 crossovers per chromosome during each meiosis. This high recombination rate will allow genetically unique migrants, upon entering a local population, to quickly acquire and/or spread genes that promote adaptation to the native climate. While the neutrality of the nine STR markers are ideal for characterizing *A. fumigatus* population structure, further research is required to genetically explain the observed variance in thermal adaptation in our *A. fumigatus* population. Multiple *A. fumigatus* genetic pathways are known to be upregulated during thermal stress (Feng et al., 2022; Lembrechts et al., 2022; Margesin et al., 2006; Xu, 2004). For example, the nucleolar protein CgrA is upregulated in *A. fumigatus* and is thought to increase the production of proteins related to heat response (Bhabhra et al., 2004). More recently, proteins that regulate aspects of the cell wall integrity pathway have been shown to provide resistance to heat shock, such as protein chaperone HSP90 and the heat shock

transcription factor HsfA (Fabri et al., 2021; Rocha et al., 2021). In another model filamentous fungus *Neurospora crassa*, mutants of calcium/calmodulin-dependent kinases were observed to have reduced thermotolerance (Kumar & Tamuli, 2014). In future studies, a GWAS analysis may locate previously identified and/or novel gene regions under selection for thermotolerance and provide candidate genes for gene expression quantification that may explain the observed variance in growth among strains. Additionally, a proteomic analysis of the strains may further elucidate the impact of thermal stresses on the *A. fumigatus* proteome (Bakar et al., 2020).

6.5 Conclusions

Rising global temperatures due to climate change will promote the expansion of microbial pathogens toward higher and lower latitudes, as well as cause the emergence of novel pathogenic species (Xu, 2022). More research is required to better understand the impact that rising global temperatures may have on microbial populations. Populations of *A. fumigatus* have broad global distributions, and therefore have the potential to adapt to a wide range of climatic temperatures present in these diverse ecological niches. Our findings of high variance in growth among strains across temperatures irrespective of geographic origin and genetic distance suggest the extreme capacity of local populations of *A. fumigatus* to adapt to the changing climate and global warming. Coupled with the high speed at which *A. fumigatus* disperse, strains and populations with highly adaptive mutations to thermal stresses could spread rapidly and be integrated into local populations across the globe (Auxier et al., 2022; Chowdhary et al., 2012). In additional to rising global temperatures, climate change will alter other abiotic factors within soil environmental, such as water availability and solute concentrations that fungi will need to adapt to in the coming years (Medina et al., 2015). Therefore, further investigation into the adaptability of *A. fumigatus* strains to abiotic stressors will provide insights on the remarkable ability of *A. fumigatus* populations to acquire and spread highly fit genotypes, including those that provide resistance to antifungal drugs.

6.6 Author Contributions

GK led the study, contributed to the data collection, analyses, interpretation, and manuscript drafting. EH contributed to the data collection and manuscript writing and edits. JX conceptualized the study design, contributed to data interpretation, and manuscript writing and finalization. All authors read and approved the final manuscript.

6.7 Funding

This research was supported by grants from the Natural Sciences and Engineering Research Council of Canada (Grant No. ALLRP 570780-21) and by the Institute of Infectious Diseases Research (IIDR) Antibiotic Resistance Initiative and the Faculty of Science's Global Science Initiative of McMaster University. The APC was funded by IIDR and David Braley Centre for Antibiotic Discovery. GK was supported by NSERC PGS-D Scholarship.

6.8 Conflict of Interest

The authors declare that the research was conducted in the absence of any commercial or financial relationships that could be construed as a potential conflict of interest.

6.9 Supplementary Material

Please click on the following link to access the table.

Supplementary Table 1: Full metadata about the 89 *A. fumigatus* strains used in this study. https://docs.google.com/spreadsheets/d/1uVPxdE1VO19CdLz-xcxlzec1QGoidzWQPcOVeNmKKNw/edit?usp=sharing

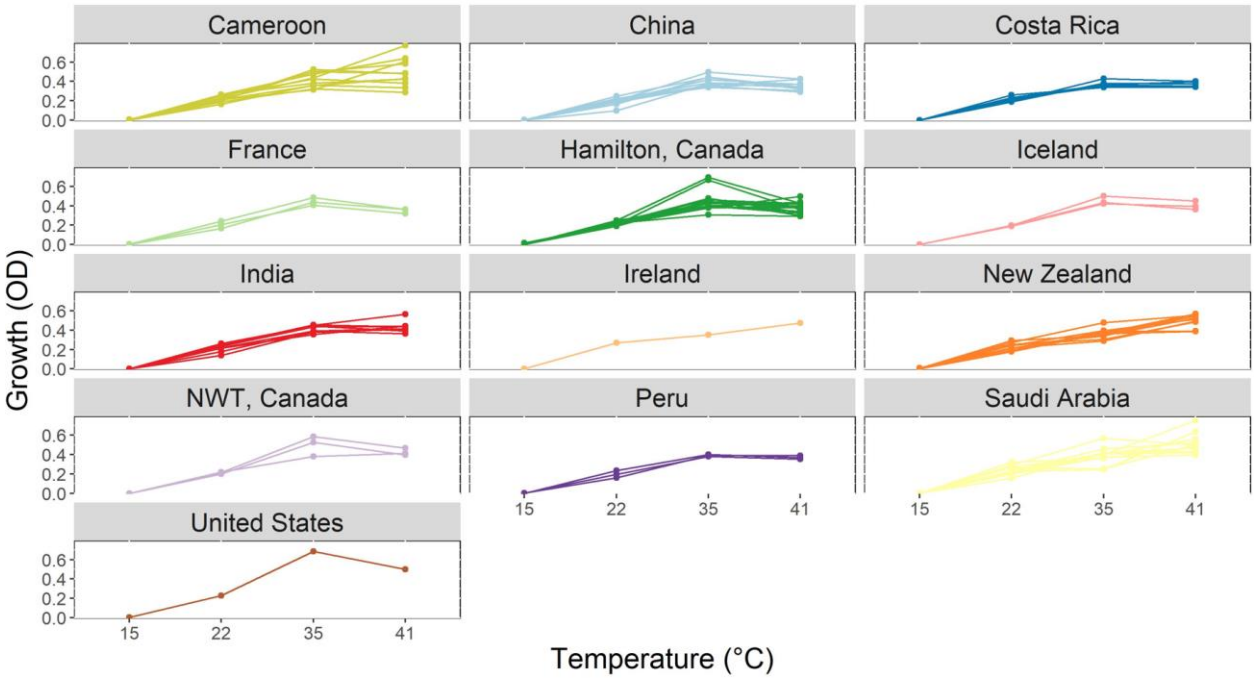

Supplementary Figure 6.1: Reaction norm plots showing strain × temperature interactions in the growth profiles of 89 strains after three days of incubation across four temperatures separated by country. NWT, Northwest Territories, Canada.

6.10 References

Alanio, A., Dellière, S., Fodil, S., Bretagne, S., & Mégarbane, B. (2020). Prevalence of putative invasive pulmonary aspergillosis in critically ill patients with COVID-19. In *The Lancet Respiratory Medicine* (Vol. 8, Issue 6, pp. e48–e49). Lancet Publishing Group. https://doi.org/10.1016/S2213-2600(20)30237-X

Arora, P., Singh, P., Wang, Y., Yadav, A., Pawar, K., Singh, A., Padmavati, G., Chowdhary, A., & Xu, J. (2021). Environmental isolation of *Candida auris* from the coastal wetlands of Andaman islands, India. *MBio*, *12*(2), 1–9. https://doi.org/10.1128/MBIO.03181-20

Ashu, E. E., Hagen, F., Chowdhary, A., Meis, J. F., & Xu, J. (2017). Global population genetic analysis of *Aspergillus fumigatus*. *MSphere*, *2*(1), e00019-17. https://doi.org/10.1128/mSphere.00019-17

Ashu, E. E., Kim, G. Y., Roy-Gayos, P., Dong, K., Forsythe, A., Giglio, V., Korfanty, G. A., Yamamura, D., & Xu, J. (2018). Limited evidence of fungicide-driven triazole-resistant *Aspergillus fumigatus* in Hamilton, Canada. *Canadian Journal of Microbiology*, *64*(2),

119–130. https://doi.org/10.1139/cjm-2017-0410

Auxier, B., Becker, F., Nijland, R., Debets, A. J. M., Heuvel, J. van den, & Snelders, E. (2022). Meiosis in the human pathogen *Aspergillus fumigatus* has the highest known number of crossovers. *BioRxiv*, 2022.01.14.476329. https://doi.org/10.1101/2022.01.14.476329

Bakar, N. A., Karsani, S. A., & Alias, S. A. (2020). Fungal survival under temperature stress: A proteomic perspective. *PeerJ*, *8*, e10423. https://doi.org/10.7717/PEERJ.10423

Barber, A. E., Riedel, J., Sae-Ong, T., Kang, K., Brabetz, W., Panagiotou, G., Deising, H. B., & Kurzai, O. (2020). Effects of agricultural fungicide use on *Aspergillus fumigatus* abundance, antifungal susceptibility, and population structure. *MBio*, *11*(6). https://doi.org/10.1128/mbio.02213-20

Bhabhra, R., & Askew, D. S. (2005). Thermotolerance and virulence of *Aspergillus fumigatus*: Role of the fungal nucleolus. In *Medical Mycology* (Vol. 43, Issue SUPPL.1, pp. 87–93). Oxford Academic. https://doi.org/10.1080/13693780400029486

Bhabhra, R., Miley, M. D., Mylonakis, E., Boettner, D., Fortwendel, J., Panepinto, J. C., Postow, M., Rhodes, J. C., & Askew, D. S. (2004). Disruption of the *Aspergillus fumigatus* gene encoding nucleolar protein CgrA impairs thermotolerant growth and reduces virulence. *Infection and Immunity*, *72*(8), 4731–4740. https://doi.org/10.1128/IAI.72.8.4731-4740.2004

Casadevall, A., Kontoyiannis, D. P., & Robert, V. (2019). On the emergence of *Candida auris*: climate change, azoles, swamps, and birds. *MBio*, *10*(4). https://doi.org/10.1128/MBIO.01397-19

Casadevall, A., Kontoyiannis, D. P., & Robert, V. (2021). Environmental *Candida auris* and the global warming emergence hypothesis. *MBio*, *12*(2), 1–3. https://doi.org/10.1128/MBIO.00360-21

Chowdhary, A., Kathuria, S., Xu, J., Sharma, C., Sundar, G., Singh, P. K., Gaur, S. N., Hagen, F., Klaassen, C. H., & Meis, J. F. (2012). Clonal expansion and emergence of environmental multiple-triazole-resistant *Aspergillus fumigatus* strains carrying the TR34/L98H mutations in the *cyp51A* gene in India. *PLoS ONE*, *7*(12), e52871. https://doi.org/10.1371/journal.pone.0052871

Cordero, R. J. B., Robert, V., Cardinali, G., Arinze, E. S., Thon, S. M., & Casadevall, A. (2018). Impact of yeast pigmentation on heat capture and latitudinal distribution. *Current Biology : CB*, *28*(16), 2657. https://doi.org/10.1016/J.CUB.2018.06.034

de Valk, H. A., Meis, J. F. G. M., Curfs, I. M., Muehlethaler, K., Mouton, J. W., & Klaassen, C. H. W. (2005). Use of a novel panel of nine short tandem repeats for exact and high-resolution fingerprinting of *Aspergillus fumigatus* isolates. *Journal of Clinical Microbiology*, *43*(8), 4112–4120. https://doi.org/10.1128/JCM.43.8.4112-4120.2005

Etienne, K. A., Berkow, E. L., Gade, L., Nunnally, N., Lockhart, S. R., Beer, K., King Jordan, I., Rishishwar, L., & Litvintseva, A. P. (2021). Genomic diversity of azole-resistant *Aspergillus fumigatus* in the united states. *MBio*, *12*(4). https://doi.org/10.1128/MBIO.01803-21

Fabri, J. H. T. M., Rocha, M. C., Fernandes, C. M., Persinoti, G. F., Ries, L. N. A., Cunha, A. F. da, Goldman, G. H., Del Poeta, M., & Malavazi, I. (2021). The heat shock transcription factor HsfA is essential for thermotolerance and regulates cell wall integrity in *Aspergillus fumigatus*. *Frontiers in Microbiology*, *12*, 735. https://doi.org/10.3389/FMICB.2021.656548

Feng, Y., Zhang, J., Berdugo, M., Guirado, E., Guerra, C. A., Egidi, E., Wang, J., Singh, B. K., & Delgado-Baquerizo, M. (2022). Temperature thresholds drive the global distribution of soil fungal decomposers. *Global Change Biology*, *28*(8), 2779–2789. https://doi.org/10.1111/GCB.16096

Gibson, A. M., & Hocking, A. D. (1997). Advances in the predictive modelling of fungal growth in food. *Trends in Food Science & Technology*, *8*(11), 353–358. https://doi.org/10.1016/S0924-2244(97)01065-0

Granade, T. C., Hehmann, M. F., & Artis, W. M. (1985). Monitoring of filamentous fungal growth by in situ microspectrophotometry, fragmented mycelium absorbance density, and 14C incorporation: alternatives to mycelial dry weight. *Applied and Environmental Microbiology*, *49*(1), 101–108. https://doi.org/10.1128/AEM.49.1.101-108.1985

Kamvar, Z. N., Tabima, J. F., & Grünwald, N. J. (2014). *Poppr* : an R package for genetic analysis of populations with clonal, partially clonal, and/or sexual reproduction. *PeerJ*, *2*, e281. https://doi.org/10.7717/peerj.281

Korfanty, G. A., Dixon, M., Jia, H., Yoell, H., & Xu, J. (2021). Genetic diversity and dispersal of *Aspergillus fumigatus* in Arctic soils. *Genes 2022, Vol. 13, Page 19*, *13*(1), 19. https://doi.org/10.3390/GENES13010019

Korfanty, G. A., Stanley, K., Lammers, K., Fan, Y. Y., & Xu, J. (2021). Variations in sexual fitness among natural strains of the opportunistic human fungal pathogen *Aspergillus fumigatus*. *Infection, Genetics and Evolution*, *87*, 104640. https://doi.org/10.1016/j.meegid.2020.104640

Korfanty, G. A., Teng, L., Pum, N., & Xu, J. (2019). Contemporary gene flow is a major force shaping the *Aspergillus fumigatus* population in Auckland, New Zealand. *Mycopathologia*, *184*(4), 479–492. https://doi.org/10.1007/s11046-019-00361-8

Kryukov, V. Y., Yaroslavtseva, O. N., Elisaphenko, E. A., Mitkovets, P. V., Lednev, G. R., Duisembekov, B. A., Zakian, S. M., & Glupov, V. V. (2012). Change in the temperature preferences of *Beauveria bassiana sensu lato* isolates in the latitude gradient of Siberia and Kazakhstan. *Microbiology 2012 81:4*, *81*(4), 453–459. https://doi.org/10.1134/S002626171204011X

Kumar, R., & Tamuli, R. (2014). Calcium/calmodulin-dependent kinases are involved in growth, thermotolerance, oxidative stress survival, and fertility in *Neurospora crassa*. *Archives of Microbiology*, *196*(4), 295–305. https://doi.org/10.1007/S00203-014-0966-2

Kwon-Chung, K. J., & Sugui, J. A. (2013). *Aspergillus fumigatus*--what makes the species a ubiquitous human fungal pathogen? *PLoS Pathogens*, *9*(12), e1003743. https://doi.org/10.1371/journal.ppat.1003743

Latgé, J. P., & Chamilos, G. (2020). *Aspergillus fumigatus* and aspergillosis in 2019. *Clinical Microbiology Reviews*, *33*(1). https://doi.org/10.1128/CMR.00140-18

Lembrechts, J. J., van den Hoogen, J., Aalto, J., Ashcroft, M. B., De Frenne, P., Kemppinen, J., Kopecký, M., Luoto, M., Maclean, I. M. D., Crowther, T. W., Bailey, J. J., Haesen, S., Klinges, D. H., Niittynen, P., Scheffers, B. R., Van Meerbeek, K., Aartsma, P., Abdalaze, O., Abedi, M., … Lenoir, J. (2022). Global maps of soil temperature. *Global Change Biology*, *28*(9), 3110–3144. https://doi.org/10.1111/GCB.16060

Letunic, I., & Bork, P. (2016). Interactive tree of life (iTOL) v3: an online tool for the display

and annotation of phylogenetic and other trees. *Nucleic Acids Research*, *44*(W1), W242–W245. https://doi.org/10.1093/NAR/GKW290

Margesin, R., Cimadom, J., & Schinner, F. (2006). Biological activity during composting of sewage sludge at low temperatures. *International Biodeterioration & Biodegradation*, *57*(2), 88–92. https://doi.org/10.1016/J.IBIOD.2005.12.001

Mattoon, E. R., Casadevall, A., & Cordero, R. J. (2021). Beat the heat: correlates, compounds, and mechanisms involved in fungal thermotolerance. *Fungal Biology Reviews*, *36*, 60–75. https://doi.org/10.1016/J.FBR.2021.03.002

Medina, A., Schmidt-Heydt, M., Rodríguez, A., Parra, R., Geisen, R., & Magan, N. (2015). Impacts of environmental stress on growth, secondary metabolite biosynthetic gene clusters and metabolite production of xerotolerant/xerophilic fungi. *Current Genetics*, *61*(3), 325–334. https://doi.org/10.1007/S00294-014-0455-9

Miyazawa, K., Umeyama, T., Hoshino, Y., Abe, K., & Miyazaki, Y. (2022). Quantitative monitoring of mycelial growth of *Aspergillus fumigatus* in liquid culture by optical density. *Microbiology Spectrum*, *10*(1). https://doi.org/10.1128/SPECTRUM.00063-21

Nielsen, K., Marra, R. E., Hagen, F., Boekhout, T., Mitchell, T. G., Cox, G. M., & Heitman, J. (2005). Interaction between genetic background and the mating-type locus in *Cryptococcus neoformans* virulence potential. *Genetics*, *171*(3), 975–983. https://doi.org/10.1534/GENETICS.105.045039

O'Gorman, C. M., Fuller, H. T., & Dyer, P. S. (2009). Discovery of a sexual cycle in the opportunistic fungal pathogen *Aspergillus fumigatus*. *Nature*, *457*(7228), 471–474. https://doi.org/10.1038/nature07528

Paoletti, M., Rydholm, C., Schwier, E. U., Anderson, M. J., Szakacs, G., Lutzoni, F., Debeaupuis, J.-P., Latgé, J.-P., Denning, D. W., & Dyer, P. S. (2005). Evidence for sexuality in the opportunistic fungal pathogen *Aspergillus fumigatus*. *Current Biology*, *15*(13), 1242–1248. https://doi.org/10.1016/J.CUB.2005.05.045

Paradis, E., & Schliep, K. (2019). ape 5.0: an environment for modern phylogenetics and evolutionary analyses in R. *Bioinformatics*, *35*(3), 526–528. https://doi.org/10.1093/BIOINFORMATICS/BTY633

R Core Team. (2022). R: a language and environment for statistical computing. *R Foundation*

for Statistical Computing Vienna, Austria (4.2.1). https://www.r-project.org/.

Rangel, D. E. N., Braga, G. U. L., Anderson, A. J., & Roberts, D. W. (2005). Variability in conidial thermotolerance of *Metarhizium anisopliae* isolates from different geographic origins. *Journal of Invertebrate Pathology*, *88*(2), 116–125. https://doi.org/10.1016/J.JIP.2004.11.007

Rangel, D. E. N., Fernandes, É. K. K., Dettenmaier, S. J., & Roberts, D. W. (2010). Thermotolerance of germlings and mycelium of the insect-pathogenic fungus *Metarhizium* spp. and mycelial recovery after heat stress. *Journal of Basic Microbiology*, *50*(4), 344–350. https://doi.org/10.1002/JOBM.200900430

Rocha, M. C., Minari, K., Fabri, J. H. T. M., Kerkaert, J. D., Gava, L. M., da Cunha, A. F., Cramer, R. A., Borges, J. C., & Malavazi, I. (2021). *Aspergillus fumigatus* Hsp90 interacts with the main components of the cell wall integrity pathway and cooperates in heat shock and cell wall stress adaptation. *Cellular Microbiology*, *23*(2), e13273. https://doi.org/10.1111/CMI.13273

Samarasinghe, H., Korfanty, G. A., & Xu, J. (2022). Isolation of culturable yeasts and molds from soils to investigate fungal population structure. *JoVE (Journal of Visualized Experiments)*, *2022*(183), e63396. https://doi.org/10.3791/63396

Sangamesh, M. B., Jambagi, S., Vasanthakumari, M. M., Shetty, N. J., Kolte, H., Ravikanth, G., Nataraja, K. N., & Uma Shaanker, R. (2018). Thermotolerance of fungal endophytes isolated from plants adapted to the Thar Desert, India. *Symbiosis*, *75*(2), 135–147. https://doi.org/10.1007/S13199-017-0527-Y

Sewell, T. R., Zhu, J., Rhodes, J., Hagen, F., Meis, J. F., Fisher, M. C., & Jombart, T. (2019). Nonrandom distribution of azole resistance across the global population of *Aspergillus fumigatus*. *MBio*, *10*(3), e00392-19. https://doi.org/10.1128/mBio.00392-19

Sugui, J. A., Losada, L., Wang, W., Varga, J., Ngamskulrungroj, P., Abu-Asab, M., Chang, Y. C., O'Gorman, C. M., Wickes, B. L., Nierman, W. C., Dyer, P. S., & Kwon-Chung, K. J. (2011). Identification and characterization of an *Aspergillus fumigatus* "supermater" pair. *MBio*, *2*(6). https://doi.org/10.1128/mBio.00234-11

Vidal, C., Fargues, J., & Lacey, L. A. (1997). Intraspecific variability of *Paecilomyces fumosoroseus*: Effect of temperature on vegetative growth. *Journal of Invertebrate*

Pathology, *70*(1), 18–26. https://doi.org/10.1006/JIPA.1997.4658

Wang, Y., & Xu, J. (2022). Population genomic analyses reveal evidence for limited recombination in the superbug *Candida auris* in nature. *Computational and Structural Biotechnology Journal*, *20*, 3030. https://doi.org/10.1016/J.CSBJ.2022.06.030

Wilson, A. M., Wilken, P. M., Van der Nest, M. A., Wingfield, M. J., & Wingfield, B. D. (2019). It's all in the genes: The regulatory pathways of sexual reproduction in filamentous ascomycetes. *Genes 2019, Vol. 10, Page 330*, *10*(5), 330. https://doi.org/10.3390/GENES10050330

Xu, J. (2004). Genotype-environment interactions of spontaneous mutations for vegetative fitness in the human pathogenic fungus *Cryptococcus neoformans*. *Genetics*, *168*(3), 1177–1188. https://doi.org/10.1534/GENETICS.104.030031

Xu, J. (2022). Assessing global fungal threats to humans. *MLife*, *1*(3), 223–240. https://doi.org/10.1002/MLF2.12036

Yadav, A., Jain, K., Wang, Y., Pawar, K., Kaur, H., Sharma, K. K., Tripathy, V., Singh, A., Xu, J., & Chowdhary, A. (2022). *Candida auris* on apples: diversity and clinical significance. *MBio*, *13*(2). https://doi.org/10.1128/MBIO.00518-22

Yong, M., Yu, J., Pan, X., Yu, M., Cao, H., Song, T., Qi, Z., Du, Y., Zhang, R., Yin, X., Liu, W., & Liu, Y. (2020). Two mating-type genes *MAT1-1-1* and *MAT1-1-2* with significant functions in conidiation, stress response, sexual development, and pathogenicity of rice false smut fungus *Villosiclava virens*. *Current Genetics*, *66*(5), 989–1002. https://doi.org/10.1007/S00294-020-01085-9

Zhang, J., Verweij, P. E., Rijs, A. J. M. M., Debets, A. J. M., & Snelders, E. (2022). Flower bulb waste material is a natural niche for the sexual cycle in *Aspergillus fumigatus*. *Frontiers in Cellular and Infection Microbiology*, *11*. https://doi.org/10.3389/FCIMB.2021.785157

Zhou, D., Korfanty, G. A., Mo, M., Wang, R., Li, X., Li, H., Li, S., Wu, J.-Y., Zhang, K.-Q., Zhang, Y., & Xu, J. (2021). Extensive genetic diversity and widespread azole resistance in greenhouse populations of *Aspergillus fumigatus* in Yunnan, China. *MSphere*, *6*(1). https://doi.org/10.1128/MSPHERE.00066-21/

Chapter 7

Conclusions and Future Research Directions

7.1 Conclusions and Perspectives

My PhD thesis makes significant contributions to our knowledge on *A. fumigatus* by investigating the genetic diversity of underrepresented soil populations, highlighting the extraordinarily high gene flow and localized genetic differentiations of *A. fumigatus* populations, and uncovering the high variations in reproductive success and thermotolerance between genetically and geographically distinct strains from diverse climatic environments.

Soil is a biodiversity hotspot for many fungal species. The abundance of fungi in even the smallest amount of soil allows for incredible genetic diversity to be present within local populations. In chapter 2, we introduced a high throughput protocol to isolate yeasts and *A. fumigatus* from soil. Many fungal populations are under sampled in many geographic/climatic regions around the world, therefore we created a protocol to quickly isolate hundreds of yeast and *A. fumigatus* strains from relatively small amounts of soil. Our protocol allows for the isolation and characterization of yeast communities and *A. fumigatus* populations with sufficient statistical power for downstream population genetic/genomic analyses. This protocol can be adapted to also isolate other mold species found within soil.

In chapter 3, we investigated the population structure of *A. fumigatus* isolates obtained from two arctic regions, Iceland and Northwest Territories (NWT) Canada. Our study was the first to investigate and characterize *A. fumigatus* populations in high latitudes regions and test the strain susceptibility to two triazole antifungals. Extensive genetic diversity was observed among strains from these two populations with evidence of both clonal and sexual reproduction present in both populations. Both arctic populations were significantly differentiated from each other as well several other populations around the world. However, the arctic population structure was still significantly influenced by populations from other

geographic regions, specifically Norway, Belgium, France, and India. Interestingly, the triazole-resistant strain found within NWT that shared a nearly identical genotype to strains in India demonstrates the complexity of managing drug resistance in *A. fumigatus* and the potential of *A. fumigatus* strains to migrate to distant regions of the world. Future research involves the investigation and identification of mechanisms influencing *A. fumigatus* adaptability and/or escape from harsh environmental stressors.

In chapter 4, we investigated the genetic diversity of 1303 soil isolated *A. fumigatus* strains obtained from 11 countries and 6 continents. We found extensive genetic diversity and historical differentiations present among soil populations, exceeding the diversity found within their clinical co-populations at country, continent, and global levels. Additionally, both clonal and sexual reproduction were present among soil populations. The exceptions to these finding were the Chinese, Indian, and Saudi Arabian soil populations, as their soil populations were dominated by clonal genotypes and were less genetically diverse. Although elements of geographic clustering were observed, the 1303 soil strains were still broadly distributed across the neighbor joining tree. Soil strains were assigned to two large genetic clusters by STRUCTURE and three genetic clusters by DAPC, similar to what was observed in previous studies (Rhodes et al., 2022; Sewell et al., 2019). Altogether, our results highlight the ability of *A. fumigatus* genotypes to spread around the world and enter diverse ecological settings while maintaining unique localized population structures. Future omics analyses will provide more insight into the differences that may exist between soil populations from different geographic/climatic regions and clinical populations. These analyses could also provide insight on how triazole resistant mutations originated and/or are maintained in some soil populations and not others.

In chapter 5, using a sample of 60 strains collected from six countries, along with two supermater strains, we investigated the presence and/or absence of reproductive barriers between these genetically and geographically distant strains. We observed that 136 crosses (15.1%) produced cleistothecia, and of these, 40.4% produced ascospores that successfully germinated. Most successful crosses produced low numbers of cleistothecia (1 to 5),

however, certain crosses produced cleistothecia in the 50 to 100 range. Intranational crosses had different mating success rates, where China showed the highest mating success (64%), followed by New Zealand (56%), Saudi Arabia (16%), and India and Cameroon (both at 4%). Interestingly, at higher geographic distances between parental strains, overall fewer cleistothecia were observed. In contrast, no relationship was observed between high genetic distance and cleistothecial formation. Large variations in ascospore germination were observed between these successful crosses, ranging from 21.1% to 0.17%. Here, China, India, and New Zealand had significantly more crosses with successful ascospore germinations than Saudi Arabia (16%), Canada, and Cameroon. Successful germination followed the same pattern as cleistothecial formation, where higher geographic distances between parental strains has significantly fewer viable ascospores while no relationship was observed between successful germination and genetic distance between strains. Ascospore germination rate decreased at higher geographic distance and increased at higher genetic distances, however, these correlations were statistically not significant. Lastly, to correct for the potential bias posed by the low reproductive success withing Canada, we analyzed a subset of strains that produced 6 to 10 cleistothecia. Similar patterns to the full dataset were observed in both mating, germination success, and germination success rate. Altogether, these results show that reproduction between geographically and genetically distant *A. fumigatus* populations are possible. Future studies should include a larger number of parental strains obtained to increase the robustness and power of our results. Additionally, genetic and phenotypic analyses on the progeny of these crosses will yield insight into the extent of genetic exchange among geographic populations and genetic clusters.

In chapter 6, using a global sample of 89 *A. fumigatus* strains, we investigated their variation in growth at different temperatures. Apart from the expected influence of temperature on strain growth, we found that growth among strains was highly variable at three of the five temperatures tested, where limited strain growth was observed only at 4°C and 15°C. Broad sense heritability analysis overall suggested genetic differences between the strains contributed to the observed difference in growth. Therefore, we calculated the coefficient of variation and observed high variability in growth across all temperatures. Additionally, the

country of origin of a strain, along with average temperature and temperature range at the isolation site of a strain, did not have a statistically significant contribution to this variability in growth. Lastly, strain mating type and genetic distance between strain did not have a statistically significant relationship to growth and variability in growth. Together, our results suggest the exceptionally ability of *A. fumigatus* strains to adapt to novel ecological niches through rapid adaptation to temperature changes. Future investigations into other phenotypic traits that provide tolerance to abiotic stressors such as salinity or reactive oxidative species. Additionally, genomic analysis may uncover mechanisms that allow *A. fumigatus* strains to quickly adapt to novel ecological niches and aid in understanding the high variation observed among strain.

Overall, my PhD thesis research broadened our knowledge on the global population structure and diversity of soil isolated *A. fumigatus* strains from diverse geographic and climatic origins. The clinical and economic burdens posed by *A. fumigatus* around the world will likely be further exacerbated by the broad variability and adaptability within most local *A. fumigatus* populations reported here. My work on the reproductive fitness of this species provided insight on the potential genetic exchange between geographic and genetic populations, including the spread of drug-resistant genes. Altogether, my work highlights how broadly distributed *A. fumigatus* strains and populations, regardless of previous historical/contemporary differentiations and selective pressures within their geographic origins, maintain the capacity to reproduce and grow in distant geographic regions and climates. Despite their capacities for growth, reproduction, and high gene flow between distant populations, *A. fumigatus* strains showed high variabilities in both reproductive success and thermal adaptability. I showed that geographic and genetic distance as well as temperature at isolation site, had little to no effect on these variabilities. Figure 7.1 illustrates a graphical summary of my thesis. My results call for further research on how local soil populations maintain their phenotypic variability and genetic diversity. Understanding this aspect of the *A. fumigatus* species is key, as foreign *A. fumigatus* strains may generate sexual progeny with native strains, potentially resulting in highly fit strains containing adaptations acquired from both sources. These fit strains may re-enter our communities and cause

increasingly devastating aspergillosis outbreaks, similar to what was first observed in India (Chowdhary, et al., 2012). Lastly, the relationships between soil populations and those from other ecological niches such as from the air and aquatic environments as well as in anthropogenic structures remain to be investigated.

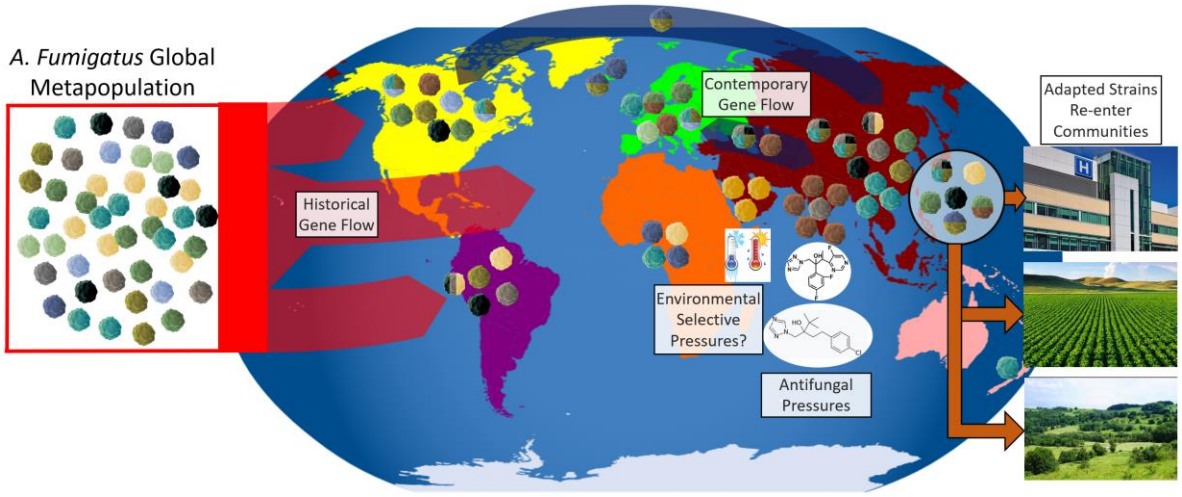

Figure 7.1: Graphical summary of my PhD thesis highlighting the global genetic diversity of *A. fumigatus* populations. The global *A. fumigatus* metapopulation, through historical differentiation and gene flow, may have generated many geographic populations of *A. fumigatus* that were highly genetically diverse within but also variably genetically differentiated (red transparent arrows). I observed strong evidence of contemporary gene flow between these geographic populations (blue transparent arrows), yet the genetic differentiation among populations persisted. Several populations were dominated by clonal strains, where antifungal selective pressures likely contributed to their expansion. However, clonal populations that were susceptible to antifungals may have expanded due to other selective pressures, such as those from the environment. Migrant strains entering foreign populations maintain their capacity to grow at different environmental pressures, and can produce sexual offspring with native strains, albeit with high phenotypic variations among strains. Potentially, these highly fit migrant strains and their progeny may re-enter our communities and cause aspergillosis outbreaks.

7.2 References

Chowdhary, A., Kathuria, S., Xu, J., Sharma, C., Sundar, G., Singh, P. K., Gaur, S. N., Hagen, F., Klaassen, C. H., & Meis, J. F. (2012b). Clonal expansion and emergence of environmental multiple-triazole-resistant *Aspergillus fumigatus* strains carrying the TR34/L98H mutations in the *cyp51A* gene in India. *PLoS ONE*, *7*(12), e52871. https://doi.org/10.1371/journal.pone.0052871

Rhodes, J., Abdolrasouli, A., Dunne, K., Sewell, T. R., Zhang, Y., Ballard, E., … Fisher, M. C. (2022). Population genomics confirms acquisition of drug-resistant *Aspergillus fumigatus* infection by humans from the environment. *Nature Microbiology 2022 7:5*, *7*(5), 663–674. https://doi.org/10.1038/s41564-022-01091-2

Sewell, T. R., Zhu, J., Rhodes, J., Hagen, F., Meis, J. F., Fisher, M. C., & Jombart, T. (2019). Nonrandom distribution of azole resistance across the global population of *Aspergillus fumigatus*. *MBio*, *10*(3), e00392-19. https://doi.org/10.1128/mBio.00392-19